Targeting cFLIP to Inhibit Residual Cancer Stem Cells after Chemotherapy

Tim Robinson

_____
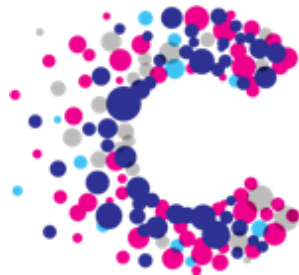
DECLARATION

This work has not been submitted in substance for any other degree or award at this or any other university or place of learning, nor is being submitted concurrently in candidature for any degree or other award.

Signed ……………………………………………Date ……………….…

STATEMENT 1

This thesis is being submitted in partial fulfillment of the requirements for the degree of PhD

Signed ……………………………………………Date ……………….…

STATEMENT 2

This thesis is the result of my own independent work/investigation, except where otherwise stated, and the thesis has not been edited by a third party beyond what is permitted by Cardiff University's Policy on the Use of Third Party Editors by Research Degree Students. Other sources are acknowledged by explicit references. The views expressed are my own.

Signed ……………………………………………Date ……………….…

STATEMENT 3

I hereby give consent for my thesis, if accepted, to be available online in the University's Open Access repository and for inter-library loan, and for the title and summary to be made available to outside organisations.

Signed ……………………………………………Date ……………….…

STATEMENT 4: PREVIOUSLY APPROVED BAR ON ACCESS

I hereby give consent for my thesis, if accepted, to be available online in the University's Open Access repository and for inter-library loans after expiry of a bar on access previously approved by the Academic Standards & Quality Committee.

Signed ……………………………………………Date ……………….…

Acknowledgments

Firstly, I would like to thank my supervisor Dr. Richard Clarkson for giving me the opportunity to undertake this PhD project within his lab and for providing me with guidance and support throughout. I would also like to thank my co-supervisors Dr. Luke Piggott and Prof. Peter Barrett-Lee for providing their expertise and knowledge. I would also like to extend my thanks to Prof. John Chester whose mentorship has, and continues to be, gratefully received.

I am also grateful to everyone who I have worked with at ECSCRI who has made my time here so enjoyable and has provided me with many memories amusement. I would like to thank all current and past members of the Clarkson lab including, Will Yang, Daniel Turnham, Andreia Silva, Rhiannon French, Aleks Gruca, Cinzia Bordoni, Gilda Giancotti and Liv Hayward, who have all contributed with ideas and help towards my work and have kept me entertained both when I was finding my feet and when results were slow to come.

I would also like to acknowledge the support of all my collaborators throughout this work, especially the staff at Velindre Cancer Centre who provided me with chemotherapy and many cups of tea in clinics. I am also grateful to Cancer Research UK who funded this work and supported my travelling to present my findings.

Finally, I would like to thank my family for rarely complaining about my absence at weekends and long days in labs. This includes my wife Polly and my two children Florence and Sybil, who will be very relieved that 'Daddy's book' has been submitted. I would also like thank my parents and parents-in-law for the babysitting that allowed both late-night working and much needed breaks. I am particularly grateful to John and Gill who have proof read this thesis.

Table of abbreviations

ACTB Beta-actin

Akt Protein kinase B

ALDH1 Aldehyde dehydrogenase 1

β catenin Beta Catenin

Bcl-2 B-cell lymphoma 2

bCSC Breast Cancer Stem Cell

BRCA-1 Breast cancer 1

BRCA-2 Breast cancer 2

c-FLIP Cellular FLICE-like inhibitory protein

CD95 Fas receptor

CNV Copy number variation

CSC cancer stem cell

DcR Decoy receptor

DED Death effector domain

DISC Death inducing signalling complex

DR4 Death receptor 4

DR5 Death receptor 5

E-cadherin- Epithelial cadherin EGF Epidermal growth factor

EGFR Epidermal growth factor receptor

EMT Epithelial-mesenchymal transition

ER Oestrogen receptor

ErbB2 erythroblastic leukaemia viral oncogene homolog

ERK Extracellular signal-regulated kinase

FACS Fluorescence activated cell sorting

FADD Fas associated death domain

FasL Fas ligand

FBS Fetal bovine serum

FEC Fluorouracil, Epirubicin, Cyclophosphamide

FLIPi c-FLIP inhibition

FLIPi/TRAIL combination c-FLIP inhibition + TRAIL treatment

Gsk3Beta Glycogen synthase kinase 3 beta

HDAC Histone deacetylase

HER2 Human epidermal growth factor receptor 2

HGF Hepatocyte growth factor

Hh Hedgehog

HIF-1 Hypoxia-inducible factor 1

HIF-2 Hypoxia-inducible factor 2

HMEC Human mammary epithelial cells

HRG Heregulin

Hsp90- Heat shock protein 90

IAPs Inhibitors of apoptosis

IFN Interferon

IGF Insulin-like growth factor

IkB Inhibitors of NF-kB IKK Inhibitor of KappaB kinase

IL-6 Interleukin 6

IL-8 Interleukin 8

JNK c-jun N-terminal kinase

LAMP1 Lysosomal marker mAb Monoclonal antibody

MAPK Mitogen-activated protein kinase

MaSC Mammary stem cell

MDR1 Multi-drug resistance protein 1

MEKK1 MAP/ERK kinase kinase 1

MET Mesenchymal-epithelial transition

MFU Mammosphere forming units

MMP Matrix metalloproteinase MMTV Mouse mammary tumour virus

mTOR Mammalian target of rapamycin

N-cadherin- Neural cadherin

NF-kB Nuclear factor binding to the intronic kappa-lightchain enhancer element in b cells

NHL Non-hodgkins lymphoma

NOD/SCID Nonobese diabetic severe combined Immunodeficiency

OH14 Novel cFLIP inhbitor

PBS Phosphate-buffered saline

PCR Polymerase chain reaction

PI3k Phosphatidylinositol 3-kinase

PR Progesterone receptor

qPCR Quantitative PCR

qRT-PCR Quantitative reverse transcription PCR

RIP Receptor-interacting protein

RNAi RNA interference

SAHA Suberoylanilide hyroxamic acid

SDS-PAGE Sodium dodecyl sulphate polyacrylamide gel

SNP Single nucleotide polymorphism

siRNA Small interfering RNA

Snail Zinc finger protein SNAI1 gene

TFU Tumoursphere-forming unit

TGF-Beta Transforming growth factor Beta

TNF-alhpa Tumour necrosis factor alpha

TIC Tumour initiating cell

TIMP Tissue inhibitors of metalloproteinases

TNBC Triple Negative Breast Cancer

TNFalpha Tumour necrosis factor alpha

TRADD TNF receptor type 1-associated death domain

TRAF TNF receptor associated factor TRAIL (APO-2L) TNF-related apoptosis inducing ligand

TRAIL TNF-related apoptosis inducing ligand

Wnt Wingless-int

ZEB1- Zinc finger E-box-binding homeobox 1

ZEB2- Zinc finger E-box-binding homeobox 2

Abstract

The emergence of the cancer stem cell (CSC) hypothesis has helped to explain previously poorly understood clinical concepts such as metastases, late tumour recurrence and resistance to chemotherapy. Triple Negative Breast Cancer (TNBC) has the worst prognosis of all types of breast cancer with a more frequent relapse rate and reduced length of survival in metastatic disease. It has been shown to contain a higher proportion of CSCs than other types of breast cancer. Paclitaxel, a taxane in widespread use in breast cancer, induces apoptosis in a ligand-independent manner through the extrinsic apoptosis pathway. cFLIP is both an antagonist of this apoptosis pathway and can interfere with the ubiquitynation and subsequent degradation of both HIF1α and β-catenin, two molecules involved in CSC-signalling. Using a novel compound targeted against cFLIP, we wanted to assess whether its combination with paclitaxel effectively targeted CSCs. Using a combination of *in vitro* models of cancer stem/progenitor-like activity and the surrogate marker of CSCs, ALDH, we demonstrated that a number of chemotherapeutic agents, including paclitaxel, docetaxel and FEC increased CSC-like behaviour. A mathematical model demonstrated that paclitaxel increased the absolute number of CSCs after treatment suggesting that CSC-like activity was being induced. OH14, a novel inhibitor of c-FLIP developed in our laboratory, abrogated the paclitaxel-mediated induction of CSC-like activity in TNBC cell lines. While apoptosis may play a role in CSC viability *in vitro*, it did not appear to play a major role in OH14-mediated suppression of CSC acquisition following paclitaxel treatment. Instead, OH14 appeared to suppress CSCs through disruption of HIF1- α, as HIF1α-mediated signalling was increased by paclitaxel and abrogated by the addition of OH14. These beneficial effects of combinatorial OH14 were confirmed in vivo, where OH14 suppressed tumour initiation of TNBC xenografts and prevented relapse of paclitaxel treated tumours in a xenograft model of systemic treatment. cFLIP thus has a dual effect in both increasing apoptosis and targeting signalling in TNBC CSCs. In a breast cancer subtype in desperate need of novel therapeutic strategies, targeting cFLIP warrants further investigation and progression towards clinical trials.

Table of contents

Table of Figures

Table of Tables

1 Introduction

1.1 Cancer

Despite a declaration of a 'war on cancer' by President Nixon in 1971, cancer remains today as one of the world's largest killers as well as being a huge economic drain on society. Cancer caused 8.2 million deaths worldwide in 2012 (CRUK 2014) and is estimated to cost the countries within the European Union €50 billion per annum in diagnosis, treatment and lost productivity (Luengo-Fernandez et al. 2013).

1.2 Breast cancer

1.2.1 Incidence and mortality

Breast cancer remains a significant burden in terms of morbidity and mortality. In 2008, 1,380,000 breast cancer diagnoses worldwide led to 458,000 deaths, ensuring that breast cancer remains one of the commonest cancer diagnoses and cause of cancer death (Ferlay et al. 2010). In the UK, age-standardised incidence of breast cancer increased by 6% over the last decade to 2010 with 50,285 new diagnoses in 2011 (CRUK 2014). It is currently estimated that there are over 500,000 people living with or after a diagnosis of breast cancer in the UK (Maddams et al. 2009) - with this population projected to triple by 2040 due to improvements in detection and treatment (Maddams, Utley and Møller 2012).

Owing to advances both in detection and in therapy, mortality rates from breast cancer have been decreasing steadily in most Western countries for the past two decades (Jemal et al. 2009). Depending on prognostic factors, up to 30% of node-negative and up to 70% of node-positive breast cancers will relapse (Cardoso et al. 2012). Approximately 5% to 10% of breast cancers are metastatic at diagnosis with an associated 20% 5-year survival. As over 90% of cancer deaths are associated with metastatic disease, new strategies are needed in order to reduce relapse rates and improve survival (G. P. Gupta and Massagué 2006). In the UK this has led to a concerted effort to identify research gaps and priorities to improve both the prevention and treatment of breast cancer (Eccles et al. 2013).

1.2.2 Breast cancer treatment

The mainstay of localised breast cancer treatment is surgery and radiotherapy. In addition to this, a wide range of hormonal, cytotoxic and targeted therapies exist for both the metastatic and adjuvant treatment of breast cancer. The focus of this work is chemotherapy, trying to increase its effectiveness by targeting cells that are both resistant to present drugs and have the potential to cause spread and recurrence.

1.3 Chemotherapy for breast cancer

1.3.1 Background

In treating breast cancer chemotherapy is given in three distinct settings. Firstly, neoadjuvantly, that is prior to surgery, to decrease tumour size and improve the success of surgery on a primary breast tumour both in terms of clinical and cosmetic outcome. Secondly, adjuvantly (within twelve weeks of surgery) to decrease the risk of tumour recurrence in the future. Lastly, in the metastatic setting, where disease is known to be incurable, chemotherapy plays a role in both improving the quality and quantity of life that a patient may experience (Rampurwala, Rocque, and Burkard 2014).

1.3.2 Development

In the early 1970s, breast cancer oncologists were some of the first to adopt chemotherapy in the treatment of their patients. The combination of cyclophosphamide, methotrexate and 5-fluoruracil (CMF) yielded impressive results with a response rate of 50% and a complete remission rate of 20% in metastatic disease (Canellos et al. 1974).

Adjuvant trials by the mid-1970s had shown a relapse rate of 24% in controls and 7% of those treated with adjuvant CMF (Bonadonna et al. 1976). By 2007, the mortality from all cancer types in the United States had fallen significantly since 1990, with half of this effect being due to the inclusion of chemotherapy in treatment regimens (DeVita and Chu 2008).

1.3.3 Adjuvant and neoadjuvant use

The allocation of chemotherapy to patients in the neoadjuvant and adjuvant settings depends on a number of factors including their tumour stage (that is itself dependent on tumour size, grade and lymph node involvement) as well as age, hormone and Her-2 receptor status of the patient (Cardoso et al. 2012). For patients, hormone or Her-2 receptor positivity not only confers a benefit in terms of survival, but also allows the use of hormone reducing drugs, such as tamoxifen or the aromatase inhibitors, or trastuzumab in the case of Her-2 receptor positive disease. The latter has transformed the care of Her-2 positive patients and, due to the multitude of targeted anti-Her-2 therapies now available, the prognosis of Her-2 positive disease has been transformed over the last decade (Denduluri et al. 2016).

If the disease is considered advanced enough, or the patient's tumour lacks expression of all three receptors, then the use of cytotoxic chemotherapy is likely to be recommended. Even then, chemotherapy sometimes only confers a small long-term survival benefit and its use needs careful consideration and discussion between oncologists and patients. This complexity has led to the development of many different algorithms to try and quantify benefit based on genetic as well as clinical factors, and include Adjuvant online and the Oncotype DX recurrence scores (Gage et al. 2015).

Much of the data used to populate these algorithms comes from the Early Breast Cancer Trialists' Collaborative Group (EBCTCG). The EBCTCG performs a meta-analysis every five years to review the data on adjuvant treatment of breast cancer based on individual patient level data.

In a meta-analysis of trials involving over 9000 patients, the EBCTCG showed the regimes containing high-dose anthrayclines (equivalent to over 240mg/m^2 of doxorubicin) were only marginally superior to the older CMF regimes, reducing the absolute risks of recurrence by 2.6%, breast cancer mortality by 4.1% and overall mortality by 3.9% (Early Breast Cancer Trialists' Collaborative Group (EBCTCG) 2012). This is fairly striking in highlighting the

small progress that has been made since the original discovery of CMF in the 1970s, some forty years ago.

The small benefit of adding the taxane class of chemotherapy agents to an anthraycline-containing regime was also demonstrated. In trials where the treatment and control regime was the same in both arms, (excluding the use of the taxane) the addition of a taxane agent led to an improvement in absolute recurrence-free survival of 4.6%, of breast-cancer specific overall survival of 2.8%, and an overall survival benefit of 3.2%. The benefits of taxane incorporation that were seen were independent of age, nodal status, tumour size, tumour grade, and oestrogen receptor status (Early Breast Cancer Trialists' Collaborative Group (EBCTCG) 2012).

1.3.4 Standard regimes in use in the neo/adjuvant setting

It is important to note that there is not a single-standard regime for breast cancer. Use of regime depends on clinician, patient and institution. However, most clinicians would agree that regimes containing both an anthraycline and cyclophosphamide (AC) as well as a taxane (T) appear to offer the best chance of reducing disease recurrence and improving overall mortality.

These regimes can take many forms: one could be a regime consisting of dose-dense doxorubicin (60 mg/m2) and cyclophosphamide (600 mg/m2 for four cycles) followed by paclitaxel (175 mg/m2 for four cycles) (AC-T) (Sparano et al. 2008). In the United Kingdom, the slightly alternative regimes of FEC (Fluorouracil (500 mg/m2), epirubicin (100 mg/m2), and cyclophosphamide (500 mg/m2) for six cycles administered every three weeks (Brufman et al. 1997) or FEC-T – (FEC every three weeks for three cycles followed by docetaxel (100 mg/m2) for three cycles; FEC for four cycles followed by weekly paclitaxel (100 mg/m2) for eight weeks) are often used (Roché et al. 2006; Martín et al. 2008). In addition the TAC regime (docetaxel 75mg/m2, doxorubicin 50mg/m2 and cyclophosphamide 500mg/m2) given every three weeks is also used. For patients who are unable to tolerate an anthracycline (for example due to pre-existing cardiac

disease), another option includes the TC regime – Docetaxel (75 mg/m2) plus cyclophosphamide (600 mg/m2) for four to six cycles, administered every three weeks (Jones et al. 2006).

The benefits of adding trastuzumab to adjuvant chemotherapy in patients with Her-2 positive disease were confirmed in a 2012 meta-analysis of eight trials of chemotherapy plus trastuzumab versus chemotherapy alone, involving nearly 12,000 patients (Moja et al. 2012). These analyses showed a improvement in disease-free survival of 40% and a reduction in mortality of 36% when combined with chemotherapy. Traditionally, in the United Kingdom, FEC would be given alone for three cycles, followed by a combination of a taxane and trastuzumab (Herceptin®) for three cycles before completing a total of one year of treatment with Herceptin. A table of the common regimes in use the adjuvant and neo-adjuvant setting can be seen in Table 1.1 (Cardoso et al. 2012; Elżbieta Senkus, Cardoso, and Pagani 2014).

Regime Name	Drugs	Frequency	Number of cycles
AC-T	Dox (60 mg/m2) Cyc (600 mg/m2) followed by Pac (175 mg/m2)	Three weekly, or dose dense (AC 2 weekly and paclitaxel weekly)	8 (4 of each)
FEC	5-FU (500 mg/m2), Epi (75 or 100 mg/m2), and Cyc (500 mg/m2)	Three weekly	6
FEC-T	FEC followed by doc (100 mg/m2)	Three weekly	6 (3 of each)
FEC-TH	As above plus trastuzumab for Her-2 receptor positivity (8mg/kg loading dose followed by 6mg/kg maintenance three weekly)	Three weekly	18, 3 of FEC, 3 of TH, 12 of H alone
TAC	DOC (75mg/m2) DOX (50mg/m2) and CYCLO (500mg/m2)	Three weekly	6

Table 1.1- Adjuvant and neoadjuvant regimes in use in the clinic for breast cancer

Key: Dox: Doxorubicin, Cyc: Cyclophosphamide, PAC: Paclitaxel, 5-FU: fluorouracil, Epi: Epirubicin, Doc: Docetaxel

1.3.5 Metastatic disease

The median survival for metastatic disease is between eighteen and twenty four months (Kiely et al. 2011) and for these patients the aim of treatment is to prolong survival and maintain a higher quality of life. Cytotoxic chemotherapy adopts a central role in treatment as all patients will invariably become resistant to both hormone and/or Her-2 targeted treatment (if their tumour type allows for its use). Nevertheless, tumours will either be resistant or acquire resistance to chemotherapy. Typically, unless disease is rapidly progressing,

patients will receive single agent chemotherapy to reduce side effects from treatment. Table 1.2 below lists the classes of chemotherapy commonly in use in the metastatic setting in breast cancer.

	Mechanism	Examples
Alkylating agents	Direct DNA damage	Cyclophosphamide
Antimetabolites	Interfere with DNA and RNA production	5-fluorouracil, gemcitabine, methotrexate
Anti-tumour antibiotics eg.Anthracyclines	Interfere with enzymes involved in DNA replication	Doxorubicin, Epirubicin
Mitotic Inhibitors	Stop mitosis in M phase of cell cycle and can prevent enzymes producing proteins needed for cell reproduction	Taxanes: Paclitaxel & docetaxel Eribulin
Platinum Agents	Inhibition of DNA, RNA and protein synthesis by cross-linking	Cisplatin, carboplatin
Vinka Alkaloids	Disrupts microtubule function	Vinorelbine

Table 1.2 Chemotherapy drugs and classes in use in metastatic breast cancer

1.3.6 Paclitaxel

Paclitaxel is a chemotherapeutic agent from the bark of the Pacific yew tree first discovered by a drug-screening programme from the National Cancer Institute in the 1960s. It has shown activity against many human tumours including head and neck, lung, pancreatic, ovarian and breast cancers (Day et al. 2006). It works by targeting the microtubule network required for cell mitosis and proliferation, ensuring that cells are stuck in G_1 and G_2/M phases (Jordan et al. 1993). Different concentration of paclitaxel can trigger distinct effects on both the microtubule network and intracellular biochemical pathways with low concentration (up to 30nM) leading to altered microtubule dynamics and G_2/M cell cycle arrest with higher concentrations (up to 30µM) causing significant microtubule damage (Tzu-Hao Wang, Wang, and Soong 2000). The main apoptotic mechanisms at higher concentrations are signalling changes in the mitogen-activated protein kinase (MAPK), Raf-1, c-jun NH(2)-terminal kinase (JNK), cyclin dependent kinase (CDK) and caspases (Stone and Chambers 2000). At lower concentrations, paclitaxel works by inducing apoptosis primarily through the extrinsic apoptosis pathway but independently of the Fas, TNFα and TRAIL receptors, but is dependent upon FADD (S.J. Park et al. 2004). Furthermore, the apoptotic process was primarily Caspase 10 dependent but also partially dependent upon Caspase 8 -with inhibitors of the former completely abrogating apoptosis and the later partially (S.J. Park et al. 2004). As discussed in a later section on the role of cFLIP and apoptosis (Chapter 5), these effects mean that the combination of paclitaxel and targeting cFLIP, a molecule involved in abrogating apoptosis through the Caspase 8/10 apoptotic pathway, holds great potential in overcoming resistance to apoptosis seen in breast cancer cells.

1.4 Reasons for treatment failure

Despite the wide array of treatment options available, current treatment strategies are clearly not eradicating all tumour cells and therefore tumours are relapsing. There are many reasons for this: often many patients present with disease that has already metastasised to distant sites within the body and they cannot be removed surgically. Even in patients with localised disease, micro–metastatic disease almost certainly exists, but often lies in a

dormant state for many years after the initial diagnosis and treatment of the cancer. There are no current methods to detect these microscopic deposits.

The major limitation of cancer chemotherapy is drug resistance, whether this is acquired by the tumour after an initial response, or innate. An example of the former is the recurrence of breast cancer after a seemingly good initial response to neoadjuvant chemotherapy, whereas pancreatic cancer is often poorly responsive to any form of chemotherapy, with response rates varying between 10-30% and the most aggressive form of chemotherapy conferring a median survival of only 11.1 months (Seufferlein et al. 2012).

Our understanding of the biology of breast cancer has grown exponentially over the past few decades. It is now apparent that a large component of the therapeutic complexity in treating breast cancer arises not only from the differences that exist in the biology of tumours in different patients (inter-tumour heterogeneity), but also from the biological differences within tumours in the same patient (intra-tumour heterogeneity). The differences between cells within tumours has led to the so-called 'Dandelion hypothesis' - certain cells are more capable of forming tumours and represent the roots of a weed. Failure to eradicate these cells will lead to a cancer returning or a failure to effectively treat it from the beginning of therapy.

1.5   Tumour heterogeneity

1.5.1   Inter-tumour heterogeneity

The treatment of breast cancer patients and prognostication has long been based on the presence or absence of several receptors based on the cell surface of breast cancer cells that are routinely tested for in clinical practice. These include the oestrogen (ER) receptor, progesterone (PR) receptors, and the human epidermal growth factor receptor 2 (Her2). Despite improving survival since the 1970s, it was clear that not all the biological heterogeneity in terms of response to treatment and molecular alterations were accurately accounted for using clinical parameters (such as tumour grade and node status) or cell surface markers.

Insights based on gene expression analyses over the last decade have shone further light on the degree of inter-tumour heterogeneity with the subdivision of breast cancer into four main molecular subtypes - Luminal A, Luminal B, Her-2 enriched and Basal-like, as well as the Normal-Breast like and Claudin-low groups that have also more recently been identified (Table 1.3) (Prat and Perou 2011).

These groups have been shown to have differences in their incidence, survival, and response to treatment, and complements and expands on the information provided by the classical clinical and pathological markers (Sorlie et al. 2001; Parker et al. 2009; Carey et al. 2007; Carey LA et al. 2006; Prat et al. 2010). Patients with basal, Claudin-low or Her-2 enriched cancers tend to respond better to initially to chemotherapy. However, significant differences in relapse free survival after initial diagnosis and treatment, as well as overall survival, were seen in patients from two patient cohorts of around 400 patients with known clinical data who have undergone molecular subtyping (Figure 1.1).   The data clearly show that Luminal A patients have the best overall survival - with while those with a Basal-like, Claudin-low or Her-2 overexpression having the worst overall survival (Prat et al. 2010).

Subtype	ER	PR	Her-2	Other features
Luminal A	+	+	-	Ki67 low
Luminal B	+	+	-/+	Ki67 can be high
Her-2 enriched	-/+	-/+	+	
Basal-like	-	-	-	
Claudin-low	-	-	-	Low expression of claudins, high mesenchymal gene expression such as vimentin
Normal-Breast like	-	-	-	Rare. Strong expression of basal epithelial genes and low expression of luminal epithelial genes.

Table 1.3- Molecular subtypes of breast cancer

Table showing the multiple different molecular subtypes of breast cancer and their distinguishing features. The Claudin-low and Normal-Breast like groups were identified later on as a subset of triple negative breast cancers (lacking expression of oestrogen, progesterone and Her2) (Sorlie et al. 2001; Prat and Perou 2011)
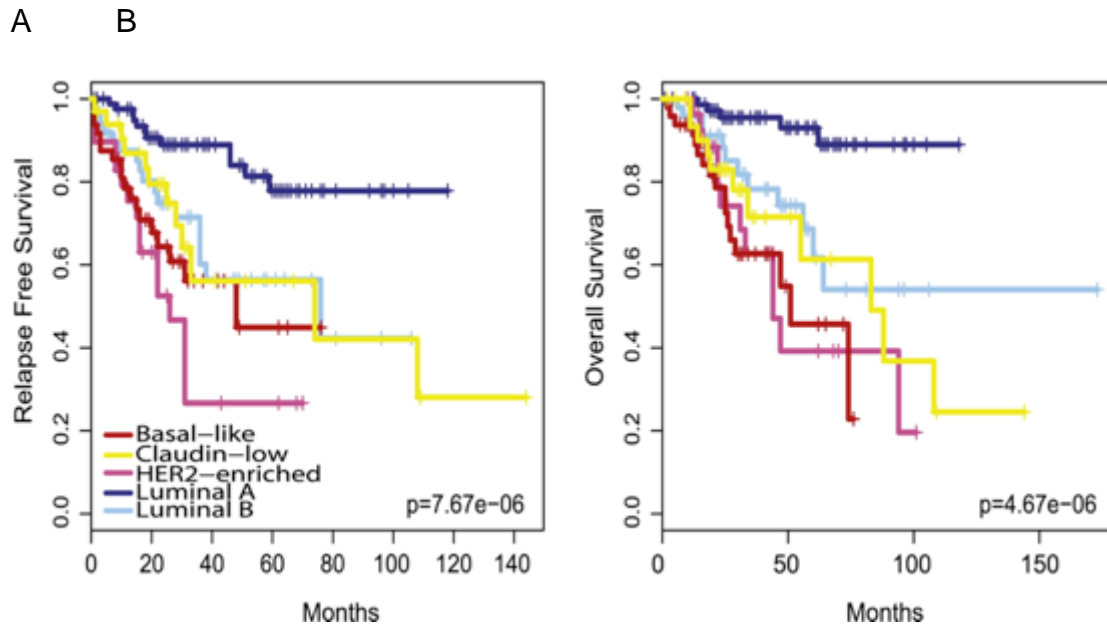
Figure 1.1- Kaplan-Meier Relapse Free Survival and Overall Survival Curves by Molecular Subtype.

Adapted from Prat et al. 2010. Graphs showing significant differences between (A) relapse free survival and (B) overall survival between different molecular subtypes.

1.5.2 ER and Her-2 receptor positive cancer

Luminal A breast cancer is characterised by overexpression of ER and PR receptors but not with Her-2 overexpression, whereas Luminal B tumours are defined by overexpression of ER and PR receptors, but Her-2 overexpression can be present or absent (when absent, it is defined by markers of high cellular proliferation (such as the Ki67)). Her-2 tumours are usually negative for the ER and PR receptors but have overexpression of the Her-2 gene and are usually aggressive.

1.5.3 Triple-negative breast cancer

Triple negative breast cancer (TNBC) accounts for between 15-20% of new diagnoses of breast cancer and is more likely to affect younger patients of African and Hispanic descent (Amirikia et al. 2011; Carey LA et al. 2006). The paradox of TNBC is that, although it has an excellent initial response to chemotherapy, patients with TNBC have a higher risk of both local and distant recurrence (Carey et al. 2007). Most relapses occur within the first three years after diagnosis before declining until 5 years, after which the recurrence

pattern is similar to those with more indolent oestrogen receptor-positive disease (see Figure 1.2). In addition, relapses are more likely to be visceral, that is affecting key body organs such as the brain, liver and lungs, compared to other forms of breast cancer. This correlates with the outcomes amongst this type of breast cancer being worse than others, with a three times increase in risk of death in the 5 years of diagnosis compared to ER and Her-2 positive breast cancers, and a significantly higher recurrence rate (Dent et al. 2007).
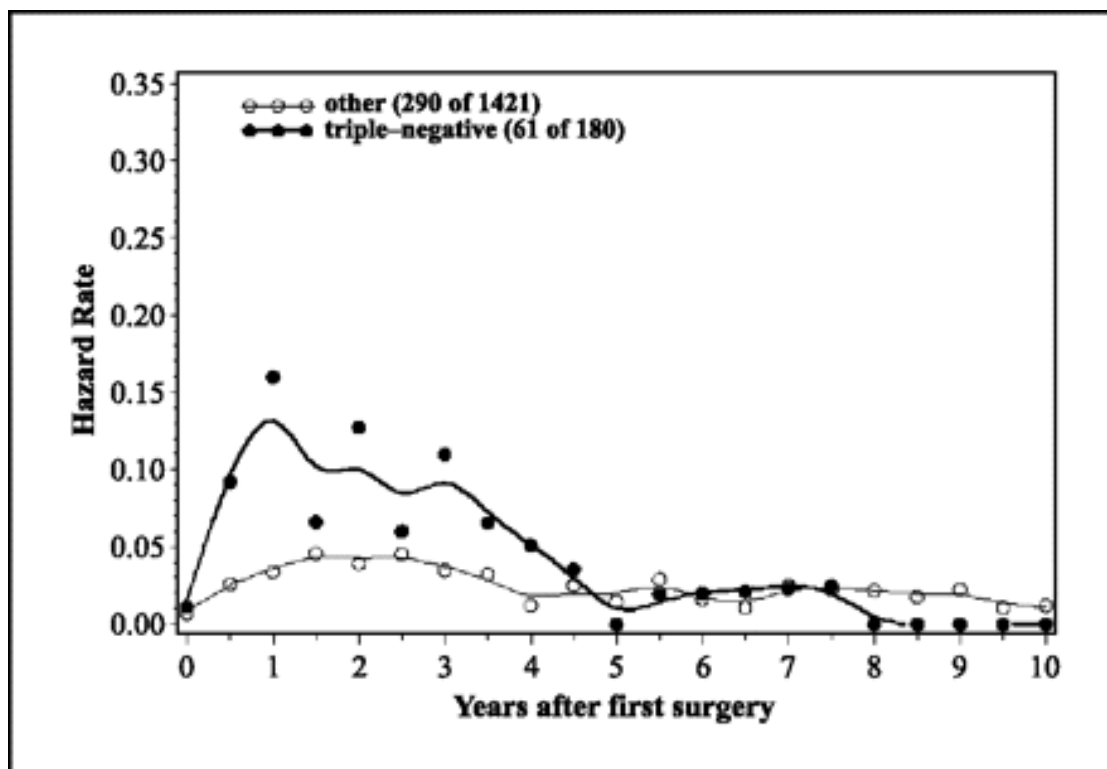
Figure 1.2- Rate of distant recurrence after surgery in triple negative and other breast cancers

Figure showing the higher initial rate of relapse from triple negative breast cancers (TNBC) up until three years. This then declines until reaching the same recurrence rates as oestrogen receptor positive from 5 years onwards. Adapted from (Dent et al. 2007).

1.5.3.1 Subtypes of TNBC

Our understanding of the biology of TNBC has increased over the past five years and we now know that in fact there is a large amount of heterogeneity within this group. Initially described as basal, Claudin-low or normal-like, our understanding of TNBC was transformed in a seminal paper in 2011. Here

Lehmann et al. characterised gene expression profiles from 21 breast cancer data sets and identified 587 TNBC cases. Cluster analysis identified 6 TNBC subtypes: 2 basal-like (BL1 and BL2), immunomodulatory (IM), mesenchymal (M), mesenchymal stem–like (MSL), and a luminal androgen receptor (LAR) subtype (Table 1.4) (Lehmann et al. 2011). These subtypes differed in their prognosis and in their sensitivity to targeted treatments. This understanding has now led to clinical trials stratifying on the basis of molecular subtype, for example with the androgen receptor drug enzalutamide, a therapy initially designed for prostate cancer, for the androgen receptor positive subtype (Moulder-Thompson 2016).

Our increased understanding of the differences between tumours over the last decade has also revealed that there are large differences between cells within a tumour. This intra-tumour heterogeneity has perhaps begun to explain why some molecular subtypes relapse more quickly than others. Interestingly, in TNBC, the focus of this work, it has been shown that tumours contain a higher proportion of cancer stem cells (CSCs) as compared to other molecular subtypes of breast cancer - perhaps explaining its poor prognosis (Habib and O'Shaughnessy 2016). This will now be explored in more detail.

Subtype	Upregulated pathways	Gene expression	Clinical Behaviour	Representative cell lines
Basal-Like 1	Cell cycle and cell division, DNA damage response, cell cycle checkpoint loss	Aurora kinases, Myc, NRAS, ATR/BRCA, Ki67	High pathological complete (pCR) response rate to chemotherapy (60-70%)	HCC1599, MDA-MB-468, HCC 1937
Basal-Like 2	Cell cycle and cell division, DNA damage response, cell cycle checkpoint loss	EGF, NGF, MET, Wnt/β-catenin, and IGF1R	High pathological complete (pCR) response rate to chemotherapy (60-70%)	SUM149, HCC70
Immunomodulatory	Immune cell signalling, cytokine signalling, ore immune signal transduction pathways	TH1/TH2 pathway, Natural Killer cell pathway, B cell receptor signalling pathway, cytokine pathway, and T cell receptor signalling, IL12, IL7 and NFKB, TNF, and JAK/STAT	Favourable prognosis (significant genetic overlap with the high-grade but prognostically favourable medullary breast cancer subtype)	HCC1187, DU4475
Mesenchymal	Cell motility ECM receptor interaction, and cell differentiation	ALK, TGF-β signalling pathway components, ZEB1, ZEB2, TWIST. Decreased E-cadherin	Pathological complete (pCR) response rate to chemotherapy around 30-	BT549, CAL-51

	pathways	and Wnt/β-catenin signaling	40%. Trend towards lower relapse rates
Mesenchymal Stem-Like	Low levels of proliferation genes, increased angiogenesis and immune signalling	ABC1, ALDHA1, HOX genes, EGFR, PDGF, calcium signalling, G-protein coupled receptor, and ERK1/2 signaling. Low expression of claudins 3, 4, and 7	Trend towards lower relapse rates	SUM 159, MDA-MD-436, MDA-MD-231
Luminal Androgen Receptor	Enriched in hormonally regulated pathways including steroid synthesis, porphyrin metabolism, and androgen/estrogen metabolism	Androgen receptor targets and co-activators (DHCR24, ALCAM, FASN, FKBP5, APOD, PIP, SPDEF, and CLDN8)	Poor pathological complete (pCR) response rate to chemotherapy (10-20%). Higher relapse rates	MDA-MB-453, SUM185

Table 1.4- Subtypes of TNBC

The different subtypes of TNBC, their signalling pathways and gene profiling, unique clinical behaviour and representative cell lines. Adapted from Lehmann et al 2011

1.5.4 Intra-tumour heterogeneity

A greater understanding of the heterogeneity of cells within tumours over the last decade has led to previously complex clinical concepts, such as therapy resistance, the ability to metastasise and cell dormancy leading to tumour recurrence, being better understood (Vermeulen et al. 2012; Hanahan and Weinberg 2011).

1.5.4.1 Clonal expansion theory

The changes leading to normal cells forming cancers were long believed to follow the clonal expansion model first proposed in the 1970s (Nowell 1976). In this model, individual cells undergo a mutation that confers an ability to divide more rapidly and outgrow their neighbours - forming a clone of cells. Through repeated acquisition of known critical genetic or epigenetic changes, perhaps half a dozen or more times, cancers form (Cho and Vogelstein 1992).

1.5.4.2 Cancer Stem Cell (CSC) model

The clonal view has been challenged by the emergence of the cancer stem cell model - a theory that a small population of cells either within or outside the tumour are responsible for both tumour growth as well as the spread of the cancer to distant sites (Visvader and Lindeman 2008). This model proposes that there are different populations within a tumour.

The CSC model is not novel. In the 1970s it was recognised that stem cells existed within numerous different cancer types and formed colonies *in vitro* (Hamburger and Salmon 1977). This model proposed that only a certain population within tumours had the ability to self-renew, differentiate and regenerate to form similar tumours. This theory was first proved in acute myeloid leukaemia in the 1990s where cells sorted according to the $CD34^+/CD38^-$ surface markers (representing 1% of total cells) were the only cells capable of leukaemia formation (Lapidot et al. 1994). Similar experiments undertaken in breast cancer, established that $CD44^{high}/CD24^{low}$ cells (representing 2% of the total tumour cells) were able to form tumours in immunocompromised mice, whereas cells without these markers were not (Al-Hajj et al. 2003). Subsequently, similar experiments were undertaken in brain

(S. K. Singh et al. 2004), colon (O'Brien et al. 2007; Ricci-Vitiani et al. 2007) and pancreatic cancer (Hermann et al. 2007).

The CSC theory has not been without controversy as debate has focused on how to integrate CSC theory with the clonal expansion tumour model. The original concept assumed that the progression from CSC to a progenitor-like cell and finally a differentiated cell was rigid and hierarchical. Once formed, the differentiated cells lost clonogenic ability to form new tumours and tumour growth and expansion was driven by the CSCs (Vermeulen et al. 2012). Cancers were formed by progressive mutations within the CSC pool leading to more aggressive cellular phenotypes.

There are however two major issues with this theory. Firstly, the rate of mutation of the pre-neoplastic stem cell population (that would form CSCs) is very low, perhaps as low as one mutation per million cell divisions (Drake et al. 1998). Combined with the generally low numbers of stem cells within a tumour, this makes the chances of mutation improbably low. Secondly, stem cells tend to divide only occasionally, with the clear majority of mitotic activity occurring in differentiated cells. As most mutations occur during DNA replication, this again leads to a conclusion that cancers arising purely as a result of mutated stem cells are unlikely (Scheel and Weinberg 2011). These issues led to a revision of the hierarchical CSC theory, with insights coming from a better understanding of the process that lead to metastases. Such processes include non-genetic determinants of CSC fates, including histone modifications and epithelial to mesenchymal transition – EMT (Kreso and Dick 2014; Mani et al. 2008).

1.5.5 Epithelial to Mesenchymal Transition (EMT)

EMT is increasingly recognised in a vital step in the progression of malignancy, with epithelial cells losing their epithelial characteristics and, via changes in their cytoskeleton, cell structure, morphology and adhesion molecules, acquiring more mesenchymal traits (Britton et al. 2011). Adhesion molecules such as E-cadherin and integrins are substituted for N-cadherin, vimentin and fibronectin that allow the cell to become detached from the

basement membrane and either begin invading into surrounding tissue or separate and spread to distant sites (J. Yang and Weinberg 2008). EMT is characterised by a scattered mesenchymal phenotype, with an increased invasive and metastatic potential of cancerous cells (Ferrand et al. 2014).

EMT has also been shown to bestow non-CSC differentiated epithelial cells with increased 'stemness' properties (Mani et al. 2008; Morel et al. 2008). It has also been shown to be an important programme in normal cell differentiation and tissue repair (Acloque et al. 2009). A number of signalling pathways are known to induce EMT including Notch, hedgehog, Wingless (Wnt), transforming growth factor-B (TGFB) and nuclear factor kappa-light-chain-enhancer of activated B cells (NFkB) (Thiery et al. 2009; Yoo et al. 2011; Takebe, Warren, and Ivy 2011; Shin et al. 2010; Jung and Yang 2015). It has also been show to confer resistance to chemotherapy (Fischer et al. 2015).

The connection between stem cells and EMT applies to both cancerous and non-cancerous cells. Cancerous cells adopt the stem cell programme to organise the complex tissues structures and behaviour that is seen at various stages of the malignant process (Scheel and Weinberg 2011). This EMT-stem cell relationship is troublesome as it confers mesenchymal characteristics on epithelial cells leading to higher degrees of motility, invasiveness and resistance to apoptosis that results in metastatic dissemination (Singh and Settleman 2010). It also confers the capacity of self-renewal that allows large colonies of cancer cells to form both as primary tumours and macroscopic metastases (Brabletz et al. 2005).

EMT also potentially solves the issues listed in the previous section - namely that mutations affecting stem cell populations are likely to be too rare to explain their role in the malignant process. Instead, cells that have already undergone cancerous mutations receive signals and can harness them to dedifferentiate and create new CSCs. It is far more likely that mutations strike a population of transient-amplifying cells that are far larger and mitotically active than the stem cell population. Mutations first gained by this pool of

cells are able to be introduced into the stem cell population via EMT where they can divide and generate progeny that harbour the mutant genotype (Scheel and Weinberg 2011). This is shown in Figure 2 below.
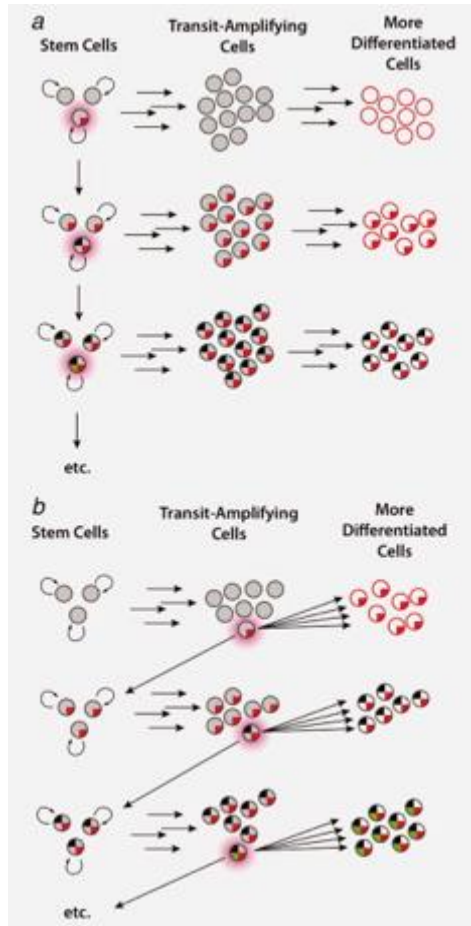
Figure 1.3- Multi-step progression and the CSC model of cancer

A) A hierarchical model. Normal stem cells acquire mutations (depicted as coloured quarters within the circles) and evolve into a mutant stem cell population. Incremental mutations lead eventually to a neoplastic stem cell population. B) Mutations do not strike the stem cells but transient-amplifying cells that are able to de-differentiate (via EMT) into stem cells. This leads to a neoplastic stem cell population. (from Scheel and Weinberg 2011).

1.5.6 EMT to Mesencyhmal Epithelial Transition (MET)

To further complicate the theory that an EMT process confers CSC traits on cancerous cells, it was shown that cells that had undergone EMT were able to invade and enter blood vessels but not form lung metastases in a mouse tumour model (Tsuji et al. 2008). EMT and non-EMT cells were both required for distant metastases to form. This led to the authors concluding that EMT cells invaded to form blood vessels to allow distant spread but that non-EMT cells were required to form these metastases.

This introduces the concept that EMT is potentially a reversible process and that cells can undergo a reverse mesenchymal to epithelial transition (MET) where cells re-express E-cadherin and regain their cellular polarity. Indeed, significant interplay between EMT and MET has been shown with cells that have undergone EMT revering to an epithelial phenotype after a couple of cell divisions (Beerling et al. 2016).

EMT has been the favoured model for explaining distant metastases in epithelial cancers such as breast cancer.   The disruption of intercellular adhesion molecules (such as E-cadherin) and tight junctions leads to cells adopting a fibroblast-like mesenchymal morphology and having increased motility, invasion and resistance to apoptotic stimuli (Scheel and Weinberg 2011). Cells that have undergone EMT also acquire cancer stem cell, tumour initiation and therapy resistant properties (Mani et al. 2008; Hennessy et al. 2009).

However, most of this evidence has come from laboratory work based on cell culture models. In patients, it is very difficult to prove EMT as samples are taken from primary and metastatic sites at different time points and may have undergone MET - thereby losing their mesenchymal features. It is also very difficult to pathologically discriminate fibroblasts from mesenchymal-like cells (Fischer et al. 2015)

1.5.7 Different breast cancer stem cell populations and their characteristics

In addition to breast CSCs (bCSCs) identified by the markers $CD44^{high}$/$CD24^{low}$, it has been demonstrated that cells with high levels of aldehyde dehydrogenase (ALDH) enzyme also possessed tumour initiating characteristics (Ginestier et al. 2007).   Both $CD44^{high}$/$CD24^{low}$ and ALDH markers identified overlapping but not identical populations that were both able to form tumours in immunocompromised mice from primary breast cancer samples.   The cells that expressed all markers were the most tumourogenic of all, with tumours being generated from as few as 20 cells. ALDH status was shown in a cohort of American breast cancer patients to

significantly correlate with overall survival (Ginestier et al. 2007). ALDH has also been shown to be associated with an ER negative, inflammatory and basal forms of breast cancer (Tiezzi et al. 2013; Charafe-Jauffret, Ginestier, Iovino, et al. 2010).

Subsequently, CD44, CD24, and ALDH were demonstrated in CSCs from a wide variety of cancers, including sarcomas, pancreas, colon, lung, ovary, prostate gland and some haematological malignancies (Suling Liu et al. 2013). The key question remained as to whether tumours contain multiple types of CSCs and whether CSC markers identify distinct CSC populations.

Subsequently, the gene expression profiles of the CD44^{high}/CD24^{low} cells showed that they were mesenchymal CSCs (or EMT-like) resembling those of basal stem cells within the normal breast, whereas the profiles of ALDH+ cells were those of the epithelial CSCs (or MET-like), resembling luminal stem cells (Suling Liu et al. 2013). These two stem cell types were shown to be distinct and able to transition between the EMT-like and MET-like states with purified CD44^{high}/CD24^{low} or ALDH+ cells generating heterogeneous populations matching the proportion of CD44^{high}/CD24^{low} or ALDH+ BCSCs present in the original cell line. This interconversion is known as plasticity.

Anatomical differences were also shown to exist between the two stem cell populations, with epithelial ALDH^{+} positive cells being shown to exist in the central hypoxic region of the tumour whilst CD44^{high}/CD24^{low} mesenchymal CSCs were identified at the invasive edge of the tumour (Fig 1.4). Importantly, the gene-expression profiles of the different CSC populations expressed similarity across all molecular subtypes of breast cancer. Also demonstrated was the increased invasiveness of the EMT-like stem cells using the matrigel assay, but also their relative quiescence compared to the proliferative potential (as measured by the Ki67 proliferative marker) of the ALDH+ MET-like cells.
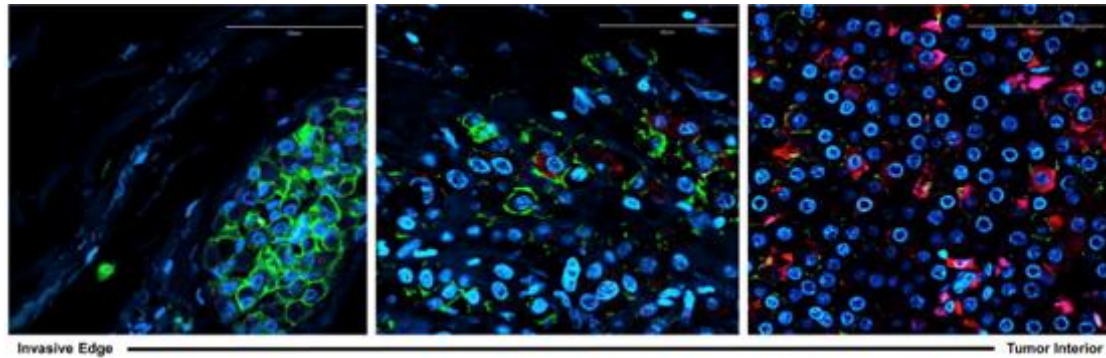
Figure 1.4- Distribution of breast cancer stem cells

Localization of CD24 (magenta), CD44 (green), ALDH1 (red), and DAPI (blue) in clinical samples of human invasive breast carcinoma as assessed by immunofluorescence staining. From Liu et al 2013 (red bar = 100 µm)
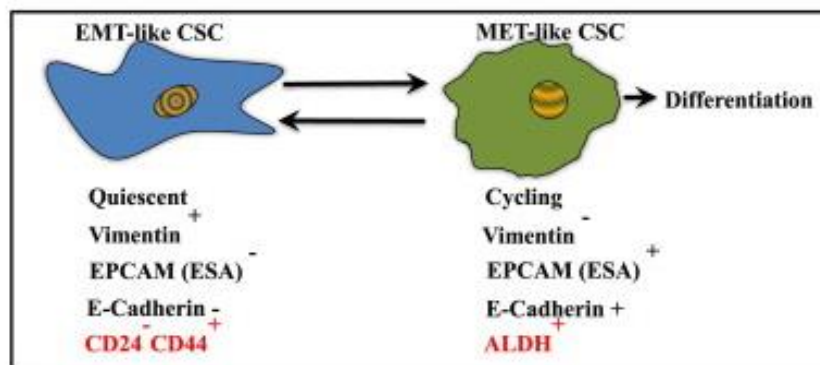
Figure 1.5- The two different CSC populations and their characteristics. From Liu et al 2013

1.6 The effect of chemotherapy on bCSCs

CSCs express high-levels of drug transporter proteins ie ABC. (Gottesman, Fojo, and Bates 2002), DNA repair enzymes (Martin, Hamilton, and Schilder 2008; M. Zhang, Atkinson, and Rosen 2010) and anti-apoptotic proteins (Piggott et al. 2011; Madjd et al. 2009; Zobalova et al. 2008; G. Liu et al. 2006).

It has been shown that cells that have been induced into EMT are resistant to both chemotherapy and radiotherapy (P. B. Gupta et al. 2009) and that these signals are both paracrine (from other cells within the tumours) as well as from stromal tissue surrounding the tumour (Farmer et al. 2009). Furthermore, It is known that cells that have undergone EMT have a slower cell cycle than non-CSC cells and as such they are likely to be damaged less

23

by the cytotoxic agents in use the clinic (Pattabiraman and Weinberg 2014). In addition to this, there are multiple drug-resistance mechanisms that mean that even dividing cells can resist cytotoxic chemotherapy (H. Liu, Lv, and Yang 2015). As such, there is accumulating evidence that although traditional chemotherapy may reduce the 'bulk' of a tumour through targeting the non-CSC population, a residual CSC population remains, that is capable of reforming tumours (Pattabiraman and Weinberg 2014; Kreso and Dick 2014).

Numerous *in vitro*, *in vivo* and clinical studies have demonstrated that chemotherapy can increase the proportion of stem cells remaining within a treated tumour.

1.6.1 Chemotherapy and ALDH[pos] 'epithelial' like bCSCs

Numerous pre-clinical studies have shown a relationship between ALDH and stem-cell like behaviour (Magni et al. 1996; Ginestier et al. 2007; Charafe-Jauffret et al. 2009; Cao et al. 2013a; Samanta et al. 2014; H. Zhang et al. 2015). High expression of ALDH in resected surgical samples is strongly associated with metastases and worse survival (Ginestier et al. 2007; Ohi et al. 2011) . ALDH has been shown to correlate with both response to chemotherapy and overall survival in breast cancer, though the relationship is not always clear cut, with some negative studies (Y. Gong et al. 2014). There is also evidence to suggest that anthracycline-containing regimes (such as epirubicin) target the ALDH population more than taxane-containing regimens (such as paclitaxel or docetaxel), though both increased ALDH staining (Alamgeer et al. 2014). There have been a number of clinical studies showing that ALDH positivity is associated with chemoresistance to both paclitaxel and epirubicin (Tanei et al. 2009), overall survival (C. Gong et al. 2010) and that the upregulation of ALDH after neoadjuvant chemotherapy is associated with worse overall survival (Alamgeer et al. 2014; H. E. Lee et al. 2011; Tiezzi et al. 2013).

The relationship between HIF1α and ALDH positivity is significant and there is good evidence to suggest that a strategy of combining HIF inhibitors alongside cytotoxic chemotherapy may be a valid therapeutic strategy.

Several groups have investigated this approach in preclinical models, Samanta et al being one (described in section 1.5.8.1) and another being Xiang et al who used ganetespib, a second-generation inhibitor of Heat Shock Protein 90 (HSP90), a molecule essential for the stability and function of many molecules including HIF1α. Treatment of both breast cancer cell lines and orthotopic mouse tumours led to reductions in growth, metastases, HIF1α protein levels and HIF1α-mediated gene expression (Xiang, Gilkes, Chaturvedi, et al. 2014). Though as ever, caution should be adopted, with a Phase 3 trial in non-small cell lung cancer combining ganetespib and docetaxel being stopped early due to no difference being noted between the combination and patients receiving docetaxel alone (Ramalingam 2016).

1.6.2 Chemotherapy and CD44^{high}/CD24^{low} 'mesenchymal' bCSCs

The relationship between CD44^{high}/CD24^{low} and clinical parameters such as overall survival and response to chemotherapy are more complex than ALDH with no clear correlation established (Angeloni et al. 2014). Treatment of breast cancer with taxanes has been reported to increase the CD44^{high}/CD24^{low} population (Bhola et al. 2013; C. C. Zhang et al. 2013; P. B. Gupta et al. 2011; X. Li et al. 2008; H. E. Lee et al. 2011) though others have demonstrated a decrease and no relationship with overall survival (Aulmann et al. 2010).

1.7 CSC Signalling

CSC rely on signalling networks to undertake behaviour associated with them such as invasion, metastases and proliferation. In breast cancer, Snail, Slug, Twist and zinc-figure E-box-binding homeobox (ZEB1 and ZEB2) are classified as EMT inducers. They can induce EMT via different cell signalling pathways of which the TGF-β (Transforming Growth Factor β), Wnt (wingless-type MMTV (mouse mammary tumor virus))/β-catenin, and Notch (a family of transmembrane proteins) pathways have been strongly implicated in inducing EMT in epithelial cells (Wu, Sarkissyan, and Vadgama 2016). There has also been considerable interest in Hypoxia Inducible Factors (HIF), that has been shown to induce EMT via ZEB1 (W. Zhang et al. 2015).

1.7.1 HIF1α

The negative impact of hypoxia of the efficacy of both chemotherapy and radiotherapy has been known for a number of decades (Gray et al. 1953; Roizin-Towle and Hall 1978). Intra-tumoural hypoxia is a hallmark of advanced breast cancer, with up to 40% of cancers known to have a hypoxic region, and is associated with an increased risk of developing metastases and treatment resistance (Vaupel, Höckel, and Mayer 2007; Chun, Adusumilli, and Fong 2005). Our understanding of the molecular basis of this phenomenon has advanced in the last twenty years with the characterisation of the HIFs. This set of transcription factors activate the gene transcription of genes that are associated with many features of breast cancer progression such as angiogenesis, invasion and metastasis (G. L. Semenza 2013; Gregg L. Semenza 2013).

Hypoxia-inducible factor-1 (HIF-1) is a transcription factor that plays a central role in development and in adaptation to hypoxia. Hypoxia has been shown to lead to the expression of CSC markers such as CD44, CD49, CD47 nanog and ALDH (Xing et al. 2011; Mathieu et al. 2011; Louie et al. 2010; Velasco-Velázquez et al. 2012; H. Zhang et al. 2015). Recently, the importance of hypoxia inducible factors in generating a CSC-phenotype has been recognized (Gregg L. Semenza 2015).

The hypoxic conditions within tumours leads to a variety of biological responses with the activation of HIF-1 being the major effect (Harris 2002). Although there are multiple subtypes of HIF, HIF1α has been implicated as the most important in breast cancer models. HIF1 is a heterodimer composed of two subunits, the hypoxic response factor HIF1α and the nuclear constitutively expressed HIF1β subunit. In the presence of oxygen, HIF1α is hydroxylated, allowing it to interact with the von Hippel-Lindau protein (pVHL), that enables it to be targeted for degradation by the ubiquitin-proteasome pathway (Huang et al. 1998). Under hypoxic conditions, HIF1α is no longer hydroxylated - resulting in its stabilization and translocation to the nucleus. It then dimerizes with HIF1β and its co-activator p300, forming an active HIF1

transcription factor that binds to a specific Hypoxia Response Element (HRE) target sequence in the promoter region of its target genes
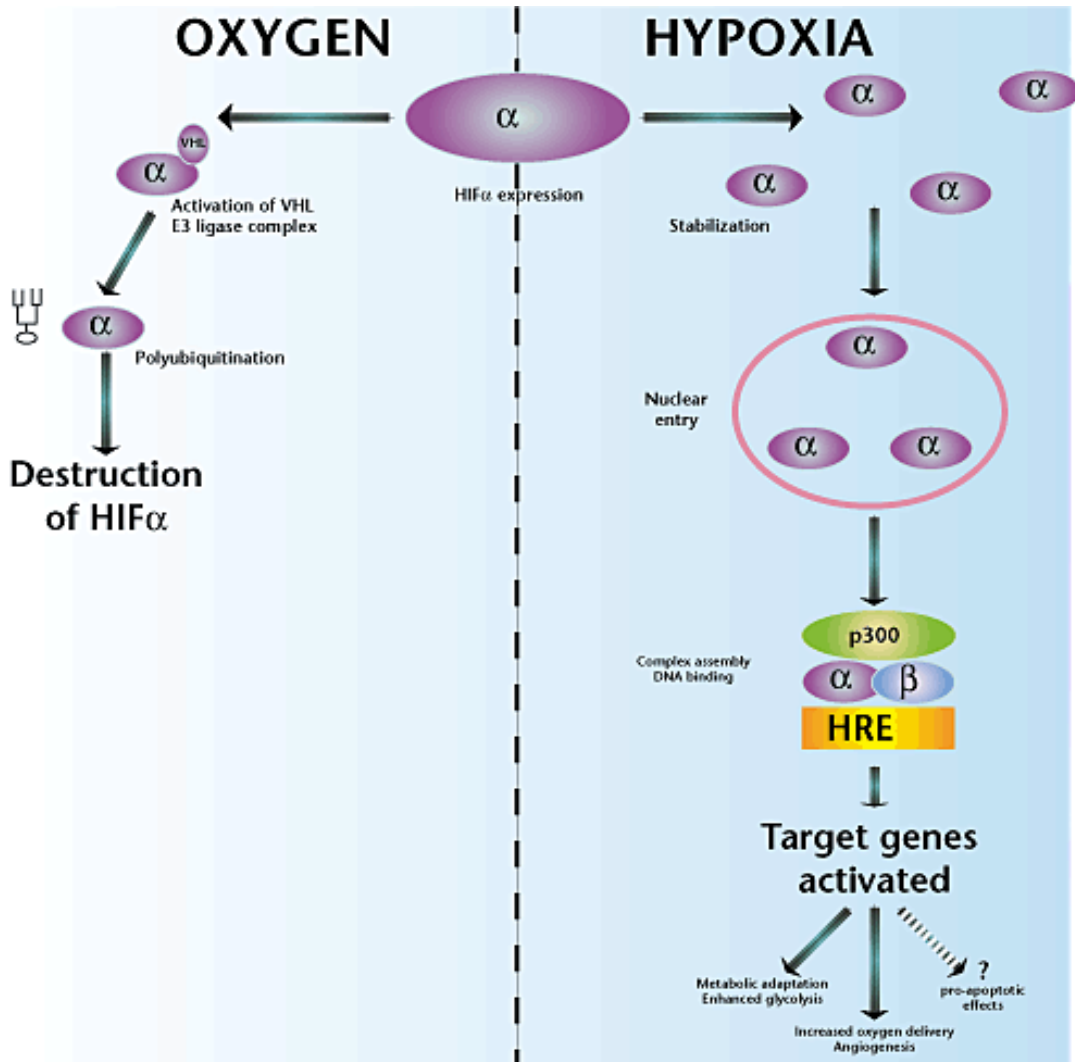
Figure 1.6- Response of HIF1α to normal and hypoxic conditions

From Ratcliffe, Pugh, and Maxwell 2000

Microarray data from more than 500 human breast cancers has shown that genes associated with HIF define the basal molecular subtype, a form of TNBC (Cancer Genome Atlas Network 2012). HIFs contribute to multiple steps in allowing metastatic spread in TNBC and immuno-histological over-expression of HIF1α is associated with increased mortality and overexpression of HIF related genes is also associated with a poor prognosis

in TNBC (Gilkes and Semenza 2013; Gregg L. Semenza 2014; Buffa et al. 2010). The importance of the HIF-related genes is further emphasised by the observation that exposure of TNBC cells to hypoxia leads to an increase in bCSCs in a HIF-dependent manner (Conley et al. 2012; Schwab et al. 2012; Xiang, Gilkes, Hu, et al. 2014). In a recent article, Samanta and colleagues showed that in both the MDA-MB-231 and MCF7 cell lines, exposure to hypoxia for 72 hours increased the mammosphere formation and ALDH positivity of both cell lines (Gregg L. Semenza 2016).

HIF1α has also been shown to confer resistance to chemotherapy (Unruh et al. 2003; Rohwer and Cramer 2011) through multiple mechanisms (see Figure 1.7 below).
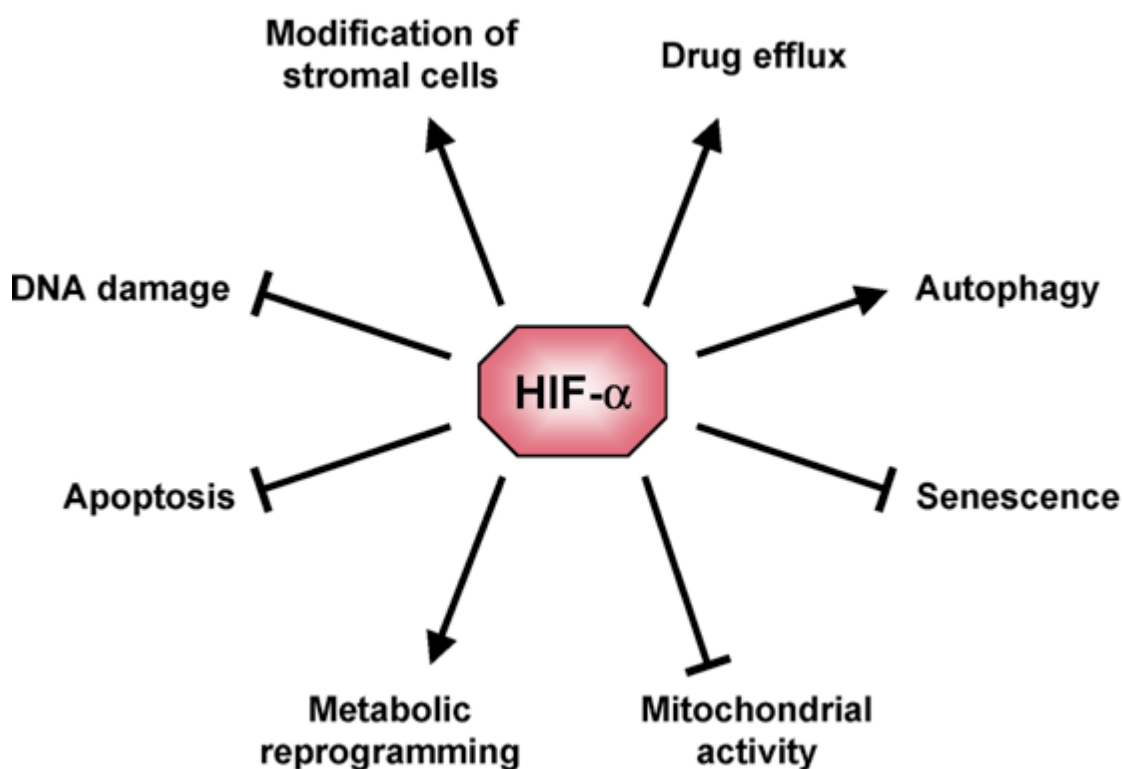
Figure 1.7- Mechanisms through which HIF1α leads to chemotherapy failure

From (Rohwer and Cramer 2011)

Of interest in this thesis is the interaction between HIF1α and apoptotic signalling. Flamant et al showed that HIF1α (as induced by hypoxia) protected against paclitaxel induced apoptosis in the TNBC cell line MDA-MB-

231 (Flamant et al. 2010). Gene expression profiling showed that five pro-apoptotic genes BAK, Caspases 3,8 and 10 and Tumor Necrosis Factor Receptor Superfamily Member 10a (TNFRSF10A, that encodes TRAIL-Receptor 1) were down-regulated when HIF1α was knocked out using siRNA, thus protecting the cells against apoptosis (Flamant et al. 2010).

Treatment of breast cancer cells with a wide-range of compounds that are in use in the clinic such as doxorubicin, paclitaxel and gemcitabine, has been shown to induce HIF1α and enrich for bCSCs (Cao et al. 2013b; Samanta et al. 2014). This was measured by both ALDH activity as well as mammosphere formation and the effect was abrogated by the use of digoxin and acraflavine, two known HIF inhibitors. ALDH has been strongly associated with HIF1α in previous studies both before and after treatment of patients with chemotherapy (Tiezzi et al. 2013). The effect of paclitaxel and gemcitabine was to induce reactive oxygen species (ROS) leading to HIF1α and HIF2α mediated upregulation of Interleukin 6 (IL-6), Interleukin 8 (IL-8) and the known drug protein Multi-Drug Resistance Protein-1 (MDR-1) (Samanta et al. 2014). Both IL-6 and IL-8 have been shown to regulate bCSC survival and self-renewal (Hartman et al. 2013; Sansone et al. 2007; Charafe-Jauffret et al. 2009) and MDR-1 is a well characterised protein that has been shown to be implicated in chemotherapy resistance and is up-regulated in bCSCs (Abdullah and Chow 2013; Pastan and Gottesman 1991).
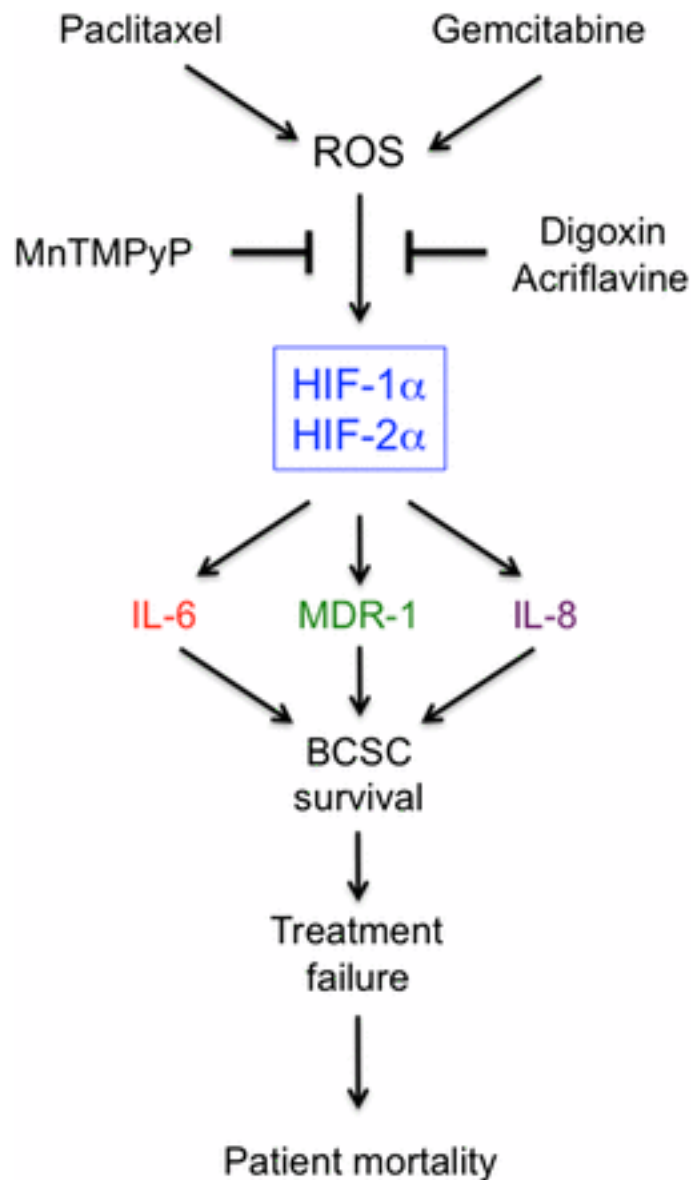
Figure 1.8- Pathway of HIF activation secondary to chemotherapy

From Samanta et al 2014. This shows that the generation of reactive oxygen species (ROS) from chemotherapy leads to the activation of HIF1α and HIF2α and the transcription of IL-6, IL-8 and MDR-1- genes associated with bCSC behaviour.

1.7.2 β catenin and WNT signaling

The Wnt/β-catenin signalling pathway was first described in colon cancer but it its activation has also been described in breast cancer (Prosperi and Goss 2010). This is particularly the case in TNBC where either cytoplasmic or nuclear accumulation of β-catenin is associated with a poor prognosis (Khramtsov et al. 2010; López-Knowles et al. 2010). In the recent identification of six TNBC subtypes, three (basal-like, mesenchymal-like and mesenchymal stem-like) have constitutive activation of the WNT pathway (Lehmann et al. 2011).

The WNT-signalling pathway has been shown to be involved in many malignancies- influencing CSC-behaviour through many mechanisms (Klaus and Birchmeier 2008). These include: increased expression of genes such as *survivin*, a WNT target gene, enhanced telomerase expression (allowing increased self-renewal capacity) and driving EMT through β-catenin signalling (Blum et al. 2009; Hoffmeyer et al. 2012; DiMeo et al. 2009). Over-expression of the WNT-target genes *Slug, Snail* and *Twist* has been shown to be associated with nuclear accumulation of transcriptionally active β-catenin as well as increasing the expression of CSC markers (Mani et al. 2008).

β-catenin is the major effector of the canonical WNT pathway and, upon stabilisation by WNT, translocates to the nucleus where it controls gene expression through its association with members of the T cell factor (TCF) family of transcription factors. Many of these targets have been associated with cell cycle progression and tumour initiation and include Cyclin D1, c-Myc, bmi-1 and Axin 2. Knockdown of β-catenin has been shown to correlate with reduced colony formation, migration in vivo tumour forming capability, as well as increased sensitivity to chemotherapy. In addition, it also decreased expression of ALDH (Jinhua Xu et al. 2015).

However, a small study of paired biopsies in a series of 29 patients receiving neoadjuvant chemotherapy showed no difference between β-catenin pre- and post-chemotherapy using immuno-histological analysis (Rosa et al. 2015).

1.8 Targeting breast cancer stem cells

Since the CSC hypothesis was first-postulated just over a decade ago, there has been considerable interest in novel ways of targeting stem cells. This approach has been varied (See Fig 1.9 below). Strategies include targeting markers associated with CSC behaviour such as CD44 and ALDH (Alamgeer et al. 2014; DeLeo 2012), targeting components of CSC signalling pathways such as Notch, WNT and Hedgehog (Schott et al. 2013) and using de-differentiation therapy to push cells from a non-differentiated to differentiated state with drugs such as vorinostat (Roy et al. 2010). The latter approach is being used to great effect in acute pro-myelocytic leukaemia with the drug all-trans retinoic acid (ATRA). There have also been attempts to target drug efflux pumps, known to be upregulated in CSCs and responsible for cytotoxic drug efflux, as well as metabolic characteristics of CSCs such as HIF1α (Y. Li, Atkinson, and Zhang 2017; Gregg L. Semenza 2016). Another pathway that has attracted much attention is apoptosis, an area to which we now focus our attention
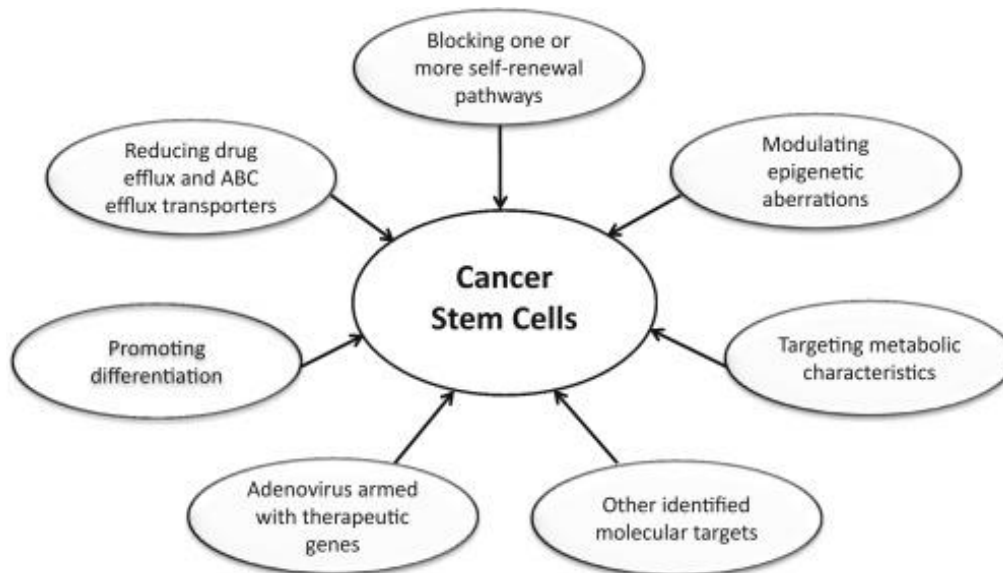
Figure 1.9- Methods of targeting Cancer Stem cells

From (Y. Li, Atkinson, and Zhang 2017)

1.9 Apoptosis and TRAIL as a therapy for breast cancer and CSCs

Apoptosis is a form of programmed cell death utilised in embryogenesis and adult cell homeostasis and has a central role in tissue development and the

immune system. It is of vital importance in a number of diseases including autoimmune disease and cancer, with its inactivation considered one of the hallmarks of cancerous cells (Hanahan and Weinberg 2011). bCSCs have been shown to be resistant to apoptosis and express high-levels of anti-apoptotic proteins (Pattabiraman and Weinberg 2014). There is a clear rationale towards the therapeutic targeting of apoptosis: genetic aberrations should drive cancerous cells towards apoptosis but blocks within these cells prevent this. Targeting these blocks may render cancerous cells susceptible to apoptosis (Avi Ashkenazi, Holland, and Eckhardt 2008).

There are two key routes that lead to apoptosis; the extrinsic and intrinsic pathways. Both pathways share common regulatory proteins called caspases (cysteine aspartic acid specific proteases) that are synthesized as inactive zymogens that are activated upon cleavage as part of signalling cascades. Common to both pathways are 'executioner' caspases that are responsible for cleaving intracellular proteins such as the cellular cytoskeleton and DNA repair proteins (Cryns and Yuan 1998).

1.9.1   The Intrinsic Pathway

The intrinsic apoptosis pathway is activated by intracellular stress such as DNA damage, hypoxia, cell cycle arrest and the loss of pro-survival factors within the cell (Khan, Blanco-Codesido, and Molife 2014; Galluzzi, Kepp, and Kroemer 2012).

A key molecule in detecting cellular damage and instigating the intrinsic pathway is the tumours-suppressor protein p53, the 'guardian of the genome' (Hanahan and Weinberg 2011). Most cytotoxic chemotherapy and radiotherapy activates the intrinsic apoptosis pathway through activation of p53 (Lowe et al. 1994). Unfortunately, as functional inactivation of p53 is one of the most commonly mutated genes in cancer, many tumours are either inherently resistant or acquire resistance to treatment.

The pathway is under tight control of both pro- and anti-apoptotic proteins that are part of the bcl-2 (B Cell Lymphoma-2) family. Central to the intrinsic pathway is the release of cytochrome C into the cytoplasm from the mitochondria that subsequently activates a caspase-activating complex called the apoptosome. The key component of the apoptosome is Apaf-1 that binds and activates pro-caspase 9 leading to the cleavage of effector caspases. This is the point where the intrinsic and extrinsic pathways converge (Hassan et al. 2014).

The anti-apoptotic members of bcl-2 family include Bcl-2 related gene A1 (A1), Bcl-2, Bcl-2-related gene, long isoform (Bcl-XL), Bcl-w, and myeloid cell leukemia 1 (MCL-1) with the pro-apoptotic members being BAD (Bcl-2 antagonist of the cell death), BID (BH3 interacting domain death agonist), BIM (Bcl-2 interacting mediator of the cell death), BMF (Bcl-2 modifying factor), PUMA (p53 up regulated modulator of apoptosis) and Noxa (Khan, Blanco-Codesido, and Molife 2014). In addition to this, there are also inhibitors of apoptosis proteins (IAPs) can also inhibit apoptosis by binding to effector caspases as well as caspase 9. There are 8 members of the IAP family - NAIP, XIAP, cIAP1, cIAP2, ILP2, livin, survivin and BRUCE (Plati, Bucur, and Khosravi-Far 2011).

1.9.2 The extrinsic pathway

The extrinsic apoptosis pathway causes apoptosis through binding of various compounds to trans-membrane death receptors (DRs) on the cell surface. There are functional surface receptors that have an extracellular cysteine rich domain (CRD) and an intracellular death domain (DD) as well as decoy receptors (DcRs) that have the CRD but no intracellular component. Ligands that bind to these receptors include TRAIL (DR4 and DR5), FasL (Fas/APO1/CD95) and TNF (TNF-R1).

Binding of the ligand to the receptor leads to trimerization and clustering of multiple death receptors that is thought to amplify the apoptotic response (Khan, Blanco-Codesido, and Molife 2014). The death effector domain (DED)

of the adaptor protein Fas-associated death domain protein (FADD) recruit the initiator caspases 8 and 10 to the cytoplasmic tail of the receptor to form the death-inducing signaling complex (DISC). This provides the platform for the autocatalytic activation of these initiator caspases allowing them to initiate the proteolytic cascade and activate the effector caspases 3, 6 and 7 allowing apoptosis and cross-talk with the intrinsic apoptosis pathway (Ashkenazi and Dixit 1998).

The extrinsic apoptosis pathway is mainly under negative control at the level of the DISC. Here it has been traditionally thought that Cellular FLICE-Like Inhibitory Protein (cFLIP), antagonizes caspases 8 and 10 by binding FADD via its own DED domains and prevents them forming part of the DISC and becoming activated (Safa 2012). An alternative method of inhibition is the use of the decoy receptors DcR1 (TRAIL-R3) and DcR2 (TRAIL-R4) that lack either an intracellular death domain (DcR1) or have a truncated form (DcR2) that is unable to initiate apoptosis. This results in no apoptosis when these receptors are bound by TRAIL. However, recent work has demonstrated that cFLIP has a complex role in the extrinsic apoptotic pathway. Whilst traditional thinking has been that cFLIP competed with pro-caspase 8 binding to FADD, Hughes et al showed that different mechanisms exist (Hughes et al. 2016). In this paper it was demonstrated that cFLIP binding to the DISC is a co-operative pro-caspase 8 dependent process. Even low levels of cFLIP-S inhibited DED-mediated caspase-8 oligomerization (and apoptosis) preventing the functional alignment of catalytic dimers that lead to apoptosis. The relationship with cFLIP-L was more complex with high levels of cFLIP-L being required to form pro-caspase-8:cFLIP-L heterodimers and prevent apoptosis. Therefore, rather than competing for binding with caspases, cFLIP forms heterodimers with their pro-caspase precursors that prevents their catalytic activity and activation of the apoptotic cascade.
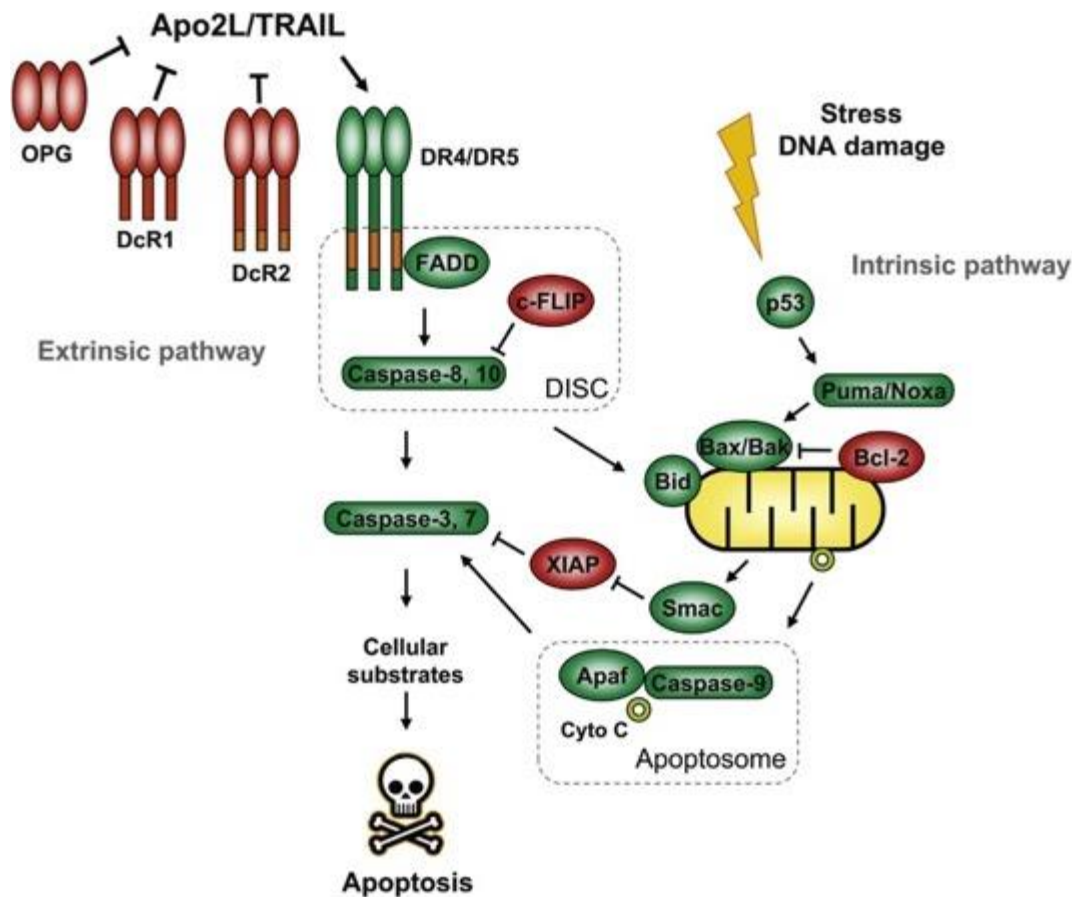
Figure 1.10- Intrinsic and extrinsic apoptosis pathways

Figure showing both the extrinsic and intrinsic apoptosis pathways and their interactions. The inhibitory role of cFLIP as it competes with Caspases 8 and 10 for binding with FADD is also shown (figure taken from Holland 2014).

1.9.3   Targeting apoptosis in breast cancer with TRAIL

Whilst chemotherapy and radiotherapy target proliferation, the targeting of apoptosis has the potential to eliminate cancerous cells entirely - potentially leading to cure (Lemke et al. 2014). Whereas conventional chemotherapy and radiotherapy depends on p53 to induce apoptosis, targeting the extrinsic apoptosis pathway bypasses this often-redundant protein in malignant cells.

Since its discovery in the late 1990s, tumour necrosis factor-related apoptosis-inducing ligand (TRAIL) has shown promising activity against a range of malignancies including leukaemia, multiple myeloma, neuroblastoma, lung, colon, breast, prostate, pancreas, kidney and thyroid carcinoma in *in vitro* models (Kruyt 2008). It also selectively targeted

malignant cells and showed minimal systemic toxicity in mouse models (Walczak et al. 1999). TRAIL works by binding to the external DR4 and DR5 receptors and induces apoptosis via both the extrinsic and intrinsic apoptosis pathways through molecular crosstalk. It also displays minimal cytotoxic activity against normal non-cancerous cells (Rahman et al. 2009). Unfortunately, there does appear to be resistance amongst some tumour types to TRAIL (LeBlanc and Ashkenazi 2003), particularly amongst breast cancer cell lines (Rahman, Pumphrey, and Lipkowitz 2009a) and Phase 1 and Phase 2 clinical trials have been largely disappointing in a wide variety of tumour types (Holland 2014). The phenotypic markers such as triple-negative/basal-like features and mesenchymal gene expression seemed to predict response to TRAIL therapy, whereas epithelial gene expression and oestrogen receptor-positivity (expressed in 70% of breast cancers) predicted resistance (Rahman, Pumphrey, and Lipkowitz 2009b). Despite this, a Phase 2 clinical trial in triple negative, 'mesenchymal-like' breast cancer failed to show any difference in progression-free or overall survival between nab-paclitaxel (a cytotoxic chemotherapy agent) in combination with either tigatuzumab (an anti-DR5 antibody) or placebo (Forero-Torres et al. 2015).

Despite this, there is some evidence that TRAIL targets the CSC component of many breast cancer cell lines (Piggott et al. 2011 and French, unpublished work). There has also been considerable interest in whether breast cancer cells can be sensitised to TRAIL.

1.9.4 Sensitising breast cancer to TRAIL

1.9.4.1 Chemotherapy

A wide variety of classes of cytotoxic agents have been used to sensitise tumours to TRAIL-induced apoptosis including platinums, anthracyclines, taxanes, topoisomerase inhibitors and vinka alkaloids across a broad range of tumour types (El-Zawahry, McKillop, and Voelkel-Johnson 2005; Shankar, Chen, and Srivastava 2005; Shankar, Singh, and Srivastava 2004; Shamimi-Noori et al. 2008; Ray and Almasan 2003).

In breast cancer, it has been demonstrated that a synergistic relationship between chemotherapy and TRA-8 (an antibody to DR5) exists with TRA-8 treatment and doxorubicin or paclitaxel, producing synergistic cytotoxicity against 12/14 or 10/14 basal-like cell lines respectively, as well as some luminal and Her-2 positive lines that were resistant to TRA-8 treatment alone (Oliver et al. 2012). Though, as stated above, clinical trials were a disappointment.

Two studies have examined the effect of combining chemotherapy with TRAIL treatment on CSCs in breast cancer. One study showed promising effects on triple-negative cell lines *in vitro* (as measured by ALDH and mammosphere activity) with a reduction in CSCs from 36% to 24% with docetaxel, 21% with cisplatin, 30% with TRAIL and 1% with cisplatin and TRAIL (Yin et al. 2011). This was mediated via a decrease in Wnt-1 signaling and its downstream targets, β-catenin and cyclin D1 and led to increased apoptosis, reduced proliferation and mammosphere formation. The effects on CSCs of chemotherapy regimes in common use in the clinic, such as the combination of FEC and the drug docetaxel, in combination with TRAIL have not been examined.

Various mechanisms have been proposed to underlie chemotherapy-induced TRAIL sensitization, including increased DISC formation, upregulation of pro-apoptotic (including caspases) and suppression of anti-apoptotic proteins (ie IAPs, cFLIP and bcl2) including of the pro- (ie DR5) and potentially anti-apoptotic TRAIL-Rs (ie DcR1) (Zinonos et al. 2014; Yin, Rishi, and Reddy 2015; X. Liu et al. 2013; Oh et al. 2012; Newsom-Davis, Prieske, and Walczak 2009).

1.9.4.2 Targeted treatments to sensitise to TRAIL

The identification of mechanisms of TRAIL resistance has led to extensive efforts to try and increase the sensitivity of cancerous cells to TRAIL through using targeted blockers against TRAIL-antagonistic pathways. These include inhibitors of XIAP, Src, the Jak-2-Stat3-Mcl1 pathway, Bcl2 and Wee1. Some

have promising pre-clinical results but none have yet made it into clinical trials (S. Park et al. 2014; Garimella et al. 2014; De Luca et al. 2014; Jing Xu et al. 2013; Abdulghani et al. 2013; Kisim et al. 2012; Garimella, Rocca, and Lipkowitz 2012). One key regulatory component of the extrinsic apoptosis pathway down-stream of the death receptors activated by TRAIL is cFLIP.

1.9.5 cFLIP

cFLIP is an anti-apoptotic protein that antagonises the activation of caspases 8 and 10 in the death-receptor signalling pathways. It consists of three forms: cFLIP long (cFLIP-L), cFLIP short (cFLIP-S) and cFLIP-R. All of these can bind to FADD (Fas-associated death domain), caspase-8 or -10 and TRAIL receptor 5 (DR5) in a ligand-dependent and -independent fashion to form an apoptosis inhibitory complex (AIC). All three forms contain two DED domains, DED1 and DED 2, and in addition cFLIP-L contains a large (p20) and small (p12) caspase-like domain with no catalytic activity. cFLIP-S and cFLIP-R lack these domains and instead have a small c-terminus and all forms of cFLIP can be cleaved by Caspase 8 at D376 to form two cleaved products (p43-FLIP and p22-FLIP). All of these variants can act as anti-apoptotic proteins (Safa 2012) (Fig 1.11).
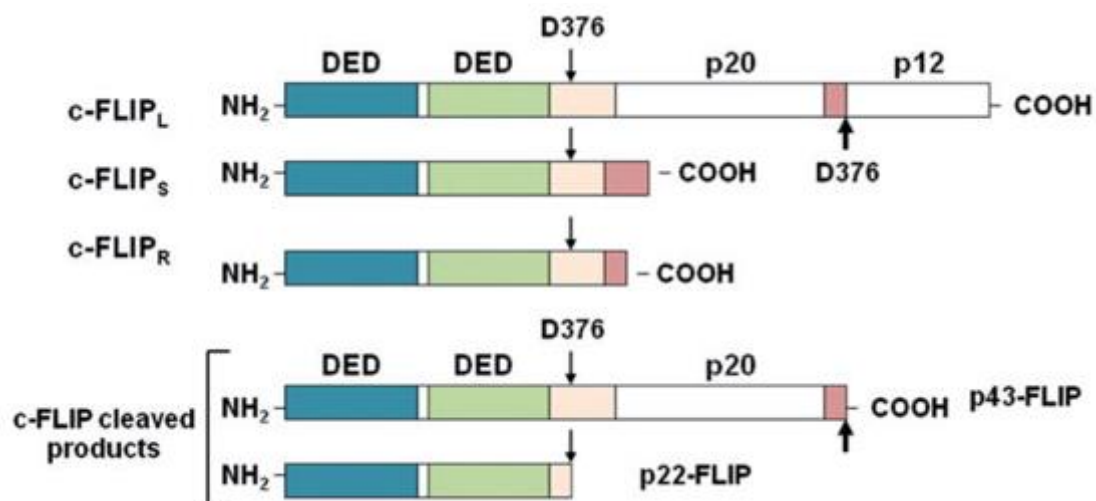
Figure 1.11- Alternative variants of cFLIP

From (Safa 2012)

Interference with cFLIP expression sensitises tumour cells to both TRAIL and chemotherapy (Day, Huang, and Safa 2008a, 2008a; Piggott et al. 2011). cFLIP has been shown to be upregulated in many malignancies and has been correlated with overall survival, though neither of these has been shown in breast cancer (Safa 2012). cFLIP has been shown to be important in chemotherapy mediated apoptosis in colorectal cancer (Longley et al. 2005).

In addition to its anti-apoptotic role, cFLIP has been shown to up regulate both proliferative and survival pathways such as NFkB, ERK, AKT and WNT – the latter being a key component in inducing EMT (Safa 2012, French unpublished work). It has also been shown to have a role in the ubiquitynation of both β catenin and HIF1 (Ishioka et al. 2007)

cFLIP is an exciting target for therapeutic intervention. However, its high homology with pro-caspase 8 makes the design of a cFLIP specific inhibitor, (i.e. one which does not also inhibit the pro-apoptotic caspase-8), highly challenging (Day, Huang, and Safa 2008). Previous studies have focused on chemotherapeutics that down-regulate cFLIP transcription and sensitise to death-receptor triggered apoptosis and include cisplatin and doxorubicin (Longley et al. 2005; Abedini et al. 2008; Song et al. 2003; El-Zawahry, McKillop, and Voelkel-Johnson 2005; Chatterjee et al. 2001). Other agents that have also been found to have an effect on cFLIP on both the transcriptional and translational level are the histone deacetylase inhibitors (HDACi), of which vorinostat is the most promising (Frew et al. 2008; Piggott et al. 2011).

In breast cancer specifically, low dose paclitaxel has been shown to induce apoptosis in a FADD- and cFLIP-dependent manner in the MCF7 cell line. Less than 10nM of paclitaxel, down-regulated cFLIP and led to apoptosis mediated through Caspases 8 and 10 (Day et al. 2006). In the same cell line, siRNA knockdown of cFLIP led to DR5- and FADD-mediated apoptosis (Day, Huang, and Safa 2008a). There is also evidence that overexpression of cFLIP in MCF7 cell lines protects against paclitaxel mediated-apoptosis (Z.

Wang et al. 2005), although this effect was not seen for docetaxel. cFLIP has also been shown to mediate resistance to paclitaxel and carboplatin in ovarian cancer cell lines and hepatocellular carcinoma (Vidot et al. 2010; Chen et al. 2010). A further study from our laboratory, combining TRAIL with a siRNA knockdown of cFLIP, demonstrated that four breast cell lines (MCF7s, MDA-MB-231s, SK-BR3 and BT474) were sensitised to TRAIL-induced apoptosis. Strikingly, this combination seemed to preferentially target the CSCs within these populations (leading to a 80% reduction in primary tumours and a 98% reduction in metastases following transplantation in a mouse xenograft model) (Piggott et al. 2011).

1.10 Linking cFLIP to the degradation of HIF1α and Wnt/β-catenin- the ubiquitin-proteosome system (UPS)

The ubiquitin-proteasome system (UPS) controls the stability of many cellular proteins including HIF1α and Wnt/β-catenin (J. C. Lee and Peter 2003). Under normal conditions, the expression of HIF1α and β-catenin is maintained at a low level in the cytoplasm through degradation by the UPS (Kitagawa et al. 1999; Tanimoto et al. 2000). When either system is stimulated, by hypoxia or WNT signalling respectively, the ubiquitynation is inhibited leading to translocation of these proteins to the nucleus and altered gene transcription (Forsythe et al. 1996; Polakis 2000). It has been reported that protein aggregates within cells can alter the UPS, leading to accumulation of proteins that would normally be degraded. cFLIP-L has been shown to interfere with the degradation of both HIF1α and β-catenin (Naito et al. 2004; Ishioka et al. 2007) by aggregating both with itself and with FADD, a component of the extrinsic apoptosis system. Homotypic interaction between the DEDs of cFLIP leads to filamentous structures called death effector filaments that interfere with the UPS (Tibbetts, Zheng, and Lenardo 2003). It has been demonstrated that mutation of the DEDs on cFLIP-L lead to reversal of the impairment of the UPS and, in a lung cancer cell line, knockdown of cFLIP using shRNA led to a reduction in both HIF1α and β-catenin (Ishioka et al. 2007). The reduction in β-catenin was confirmed in two breast cancer cell lines (MCF7 and MDA-MD-231) using siRNA-mediated knockdown of cFLIP (French et al. 2015). The

effect has also been shown to be medicated through the UPS as well as through cFLIP co-localising with transcription factors within the nucleus to enchance β-catenin dependent gene expression (Naito et al. 2004; French et al. 2015)

1.11 Development of a small molecule inhibitor of cFLIP

Recently our laboratory has identified, through in silico protein modelling, a small-molecule that is able to specifically interfere with the binding pocket on DED1 of cFLIP.   As has been shown recently, DED1 is considered the most important of the two DED domains contained on cFLIP and has a role in both in the inhibition of apoptosis as well as the formation of the filamentous structures that inhibit the UPS (Hughes et al. 2016; Ishioka et al. 2007). Importantly, this small molecule, named OH14, does not interfere with pro-caspases 8 or 10, as such apoptosis can still be induced via formation of the DISC.   Our c-FLIP inhibitor, OH14, has shown synergistic activity in combination with TRAIL on both bulk and stem cells in the TRAIL resistant MCF-7 and BT474 cell lines (Hayward, unpublished work).   One of the aims of this work will be to assess its role in combination with chemotherapy.

1.12 Projects aims and objectives

It has been demonstrated that standard chemotherapy regimes currently in use in breast cancer may differ in their effectiveness in targeting breast CSCs and potentially increase the proportion of CSCs remaining after treatment. One reason for failure may be the resistance to apoptosis displayed by CSCs as well as increased CSC signalling.

Previously we have demonstrated that siRNA-mediated knockdown of cFLIP, in combination with TRAIL, targets CSCs. This subsequently led to the development of a novel compound targeted against the DED1 binding site of cFLIP that prevents activity. In this project, we want to target residual CSCs remaining after chemotherapy using TRAIL, in combination with the c-FLIP inhibitor OH14. This may increase its effectiveness in targeting both the bulk and CSC components of these tumours. This effect could be mediated by increased apoptosis in those cells but also through potentially affecting CSC pathways such as WNT/ β-catenin and HIF1α signalling.

Therefore, the aims of this project are to:
- Employ *in vitro* models through which the effect of regimens in common use in breast cancer clinic on CSCs can be evaluated
- Establish that a combination of the c-FLIP inhibitor OH14 and TRAIL targets CSCs in breast cancer after chemotherapy
- Assess the effect mechanism of any CSC-targeted effect. Potential mechanisms include apoptosis and HIF1α/ β-catenin signalling.

2 Materials and Methods

2.1 Cell lines and cell culture

2.1.1 Experimental Cell Lines

The human breast cancer cell lines MCF-7, HCC1954, MDA-MB-231 and MDA-MB-436 were gifts from other members of the Clarkson laboratory and the cell line SUM 149 was purchased from Asterand Bioscience (Detroit, USA). These cell lines were chosen as they have been well characterised in regards to stem cell assays in regards to ALDH (Bhola et al. 2013; Conley et al. 2012; Charafe-Jauffret et al. 2009) and represent a wide-spectrum of the molecular subtypes of breast cancer. Breast cancer cell lines have been used extensively to investigate the biology of breast cancer as well as to screen and investigate novel therapeutics (Kao et al. 2009). They have yielded a wealth of information concerning the genes and signalling pathways that regulate the malignant process. Cell lines are advantageous in that they are easily propagated, relatively easy to genetically modify, and can yield reproducible results (Vargo-Gogola and Rosen 2007). However, there has been some debate as to how representative of human breast cancers cell lines are. Comparison of the gene-expression profiles of 51 human breast cancer cell lines and primary breast cancers has shown that there is some loss of the variation of genome copy number variations (CNVs) between luminal and basal subtypes of breast cancer when propagated as cell lines-suggesting that the process of establishment and propagation in culture has selected for a certain degree of genomic alteration (Neve et al. 2006). In addition this study also showed that not all the molecular subtypes of breast cancer were represented with no clear distinction between luminal subtypes. These differences can probably be explained by the fact that most of the cell lines were obtained from advanced-stage tumours as well as pleural effusions and therefore may represent the most malignant variants that could be adapted to culture.

2.1.1.1 MCF-7

The MCF-7 cell line is an oestrogen-dependent luminal human breast adenocarcinoma that was isolated from a pleural effusion. It is generally recognised to have poor metastatic properties and expresses receptors to

both oestrogen and progesterone but does not overexpress the Her-2 receptor (Neve et al. 2006).

2.1.1.2 HCC1954

HCC 1954 is a moderately invasive basal invasive ductal adenocarcinoma obtained from a grade three primary breast carcinoma. It lacks receptors to oestrogen, progesterone but overexpresses the Her-2 receptor (Neve et al. 2006).

2.1.1.3 MDA-MB-231

The MDA-MB-231 cell line is a invasive basal B adenocarcinoma obtained from a pleural effusion. It lacks receptors to oestrogen, progesterone and Her-2 receptor and has one mutant p53 allelle (Neve et al. 2006).

2.1.1.4 MDA-MB-436

MDA-MB-436 is a moderately invasive basal invasive ductal carcinoma obtained from a pleural effusion. It lacks receptors to oestrogen, progesterone and Her-2 receptor (Neve et al. 2006).

2.1.1.5 SUM 149

SUM 149 is a highly-aggressive inflammatory ductal carcinoma that is basal in origin and is negative for the oestrogen and progresterone receptors and does not overexpress the Her-2 receptor (Neve et al. 2006).

2.1.2 Maintenance of cell lines

The MCF-7, HCC 1954, MDA-MB-231 and MDA-MB-436 cell lines were cultured in RPMI medium (Invitrogen, Paisley, UK) with 10% fetal bovine serum (FBS; Sigma, Dorset, UK) and 2mM L-glutamine (Invitrogen). Cells were treated with 1% penicillin/streptomycin (Sigma, Dorset, UK). The SUM 149 cell line was cultured in Hams F12 media (Invitrogen, Paisley, UK) supplemented with 5% fetal bovine serum (FBS; Sigma, Dorset, UK), 2mM L-glutamine (Invitrogen), 10mM HEPES (Invitrogen), 1µg/ml Hydrocortisone (Invitrogen) and 5µg/ml insulin (Invitrogen).

Cells were maintained in a sterile, humidified 37°C incubator and CO_2 levels were kept at 5%. All cell lines were routinely cultured in either T25 or T75

tissue culture flasks (Nunc, Leics, UK). When cells reached a confluency of 80-90%, they were passaged on at a split ratio of 1:6- 1:10 at appropriate times (See Table 2.1). Cell passaging was carried out by removing used medium followed by the addition of 0.05% Trypsin/EDTA (Invitrogen, Paisley, UK) to each flask and left to incubate at 37°C for 5-10 minutes. Following this incubation period, cells were checked under the microscope to ensure that all cells had detached and were then diluted with culture medium according to appropriate splitting ratios. All cell lines were not maintained for any more than 30 recorded passages.

Cell line	Molecular subtype	Passaging ratio
MCF7	ER positive	1:8-1:10
HCC 1954	Her2 positive	1:5
SUM149	TNBC, inflammatory	1:6
MDA-MB-231	TNBC	1:8-1:10
MDA-MB-436	TNBC	1:6

Table 2.1 List of cell lines and passaging ratios

2.1.3 Long term storage of cell lines

In order to maintain a low passage number, cells were frozen and cryo-stored in liquid nitrogen. Confluent flasks were detached using 0.05% Trypsin/EDTA (Invitrogen, Paisley, UK), transferred to a 15ml falcon tube (BD Biosciences) and resuspended in at least the equivalent volume of media to 0.05% Trypsin/EDTA. Cell were then spun at 1200rpm for 5 minutes before the pellet was resuspended in freezing medium (10% v/v dimethyl sulfoxide (DMSO, Sigma, Dorset, UK) and 1ml aliquots were placed in 1.5ml cryo-tubes (Nunc, Leics, UK). These tubes were then placed in a container containing isopropanol to facilitate gradual freezing at -80°C overnight. After this, cells were transferred in dry ice to the liquid nitrogen container. For retrieval of cells, cells were quickly defrosted in a 37°C waterbath, resuspended in 10ml of complete media, centrifuged for 5 mins at 1200rpm, the supernatant removed and the pellet resuspended in 7mls of culture medium in a T25 flask.

2.1.4 Cell Seeding

After cell detachment using trypsin, cells were collected in a 15 mL falcon tube.To ensure correct cell seeding densities, cells were counted using Fast Read Slides (Immune Systems,   UK),). Single cells were counted automatically by adding 9 µL of cell suspension to the each well of the counting slides. Cells were then diluted accordingly with culture medium and seeded into appropriate culture plates depending on the assay being performed (Table 2.2).

Plate	Relative Surface Area	Volume (µL)
96-well (Costar)	0.2	100
24-well (Costar)	1	500
12-well (Costar)	2.5	1000
6-well (Costar)	5	2000
60mm dish (Costar)	20	5000

Table 2.2- List of plate formats and normal media volumes

2.2   Viability

2.2.1   Chemotherapy protocol

Cells were plated at different concentrations based on the rate of growth of the cells in culture. On Day 1 50000 cells/ml of the MCF-7, HCC 1954 and MDA-MB-436 cell lines and 25000 cells/ml cells of the SUM 149 and MDA-MB-231 cell lines were plated in 96-well plates and allowed to grow for 24 hours in 90uL of media. At this point an eight-log range of doses of chemotherapy was added (10uL of chemotherapy, leading to a total volume of 100uL) and cells were treated for 72hrs. Viability was assessed using the CellTiter Blue assay.

The chemotherapy agents 5-FU, Epirubicin, Paclitaxel and Docetaxel were produced by Cayman Chemicals and purchased from Cambridge Biosciences, Cambridge, UK. Cyclosphosphamide was purchased in the form of 4-Hydroperoxycyclophosphamide as this is the active metabolite that is formed from the degradation of cyclophosphamide *in vivo* from Niomech,

Bielefield, Germany. Cells were diluted in DMSO for long-term storage with aliquots being thawed and diluted in cell-appropriate media prior to use. DMSO concentration did not exceed 0.1% and controls contained the same amount of DMSO as the maximum concentration that was used in any experiment.

For dose finding experiments, chemotherapy was made near to a maximal concentration that 0.1% DMSO would allow and then diluted in an 8 log-fold fashion by diluting the media containing chemotherapy by 10. This was used to generate an IC50 value that was used for further experiments that was controlled by the addition of the relevant DMSO concentration to control wells.

For combination chemotherapy, the IC50 value of each individual compound was taken and tripled to represent a value of 300% of its individual IC50 value and combined with other compounds again at the same 300% concentration This was then diluted and added to cells to calculate a percentage value of the 100% IC50 concentration. This method ensures that each individual compound remains in a fixed dilution in any given mixture and is a recognized method of testing combinations of drugs (T. C. Chou and Talalay 1984; T.-C. Chou 2006).

2.2.2 OH14 and TRAIL protocol

Cells were plated at the confluencies listed above but different amounts of media was used depending on the plates used and the experiments being undertaken (Table 2.2 and Section 2.2.1)

The cytoxicity of OH14 (produced by Cardiff University) and TRAIL (SuperKillerTRAIL, Enzo Life Sciences) was assessed using a log-range of both with viability being assessed using the CellTiter Blue assay (Section 2.2.3). For experiments combining chemotherapy and TRAIL or OH14, TRAIL was added 72hrs after the addition of chemotherapy with OH14 being added one hour before. OH14 was diluted from DMSO stock solutions at 100mM in cell appropriate media, leading to a concentration of DMSO never exceeding 0.1% with controls containing the same amount of DMSO. TRAIL was diluted

in TRAIL buffer and stored at -80^{0}C before being diluted in media and applied to cells. For some cell lines the IC50 value of TRAIL was calculated, whilst for the MDA-MB-231 cell line 20ng/ml was used as this level has previously been shown by others in our laboratory to lead to the maximal amount of caspase activity (Piggott et al. 2011).

2.2.3 Cell Titer Blue

The CellTiter Blue assay (Promega, Southampton, UK) provides a fluorometric method for the number of viable cells present. This assay measures the metabolic capacity of cells using resazurin as an indicator dye. Viable cells have the ability to convert resazurin into resofurin, a highly fluorescent derivative. Any non-viable cells will lack the metabolic capability to make this conversion and thus fail to produce a fluorescent signal.

Before use, CellTiter Blue reagent was thawed to room temperature. 20µl of CellTiter Blue reagent was added per 100µl of culture media and incubated at 37^{0}C with 5% CO_2 for a minimum of 90 minutes. The resulting fluorescence was then measured by setting excitation/emission wavelengths to 560/590nm on a Fluostar Optima plate reader (BMG Labtech, Bucks, UK).

2.3 Tumoursphere formation assay

The tumoursphere assay is a functional assay designed to isolate the cancer stem cells from cell lines or primary cultures by exploiting their capacity to resist anoikis. Cells are cultured in suspension which induce anoikis in the bulk population but allow the stem cells to remain. These cells continue to self renew and divide and as a result produce small colonies termed tumourspheres. These can be subjected to serial passaging to assay for self-renewal. Quantification of tumourspheres is therefore indicative of stem cell number (Dontu et al. 2003; Shaw et al. 2012). Whilst the formation of primary mammospheres is a measure of both stem cell and early progenitor activity, their harvesting and dissociation into single cells before passaging them again allows for quantification of their self-renewal- a property of CSCs (Shaw et al. 2012). Tumoursphere assays were carried out in non-adherent conditions in

a serum-free epithelial growth medium (MEBM, Lonza), supplemented with B27 (Invitrogen), 20 ng/ml EGF (Sigma), Insulin (Sigma), and hydrocortisone (Sigma) for initial experiments. Further optimisation of the tumoursphere assays used MammoCult Media (Stem Cell Technologies) with the addition of heparin (Stem cell Technologies), hydrocortisone (Sigma) and 1% Penicillin/Streptomycin (Life Technologies). For all tumoursphere experiments after a four day adherent treatment, MammoCult media was used. Cells were plated in ultra-low attachment plates (Costar, Corning) at a density of 5000 cells/ml. After 7 days tumourspheres were counted, then collected by gentle centrifugation (300rcf), dissociated in 0.05% trypsin, 0.25% EDTA (Invitrogen) and re-seeded at 5000 cells/ml for subsequent passages.

2.4   Mathematical model for absolute CSC number

To determine the absolute number of CSCs that were present at the end of treatment in adherent conditions a simple mathematical model was constructed. In this model we determined that a well of untreated cells in a 96 well plate contained approximately 10000 cells and that this equated to a viability of 100% as measured by Cell Titer Blue. For each chemotherapeutic agent we then entered the mean viability of the IC50 value calculated previously assuming a linear relationship between CTB and absolute cell number, a 50% reduction in CTB equates to a 50% reduction in cell number. This viability was then multiplied by the percentage mammosphere formation in Passage 2 for the corresponding treatment condition to give an absolute number of CSCs remaining at the end of the treatment for that condition. This can be calculated by the following equation:

Absolute CSC number= (10000 x viability) x Percentage mammosphere formation in Passage 2

2.5   Colony formation assay

To assess the ability of individual cells to survive, proliferate, and expand into small colonies, the colony formation assay was performed. (Locke et al. 2005) Cells were seeded at low density of 125 cells per/mL in 6-well plate format, in

normal growth medium, and left for 6 days. To quantify colonies, media was removed and cells gently washed with PBS before being stained with crystal violet/ethanol solution for 15 min at room temperature. The crystal violet solution was then removed before cells were washed twice with PBS and if necessary under running water to remove any excess solution. Colonies were then either counted manually or automatically using a GelCount plate reader, and software set to count colonies of sizes between 100-1000 μm.

2.6 siRNA transfection

Short interfering RNA (siRNA) targeting an irrelevant scrambled control, cFLIP and HIF1α were transfected into selected cells (ON-Target plus SMART pool, GE Dharmacon, Bucks, UK. Each siRNA pool was resupended according to the manufacturers protocol in 250 μL of RNA-free water to obtain a 20 μM concentration. Transfection was performed on cell using Lipofectamine RNAiMAX (Invitrogen) and serum-free Opti-MEDM (Invitrogen) according to the manufacturers protocols to give a final concentration of 10nM. Volumes and concentrations of each of the reagents used are listed in Table 2.3. The appropriate volume of siRNA was diluted in Opti-MEM before the appoproate volume of Lipofectamine RNAiMAX was added. This mixture was then vortexed for 15secs and left to incubate for 5 mins at room temperature.

Tissue Culture Vessel	Surface Area (cm^2)	Volume of plating media	Volume of OptiMEM medium	Final SiRNA conc. (nM)	Volume of Lipo-fectamine RNAiMAX
96 well	0.2	100µL	10 µL	20 nM	0.1 µL
6 well	10	2mls	250 µL	20 nM	5 µL
60mm dish	20	4mls	552.5 µL	20 nM	10 µL

Table 2.3- Volumes and concentrations for SiRNA transfections

siRNA	Target Sequence (5'-3')	Catalogue Number
Human control ON-Target plus SMART pool	UGGUUUACAUGUCGACUAA UGGUUUACAUGUUGUGUGA UGGUUUACAUGUUUUCUGA UGGUUUACAUGUUUUCCUA	Dharmacon D-001810-10
Human cFLAR ON-Target plus SMART pool	GUGCCGGGAUGUUGCUAUA CAAGCAGUCUGUUCAAGGA CAUGGUAUAUCCCAGAUUC CCUAGGAAUCUGCCUGAUA	Dharmacon L-003772-00-0005
Human HIF1A ON-Target plus SMART pool	GAACAAAUACAUGGGAUUA AGAAUGAAGUGUACCCUAA GAUGGAAGCACUAGACAAA CAAGUAGCCUCUUUGACAA	Dharmacon L-004018-00-0005

Table 2.4- SiRNA sequences used in this project

2.7 Flow cytometry

2.7.1 Aldefluor assay

The Aldefluor assay (Stemcell Technologies, Grenoble, France) is a method to identify stem cells on the basis of their high aldehyde dehydrogenase (ALDH) activity. A fluorescent aldefluor reagent diffuses into cells and is a substrate for ALDH. The amount of fluorescent ALDH reaction product is directly proportional to the ALDH activity in cells. Cells with high expression of ALDH are recognised by comparing the fluorescence of test cells with that of a control sample containing the specific ALDH inhibitor, diethylaminobenzaldehyde (DEAB).

Aldefluor reagents were prepared according to manufacturer's instructions. Transfected cells were removed from tissue culture plates using 1mM EDTA and centrifuged at 1100rpm for 5 minutes. The cells were washed twice in FACS buffer by resuspension and centrifugation. Cells were suspended in 1ml of aldefluor assay buffer and counted. The samples were adjusted to a concentration of 2×10^5 cells/ml with aldefluor assay buffer. A 'control' and a 'test' tube were prepared for each sample to be tested and 1ml of the cell suspension was placed into each 'test' tube. 5µl of DEAB reagent was added to the control tube and recapped immediately before 5µl of activated aldefluor substrate was added per ml of test suspension in the 'test' tube. The suspension was mixed and 0.5ml was immediately transferred to the 'control' tube containing the DEAB substrate. The 'test' and 'control' tubes were incubated for 45 minutes at 37°C. The tubes were then centrifuged at 1100rpm for 5 minutes, the pellets resuspended in aldefluor buffer and placed on ice. The fluorescence of cells was measured in the green fluorescence channel of a FACS Accuri flow cytometer (BD Biosciences). Analysis was performed using FlowJo software.

2.8 DAPI/Annexin V assay

2.8.1 DAPI Cell Cycle

For analysis of cell cycle progression the nuclear marker DAPI to determine the DNA content of individual cells which was used to determine the cell cycle

stage of cells. On the day of analysis cells were harvested, counted and diluted in PBS to equal cell numbers up to 1 x 10^6 cells/mL. Cells were then pelleted again be centrifugation for 5 min at 1200 rpm before being resuspended in DAPI solution containing 5 µg/mL DAPI (ThermoFisher scientific) in 0.01% IGEPAL CA-630 (Sigma) in PBS and incubated for 5 min at room temperature. Cells were then placed on ice and covered from light until analysed.

To analyse DAPI stained cells, each sample was filtered through a 40 µm cell strainer (BD Biosciences) into a flow cytometry collection tube (BD Biosciences) to form a single cell suspension. Flow cytometry was performed on a BD LSRFortessa flow cytometer (BD Biosciences) and analysed using FlowJo analysis software. Cells were gated by FSC-area/SSC-area and by FSC-area/FSC-height to obtain a single cell population and to remove artefacts and doublets. Single cells were then analysed by histogram plots using DAPI-area to determine the DNA content of cells.

2.8.2 Annexin V apotosis assay

To analyse the levels of early and late apoptotic cells in differentially treated cells the annexin V apoptosis assay (ThermoFisher scientific) was used to detect levels of external phosphatidylserine on apoptotic cells. On the day of analysis cells were harvested, pelleted and washed in cold PBS before being recentrifuged. Washed cells were resuspended in 100 µL of 1X annexin-binding buffer and counted. Cells were then diluted in 1X annexin-binding buffer to 1 x 10^6 cells/mL, with 100 µL of diluted cell suspension used per assay. To 100 µL of cells, 5 µL of FITC annexin V was added and left to incubate for 15 min at room temperature. After the incubation period a further 400 µl of 1X annexin-binding buffer was added along with 5 µL of 5 µg/mL DAPI in PBS, with cells mixed and kept on ice for a minimum of 5 min before analysis. Cells were then analysed by flow cytometry using a BD LSRFortessa flow cytometer (BD Biosciences) and analysed using FlowJo analysis software. Cells were gated by FSC-area/SSC-area and by FSC-area/FSC-height to obtain a single cell population and to remove artefacts and

doublets. Single cells were then gated based on the expression of green-FITC conjugated to annexin V and DAPI expression to determine cells that were either alive, dead, early apoptotic or late apoptotic

2.9 Protein analysis by Western Blotting

2.9.1 Protein extraction from cells

Cell culture plates or dishes were removed from the incubator and placed on ice. Media was completely aspirated from cell culture plates before an appropriate amount of ice-cold PBS was added. Cells were then removed using a cell scraper before being placed into 15ml falcon tubes. Cells were then centrifuged at 1200rpm at 4^0C for 5 minutes and the supernatant removed. Cells were then either stored at -80^0C or immediately lysed by the addition of 100µL of RIPA buffer (150mM sodium chloride (Fisher Scientific), 1% v/v Nonidet-P40 (Roche), 0.5% w/v sodium deoxycholate (Sigma), 0.1% w/v sodium dodecyl sulphate (SDS; Sigma), 50mM Tris (Sigma), pH8) containing 1:100 protease and phosphatase inhibitor cocktail (Cell Signalling Technologies, MA, USA). Lysates were centrifuged at 10,000rpm for 15 minutes at 4^0C to pellet cell debris and the supernatant was aliquoted into fresh tubes for protein quantification.

2.9.2 Determination of protein quantification

Protein concentrations were analysed using the Pierece BCA protein assay kit (ThermoFisher Scientific) according to the manufacturers intstructions. Briefly, protein standards were prepared by diluting 2mg/ml BSA in PBS to produce a range of 7 known protein concentrations (2mg/ml, 1mg/ml, 0.5mg/ml, 0.25mg/ml, 0.125mg/ml, 0.0625mg/ml, and 0mg/ml) and 10µL of these standards or of sample were added to 100µL of solution containing BCA protein assay reagent A and BCA protein assay reagent B in a ratio of 50:1 in a 96 well plate. Samples were mixed and then incubated at 37^0C for 30 minutes before being analysed on a Fluostar Optima plate reader (BMG Labtech, Bucks, UK) at 562nm. The standards were used to generate a standard curve from which the concentration of protein in each sample could be extrapolated.

2.9.3 Western Analysis

2.9.3.1 Preparation of protein samples

After protein concentrations were determined, 25µg of protein were diluted in RIPA buffer to produce a final volume of 8µl. To this, 2 µl of 5X laemmli buffer (0.125M Tris-HCL pH6.8, 4% w/v SDS, 40% v/v glycerol, 0.1% w/v bromophenol blue [Sigma], 6% v/v beta- mercaptoethanol [Sigma] in ddH20) was added to each sample. Just before loading, the samples were heated to 95oC for 5 minutes to denature the proteins.

2.9.3.2 Gels and gel electrophoresis

After denaturing samples were stored on ice before loading into gels. Precast gels were purchased from BioRAD (4–20% Mini-PROTEAN® TGX™ Precast Protein Gels) and placed in the Mini-Protean III (Bio-Rad) electrophoresis tank and immersed in 1 x Tris-Glycine-SDS running buffer (Biorad). Protein molecular weight marker (PageRuler, ThermoFisher) was loaded into the first and last lane of each gel and prepared protein samples were loaded into the appropriate remaining wells. The samples were resolved down gels for approximately 45-60 minutes at 150V until the dye front reached the bottom of the gel.

2.9.3.3 Western transfer to membrane

After electrophoresis, gels were removed carefully from their plastic cassettes using the specific tool (BioRad). They were kept moist by dripping running buffer onto them and excess gel was trimmed. They were then placed into a membrane system purchased from BioRAD in the correct orientation (Trans-Blot® Turbo™PVDF, BioRAD) before being rolled to remove any air bubbles in Trans-Blot® Turbo™ Transfer System (BioRAD) Cassettes. Cassettes were then placed in to the Trans-Blot® Turbo™System and run on a MIXED MW protocol for 7 minutes.

2.9.3.4 Blocking and antibody incubation

Following Western transfer, sandwiches were disassembled and membranes washed 3 x 5 min in PBST (1 x PBS solution (Fisher): 5 tablets 500 ml dH2O with 0.5 ml Tween (Sigma)) before being incubated in blocking buffer (5% w/v non-fat milk powder (Marvel): 0.75 g in 15 ml PBST per transfer membrane) with shaking for 1 h. The membranes were then transferred to 30ml universal tubes (Fisher) containing 2 ml of the desired primary antibody diluted in 5% w/v non-fat milke powder (Marvel) in PBST. Membranes were incubated in the primary antibody solution overnight at 4 ℃ on a roller.

Antibody	Dilution	Supplier	Cat. No	Species	MW
HIF1A	1:500	Novus	NB100-105	Mouse	93kDA
Beta Catenin (mAb)	1:1000	BD Biosciences	610154	Mouse	100 kDA
cFLIP (7F10)	1:1000	Enzo	ALX-8084-961-0100	Mouse	55kDA
GAPDH	1:1000	Santa-Cruz	sc-32233	Mouse	35kDA

Table 2.5- Primary antibodies used in Western Blotting

2.9.3.5 Detection and quantification

Membranes were then washed 3 times for 5 min in PBST and transferred to a 30 ml tube containing 2 ml of the appropriate mouse horseradish peroxidise-conjugated secondary antibody (Dako) diluted 1:2000 in 5% BSA in PBST. Membranes were incubated in secondary antibody at room temperature for 1 h on a roller. Finally, membranes were washed 3 times for 5 min in PBST. Antibody binding was detected using ECL prime detection reagent (Amersham) before being developed in a Biorad Chemidoc MP Imaging System. Diigital images were then quantitatfed by densitometry using the program Image J (http://imagej.nih.gov/ij/).

2.10 RNA Analysis

Prior to working with RNA all equipment and work surfaces were cleaned using RNAseZAP (Ambion) to prevent contamination from RNAses.

2.10.1 RNA extraction

Cultured cells were pelleted via centrifuge at 1200 rpm for 5 min before being resuspended in 350 µL RLT buffer (Qiagen) and placed on ice for immediate extraction or frozen at -80°C for future extraction. RNA extraction was performed using the Qiagen RNEasy kit following the manufacturer's instructions. The concentration and quality of RNA was analysed using a nanodrop 3000 spectrophotometer (Thermo Scientific).

2.10.2 cDNA synthesis

Previously isolated RNA was synthesized into cDNA using the QuantiTect Reverse Transcription kit (Qiagen). Frozen template RNA was thawed on ice along with gDNA Wipeout buffer, Quantiscript Reverse Transcriptase, Quantiscript RT buffer and RT Primer mix. 1 µg of RNA was diluted in 2 µL of gDNA Wipeout buffer and RNase-free water to a total volume of 14 µL and incubated for 2 min at 42°C before being placed immediately on ice. A master mix (Table 2.5) was then added to each reaction and incubated for 30 min at 42oC followed by 3 min at 95°C to inactivate the reverse transcriptase. The cDNA product was then either used immediately or stored at -20°C for future use.

Component	Volume per 1 µg reaction
Quantiscript Reverse Transcriptase	1 µL
Quantiscript RT Buffer, 5x	4µL
RT Primer Mix	1 µL

Table 2.6- ctDNA synthesis reagents and volumes

2.10.3 Quantitive-real time-polymerase chain reaction (qRT-PCR)

2.10.3.1 Primer selection

All primers were selected and bought from ThermoFischer Scientific using their inventoried TaqMan gene expression assay search tool and were selected to target human sequences (Table 2.6). Each primer was designed to carry a FAM-reporter dye with the exception of ACTB controls which were designed to carry a VIC-reporter dye so multiplex PCR reactions could be performed.

Target Name	Assay ID
HIF1A	Hs00153153_m1
IL6	Hs00985639_m1
IL8	Hs00174103_m1
ABCB1(MDR1)	Hs00184500_m1
SNAI1 (Snail)	Hs00195591_m1
ACTB	Hs99999903_m1

Table 2.7- Taq man probes used for gene expression analysis

2.10.3.2 qRT-PCR reaction

All qRT-PCR experiments were designed to include both target gene probes as well as an ACTB control probe, which was selected as expression levels should remain constant across cell lines and therefore can be used to normalize target amplification to the amount of cDNA present in each sample. No template controls were also run alongside where cDNA was replaced with dH2O to control for the presence of contaminating DNA.

For each experiment TaqMan Universal Master Mix II, with UNG (ThermoFischer Scientific) was used, which includes: AmpliTaq gold DNA polymerase, dNTPs (with dUTP), ROX passive reference dye, Uracil-N glycosylase (UNG) and optimized buffer components. TaqMan master mix was added to target and ACTB control probes as well as RNase free H2O to make individual target master mixes containing all reaction components, with the exception of cDNA, which was then added to either 96-well or 384-well

qPCR plates (Applied Biosystems) (Table 2.7). Either 18 µL or 8 µL of master mix was added to 96 or 384-well plates respectively before the appropriate amount of cDNA was added to each well.

qRT-PCR Component	Volume added per well for 96-well	Volume added per well for 384-well
Target primer/FAM-probe (20x)	1 µl	0.5 µL
ACTB primer/VIC-probe (20x)	1 µl	0.5 µL
TaqMan master mix (2x)	10 µl	5 µL
RNase free-H2O	6 µl	3 µL
cDNA	2 µl	1 µL
Total Volume	20 µL	10 µL

Table 2.8 - qRT-PCR master mix components

Once each component had been added, plates were sealed with Micro AMP optical adhesive films (Applied Biosystems) before being shaken for 30 sec and centrifuged for 1 min at 1200 rpm at 4ºC. Plates were then run on a QuantStudio 7 Real-Time PCR machine (Applied Biosystems) set to the following protocol: initial denaturation at 95ºC for 10 min, followed by 40 cycles of 95ºC for 15 sec (denaturation), and 60ºC for 1 min (annealing/elongation).

2.10.3.3 qRT-PCR data analysis

Data was analysed in the automated Thermo cloud software (ThermoScientific) using relative quantification whereby samples are quantified to a reference sample. First, target Ct values were subtracted from ACTB control Ct values for individual wells to create a ΔCt value, which was then averaged from triplicated wells for each sample. A relative value for the difference in transcript levels between samples was then calculated as a difference of ΔCt between samples and a reference sample resulting in the ΔΔCt value. This value was the calculated as 2-ΔΔCt to give the relative fold

change which was then transformed on a log10 scale. Statistical analysis was then performed by assessing the overlap between 95% confidence intervals as described in (Cumming, Fidler, and Vaux 2007)

2.11 Caspase Inhibition

For expimerents involving Caspase Inhibtiion, the pan-caspase inhibitor Z-VAD-FMK was purchased from R & D Systems (Abingdon, UK) (Product Number FMK001). Product was made up in DMSO and stored at -20^0C. This was diluted 1:100 in cell culture plates and added onto cells one hour before the addition of the compound that we were attempting to block apoptosis in. This gave a final concentration of 20ng/ml.

2.12 Animal experiments

2.12.1 Licensing

All procedures involving the use of animals were carried out according to institutional guidelines in accordance with UK Home Office Regulations (Animals (Scientific Procedures) Act 1986) under UK HO licence 3003433.

2.12.2 Animals

For immune-compromised animal transplantation experiments, NOD/SCID/Balbc mice were obtained from Charles River Laboratories (Wilmington, US) or Athymic Nude (Hsd:Athymic Nude-Foxn1nu) mice were obtained from Harlan Laboratories (Indianapolis, US). Animals were acquired at six to eight weeks of age and maintained in individually ventilated cages (Allentown Inc. NJ, US) with a 12hr day/night cycle. Mice received a Teklad global 19% protein extruded rodent diet (Harlan Laboratories) and water *ad libitum*. All food, drink, saw dust and water bottles were sterilised by autoclaving prior to use. All procedures and animal husbandry was performed within a laminar flow hood (Allentown).

2.12.3 Experimental procedures involving animals

2.12.3.1 Subcutaneous xenograft tumour models

Prior to transplantation, cells were either treated under the conditions of interest (for serial dilution experiments) or grown to 70-80% confluency before

being detached with trypsin and agitated to form a single cell suspension. Cells were washed in 5mls RPMI media containing no additives (Invotrogen, Paisley, UK) and spun at 1200rpm for 5 minutes three times before being prepared at the concentrations required in a mix of 50% RPMI with no additives and 50% Matrigel (ThermoFisher) that had been thawed overnight at 4^0C and kept on ice until transplantation. For MDA-MB-231 and PDX 151 cell transplants, Athymic nude mice and NOD/SCID/Balbc mice were used respectively. Cells were injected into the mammary fat pads bilaterally on the dorsum of mouse and allowed to grow.

2.12.3.2 *In vivo* treatment of mice

For some experiments mice were treated *in vivo* with paclitaxel and either OH14 or DMSO control. Paclitaxel was obtained from our local oncology until (Velindre Cancer Centre, Cardiff, UK) at a maximum age of constitution of 48 hours prior to injection. For our protocol Paclitaxel was injected twice a week (Tuesdays and Fridays) for a total of seven injections at a concentration of 20mg/kg intraperitoneally (IP). Mice were also treated with OH14 at a concentration of 20mg/kg IP, prepared by diluting powdered compound in DMSO) and being treated five days per week finishing with the last dose of paclitaxel. The DMSO was controlled for by using the same concentration of DMSO injected into mice at the same time as OH14.

2.12.3.3 Tumour monitoring and measurements

Mice were inspected at least twice weekly for tumours via palpation and measurements were taken with digital calipers (Fisher Scientific, Loughborough, UK). The size of tumours was calculated as volume in mm^3 using the widely used formula: Volume= (Length x(Width^2))/2 (Jensen et al. 2008).

2.13 Statistical analysis

Error bars on all graphs represent standard error values with the exception of gene expression data which are represented by 95% confidence intervals.

An unpaired student's T-test was used to determine statistical differences between normally distributed data sets and between data sets with sample sizes of n=3 unless stated, which was performed using Graphpad prism.

For calculation of IC50 values, non-linear regression was used with a standard Hill Slope (=-1.0) using GraphPad Prism.

For calculation of significance in RT-PCR experiments, significance was determined by calculating overlap of error bars as described in (Cumming, Fidler, and Vaux 2007).

3 Investigating the Viability and Stem Cell-like Activity of Breast Cancer Cells in Response to Chemotherapy

3.1 Introduction

Our increasing understanding of the heterogeneity of breast cancer has led to advances in targeted therapy that have improved the outcome of those with certain subtypes of breast cancer, for example those with oestrogen receptor positive disease (Elżbieta Senkus, Cardoso, and Pagani 2014; Turner et al. 2016). Despite these advances the prognosis for patients with metastatic disease can be as low as a few months, particularly for those with TNBC for whom no targeted agents exist (Cardoso et al. 2012).

Breast cancer stem cells (bCSCs) have been implicated in both inherent and acquired resistance to chemotherapy since their existence was first proposed over a decade ago. bCSCs have been implicated in breast cancer recurrence as well as resistance to chemotherapy and, naturally, there has been significant interest in exploring how chemotherapy impacts on bCSC populations (Liu, Lv, and Yang 2015).

Cytotoxic chemotherapy has been one of the main components of breast cancer treatment since the 1970s but its use is associated with both significant side effects as well as an incomplete response. This is manifest as either a failure of tumours to shrink with chemotherapy in the neo-adjuvant or metastatic setting or a recurrence of disease- often many years later.

Previous studies have shown that chemotherapeutics in use in the breast cancer clinic, including FEC, paclitaxel and docetaxel, increase CSC-like activity (eg. tumoursphere-forming capability) of treated breast cancers from patients *ex vivo* (Samanta et al. 2014; Li et al. 2008). There are also data showing an increase in the proportion of cells expressing markers associated with bCSC behaviour after chemotherapy in vivo, such as ALDH1 enzyme and the cell surface markers CD44 and CD24 (Alamgeer et al. 2014). ALDH1 expression has been shown to correlate with lymph node metastases and early recurrence in ER-positive/Her2 negative breast cancer receiving either adjuvant endocrine therapy or chemotherapy (Miyoshi et al. 2016).

The purpose of this chapter was to establish an *in vitro* cell line based model through which the effect of a wide-range of chemotherapeutic agents in use in the clinic on bCSCs could be evaluated in more detail at the molecular level.

3.2 Results

3.1.1 Establishing the susceptibilities of a range of cell lines to chemotherapy

Before assays examining the effect of chemotherapy on bCSCs could be undertaken a range of cell lines representing the broad molecular subtypes of breast cancer were tested for their overall susceptibility to different chemotherapy agents. The cell lines tested were MCF-7 (Luminal A, ER positive, Her-2 negative), HCC 1954 (Basal, ER positive, Her-2 negative) and SUM 149 (Basal, ER negative, Her-2 negative) (Neve et al. 2006). These cell lines also have the advantage of being able to form mammospheres and have had their stem cell populations well characterised (Suling Liu et al. 2013).

These cells were then subjected to a range of doses of 5- Fluorouracil (F), Epirubicin (E), Cyclophosphamide (C), the combination FEC and docetaxel (D) in order to establish the concentration needed to inhibit half of the maximum biological response of the individual drugs (IC50). The regime of FEC or D is one that is widely used in the clinic within the UK and is a recognised first-line adjuvant and neo-adjuvant regime for breast cancer regardless of molecular subtype (Early Breast Cancer Trialists' Collaborative Group (EBCTCG) 2012). It is also a combination whose effects have not been tested on bCSCs *in vitro*, though some have examined it in combination with other compounds with respect to bulk cell viability and on *ex vivo* samples (Konecny et al. 2001; Ari et al. 2011).
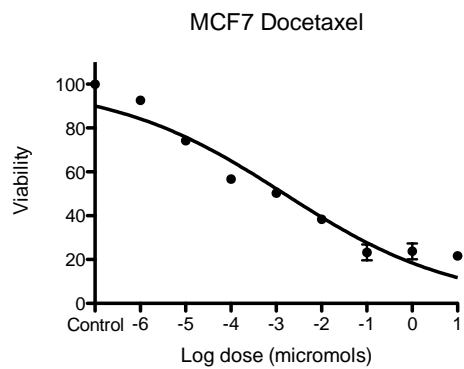
Though others have looked at susceptibility of cell lines to chemotherapy, the use of different cell densities, treatment times and assays mean that IC50 values derived from the literature vary substantially. A standardised approach to screening drug sensitivities is one of plating at around 15-20% confluency, allowing cells to seed overnight and then treating for 72 hours before

performing a viability assay (W. Yang et al. 2013). This correlated to a plating density of 50000 cells/ml for the MCF7 and HCC1954 cell lines and a density of 25000 cells/ml for the faster proliferating SUM149 cell line. This ensures that the cells remain pre-confluent, in a logarithmic growth phase, for the majority of the extended treatment period.

Therefore, an 8-fold log dose range of chemotherapy doses was used to establish IC50 values for all four drugs against all three cell lines (Fig 3.1). The IC50 value for the combination of FEC chemotherapy was performed according to the Chou-Talay method (T. C. Chou and Talalay 1984), where each drug remains in fixed amount of any mixed solution. In this experiment, drugs were tested in combination in a range starting at twice their individual IC50 values. This was presented as a percentage of the individual IC50 values.(Fig 3.2).

The IC50 values obtained highlighted the fact that different cell lines have vastly different susceptibilities to different chemotherapy agents and justified the decision not to use a standard concentration across all cell lines. For example, the IC50 value of the MCF7 cell line for epirubicin was twenty-two times that of the SUM149 cell line (220nm and 10.6nM respectively). These IC50 values were used to perform further experiments on assessing the effect of chemotherapy on CSC formation in breast cancer cell lines for the remainder   of   this   work.

A

MCF7 5-FU

MCF7 Epirubicin

MCF7 4-HC

MCF7 Docetaxel

B

HCC 1954 5-FU

HCC 1954 Epirubicin

HCC 1954 4-HC

HCC 1954 Docetaxel
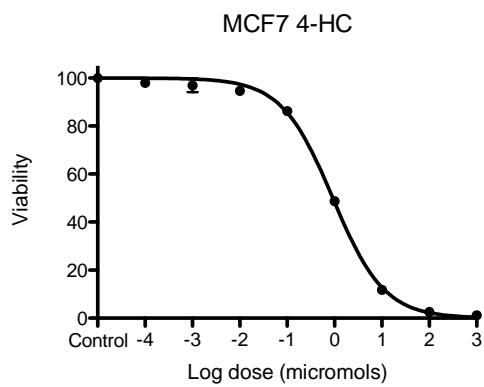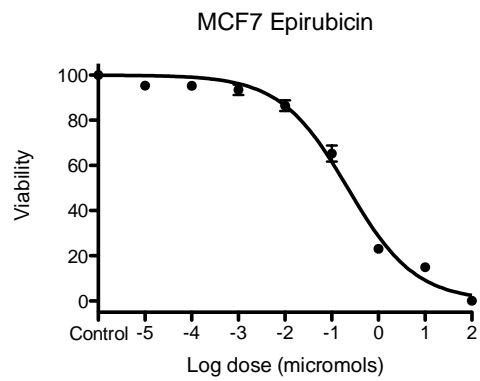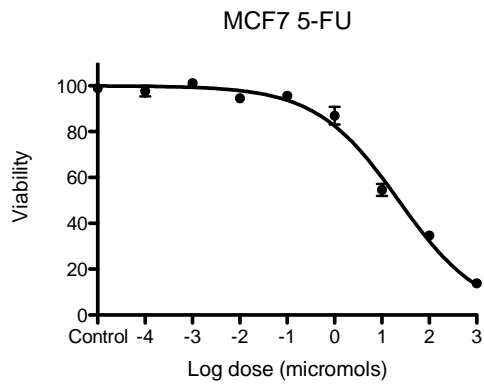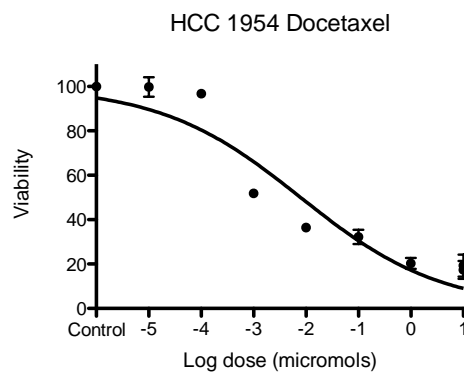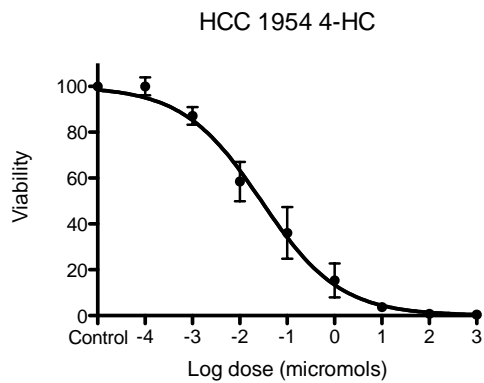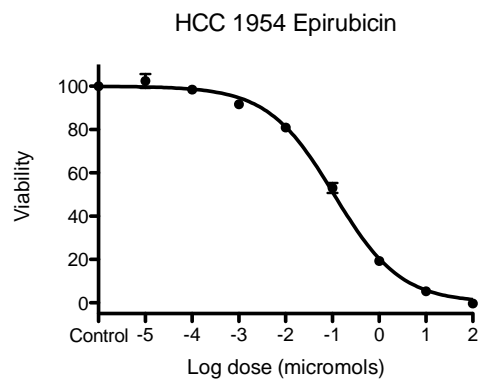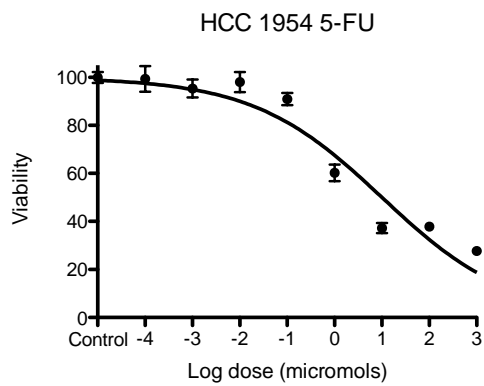
C
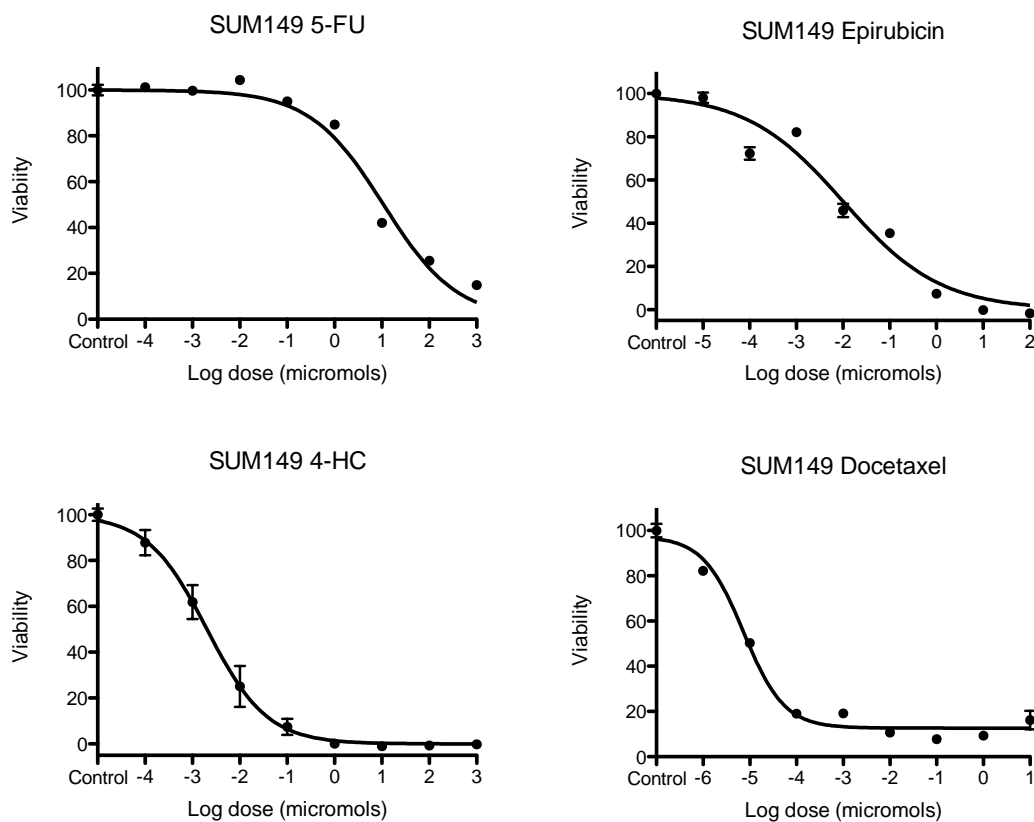
Figure 3.1- Three-day dose-response curves of MCF7, HCC 1954 and SUM149 cell lines to individual chemotherapy drugs

A MCF7 **B** HCC 1954 and **C** SUM 149 cells were plated in 96 well plates and allowed to adhere overnight. Reducing doses of chemotherapy drugs were added as indicated and at 72 hours cell viability was assessed using cell titer blue. All results are averages of a minimum of three independent experiments each performed with three internal technical replicates. Error bars represent Standard Error of the Mean (SEM).

A   B

C
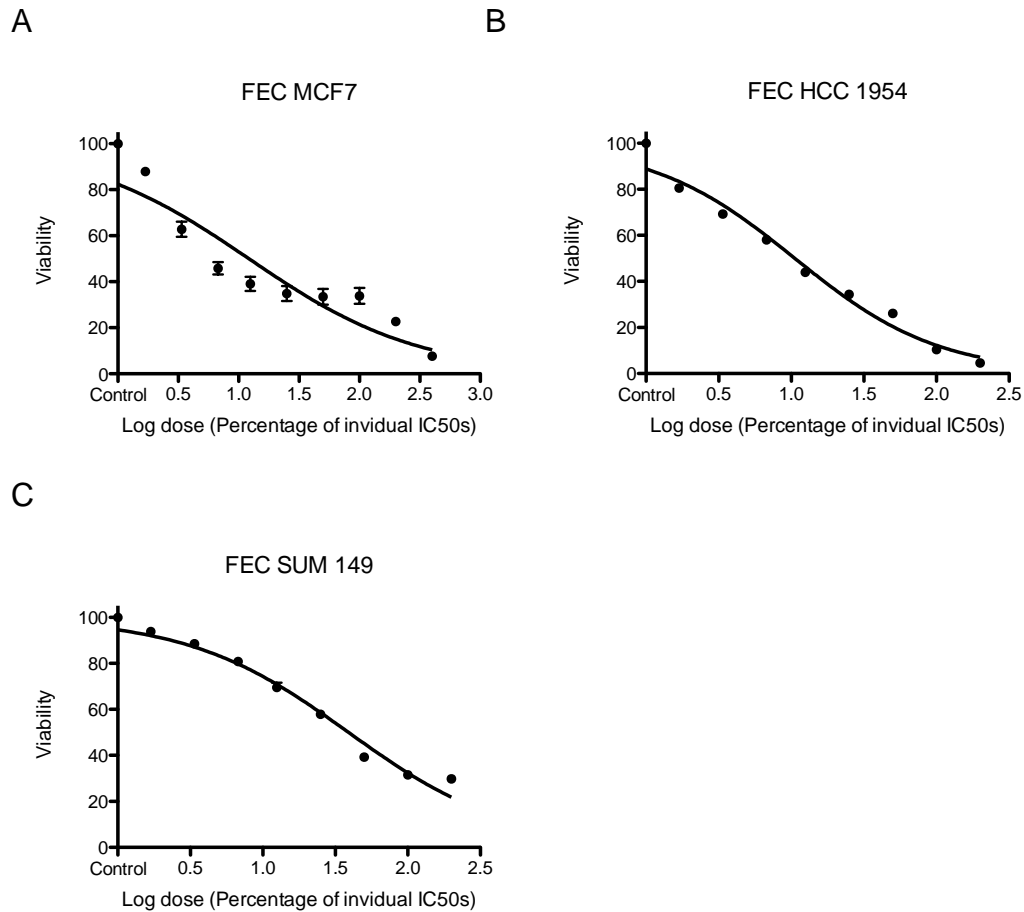
Figure 3.2- Three-day dose-response curves of MCF7, HCC 1954 and SUM149 cell lines to FEC chemotherapy.

A MCF7 **B** HCC 1954 and **C** SUM 149 cells were plated in 96 well plates and allowed to adhere overnight. Reducing doses of FEC chemotherapy were added and viability was assessed 72 hrs later using the Cell Titer blue assay. All results are averages of a minimum of three independent experiments each performed with three internal technical replicates. Error bars represent Standard Error of the Mean (SEM).

Cell line/Drug	F	E	C	FEC*	D
MCF7	22.5µM	220nM	0.918µM	12.16%	1.5nm
HCC 54	10µM	108nM	28µM	10.59%	7.9nm
SUM 149	10.8µM	10.6nM	2µM	38.99%	0.73nM

Table 3.1- Three day IC50 values of cell lines to F,E,C, FEC and D

Tabular representation of the IC50 values of both individual and combined chemotherapeutic agents for all three cell lines.   F= 5-fluorouracil, E=Epirubicin, C=4-Hydroxycyclophosphamide, FEC= all three drugs, D= Docetaxel. *= percentage of IC50 values of individual drugs that led to IC50 in combination

3.1.3 bCSC-like activity is responsive to cytotoxic chemotherapy in a range of different treatment conditions

Having established IC50 treatment concentrations for our cell lines and chemotherapeutics, the MCF7 cell line was arbitrarily selected to begin assessing the effect of chemotherapy on bCSCs (Dontu et al. 2003). As CSCs have been shown to be resistant to chemotherapy (Suling Liu and Wicha 2010), it was hypothesised that treatment with chemotherapy would potentially increase the proportion of bCSCs relative to non-bCSC cells remaining at the end of chemotherapy treatment. For example, if we assume that the proportion of bCSCs within the MCF7 cell line is 2% but that these cells are completely resistant to chemotherapy, we could expect that, if 50% of the non-bCSC cells in the dish had been killed by chemotherapy, that the proportion of bCSCs in the remaining viable cell population would increase to 4%; thus representing a two-fold increase in bCSCs in the treated group compared to control. To test this hypothesis, cells were treated in adherent conditions for 72 hours before being trypsinised and plated into mammosphere forming conditions, a well-established in vitro test for CSC-like activity which quantifies the absolute number of sphere-forming cells within a tumour cell population (Charafe-Jauffret et al. 2009; Shaw et al. 2012; Dontu et al. 2003).

While the MCF7 cells formed the predicted well-rounded uniform spheres in control conditions (Shaw et al. 2012) (Fig 3.3A), contrary to expectation pre-treatment with both FEC and docetaxel at their IC50 values significantly decreased mammosphere formation (Fig 3.4). In chemotherapy pre-treated cells, cells formed loose associations, did not grow well in spheres and often demonstrated the presence of vacuoles when grown in non-adherent conditions. This is a phenomenon that has been observed in mammospheres that are entering senescensce and are no longer dividing (Dey et al. 2009) (Figs 3.3B and 3.3C). The reduction in the number of spheres was present in the secondary passage of the mammosphere culture, confirming a reduction in self-renewing sphere-forming cells within the cell population (see Section 2.3).

This result was inconsistent with the weight of published data for the individual FEC agents and docetaxel as previously both regimes had been shown to increase stem cell activity (as measured by mammospheres and ALDH1 expression) both *in vivo* and in *ex vivo* mammosphere conditions (Alamgeer et al. 2014; X. Li et al. 2008).

We found that a number of different conditions had been employed by other groups that had demonstrated chemotherapy increased mammosphere formation. These included: allowing cells to recover in fresh media for three days after treatment with paclitaxel before plating on into mammosphere conditions (Bhola et al. 2013), treating in mammosphere conditions rather than pre-treating the cells (Hirsch et al. 2009; Sims-Mourtada et al. 2014; Li et al. 2008) and exclusion of non-viable cells before plating into mammosphere conditions (Samanta et al. 2014).

Repeating the same experiments in the MCF7 cell line but with these additional parameters yielded the same results as our original experiment, with the different conditions of a tryphan blue exclusion dye before plating, a three day rest period after chemotherapy or treatment in mammosphere conditions (Fig 3.5 A-C) all showing a significant reduction in mammosphere formation in both Passage 1 and Passage 2.
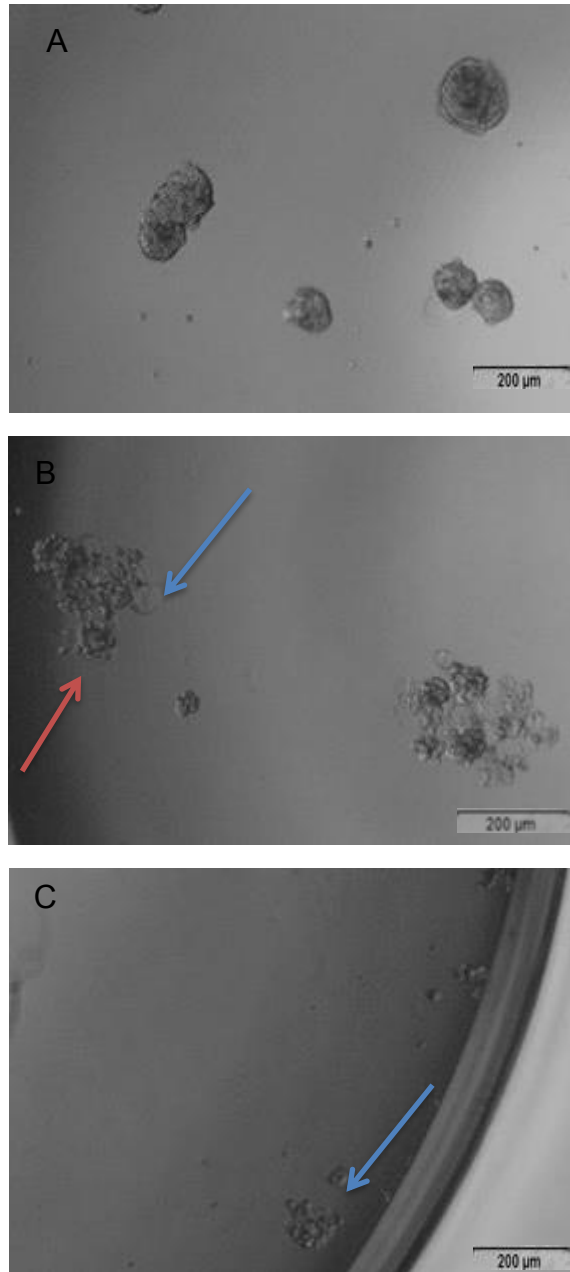
Figure 3.3- MCF-7 mammospheres decrease after chemotherapy after one week of non-adherent culture

MCF7 cells were plated into adherent conditions, allowed to adhere overnight and then treated with either control (A) or IC50 values of FEC (B) or Docetaxel (C) as shown in Table 3.1. Whilst spheres formed in the control arm (A), mammosphere formation was less than in control groups after chemotherapy- often with loose association of cells (B, red arrow) and vacuole formation (B and C, blue arrows). Magnification= x4
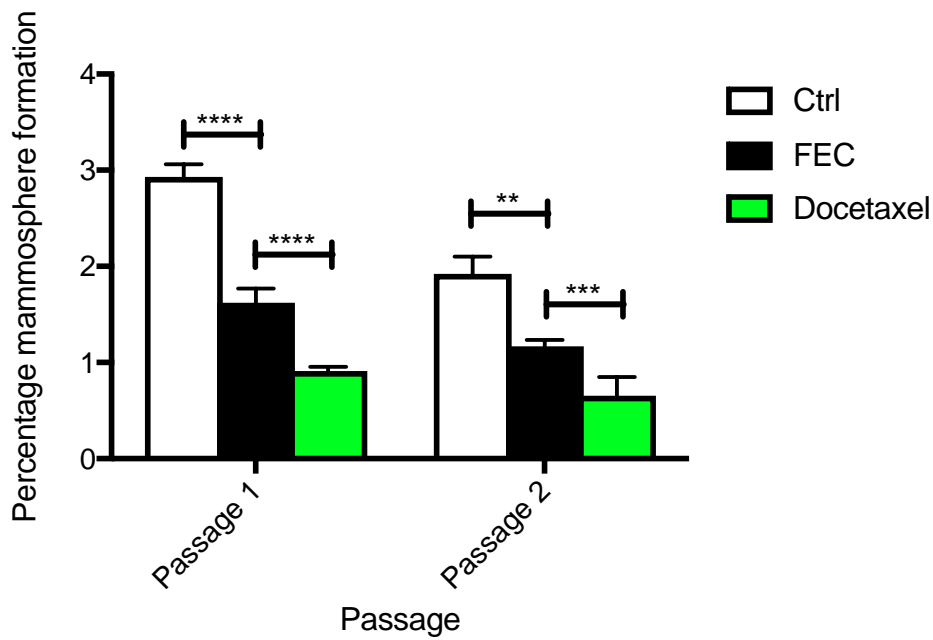
Figure 3.4- Number of MCF7 mammospheres reduces after treatment with either FEC or docetaxel.

After 3 days treatment in adherent conditions with the IC50 values of both FEC and docetaxel there was a significant decrease in sphere formation in the MCF7 cell line. Cells were dissociated and then grown in non-adherent conditions for 7 days (Passage 1) before being dissociated and seeded again as single cells into Passage 2. Error bars represent SEM of the mean and results are an average of three experiments performed in triplicate. (T-test, *=p<0.1, **=p<0.01, ***=p<0.001 ****=p<0.0001).
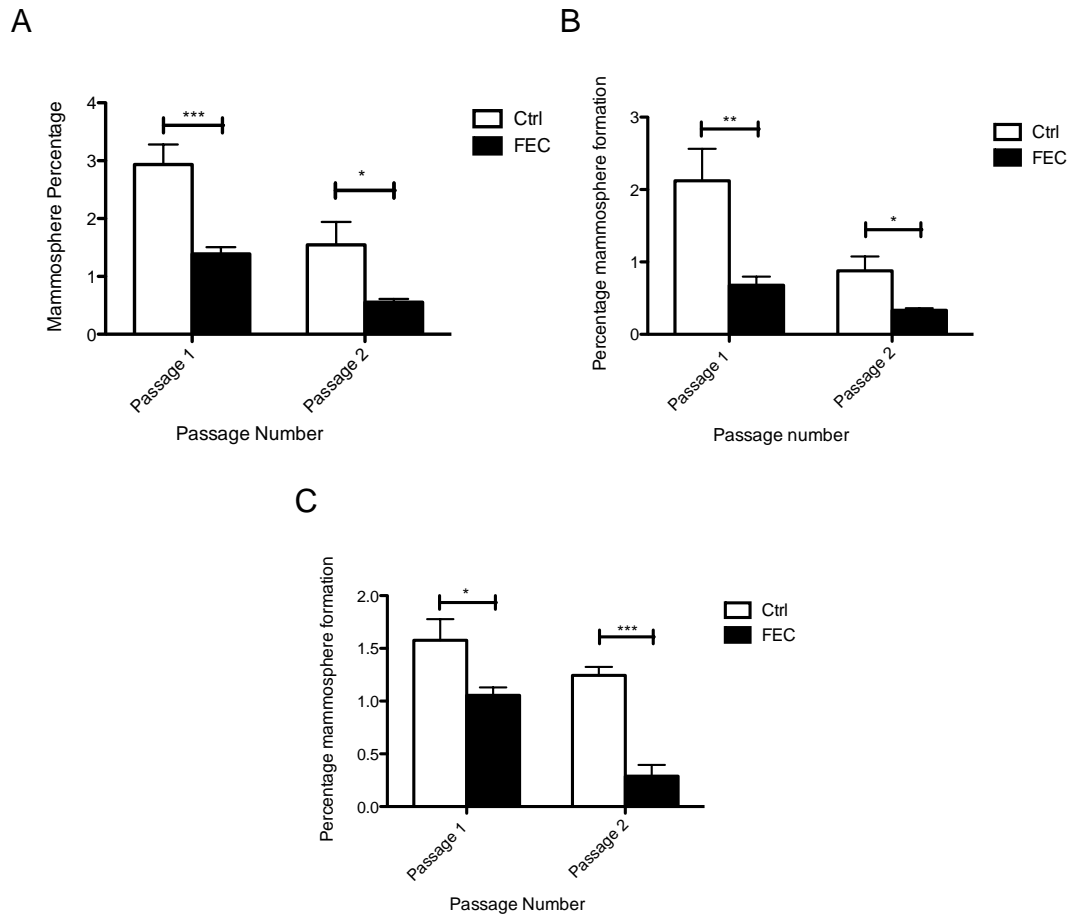
Figure 3.5- MCF7 mammospheres decrease after FEC chemotherapy in a number of different plating conditions

In order to assess the effect of different plating conditions on mammopshere formation, MCF7 cells were treated with FEC at its IC50 value in adherent conditions for 3 days and then plated into non-adherent mammopshere conditions after **A** a tryphan blue exclusion stain or **B** three days rest in fresh media after treatment. For **C**, cells were treated at the IC50 value in mammosphere conditions. Error bars represent SEM of the mean and results are an average of three experiments performed in triplicate. (T-test, *=p<0.1, **=p<0.01, ***=p<0.001   ****=p<0.0001).

3.1.4 Treatment with docetaxel for four days increased mammosphere formation in the MCF7 cell line

A study in which bCSC-like activity (as measured by mammospheres and ALDH positivity) was enriched following treatment with paclitaxel in a panel of TNBC cell lines as well as the MCF7 cell line, included three additional alternative parameters: the length of time (four days versus three), the use of the drug paclitaxel and the non-adherent media used (Mammocult, Stem Cell Technologies instead of MEBM, Lonza) (Samanta et al. 2014). The authors eloquently demonstrated that levels of HIF1α increased at four days after treatment with chemotherapy and that this was responsible for the increased bCSC seen at this time point (Samanta et al. 2014). The proposed mechanism was through interleukin 6 and 8 signalling leading to both increased expression of the multi drug resistance 1 (MDR1) protein as well as bCSC behaviour.

We therefore sought to replicate this experiment but realised that an unknown variable was the initial plating density of cells within the experiment. We reasoned that cell density could influence the clonal potential of resident stem cells within the tumour cell populations *in vitro*. Thus experiments were performed at a range of cell densities (25000/ml, 50000/ml, 100000/ml and 200000/ml) and treatment for four days at two concentrations of docetaxel (1nM and 5nM) in the MCF7 cell line (Fig 3.6). We did not use the previously calculated IC50 value as we reasoned that this would be altered by both the different cell densities as well as the treatment time. Cells were plated out at the different cell densities, allowed to adhere overnight and then treated with chemotherapy for 96hours. They were then dissociated and plated into non-adherent conditions as described in Section 2.6 using Mammocult media (Stem Cell Technologies)

After exposure of different concentrations of MCF7 cells to docetaxel for four days the proportion of self-renewing mammosphere forming cells increased for all densities of cells plated but significantly for cells at 50000 and 100000 cells/ml (Figs 3.6A and B and 3.7). The dose of 1nM corresponded roughly with our previous IC50 value for MCF7 cells for three days of treatment

(1.5nM). At 5nM cells failed to form tight aggregates as previously observed (Fig 3.7C).

As 50000 cells/ml was the cell density used in previous experiments, there were two differences between this experiment and the previous ones performed: the length of treatment and the non-adherent culture media used.
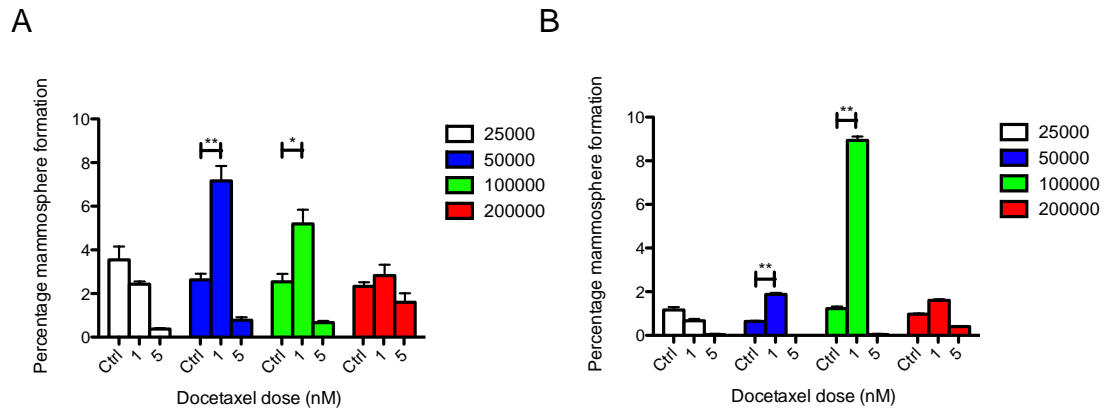
Figure 3.6- MCF7 mammosphere formation increases with docetaxel at certain cell densities and drug concentrations

When MCF7s were plated at different cell densities, allowed to adhere overnight and then treated with two concentrations of docetaxel (1nM and 5nM) for 96 hours before being dissociated and plated into mammosphere conditions. After 7 days (A, Passage 1) cells were counted and dissociated before being passaged on into Passage 2 (B) where they were counted a further seven days later. Error bars represent SEM of the mean and results are an average of two experiments performed in triplicate. (T-test, *=p<0.1, **=p<0.01, ***=p<0.001 ****=p<0.0001).
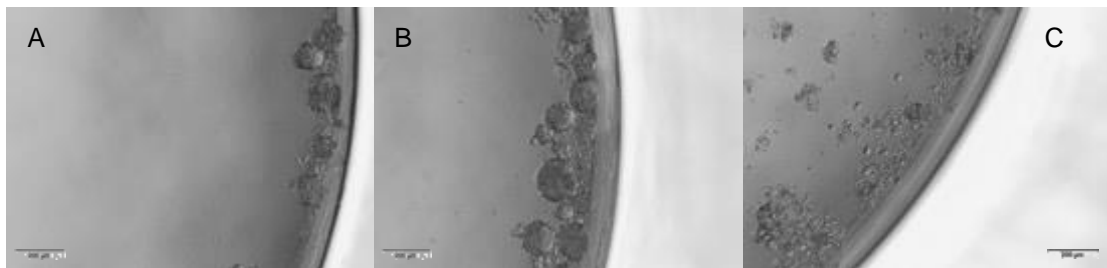
Figure 3.7- MCF7 mammospheres increase after chemotherapy

After 96 hours of treatment in adherent conditions, mammosphere count increased from control **(A)** to 1nM of docetaxel treatment **(B)** but decreased with 5nM of docetaxel **(C).** Cells looked sick at the higher concentration and did not form mammospheres in Passage 2. Plating density 100000cells/ml. Picture taken at the end of Passage 1. Scale bar 200μM.

3.1.5 Re-establishing 96 hour IC50 values for all cell lines

The docetaxel doses in the previous experiment were based on the IC50 determinations from 72 hour experiments. Thus, on the basis that future experiments would need to be performed at 96 hours to further investigate the effects of chemotherapy on bCSC increases, dose response curves were repeated for 96 hour assays. In addition, the drug paclitaxel, a taxane related to docetaxel, was also tested. Although not licensed for adjuvant or neo-adjuvant use in the UK, paclitaxel is in use in the metastatic setting and is commonly used worldwide in a weekly format in the adjuvant setting (Sparano et al. 2008). As has been demonstrated by others, docetaxel is a more potent drug than paclitaxel with our IC50 values demonstrating that the concentration of paclitaxel needed to reach an IC50 values is 3-4 multiples of docetaxel (Izbicka et al. 2005). The IC50 doses of the individual drugs forming the regime FEC were not recalculated. Instead the same method as above was used to make a mix of all three drugs representing the 72-hour IC50 dose that was then serially diluted so that all drugs remained in fixed proportions. This dilution was then used for all future experiments. As expected, the IC50 doses differed from the 72 hour treatment (Fig 3.8 and Table 3.2). Cell plating density was the same as the 72 hour experiments (see Section 2.2.1).

A

MCF7 Docetaxel

MCF7 Paclitaxel

MCF7 FEC

B

HCC54 Docetaxel

HCC54 Paclitaxel

HCC54 FEC

79
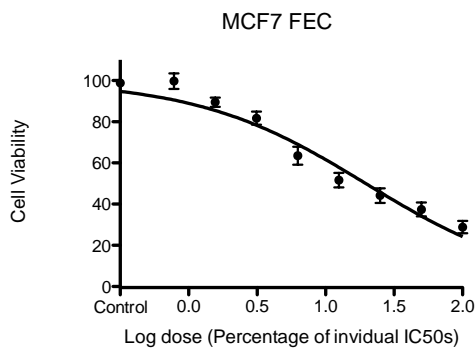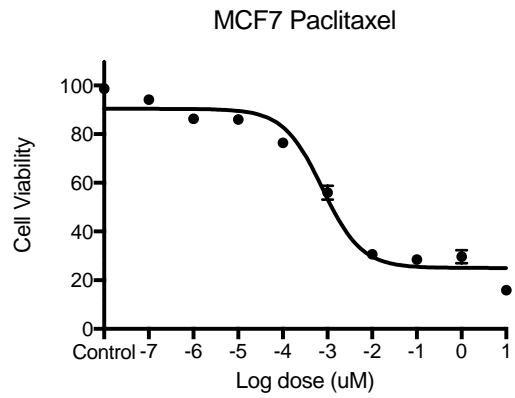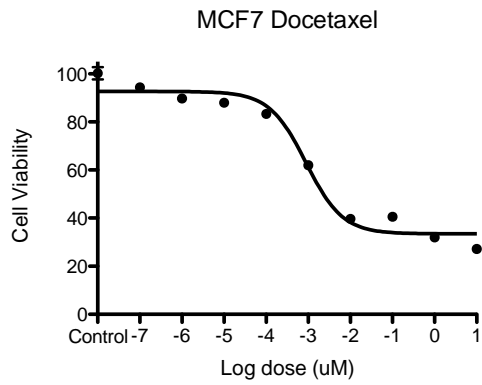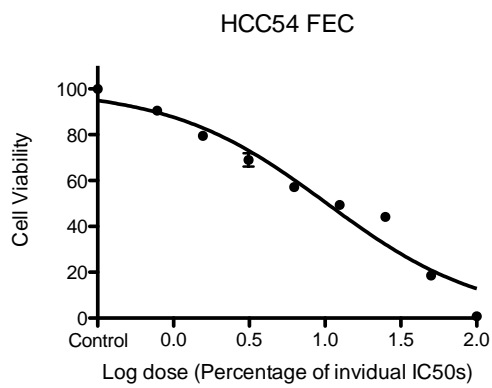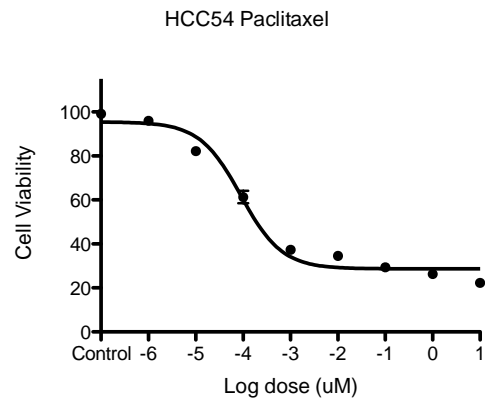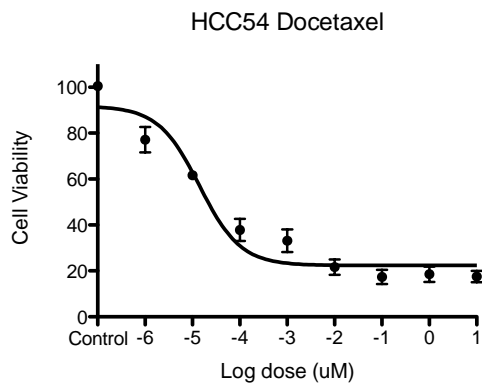
C
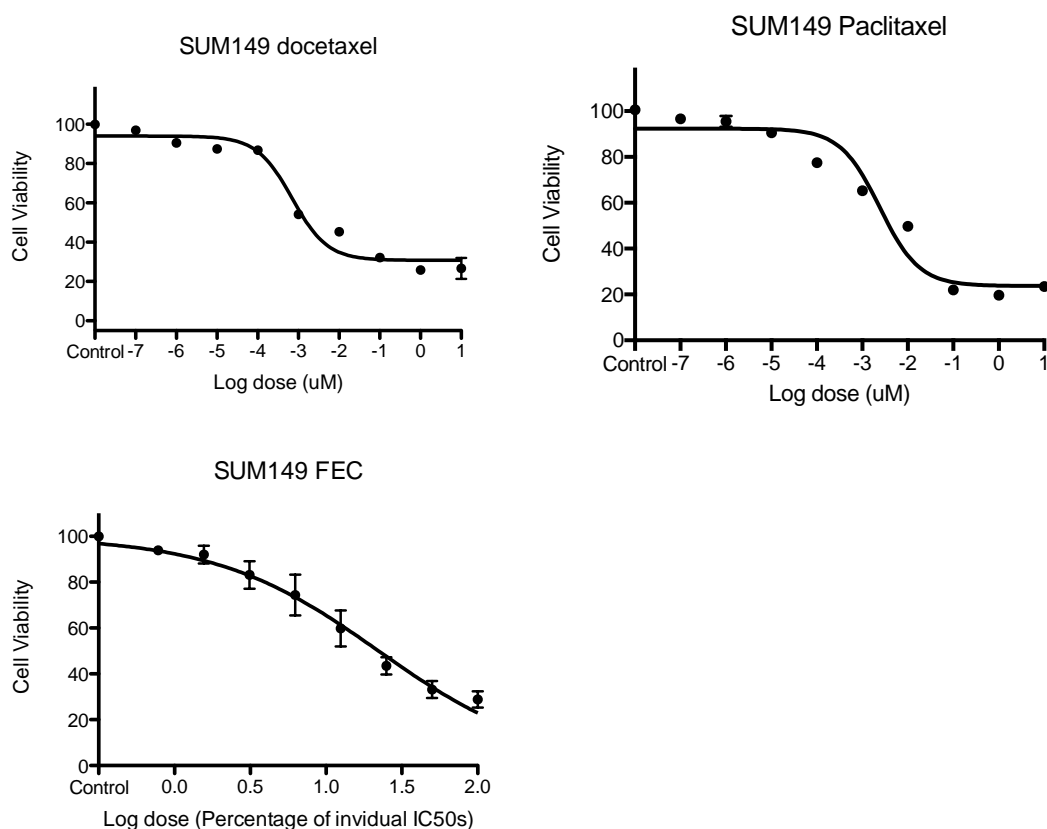
Figure 3.8- Four-day dose response curves of MCF7, HCC 1954 and SUM149 cell lines to paclitaxel, docetaxel and FEC chemotherapy

A MCF7 **B** HCC 1954 and **C** SUM 149 cells were plated in 96 well plates and allowed to adhere overnight. Reducing doses of paclitaxel, docetaxel and FEC chemotherapy were added and viability was assessed 96 hrs later using the cell titer blue assay. All results are averages of a minimum of three independent experiments each performed with three internal technical replicates. Error bars represent Standard Error of the Mean (SEM).

Cell line/Drug	FEC[*]	Paclitaxel	Docetaxel
MCF7	19.83%	3.58nM	0.88nM
HCC 54	10.29%	1.62nM	0.57nM
SUM 149	22.19%	2.41nM	0.70nM

Table 3.2- Four day IC50 Values

Tabular representation of the IC50 values of both individual and combined chemotherapeutic agents for all three cell lines. F= 5-fluorouracil, E=Epirubicin, C=4-Hydroxycyclophosphamide, FEC= all three drugs [*]= percentage of IC50 values of individual drugs that led to IC50 in combination

80

3.1.6 Treatment at IC50 values for 96 hours increased the proportion of mammospheres in all cell lines

Having established the new 96 hour IC50 values, the MCF7, HCC 1954 and SUM149 cell lines were plated, allowed to adhere overnight and exposed to either paclitaxel, docetaxel or the combination of FEC for 96 hours, before being plated into non-adherent, mammosphere forming conditions. After 7 days they were dissociated and passaged again for a further 7 days.

The results showed that in all cell lines, across all chemotherapies, mammosphere formation increased in response to treatment (Fig 3.9 A-E). This was the reverse of what was seen after 72 hours of treatment in the MCF7 cell line (Figs 3.3 and 3.4). There were however some differences between the cell lines, for example in the MCF7 cell line both paclitaxel and docetaxel significantly increased the mammopshere formation in both Passage 1 and Passage 2 more than FEC. In the SUM149 cell line, FEC only had a small effect on increasing mammosphere formation in Passage 1 that was significantly less than both paclitaxel and docetaxel. In Passage 2, this situation was reversed with FEC increasing the mammosphere formation significantly more than that of both paclitaxel and docetaxel. In the HCC 1954 cell line, there was a significant increase in mammospheres seen in Passage 1 with paclitaxel compared to the other chemotherapeutics that did not carry over into Passage 2, with no significant differences seen between the three agents.

Passage 1

Passage 2

A

B
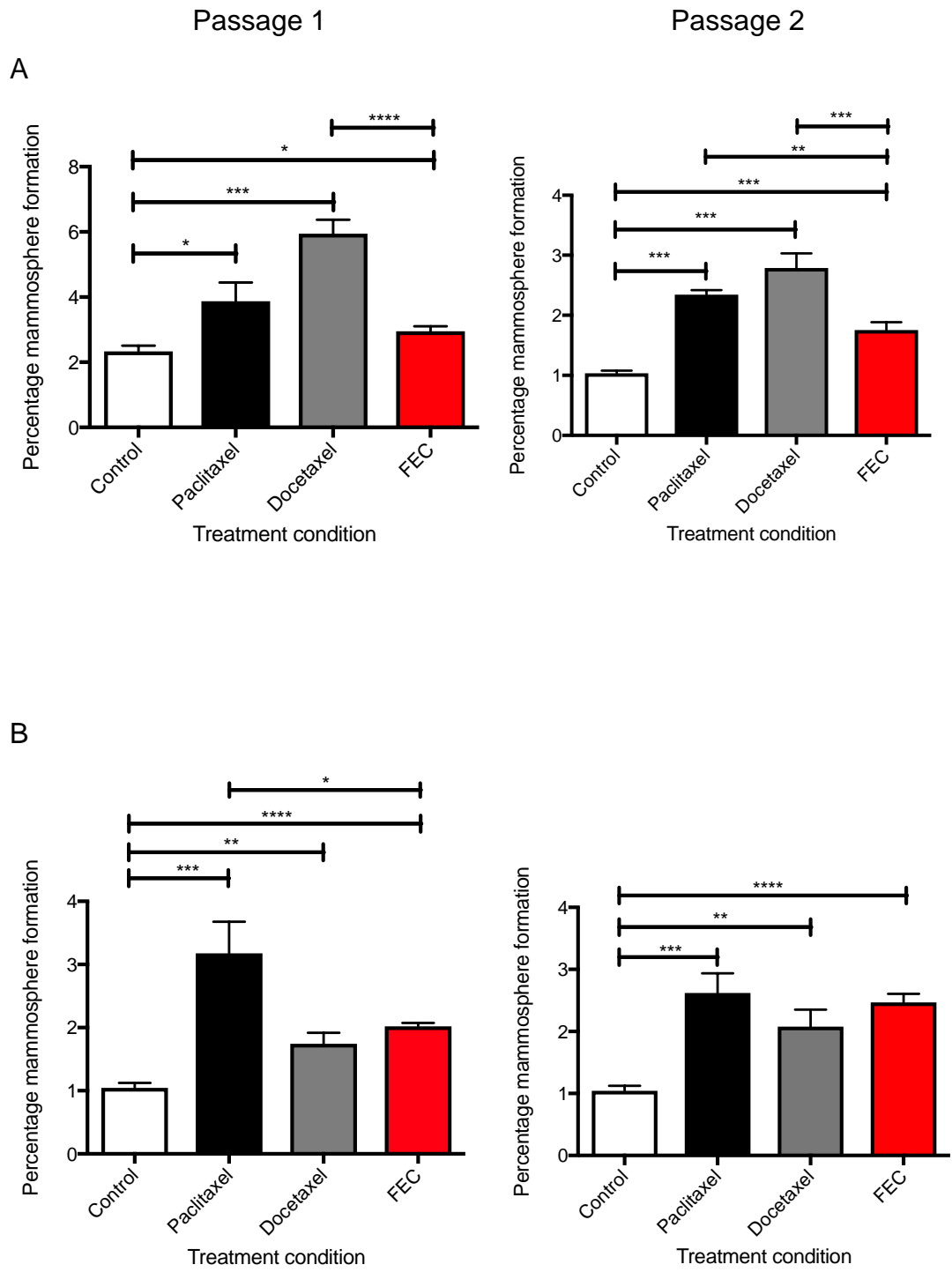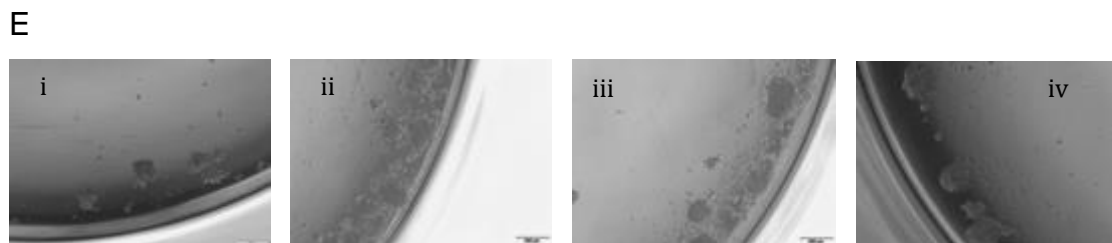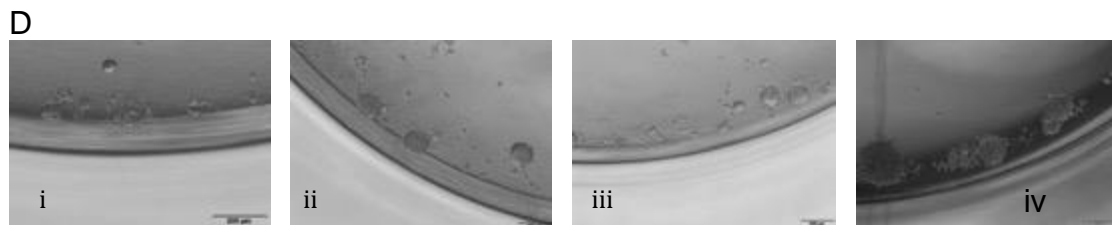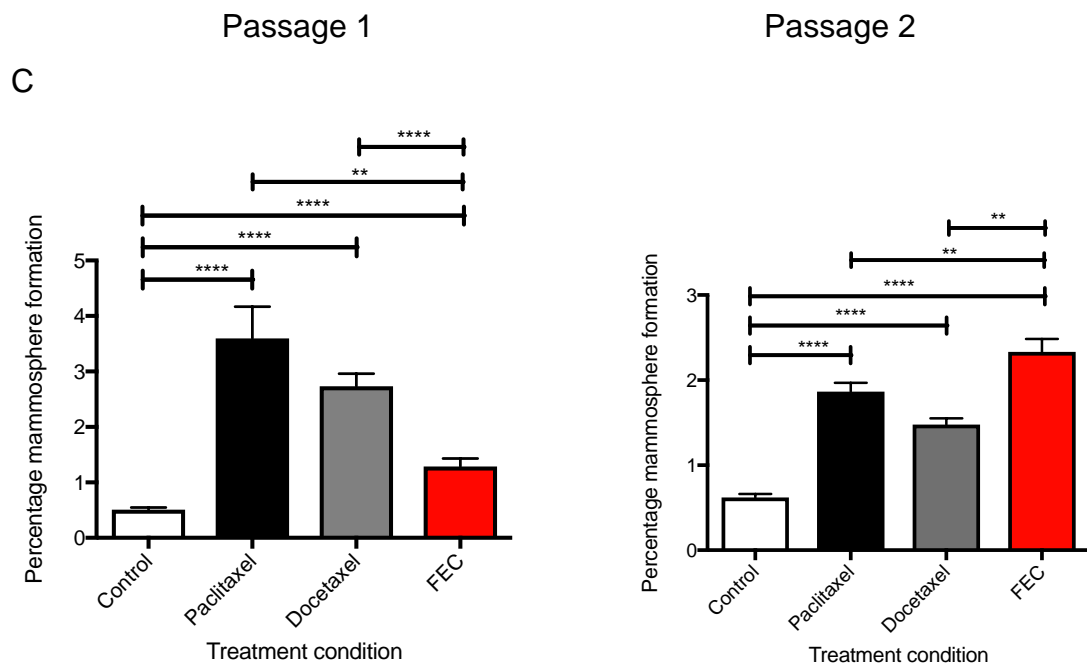
Figure 3.9- Increasing mammosphere formation induced by chemotherapy across a broad range of cell lines and chemotherapeutics

In the MCF7 (A), HCC 1954 (B) and SUM 149 (C) cell lines there were significant increase in mammosphere formation in both Passage 1 and Passage 2 after treatment with 96hours of chemotherapy. Figs 19D and 19E show representative pictures of the HCC 1954 and SUM149 P1 mammospheres respectively after treatment with DMSO (i), or the IC50 values of Paclitaxel (ii), Docetaxel (iii) and FEC (iv). Error bars represent SEM of the mean and results are an average of three experiments performed in triplicate. (T-test, *=p<0.1, **=p<0.01, ***=p<0.001 ****=p<0.0001). Scale bar 200μM.

3.1.7 A mathematical model demonstrates that chemotherapy increases the actual number of CSCs remaining in a cell population after treatment

In an attempt to assess whether chemotherapy simply ineffectively targets CSCs (leading to a reduced overall number but increased overall percentage in a remaining population) or leads to an absolute increase in their total number mediated by a mechanism such as CSC signaling (leading to an increased overall number and percentage) a basic mathematical model was constructed (see Section 2.4). There has been much interest in this area with tumours evaluated after both hormone and chemotherapy showing increased mesenchymal and tumour initiating features after chemotherapy (Creighton et al. 2009).

The results show differing effects of chemotherapy depending on cell line (Tables 3.3A-C and Fig 3.10). For example, in the SUM149 TNBC cell line, all chemotherapeutics significantly increased CSC number, but in the HCC1954 cell line, only paclitaxel did. For the MCF7, ER positive cell line, both paclitaxel and docetaxel led to an increase but not FEC. Although this is a result based on a hypothetical mathematical model, this implies that chemotherapy is likely not only ineffective in targeting CSC-like cells but, in some situations, also leads to an induction of new CSC formation. This is particularly true for the SUM149 TNBC cell line- a molecular subtype of cancer known to contain large numbers of CSCs (Habib and O'Shaughnessy 2016).

A

	Viability (%)	Total cell number	P2 sphere formation (%)	CSCs in plate
Control	100	10000	1.033	103
Paclitaxel	61.5	6153.4	2.344	144
Docetaxel	58.0	5805.2	2.7899	162
FEC	65.8	6580	1.7556	116

B

	Viability (%)	Total cell number	P2 sphere formation (%)	CSCs in plate
Control	100	10000	1.044	104
Paclitaxel	58.645	5864.5	2.622	154
Docetaxel	57.5	5750	2.077	119
FEC	43.79	4379	2.466	108

C

	Viability (%)	Total cell number	P2 sphere formation (%)	CSCs in plate
Control	100	10000	0.6222	62
Paclitaxel	58.045	5804.5	1.8667	108
Docetaxel	62.398	6239.8	1.4778	92.2
FEC	59.675	5967.5	2.3333	139

Tables 3.3A-C A Model to demonstrate the effect of chemotherapy on CSC number in breast cancer cell lines

IC50 value viability was used to calculate viable cells left at the end of a 96hour treatment period with chemotherapy. This was then multiplied by the percentage mammosphere formation at the end of Passage 2 to give a total CSC number remaining in the plate at the end of chemotherapy treatment in the MCF7 (A), HCC 1954 (B) and SUM149 (C) cell lines. Results are the mean of three independent experiments each performed in triplicate.
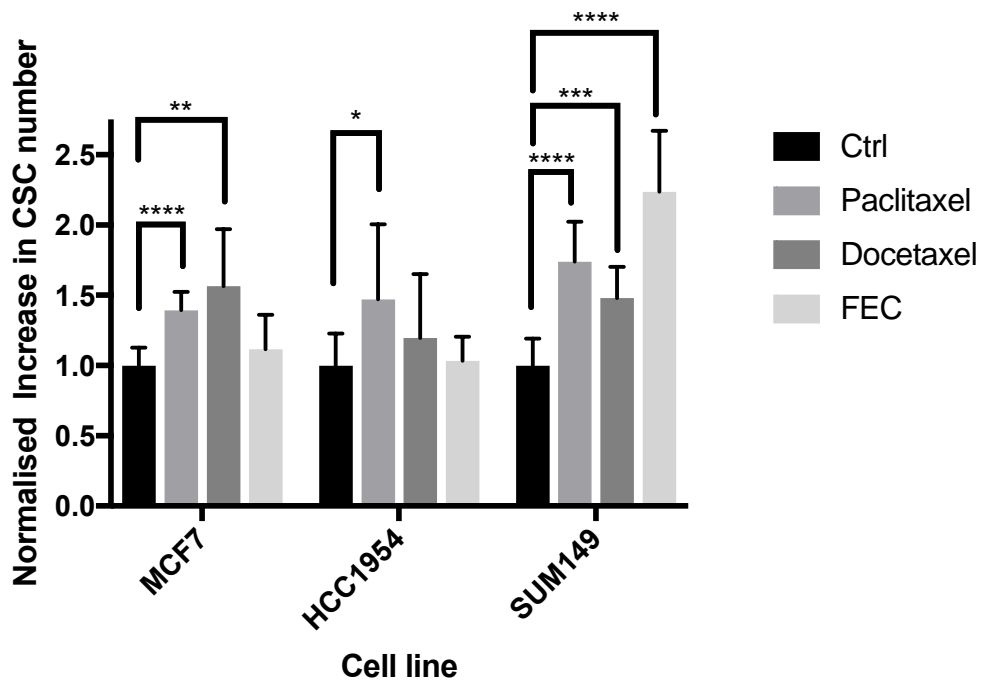
Figure 3.10- Chemotherapy increases the total number of CSCs remaining in a cell population after treatment.

Graphical representation using cell viability to calculate the number of stem cells remaining after treatment multiplied by the sphere formation of the same treatment condition to give an actual number of CSCs left at the end of treatment. Error bars represent SEM of the mean and results are an average of three experiments performed in triplicate. (T-test, *=p<0.1, **=p<0.01, ***=p<0.001 ****=p<0.0001).

3.1.8 The proportion of ALDH MCF7 and SUM149 positive cells increase in response to chemotherapy

ALDH has been identified as a marker associated with bCSC activity in all molecular subtypes of breast cancer and has been linked with prognosis (Alamgeer et al. 2014; Ginestier et al. 2007; Charafe-Jauffret, Ginestier, Iovino F, et al. 2010). For example, it has been shown in paired biopsies of breast cancer patients before and after anthracycline and taxane containing chemotherapy that ALDH staining increased (Alamgeer et al. 2014; Tanei et al. 2009; Tiezzi et al. 2013). The MCF7 cell line has been shown to have a baseline activity of around 1%, the HCC 1954 line 1-5% and the SUM 149 line around 5% (Suling Liu et al. 2013; Charafe-Jauffret, Ginestier, Iovino F, et al. 2010).

The Aldeflour assay (StemCell Technologies, Vancouver, Canada) was used to ascertain whether the increase in ALDH positivity correlated with mammosphere formation after treatment with chemotherapy. After exposure to IC50 values of chemotherapy drugs for 96 hours, ALDH positivity significantly increased from 2.3% at baseline in the MCF7 cell line to 23.8% with paclitaxel, 25.8% with docetaxel and 24.8% with FEC. In the SUM149 cell line the results were more varied, increasing from 4.1% at baseline to 32.2%, 16.1% and 31.8% with paclitaxel, docetaxel and FEC respectively (Fig 3.11). The almost ten-fold increase in ALDH positivity is markedly more than the increase in mammosphere formation that was witnessed in these two cell lines. Although ALDH has been correlated with CSCs and drug resistance (Januchowski, Wojtowicz, and Zabel 2013), this surrogate marker of CSC-like activity fails to precisely overlap with the functional CSC mammosphere assay. Nevertheless, the increase in ALDH correlates with the increase in functional CSC number seen in our mathematical model. As will be discussed in Chapter 4, the ALDH positivity of the HCC1954 line was not examined as the focus of this work changed to focusing on triple negative breast cancer.

A

MCF7

DEAB	Control	Paclitaxel	Docetaxel	FEC
ALDH Positive 0.15	ALDH Positive 2.02	ALDH Positive 22.7	ALDH Positive 24.2	ALDH Positive 26.4

SUM149

DEAB	Control	Paclitaxel	Docetaxel	FEC
ALDH Positive 0.20	ALDH Positive 4.13	ALDH Positive 36.8	ALDH Positive 20.0	ALDH Positive 39.1

ALDH1 +ve

B

C
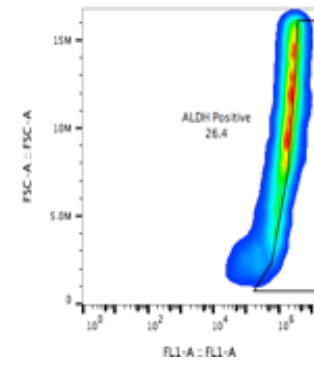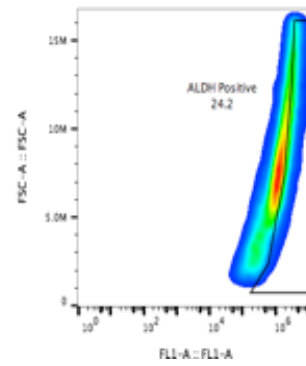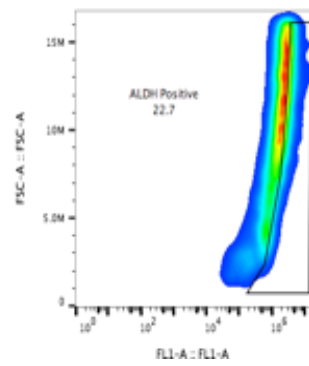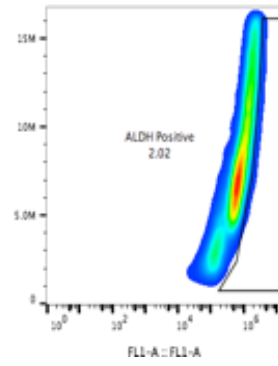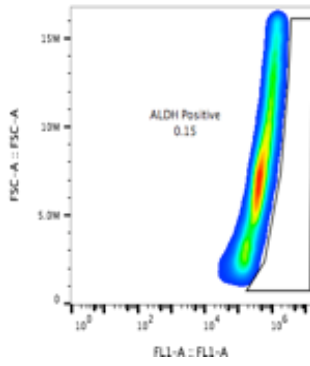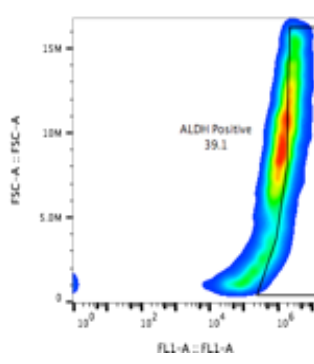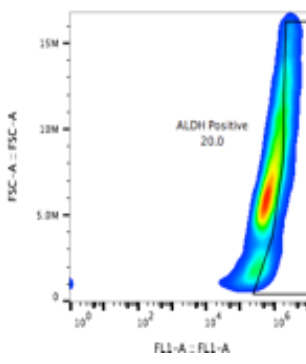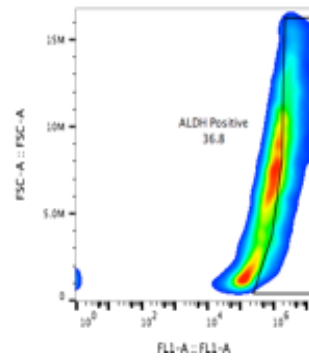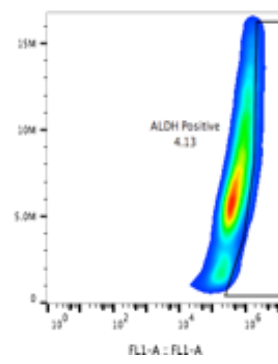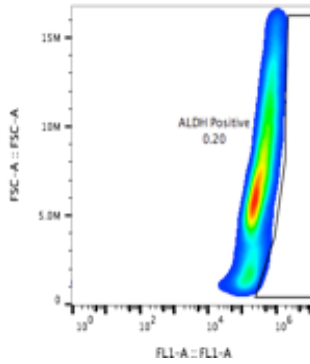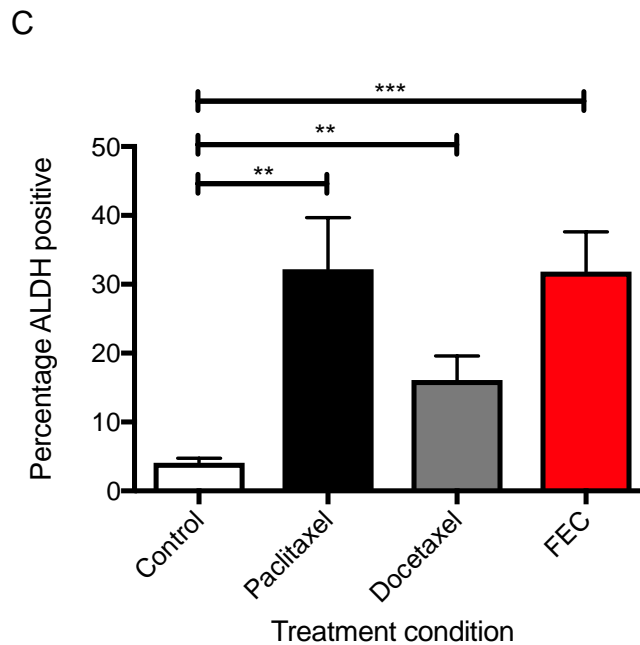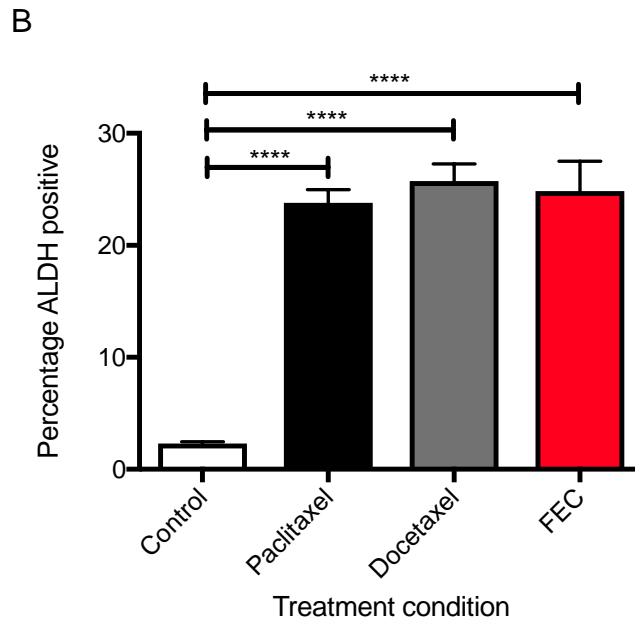
Figure 3.11- ALDH1 positivity increases in response to chemotherapy

The treatment of MCF7 and SUM149 cells with paclitaxel, docetaxel or FEC chemotherapy significantly increases the proportion of ALDH1 positive cells compared to controls. A, representative FACS plots of ALDH1 positivity in the MCF7 and SUM149 cell lines. B and C, Percentage of ALDH1 +ve cells in the MCF7 and SUM149 cell lines respectively after treatment with respective chemotherapy agent at IC50 concentration for 96hours. Error bars represent SEM of the mean and results are an average of three experiments performed in triplicate. (T-test, *=p<0.1, **=p<0.01, ***=p<0.001   ***=p<0.0001).

3.3 Discussion

In this chapter, the sensitivities of a broad panel of cell lines representing the different molecular subtypes of breast cancer (MCF7- ER positive, HCC1954 – HER2 positive and SUM149- triple negative) to different chemotherapeutic agents representing the current standard of care in breast cancer was established (E. Senkus et al. 2013). This was done to establish an *in vitro* model through which the effect of these agents on the bCSC population within these three cell lines could be established. Having established the IC50 values for FEC and Docetaxel (Fig 3.2 and Table 3.1) our initial findings that chemotherapy effectively targets the mammosphere formation of this panel of cell lines (Fig 3.4) were unexpected, as they appeared to be inconsistent with the overwhelming weight of literary evidence that had suggested that bCSCs were resistant to chemotherapy. Indeed, extensive literature searches yielded no evidence that cytotoxic chemotherapy effectively targets CSCs but a multitude of papers on approaches to target residual CSC populations that remained after chemotherapy ((Ranji et al. 2016; Angeloni et al. 2015; Dragu et al. 2015). Our data did also not fit with clinical outcomes, if chemotherapy was so effective at targeting CSCs then there would be an expectation that these cells would not survive, reform tumours and lead to both recurrences and metastatic disease often years after the original treatment.

This led us to re-evaluate a number of experimental parameters that could explain the disparity between our data and other published evidence (Fig 3.5). Eventually, treating the cells for 96 rather than 72 hours with chemotherapy and changing the mammosphere media (to Mammocult©) led to increasing mammosphere formation across all chemotherapeutic agents in all cell lines (Figs 3.6-3.9). Although we did not assess the effect of both different mammosphere media at 96 hours, we feel it is unlikely that the difference in media would explain the highly significant differences in mammosphere formation seen between the 72 and 96 hours treatment time points. In the absence of publically available data as to the composition of the Mammocult© media (as compared to the original MEBM media used) any potential

difference would have been assessed. Unfortunately there was insufficient time to evaluate this.

Chemotherapy

Initial tumour

Survival of CSC and stimulation of CSC signaling

Tumour relapse
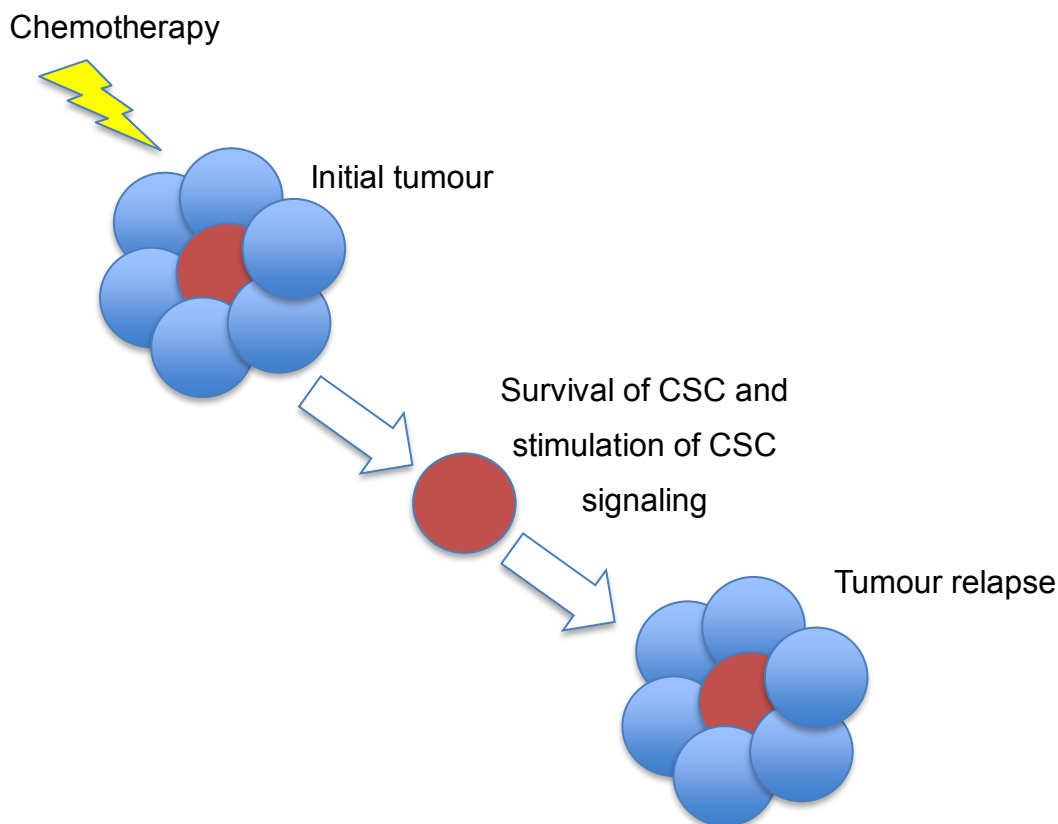
Figure 3.12- Effect of chemotherapy on CSCs

After treatment with chemotherapy, the bulk of tumours cells (blue) are killed but the CSC remains (red). Over time, this cell is able to divide and reform the tumour- leading to recurrence of the tumour at a later time point.

As the mammosphere assay is a surrogate for measuring CSC-like behavior, this would suggest that chemotherapy is having a number of potential effects. The first possibility is that chemotherapy is ineffective at targeting CSCs and that they enjoy a preferential survival advantage over non-CSCs, meaning that they are present at an increased proportion of the remaining viable cell population which then translates into increased mammosphere formation when these cells are plated out at a fixed density. Indeed, there is evidence that cells are inherently resistant to chemotherapy through utilizing mechanisms such as increased drug efflux pumps, DNA damage repair enzymes and resistance to apoptosis (Gottesman, Fojo, and Bates 2002; G. Liu et al. 2006; M. Zhang, Atkinson, and Rosen 2010) . Our data would

potentially go against this as we saw an inhibition of mammosphere formation by chemotherapy at 72 hours when, presumably, CSCs should be able to form spheres as a functional surrogate of their activity at this time point.

Another possibility is that cell signaling induced by chemotherapy leads to an induction of a CSC-like phenotype leading to non-CSCs being transformed into CSC-like cells. This could be mediated through a process such as EMT and, indeed, there is evidence supporting the role of chemotherapy in inducing EMT and an increase in CSC-like behaviour (Pattabiraman and Weinberg 2014; Li et al. 2008; Mani et al. 2008; Chang et al. 2005).

Combining both our cell viability and mammosphere data we then constructed a simple mathematical model to demonstrate this phenomenon. The results differed depending on both cell line and chemotherapy with the most aggressive cell line, the TNBC SUM149 cell line, being the only line to have its actual number of CSCs significantly increased by all types of chemotherapy. This is an interesting observation and correlates with the fact that TNBC is known to contain larger numbers of CSCs compared to other molecular subtypes of breast cancer (Habib and O'Shaughnessy 2016) (Tables 3.3A-C and Fig 3.10). Whilst in the MCF7 cell line the taxane compounds significantly increased the number of CSCs, FEC did not and in the HCC1954 cell line only paclitaxel led to a significant increase. Nevertheless, it is still important to remember that no chemotherapeutic led to a reduction compared to control, confirming that chemotherapy poorly targets CSCs (Suling Liu and Wicha 2010)

The increase in CSC-like activity at 96 hours was confirmed through the use of ALDH as a surrogate marker of CSC-like activity (Figure 3.11). Numerous studies have shown a relationship between ALDH and stem-cell like behaviour (Magni et al. 1996; Ginestier et al. 2007; Charafe-Jauffret et al. 2009; Cao et al. 2013a; Samanta et al. 2014; H. Zhang et al. 2015) Additionally, the upregulation of ALDH after neoadjuvant chemotherapy is associated with worse overall survival (Alamgeer et al. 2014; H. E. Lee et al. 2011; Tiezzi et al. 2013). ALDH has also been shown to correlate with

chemoresistance and is associated with the more aggressive molecular subtypes of breast cancer such as triple negative and Her-2 positive disease (Kida et al. 2015). Our data would suggest that in this setting, the increase in ALDH positivity is more than the increase in mammosphere formation witnessed after treatment with chemotherapy suggesting that ALDH positive cells do not exclusively represent CSCs but may represent a response to chemotherapy.

These data have two potential implications. Firstly, it means that perhaps standard protocols for testing oncology drugs may underestimate their effect on stem cell function as they commonly last 24-72 hours (W. Yang et al. 2013). As more is understood about patterns of recurrence and metastatic disease, it is clear that effectively targeting CSCs can only be beneficial to outcomes and the ability to target CSCs needs to be incorporated into standard novel drug testing. Secondly, it also implies that there is a key event that occurs between 72 and 96 hours and that this event may represent a target against which a novel CSC compound could be targeted.

When trying to elucidate this potential mechanism, attention turned to known CSC pathways such as TGF-β (Transforming Growth Factor β), Wnt (wingless-type MMTV (mouse mammary tumor virus), β-catenin, Notch and HIF1α (H. Zhang et al. 2015; Wu, Sarkissyan, and Vadgama 2016; Xie et al. 2016). As stated previously, one particular study examining the effect of chemotherapy on a panel of triple negative cell lines as well the MCF7 cell line demonstrated that four days rather than three of chemotherapy is needed to induce HIF1α expression leading to upregulation of IL-6 and Il-8 expression and CSC like features (Samanta et al. 2014). Though a recent paper by the same group has now shown three days treatment may increase mammospheres in triple negative cell lines (Lu et al. 2015). IL6 has been shown to be important in the ability of CSCs to self-renew and can force non-CSCs into a CSC-like state (Iliopoulos et al. 2011). IL8 leads to a pro-inflammatory response, increases CSC invasion, has been shown to be upregulated in ALDH positive cells and leads to increased mammosphere formation when added to cell culture (Charafe-Jauffret et al. 2009). The

93

relationship between HIF1α and chemotherapy will be explored in later chapters to assess whether this is at least partially responsible for the change in mammosphere number seen after 96 hours of treatment.

Having established a model through which an increase in CSC-like behaviour can be induced by chemotherapy *in vitro* the aims of subsequent chapters are to assess whether this increase can be either stopped, or preferably, reversed so that chemotherapy leads to both a reduction on both CSCs and their non-CSC counterparts.

4 Investigating Breast Cancer Cell Viability and Stem Cell Activity following chemotherapy combined with cFLIP-inhibition and/or TRAIL

4.1 Introduction

Having demonstrated that conventional cytotoxic chemotherapy targets bulk cells but increases CSC-like activity (Chapter 3), our attention turned towards targeting this residual stem-like population with a combinatorial therapeutic. TRAIL, a ligand for activating the extrinsic apoptosis pathway, and cFLIP, a key regulator of this pathway, are potential targets with which to overcome resistance to apoptosis seen in bulk cells but particularly in CSCs (Hanahan and Weinberg 2011; Fulda 2013). This chapter aims to explore whether targeting this pathway leads to a further reduction in bulk-cell viability when combined with chemotherapy, and moreover whether this combinatorial approach stems the increase in CSC-like activity observed when chemotherapy is used alone.

4.1.1 TRAIL

Despite promising pre-clinical activity, especially against mesenchymal cell lines (that broadly represent the TNBC molecular subtype of breast cancer), and evidence of synergistic activity with both anthracycline and taxane chemotherapeutic classes (of which epirubicin, paclitaxel and docetaxel are members), a recent trial of paclitaxel with or without tigatuzumab, a DR5 monoclonal antibody, showed no difference in recurrence-free or overall survival in triple-negative breast cancer (Oliver et al. 2012; Buchsbaum et al. 2003; Forero-Torres et al. 2015). This was a disappointment but fits in with the overall picture that, despite promising pre-clinical data, multiple TRAIL receptor agonists have failed in clinic trials (Holland 2014). Further work is needed to identify those patients with breast cancer who may benefit from TRAIL- with strategies adopted that may sensitise cells to TRAIL mediated apoptosis both with and without chemotherapy.

4.1.2 cFLIP

The intensive efforts to sensitise resistant cells to TRAIL have identified cFLIP as a key factor in resistance to TRAIL-induced apoptosis (Safa 2012). Previous work in our laboratory using siRNA-mediated knockdown of cFLIP combined with TRAIL has shown promising activity against CSC-like activity across a broad-range of molecular subtypes of breast cancer (Piggott et al.

2011). This has led to the development of an experimental compound named OH14 that binds to the DED1 domain on cFLIP, preventing incorporation of cFLIP into the Caspase 8 / 10 chain complexes recruited to the DISC and thus de-repressing apoptosis induced by death ligands (see Chapter 1.9). Whilst others in our laboratory have demonstrated an effect on CSC-like behaviour of this experimental compound in combination with TRAIL (Hayward et al, unpublished work) we wanted to assess whether this effect could be replicated after treatment with chemotherapy.

4.1.3 Combination of TRAIL and cFLIP inhibition with chemotherapy

There have been many attempts to combine TRAIL with a wide-range of chemotherapeutics across almost all tumour types (Holland 2014; Yang, Wilson, and Ashkenazi 2010). We hypothesis that by preventing the inhibition of apoptosis induced by TRAIL by using a cFLIP inhibitor, that any cytotoxic effect of chemotherapy would be enhanced. A review of the literature highlighted that, interestingly, there is evidence to show that paclitaxel in particular is dependent upon the extrinsic pathway to induce its apoptotic effect (Day et al. 2006). This raised the possibility that inhibition of cFLIP alone, in combination with paclitaxel in particular, may be sufficient to sensitise to chemotherapy-induced death.

Paclitaxel mediates its apoptotic effects through Caspases-8 and -10, increases expression of the DR5 death receptor and increased apoptosis- even in the absence of a ligand binding to this receptor. Knockdown of cFLIP significantly enhances the apoptosis induced by paclitaxel (Day, Huang, and Safa 2008a; Day et al. 2006) and it has been shown that paclitaxel induced apoptosis in a leukaemic cell line in a FADD-dependent manner, mediated primarily thorough Caspase 10 (Park et al. 2004). In this paper, neutralising antibodies to the external apoptotic pathway receptors Fas, TNF-Receptor 1, DR4 or DR5 did not reduce the apoptosis induced by paclitaxel suggesting that its apoptotic effect was mediated downstream of the extrinsic apoptosis pathway receptors. In cells that were transfected with FADD lacking a DED domain, apoptosis was reduced in cells treated with paclitaxel, showing that its apoptotic effect is dependent upon FADD. MCF7 cells overexpressing

cFLIP were resistant to apoptosis induced by paclitaxel but not docetaxel, possibly showing that the former is more dependent upon the extrinsic apoptosis pathway to induce apoptosis (Wang et al. 2005). Paclitaxel has been shown to elevate both Caspase-8 and TNF-α components of the extrinsic apoptosis pathway, whereas docetaxel has not. siRNA-mediated knockdown of cFLIP has also shown to sensitise a panel of ovarian carcinomas to apoptosis mediated by either paclitaxel or carboplatin (Vidot et al. 2010). Therefore, although the potential interactions between paclitaxel, docetaxel and FEC with both OH14 and TRAIL will be explored, there will be a particular focus on cFLIP inhibition with paclitaxel in this chapter as a route to assess whether cFLIP inhibition alone, as opposed to its combination with TRAIL therapy, after chemotherapy leads to a targeting of remaining CSCs after chemotherapy.

4.2 Results

4.2.1 Assessing the effect of OH14 and TRAIL on bulk cell viability

4.2.1.1 The MCF7, HCC 1954 and SUM149 cell lines are resistant to cell death induced by OH14

We tested the viability of the MCF7, HCC1954 and SUM149 cell lines after being treated with OH14 for 24hours after cells had been allowed to grow for 96 hours. This time point was chosen as we wanted to assess the effect of OH14 on CSC surrogate assays (such as mammospheres and ALDH1 positivity) and, as was established in Chapter 3, treatment for 96 hours with chemotherapy was needed to increase CSC-like behaviour. There was no significant difference in toxicity between 0.01 and 10μM, though the MCF7 cell line was the most sensitive at this level with around a 20% drop in viability, and the SUM149 cell lines the most resistant (Fig 4.1). There was a significant drop in viability at 100μM for all cell lines to around 40% for the MCF7 and HCC 1954 cell lines and 20% for the SUM149 cell line. As such a dose of 10μM was selected for further experiments as it was felt that this would offer the potential to observe sensitization in combined treatments.

A
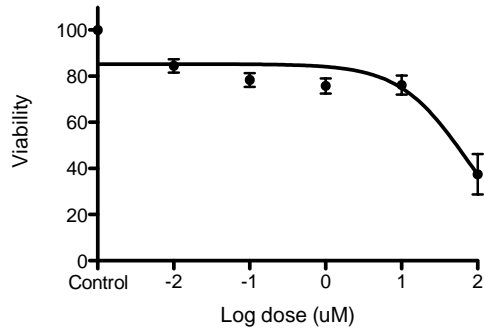
B
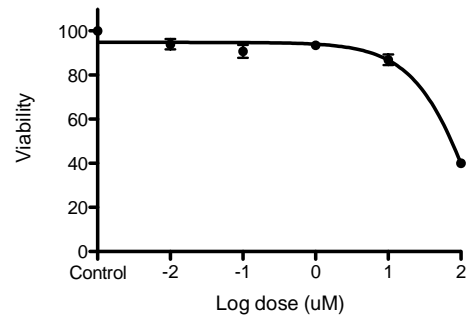
C
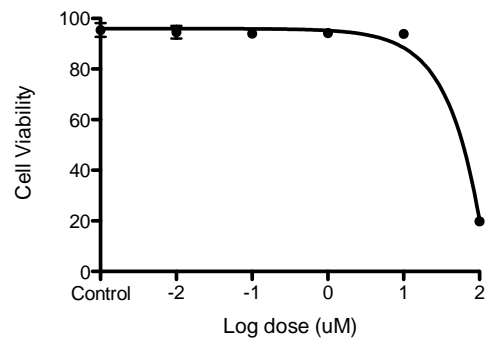
Figure 4.1- Viability of cell lines in response to OH14

The MCF7 (A), HCC 1954 (B) and SUM149 cell lines were plated and allowed to grow for 96 hours before a 24 hour treatment with OH14 at a 5-log dose range. Viability was assessed via Cell Titer Blue. Error bars represent SEM of the mean and results are an average of three experiments performed in triplicate.

4.2.1.2 The MCF7, HCC 1954 and SUM149 cell lines have different sensitivities to TRAIL

Previous studies have shown a wide range of response to TRAIL: varying from sensitive mesenchymal cell lines, such as SUM149, to resistant oestrogen receptor positive lines, such as MCF7. Her-2 receptor positive lines, such as HCC 1954, lie somewhere in the middle of the spectrum (Rahman, Pumphrey, and Lipkowitz 2009). Previous experiments in our laboratory have identified that TRAIL at 20ng/ml was the minimum concentration that led to the maximum amount of Caspase-8 activation (Piggott et al. 2011) and as such, in the absence of a reduction in viability of cell lines to TRAIL, this was used as a treatment dose.

Cells were plated out at 50000 cells/ml (25000 cells/ml for the SUM149 and MDA-MB-231 cell line) and treated at a time point that would correlate with the end of a four-day chemotherapy experiment (allowed to adhere overnight, left for 72 hours and then treated for 24 hours before analysis). This ensured that they were allowed to reach near-confluency before being treated for 24 hours with TRAIL. The MCF7 and HCC54 cell lines were resistant to TRAIL-induced apoptosis with a maximal reduction in viability of around 20% above 10ng/ml. In contrast to this, and as expected, the SUM149 cell line was exquisitely sensitive to TRAIL with an IC50 value of 0.13ng/ml (Fig 4.2).
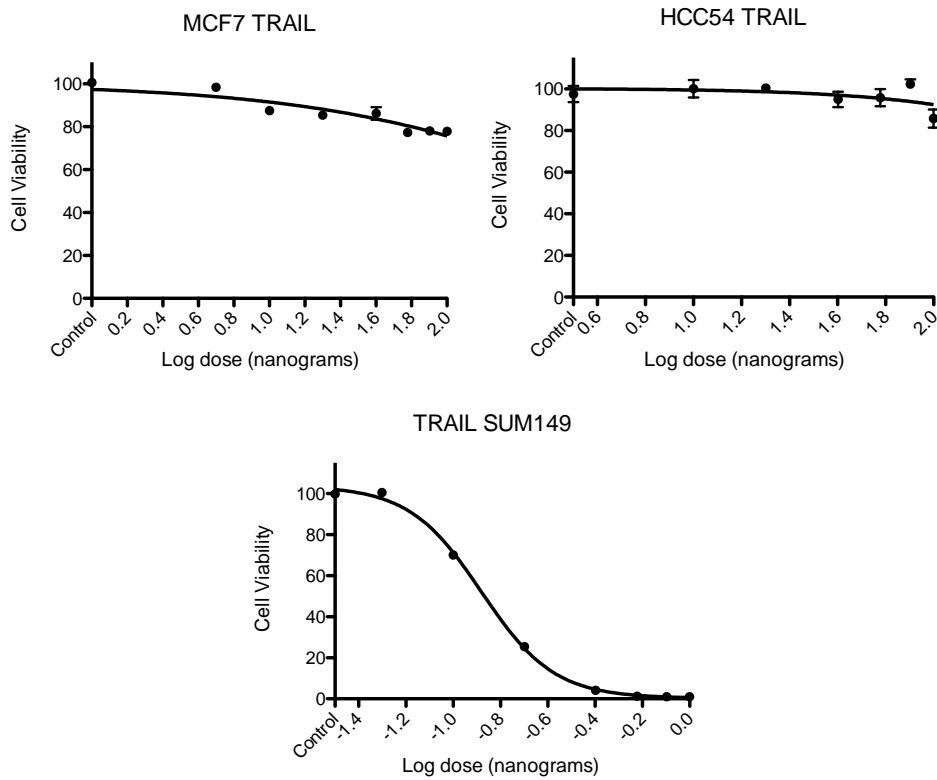
Figure 4.2- Susceptibility of cell lines to TRAIL

The MCF7 (A), HCC 1954 (B), and SUM 149 (C) cell lines were plated and left for four days (to near confluency) and treated for 24 hours. Viability was assessed via Cell Titer Blue. Error bars represent SEM of the mean and results are averages of a minimum of three independent experiments each performed with three internal technical replicates.

4.2.1.3 The combination of OH14 and TRAIL has different effects on the viability of the MCF7 and SUM149 cell lines

To determine the effect of cFLIP inhibition on TRAIL sensitivity we took the two cell lines that represented both TRAIL resistance (MCF7 cell line) and TRAIL sensitivity (SUM149 cell line). The respective cell lines were then plated into adherent conditions, allowed to grow for 96 hours and then treated with either control (DMSO vehicle), 10 μM OH14, TRAIL or a combination of 10 μM OH14 one hour before TRAIL for 24 hours. Viability was then assessed using a Cell Titer Blue assay.

Our results in the MCF7 cell line concur with those seen by other member of our group when using both OH14 (Hayward, unpublished work) and siRNA-mediated knockdown of cFLIP (Piggott et al. 2011). We saw a small but significant reduction in viability of around 10% compared to control when cells were treated with either single agent OH14 or TRAIL. The combination led to a further 10% reduction (to around 75% overall viability) that was significant compared to control and significantly more than either single agent OH14 or TRAIL (Fig 4.3A). However, it is likely that this effect is additive as the reduction in viability of the combined treatment is no more than the single effect of each compound alone added together.

The SUM149 cell line showed a different pattern of response, these cells were highly sensitive to TRAIL consistent with previous studies (eg. (Rahman et al. 2009) and there was no significant reduction seen with either single agent OH14 or the addition of OH14 to TRAIL as compared to TRAIL alone (Fig 4.3B)
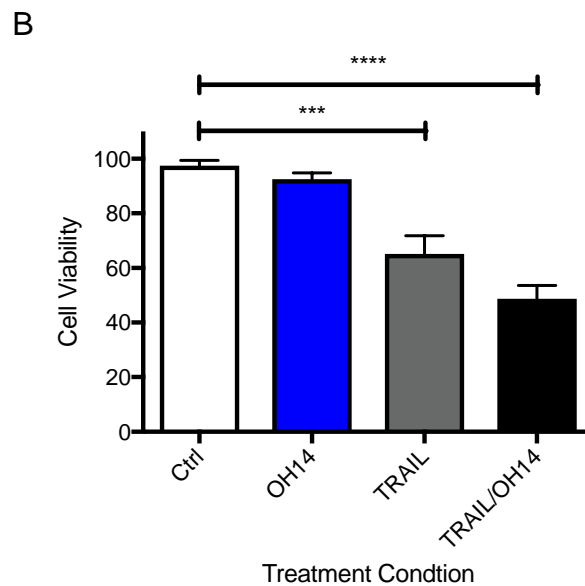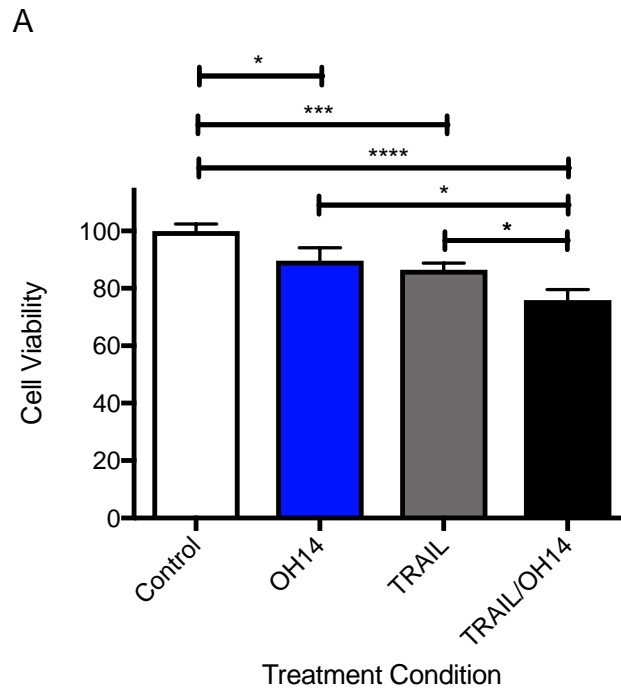
Figure 4.3 Susceptibility of the MCF7 and SUM149 cell lines to OH14 and TRAIL

The MCF7 (A) and SUM149 (B) cell lines were plated in adherent conditions for 96 hours before being treated with a vehicle control, 10 µM OH14, IC50 TRAIL or a combination of both 10µM OH14 and IC50 TRAIL (with OH14 added one hour before TRAIL) and left for 24 hours. Cell viability was assessed via Cell Titer Blue assay. Error bars represent SEM of the mean and results are an average of three experiments performed in triplicate. (T-test, *=p<0.1, **=p<0.01, ***=p<0.001 ****=p<0.0001).

4.2.2 Assessing the effect of TRAIL and OH14 on CSC-like behaviour

4.2.2.1 The combination of OH14 and TRAIL abrogates mammosphere formation in the MCF7, SUM149 and MDA-MB-231 cell lines

Previous work in our laboratory has shown that siRNA-mediated knockdown of cFLIP and treatment with TRAIL leads to the abrogation of mammosphere formation across a broad panel of breast cancer cell lines (Piggott et al. 2011; French et al. 2015) and further work with OH14 has repeated this finding (Hayward et al, unpublished work). The aim was to confirm that this was still the case after treatment with chemotherapy.

In these experiments, cells were plated into adherent conditions, allowed to grow for 96 hours and then treated with 10µM OH14 at least one hour before treatment with TRAIL at either 20ng/ml in the MCF7 cell line or 0.13ng/ml in the SUM 149 cell line.

There was a significant reduction in mammosphere formation in both Passage 1 and Passage 2 (Fig 4.4A) with the addition of TRAIL and TRAIL/OH14 In the MCF7 cell line. This was more than the effect of these treatments on the bulk cell population and therefore we can conclude that the combination of OH14 and TRAIL seems to preferentially target the CSC-like cells within the MCF7 cell line.

The same effect was seen on the SUM149 and MDA-MB-231 cell lines (Figs 4.4B-E), with significant reductions seen in mammosphere formation in both Passage 1 and 2 with the addition of TRAIL and OH14 and also a significant reduction between the TRAIL and OH/14 treatment arms in both passages. Here though, the results mirrored more closely the effect seen on the bulk cell population. The TNBC MDA-MB-231 cell line was added at this point as, as will become apparent, the focus of this work shifted to TNBC.

Passage 1

Passage 2

A

B

C

D

E
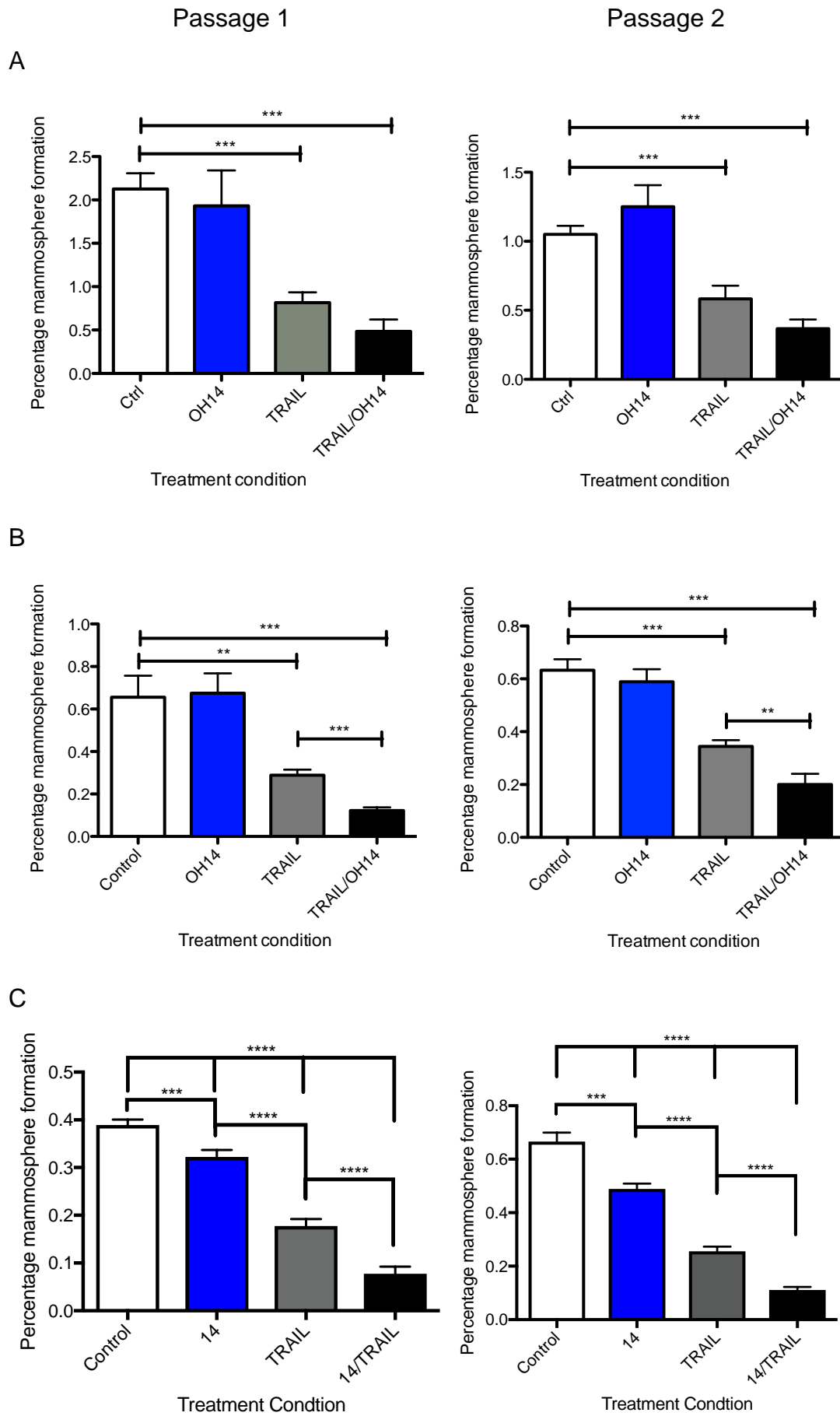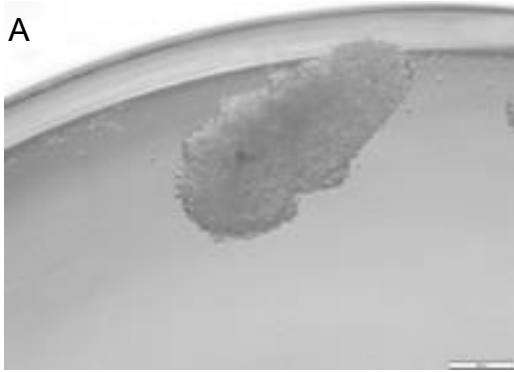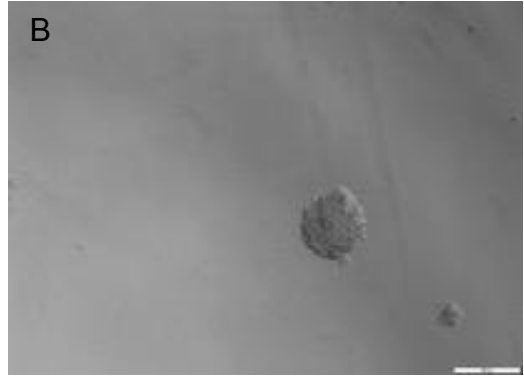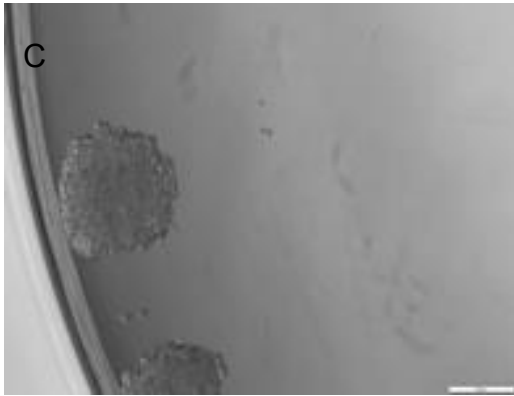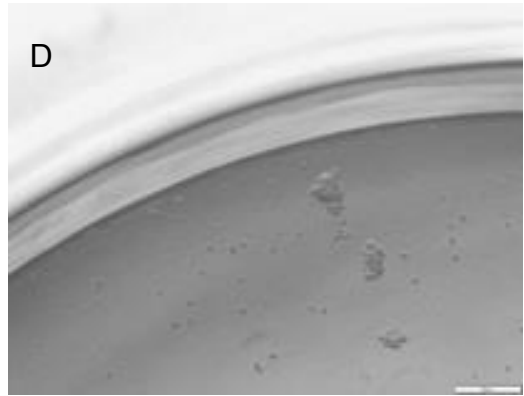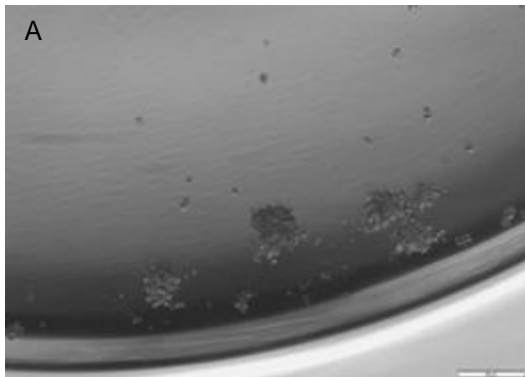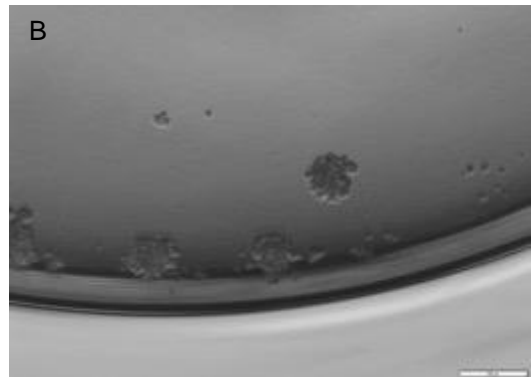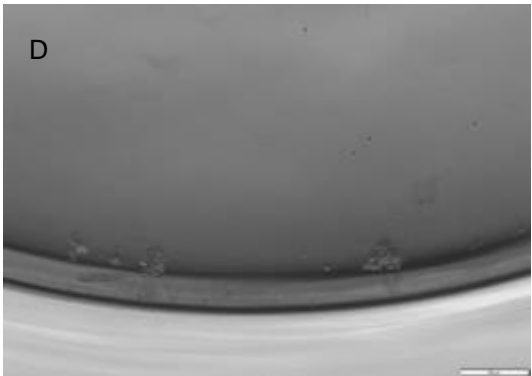
Figure 4.4 – Effect of TRAIL and OH14 on mammosphere formation in the MCF7 and SUM149 cell lines

The MCF7 (A) SUM149 (B) and MDA-MB-231 (C) cell lines were plated in adherent conditions for 96 hours before being treated with a vehicle control, OH14, TRAIL or a combination of both OH14 and TRAIL (with OH14 added one hour before TRAIL) and left for 24 hours. Cells were then dissociated and plated into non-adherent conditions at a fixed concentration for seven days before being counted (Passage 1), dissociated and plated again in a fixed concentration and counted seven days later (Passage 2). D and E, These pictures show mammosphere formation at the end of Passage 2 for A) control B) OH14 C) TRAIL and D)TRAIL/OH14 in the MDA-MD-231 (D) and SUM149 (E) cell lines respectively. Error bars represent SEM of the mean and results are an average of three experiments performed in triplicate. (T-test, *=p<0.1, **=p<0.01, ***=p<0.001 ****=p<0.0001). Scale bars 200μM.

4.2.2.2 A mathematical model shows that TRAIL and TRAIL/OH14 reduces absolute CSC number

Next we employed the same mathematical model that we used in Section 3.17 (Explained in detail in Methods section 2.4) to demonstrate the effect of OH14, TRAIL and the combination of the two on absolute CSC number surviving at the end of adherent treatment. In the MCF7 cell line, TRAIL led a significant reduction in CSC number as a single agent and this was proportionally more than the effect of single agent TRAIL on overall cell viability, suggesting it is an effective agent at targeting CSCs (Figs 4.5 A and C). This concurs with previous work (French et al. 2015; Piggott et al. 2011). This effect was further increased by the addition of OH14 with its magnitude, a roughly 50% further decrease in mammospheres, being proportionally more than the extra reduction in bulk cell viability seen with the addition of OH14 to TRAIL. This suggests some synergy in targeting CSCs when OH14 is added to TRAIL.

In the SUM149 cell line, OH14 alone led to a small reduction in absolute CSC number whereas TRAIL and TRAIL with OH14 led to large drop to around a third of the control treated group and a half of the TRAIL alone treated group respectively (Figs 4.5 B and C). As with the MCF7 cell line, the effect on CSC number was proportionally more than the reduction in bulk cell viability suggesting that TRAIL targets CSCs within the SUM149 cell line and that there is likely some synergism with the addition of OH14 on this CSC population.

A

	Viability (%)	Total cell number	P2 sphere formation (%)	CSCs in plate
Control	100	10000	1.05	105
OH14	89.6	8960	1.25	112
TRAIL	86.4	8640	0.58	50
TRAIL/OH14	76	7600	0.37	28

B

	Viability (%)	Total cell number	P2 sphere formation (%)	CSCs in plate
Control	97.5	10000	0.63	63
OH14	92.5	9250	0.59	55
TRAIL	65.2	6520	0.34	22
TRAIL/OH14	48.7	4870	0.2	10

C
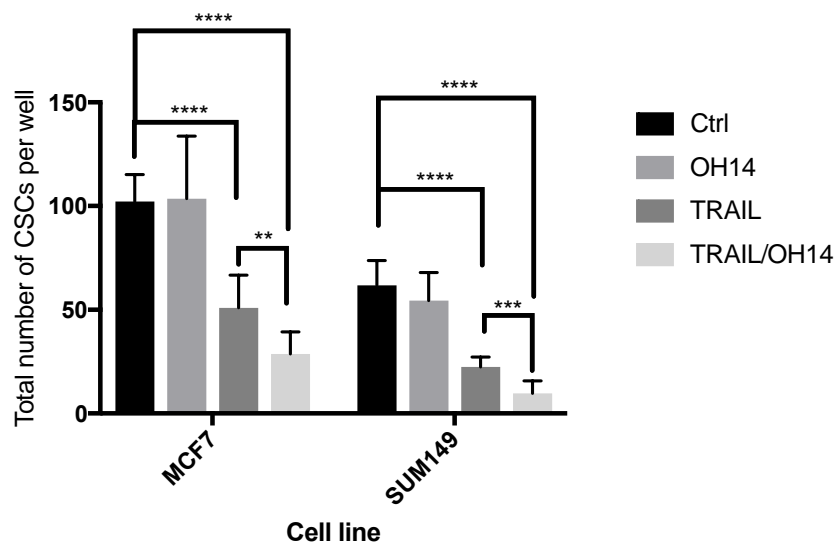
Figure 4.5 Effect of OH14 and TRAIL on absolute CSC number

The overall cell viability of the MCF7 (A) and SUM149 (B) cell lines was multiplied by the percentage mammosphere formation at the end of Passage 2 for the respective treatment condition to give an absolute CSC number remaining at the end of adherent treatment (C). Error bars represent SEM of the mean and results are an average of three experiments performed in triplicate. (T-test, *=p<0.1, **=p<0.01, ***=p<0.001 ****=p<0.0001).

4.2.3 Establishing the efficacy of OH14 and TRAIL after Chemotherapy

4.2.3.1 The combination of OH14 and/or TRAIL reduces mammosphere formation in the MCF7 and SUM149 cell lines after chemotherapy

We next wanted to assess whether the addition of OH14 and/or TRAIL had the same effect on mammosphere formation following chemotherapy. Cells were treated with chemotherapy (paclitaxel, docetaxel and FEC) at the IC50 doses described in Chapter 3 for 96 hours. At 72 hours either OH14, TRAIL or both (with OH14 being added 1 hour before TRAIL) were added and left for 24hrs before plating into mammosphere conditions.

Interestingly, for the MCF7 cell line, OH14 alone after chemotherapy led to a significant reduction in mammosphere formation in both Passages 1 and 2 in almost all types of chemotherapy tested- with the only non-significant result being in Passage 1 of the paclitaxel treated arm and most significant in the FEC treated samples (Fig 4.6 A-C). TRAIL after chemotherapy led to an even greater reduction in sphere formation and for almost all passages and chemotherapeutic agents and this effect was enhanced further by the addition of OH14 to TRAIL after chemotherapy (with the exception of Passage 1 after FEC treatment)

In the SUM149, triple negative inflammatory cell line across all chemotherapeutic agents and passages, there was a significant reduction in mammosphere formation after treatment with chemotherapy with single agent OH14, often at the same level as, or more than, the addition of TRAIL or TRAIL and OH14 (Figs 4.6 D-F and 4.7). This led us to explore whether there was a potential relationship between cFLIP, chemotherapy and a triple negative phenotype. Although the triple combination of chemotherapy, OH14 and TRAIL was not going to be excluded at this point, we wanted to assess whether there was merit in adopting a double combination approach rather than involving TRAIL as a third drug, as this would have implications for the validity and efficacy of drug administration in the clinical setting.

Passage 1 | Passage 2

A

B

110

C

Treatment condition

Treatment condition

D

Passage 1

Passage 2

Treatment condition
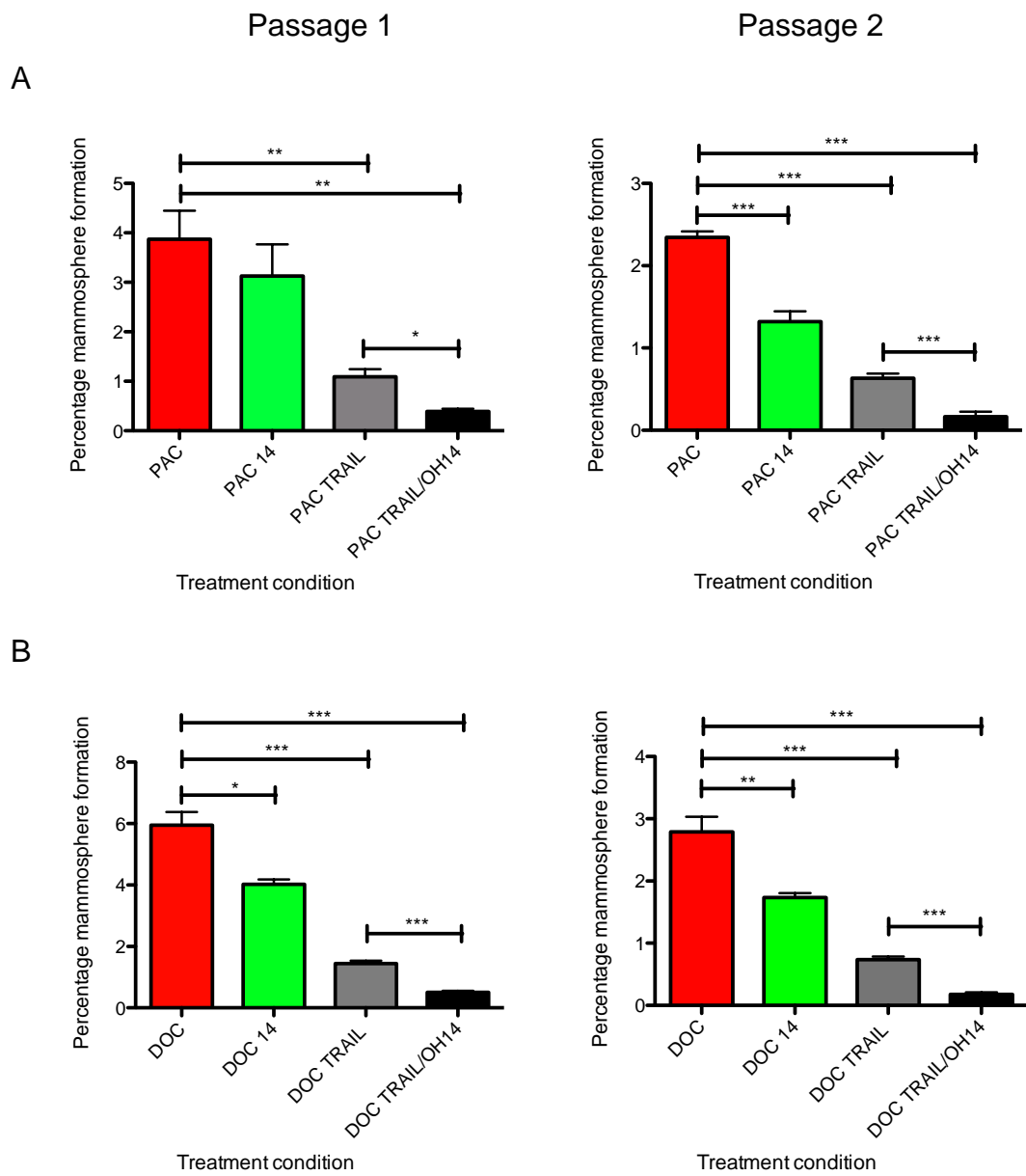
Treatment condition
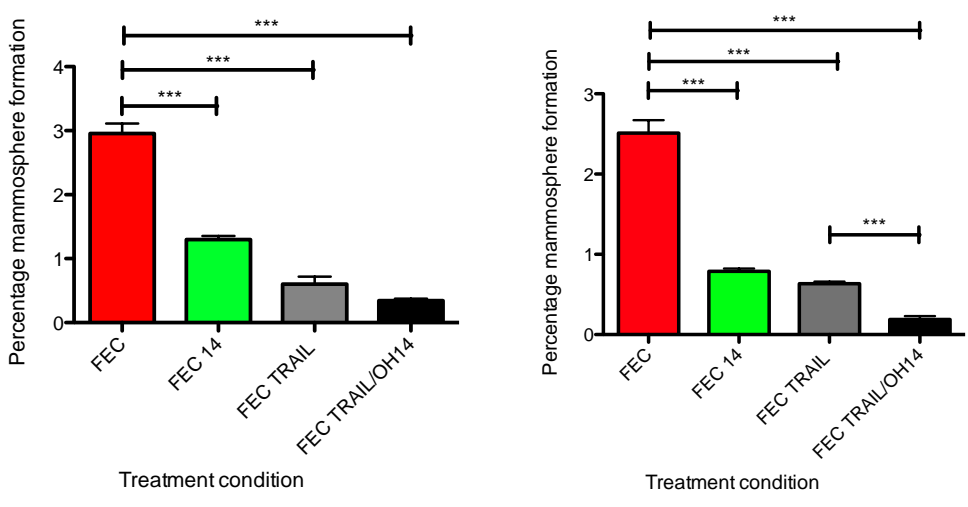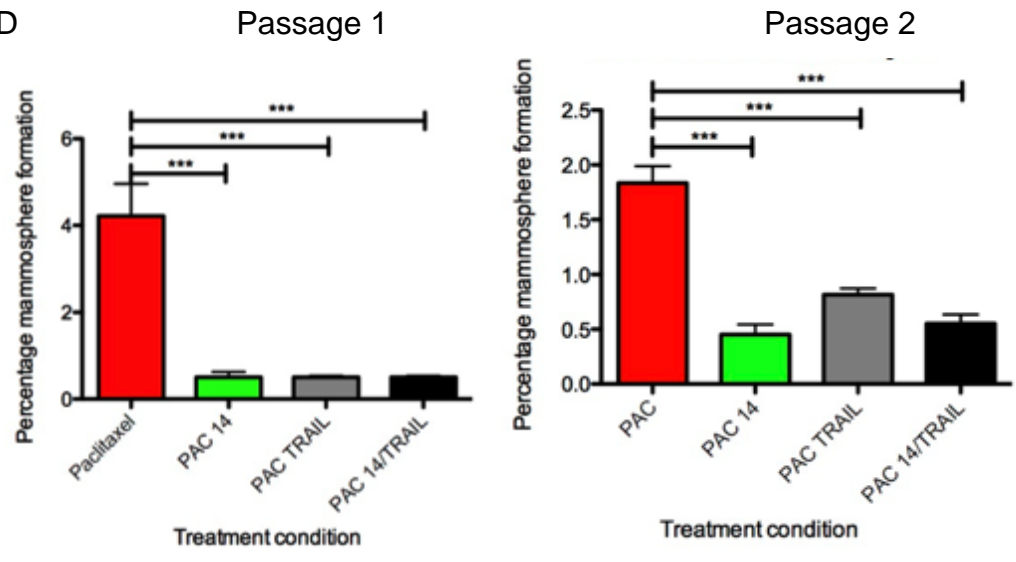
E
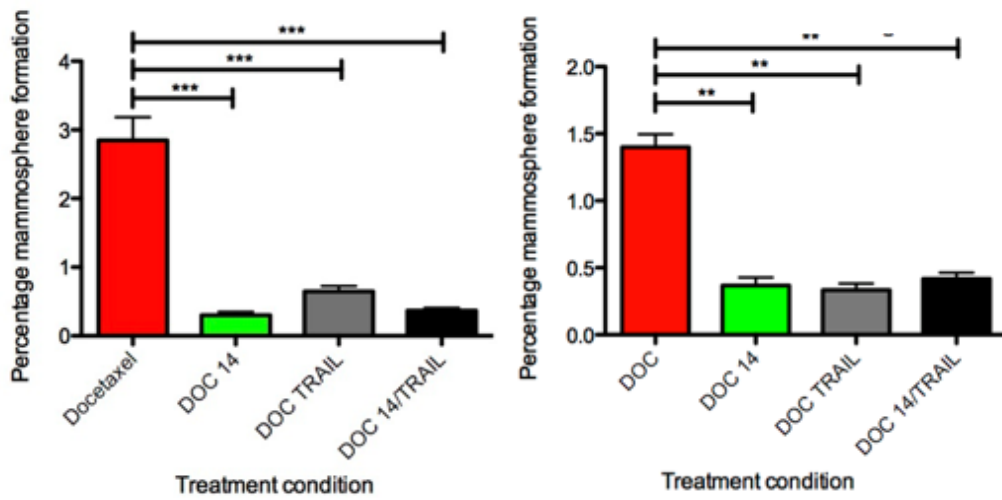
F
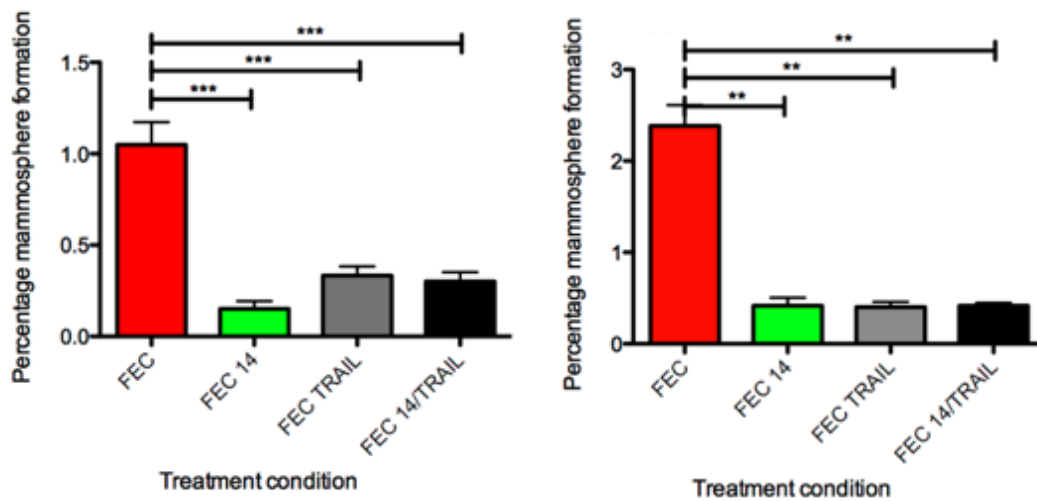
Figure 4.6 OH14 and TRAIL abrogate mammosphere formation after chemotherapy in both the MCF7 and SUM149 cell lines

The MCF7 (Fig 4.7A-C) and SUM149 (Fig 4.7 D-F) were plated into adherent conditons, treated with chemotherapy at the previously calculated IC50 values and 72 hours later OH14, TRAIL or both was added and left for a further 24 hours. Cells were then dissociated and plated into non-adherent conditions at a fixed cell concentration. After 7 days they were counted (Passage 1), dissociated and plated as single cells again at a fixed cell concentration. After a further 7 days they were counted again (Passage 2). Error bars represent SEM of the mean and results are an average of three experiments performed in triplicate. (T-test, *=p<0.1, **=p<0.01, ***=p<0.001 ****=p<0.0001).
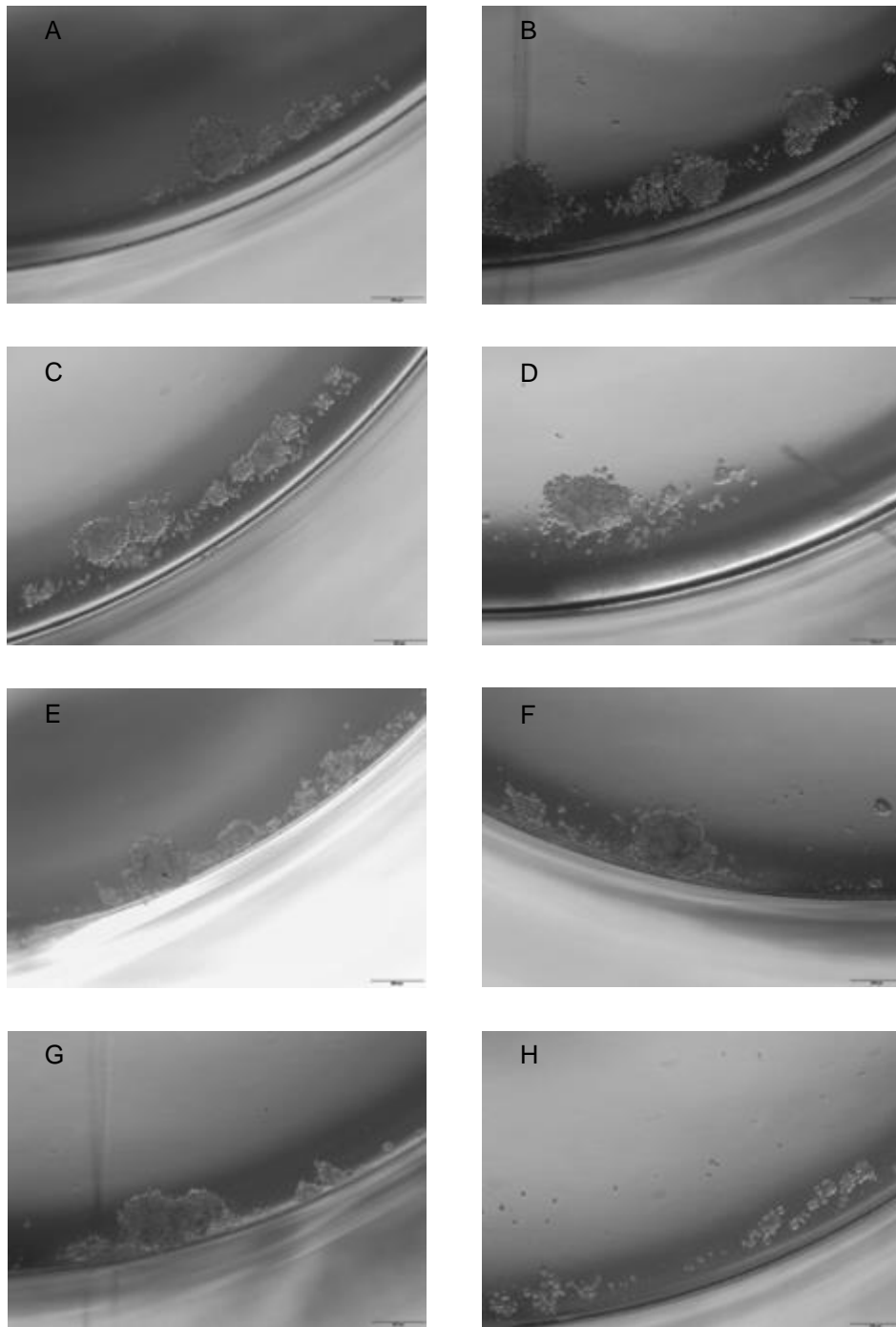
Figure 4.7 SUM149 Mammospheres increase after chemotherapy and are abrogated by the addition of OH14.

Representative pictures at the end of Passage 2 of SUM149 mammospheres that had been treated with: A) control (vehicle) B) OH14 C) Paclitaxel D) Paclitaxel and OH14 E) Docetaxel F) Docetaxel and OH14 G) FEC H) FEC and OH14. Scale bars 200μM.

4.2.4 Investigating a link between cFLIP and Paclitaxel

As stated in Section 4.1.3, a potential relationship between cFLIP and paclitaxel has previously been reported by several groups (Day et al. 2006; Day, Huang, and Safa 2008b; Park et al. 2004; Wang et al. 2005). Thus it has been reported that paclitaxel appears, at least in part, to mediate its apoptotic effects in a ligand-independent manner through the extrinsic apoptotic pathway. Although a strong relationship had been seen between FEC, docetaxel and paclitaxel and OH14 in the SUM149 cell line, a sound scientific rationale therefore existed in investigating paclitaxel alone. As an antagonist of this pathway, cFLIP is a natural target to try and increase the cytotoxic effect of paclitaxel against both bulk cells and CSCs. In addition, it was decided to assess whether this relationship existed in TNBC cell lines- as the SUM149 cell line had responded better than the MCF7, oestrogen receptor positive, cell line in the previous section. As the prognosis for TNBC is the worst of all the molecular subtypes of breast cancer and an area where novel treatments are urgently needed, two further TNBC cell lines were added, MDA-MB-436 and MDA-MB-231, in order to give a panel of three TNBC cell lines in which to examine the effect of this combination

4.2.4.1 TNBC cell lines, but not ER or HER-2 positive cell lines, are sensitized to paclitaxel by OH14.

The effect of paclitaxel and OH14 was assessed on the MCF7, HCC1954, SUM149, MDA-MD-436 and MDA-MD-231 cell lines. Cells were plated at 100000 cells/ml in 96 well plates, allowed to adhere overnight and then treated with a range of paclitaxel doses (1nM, 5nM and 10nM) for 24hrs with either vehicle or 10μM of OH14 one hour before paclitaxel.

Though the addition of OH14 to the ER-positive MCF7 and Her2-positive HCC1954 cell lines did not increase the cytotoxicity seen with paclitaxel, the three TNBC cell lines showed a significant reduction in viability of 19.6%, 19.75% and 25.45% for the MDA-MB-231, SUM149 and MDA-MB-436 lines respectively when OH14 was added one hour before paclitaxel at a 10nM dose (Fig 4.8A). This gave credence to the hypothesis that TNBC lines may be sensitive to the combination of paclitaxel and c-FLIP suppression.

In order to continue and assess the relationship between OH14 and paclitaxel in TNBC cell lines the 96hr paclitaxel IC50 value of both the MDA-MB-231 and MDA-MB-436 cell was established at 5.01nM respectively 2.1nM (Fig 4.8 B and C).

A

116
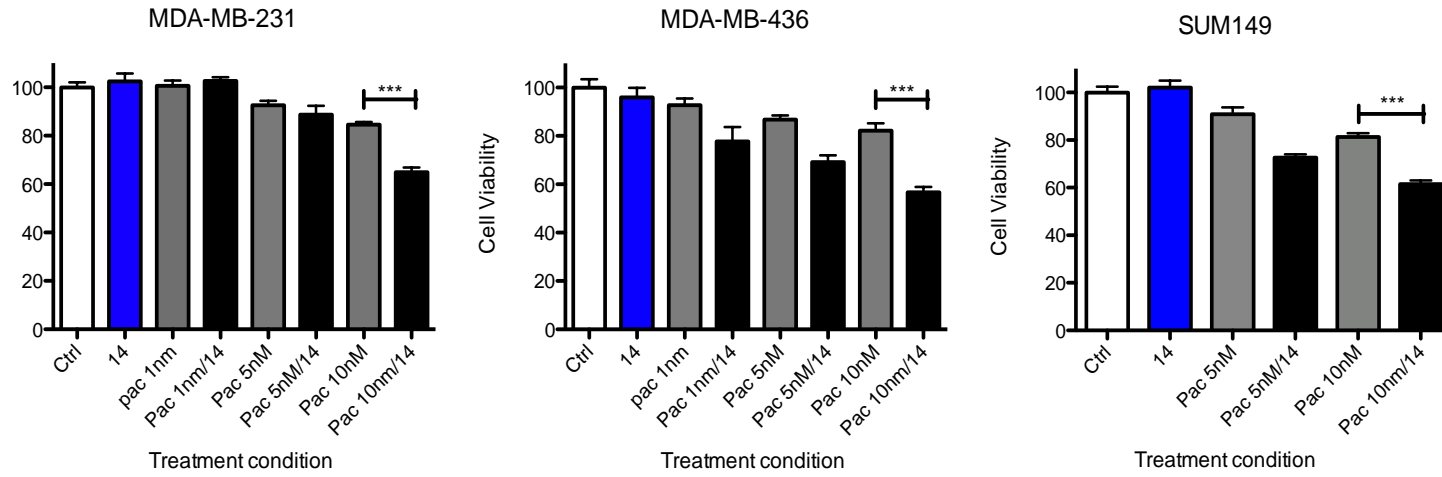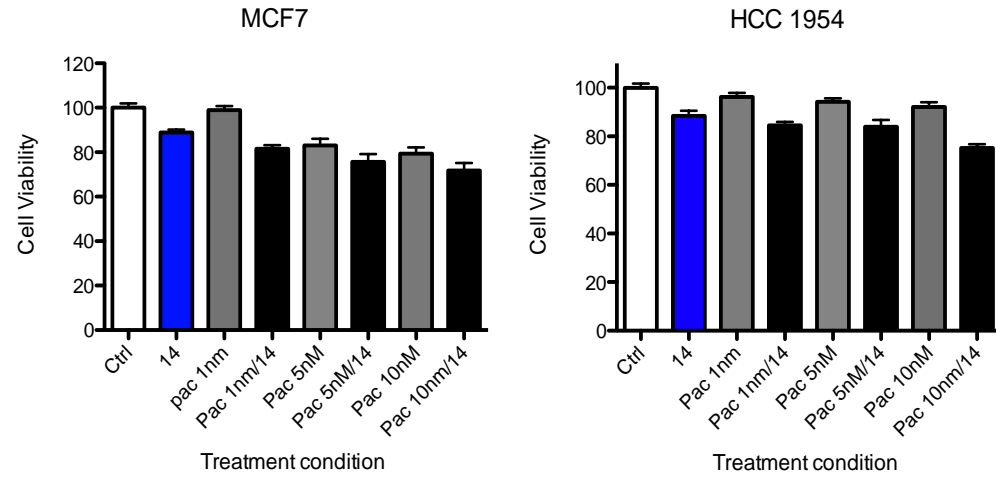
B
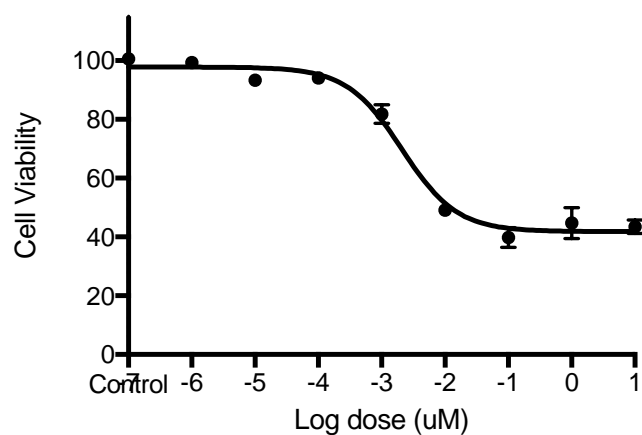
C
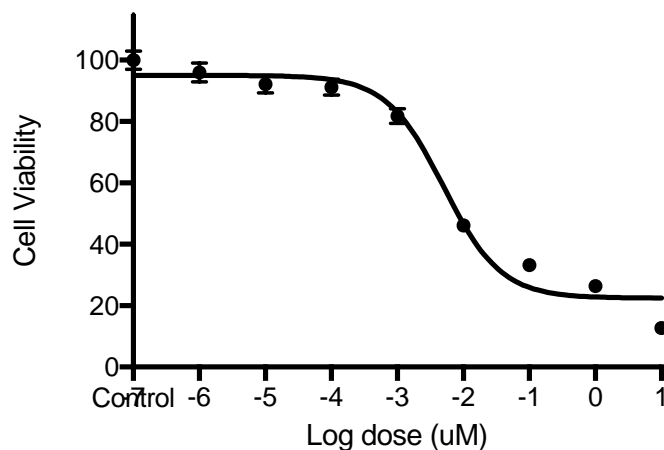
Figure 4.8- OH14 enhances the cytotoxic effect of paclitaxel in a panel of TNBC cell lines

A, the MCF7, HCC1954, MDA-MB-231, MDA-MB-436 and SUM149 cell lines were plated at 100000 cells/ml to allow near confluency before a 24 hour treatment with either vehicle control, 10µM OH14, varying doses of Paclitaxel alone or varying doses of paclitaxel with OH14. B and C, the 96hr IC50 values for both the MDA-MB-436 (2.1nM) and MDA-MB-231 (5.01nM) were then established to be used in further experiments. Error bars represent SEM of the mean and results are an average of three experiments performed in triplicate. (T-test, *=$p<0.1$, **=$p<0.01$, ***=$p<0.001$ ****=$p<0.0001$).

4.2.4.2 OH14 and TRAIL lead to a decrease in the viability of MDA-MB-231 and SUM149 cell lines both with and without chemotherapy

We wanted to assess the effect of OH14, both with paclitaxel and in combination with TRAIL, on cell viability in TNBC cell lines. 72hrs after chemotherapy was added to MDA-MB-231 or SUM149 cell lines, either vehicle, TRAIL, OH14, or OH14 and TRAIL was added for 24hrs before the cells were analysed by Cell Titer Blue.

The addition of OH14 did not lead to a reduction in viability but the addition of TRAIL led to a significant reduction in both the MDA-MB-231 (Fig 4.9 A) and SUM149 (Fig 4.9 B) cell lines. Additionally, in the MDA-MB-231 cell line, the combination of OH14 and TRAIL led to a significant drop above TRAIL treatment alone, something that was not seen in the SUM149 cell line. After treatment with paclitaxel the addition of OH14 alone led to a significant reduction in viability in the MDA-MB-231 cell line (Fig 4.9C) but not in the SUM149s (Fig 4.9D). Indeed, in the MDA-MB-231 cell line it was more effective as a single agent than TRAIL, although the combination of both was the most effective treatment with a significant drop in viability compared to all other arms. In the SUM149 line, the addition of single agent OH14 or TRAIL after paclitaxel did not lead to a significant drop in viability, although the combination treatment did.
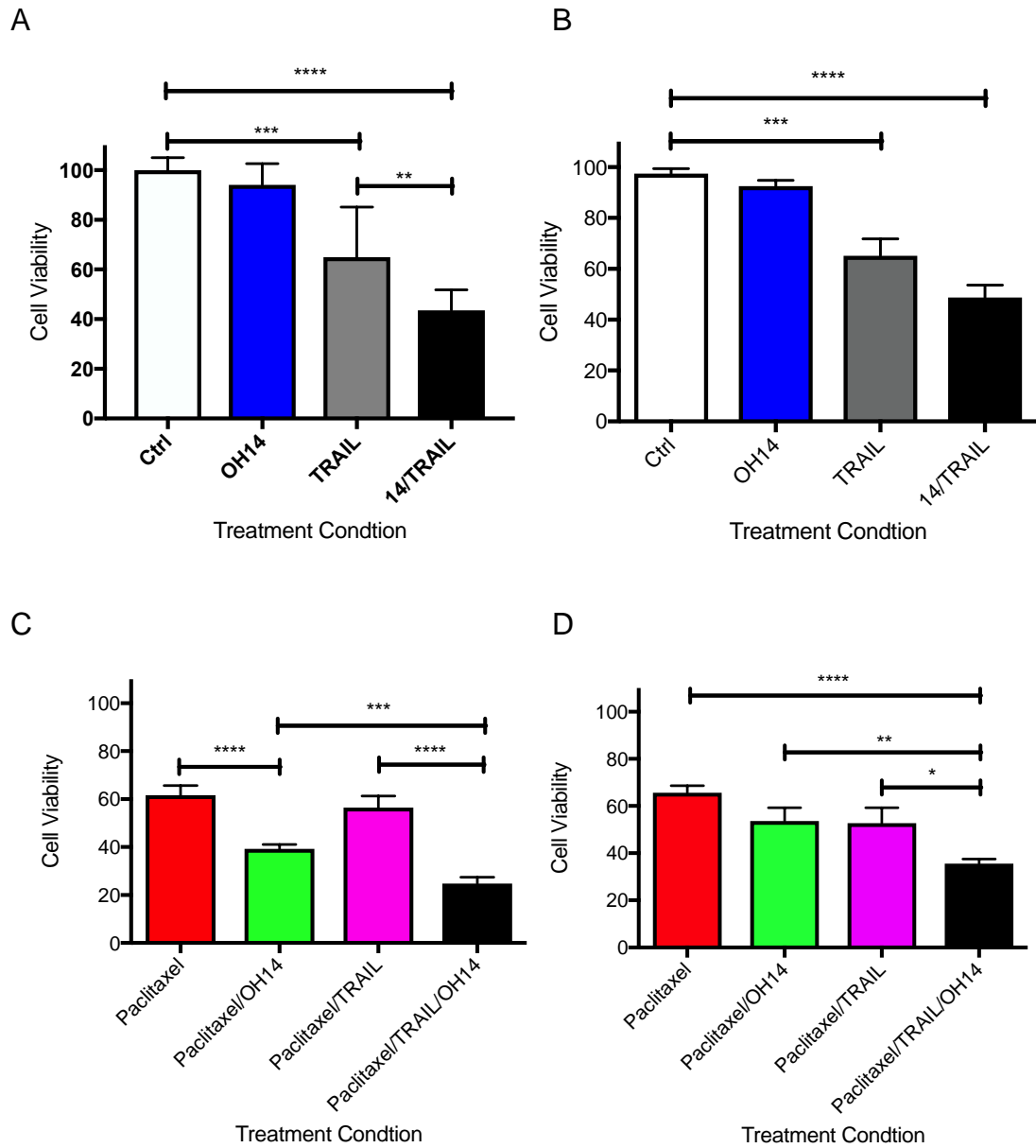
Figure 4.9- Effect of OH14 and TRAIL alone and with chemotherapy on cell viability in the MDA-MB-231 and SUM149 cell lines

The effect of OH14, TRAIL or the combination was assessed on the MDA-MB-231 (A) and SUM149 (B) cell lines. These drugs were then tested again 72hrs after the addition of IC50 paclitaxel before being left for 24hrs and analysed by CellTiter Blue (C, MDA-MB-231 and D, SUM149). Error bars represent SEM of the mean and results are an average of three experiments performed in triplicate. (T-test, *=p<0.1, **=p<0.01, ***=p<0.001 ****=p<0.0001).

119

### 4.2.5 Paclitaxel followed by OH14 reduces mammosphere formation in a panel of TNBC cell lines

Next we examined the effect of treating three TNBC cell lines (MDA-MB-231, MDA-MB-436 and SUM149) with paclitaxel for 96 hours with OH14 added at 72 hours after chemotherapy treatment. Treatment with paclitaxel increased mammosphere formation in both Passage 1 and Passage 2 across all passages in all cell lines (Fig 4.10), suggesting that as seen previously in the MCF7 and SUM149 cell lines, paclitaxel significantly increased the CSC content of these cell lines at the end of treatment.

The addition of OH14 as a single agent did not lead to a significant difference compared to the control (vehicle) arm but did reverse the significant increase seen with paclitaxel (Figs 4.10 and 4.11). This suggests that the combination of paclitaxel and OH14 may be a viable treatment option to target CSCs that are present either before chemotherapy or that are induced by chemotherapy after treatment with paclitaxel.
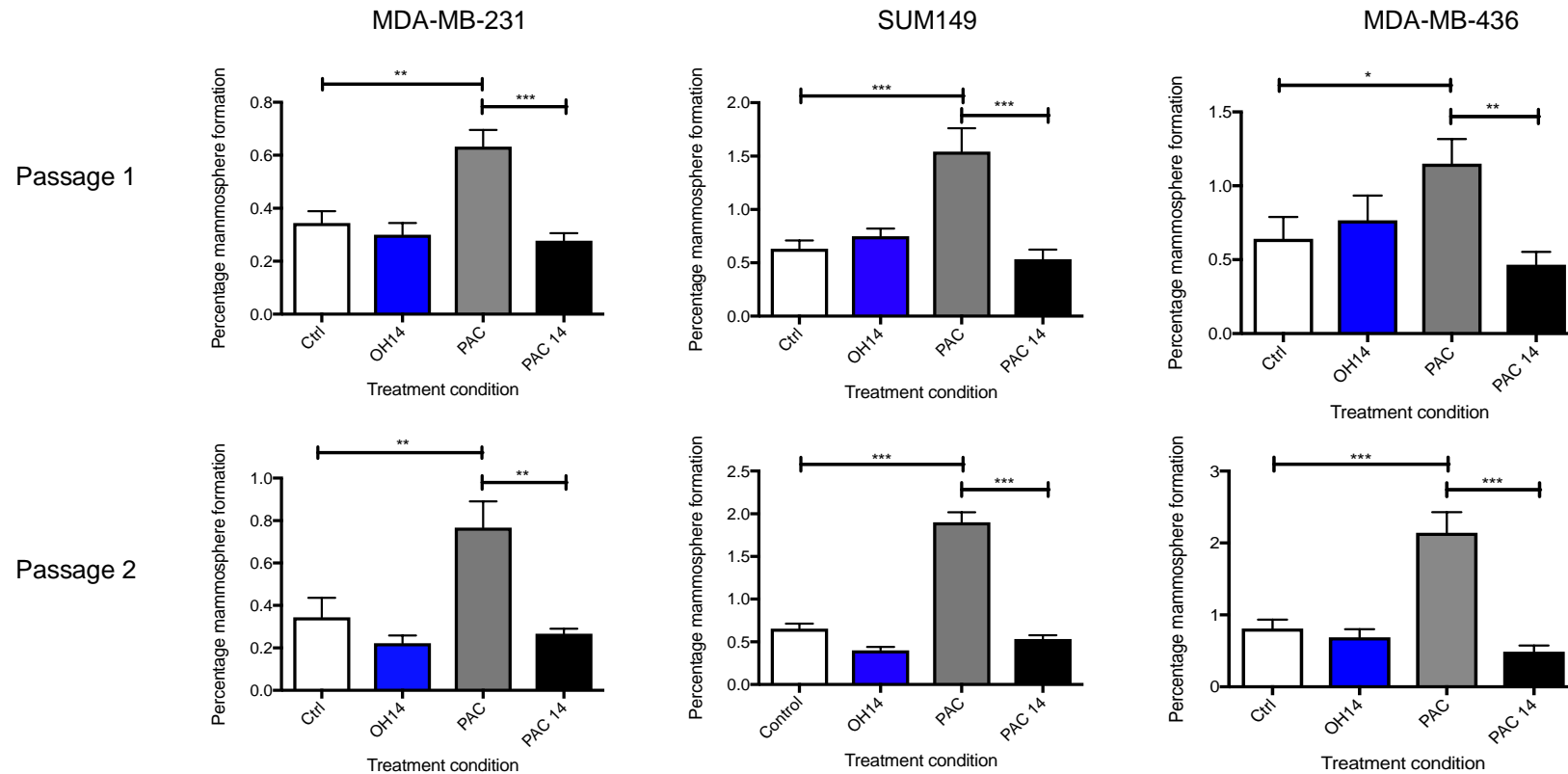
Figure 4.10- Effect of Paclitaxel and OH14 on mammosphere formation in a panel of TNBC cell lines

The MDA-MB-231, SUM149 and MDA-MB-436 cell lines were plated into adherent conditions for 96hrs and treated with IC50 paclitaxel +/- 10 μM OH14 at 72 hrs. Cells were then dissociated and plated into non-adherent conditions at a fixed cell concentration. After 7 days they were counted (Passage 1), dissociated and plated as single cells again at a fixed cell concentration and a further 7 days they were counted again (Passage 2). Error bars represent SEM of the mean and results are an average of three experiments performed in triplicate. (T-test, *=p<0.1, **=p<0.01, ***=p<0.001 ****=p<0.0001).

A)
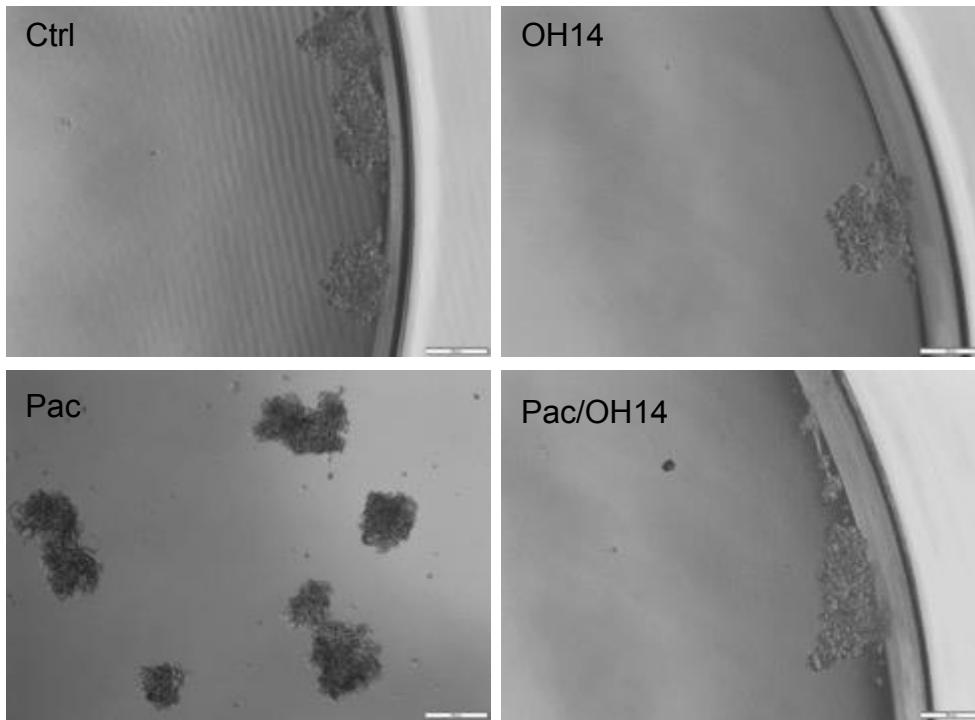
B)
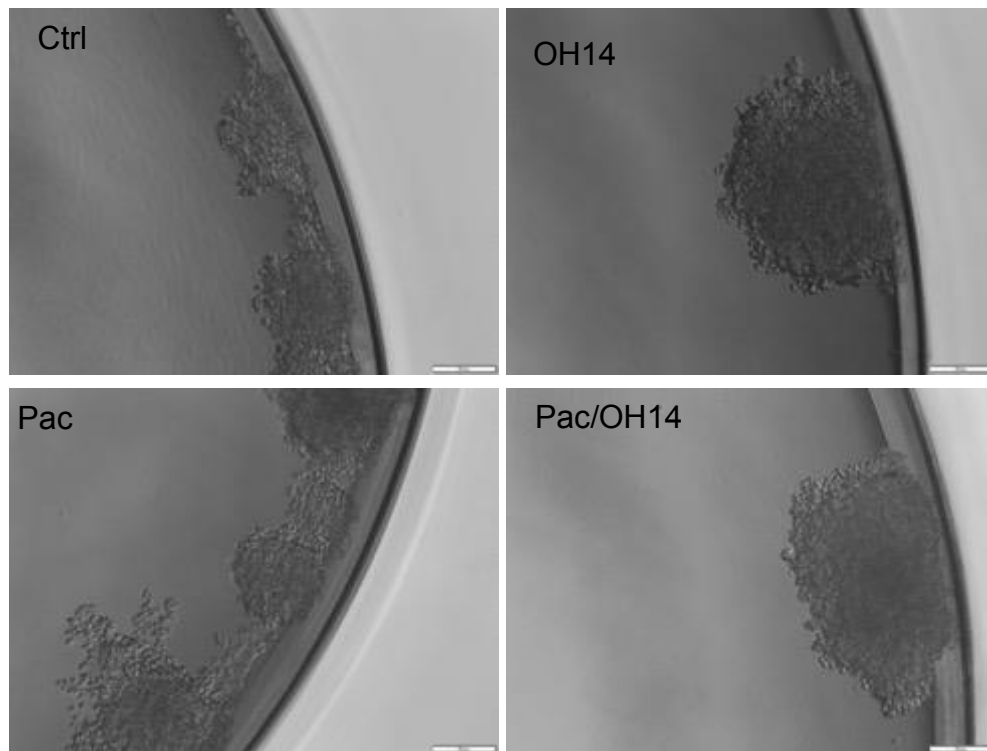
Figure 4.11- Representative pictures of mammosphere formation in the MDA-MB-436 (A) and SUM 149 (B) at the end of Passage 2 .

Scale bars 200μM.

4.2.6 Use of a mathematical model to assess whether OH14 preferentially targeted bCSCs after chemotherapy

To evaluate the effect of OH14 and paclitaxel on bCSCs in two TNBC cell lines, the mathematical model employed in Chapter 3 was used again to show the effect of treatment, with and without chemotherapy, on bCSCs.

Single agent OH14 did have an effect in reducing the total number of CSCs in both the MDA-MB-231 and SUM149 cell lines as a single agent. Although paclitaxel increased the remaining CSC population above control in the SUM149 cell line it importantly did not significantly change the number in the MDA-MB-231 cell line (Fig 4.12). This addition of OH14 after paclitaxel not only reversed the increase in bCSC number but led to a reduction in bCSCs below the level in the control group. If paclitaxel demonstrated equal efficacy in targeting CSCs and non-CSCs within the original population a proportional reduction in CSC number with viability would be expected. However, once again in these experiments the total number of CSCs actually increases above control, even though there is a significant reduction in viability. This effect is completely reversed by the addition of OH14- the addition of which leads to an almost proportional reduction of CSCs in line with cell viability. For example, in the MDA-MB-231 cell line the total number of CSCs falls from 42 to 11, a 74% reduction- this correlates with a reduction in overall cell viability of 60.7%. In Chapter 3, the point was made that chemotherapy not only poorly targets CSCs but also can increase them, likely through inducing signaling pathways. Therefore, OH14, by reducing the total number of CSCs to below control levels, must be enabling not only the paclitaxel to kill CSCs, but also blocking the signaling pathways that lead to CSC induction. This will be explored further in Chapter 5.

A

	Viability (%)	Total cell number	P2 sphere formation (%)	CSCs in plate
Control	100	10000	0.34	34
OH14	94.1	9410	0.22	21
Paclitaxel	61.7	6170	0.77	48
Paclitaxel/OH14	39.3	3930	0.27	11

B

	Viability (%)	Total cell number	P2 sphere formation (%)	CSCs in plate
Control	97.5	9750	0.66	64
OH14	92.5	9250	0.40	37
Paclitaxel	65.7	6570	1.9	125
Paclitaxel/OH14	53.7	5370	0.53	28

C
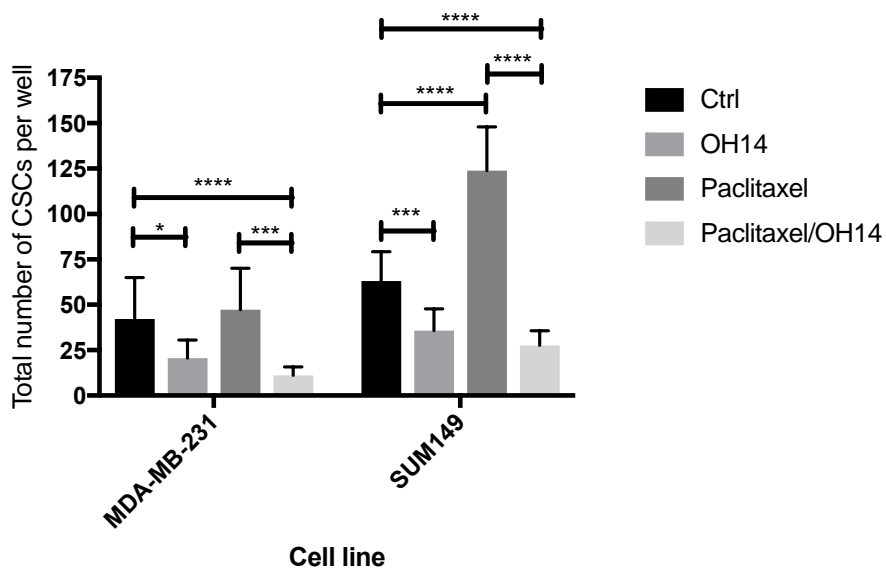
Figure 4.12- Total CSC number after treatment with paclitaxel and OH14

The overall cell viability of the MDA-MB-231 (A) and SUM149 (B) cell lines was multiplied by the percentage mammosphere formation at the end of Passage 2 for the respective treatment condition to give an absolute CSC number remaining at the end of adherent treatment (C). Error bars represent SEM of the mean and results are an average of three experiments performed in triplicate. (T-test, *=p<0.1, **=p<0.01, ***=p<0.001 ****=p<0.0001).

4.2.7 The effect of OH14 and TRAIL on the ALDH+ population of TNBC lines

In order to confirm that the effects of OH14 on PAC-induced tumoursphere numbers was due to an increase in CSCs, an independent surrogate marker of CSC-like activity was used. ALDH-positive cells are enriched for CSC-like properties, and initially we wished to confirm our previous published observations that c-FLIP suppression and TRAIL treatment reduced the proportion of ALDH-positive cells in the cancer cell population (Piggott et al. 2011). MDA-MB-231 or SUM149 cell lines were plated into adherent conditions, left for 96 hours and then treated with either TRAIL, OH14 or a combination of both for 24 hours.

In both the MDA-MB-231 and SUM149 cell lines, there was a significant reduction in the ALDH+ population with single agent OH14 and TRAIL arm as well as the combined OH14+TRAIL arm (Fig. 4.13). In the MDA-MB-231 cell line, the biggest effect was seen in the OH14 alone treatment arm.

A
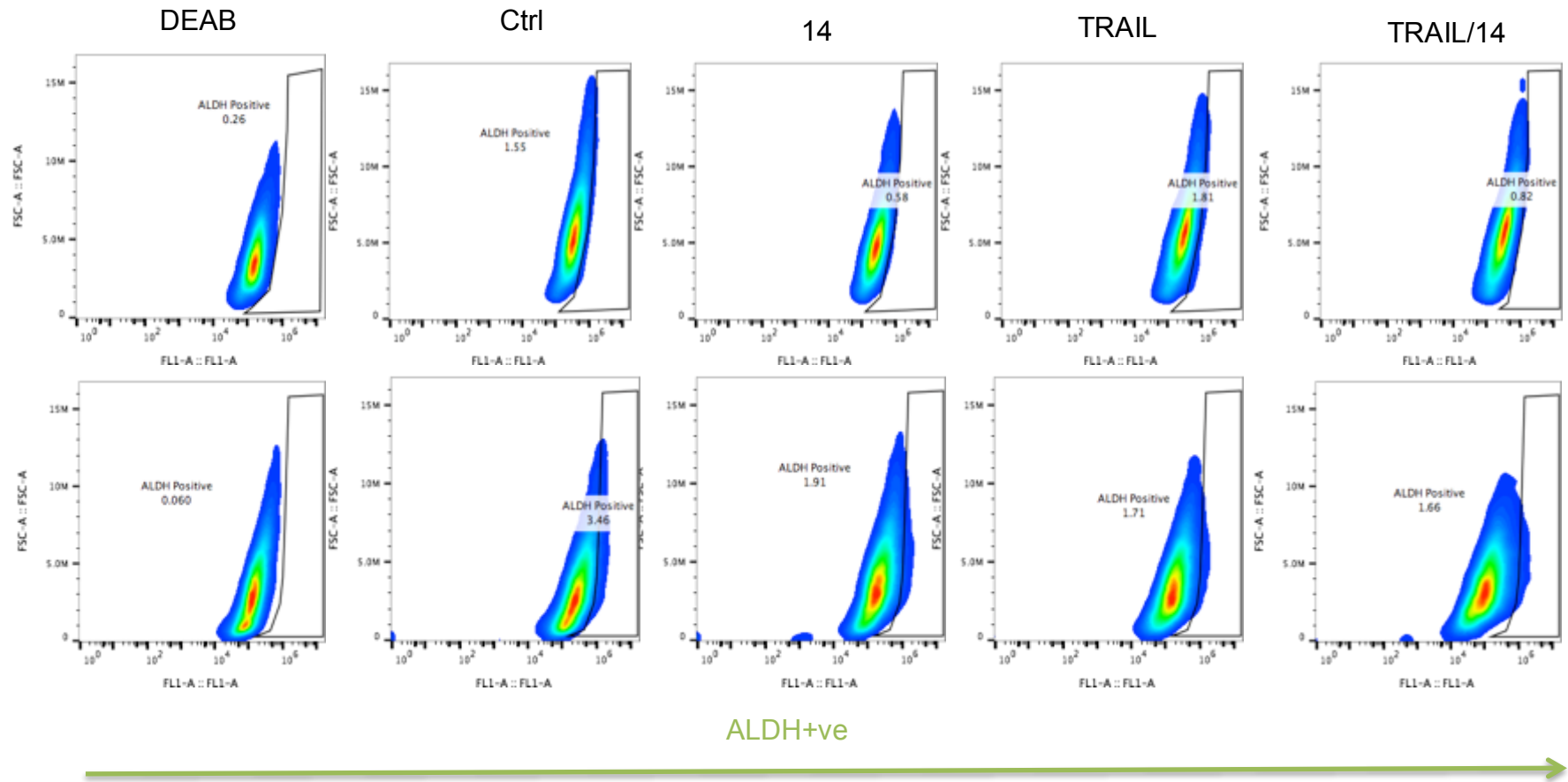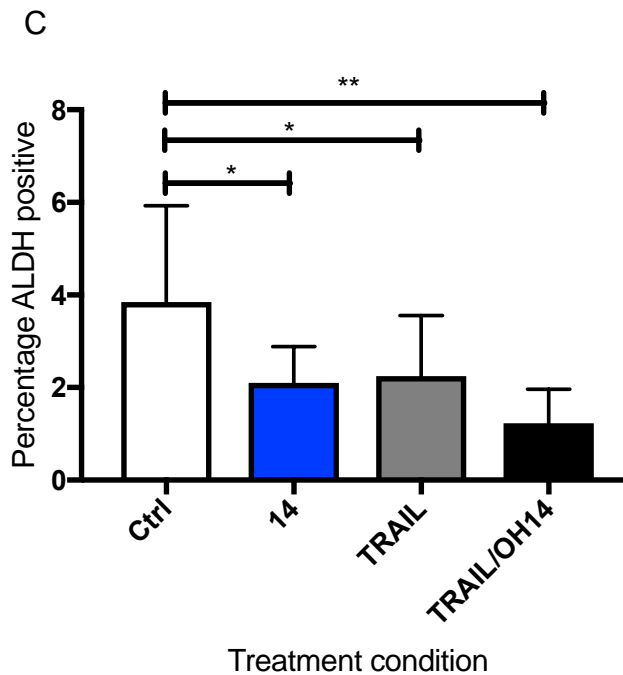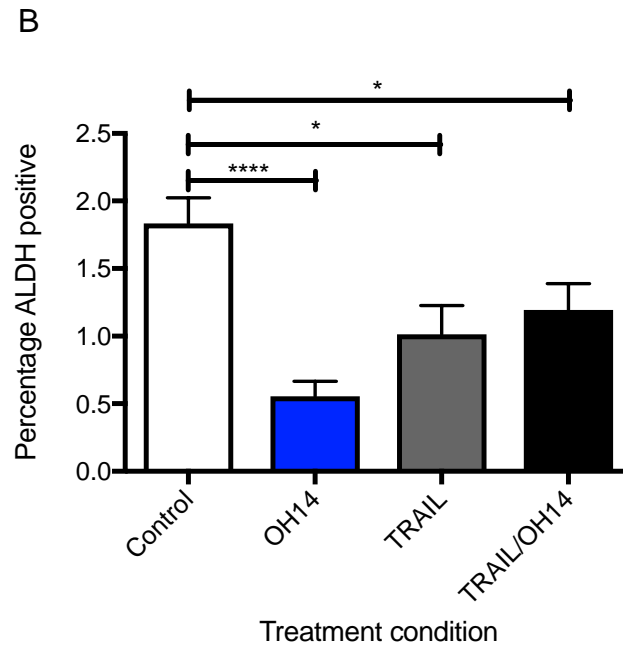
Figure 4.13 Effect of OH14 and TRAIL on mammopshere formation and ALDH+ in representative TNBC cell lines

The MDA-MB-231 (B) and SUM149 (C) cell lines were plated into adherent conditions and 96 hours later treated with Ctrl, OH14, TRAIL or TRAIL+OH14 for 24 hours. Cells were dissociated and underwent flow cytometry using the Aldeflour assay following the manufacturers protocol. Representative plots are shown in A. Error bars represent SEM of the mean and results are an average of three experiments performed in triplicate (SUM149 Flow cytometry was 2 repeats). (T-test, *=p<0.1, **=p<0.01, ***=p<0.001 ****=p<0.0001).

4.2.8 OH14+/- TRAIL with paclitaxel targets the ALDH+ population in TNBC cell lines

Next an assessment of the response of the ALDH+ population in the MDA-MB-231 and SUM 149 cells to OH14 with paclitaxel was assessed and in addition the effect of adding TRAIL with paclitaxel was assessed in the MDA-MB-231 cell line. The MD-MB-231 or SUM149 cell lines were plated into adherent conditions, the relevant IC50 value (MDA-MB-231 4.989nM, SUM149 2.41nM) of paclitaxel was added after cells were allowed to adhere overnight and left for 96 hours with OH14 +/- TRAIL being added 72hours later for the final 24 hours of the experiment.

Consistent with the mammosphere data, in the MDA-MB-231 cell line, there was a significant rise in the ALDH+ population with paclitaxel compared to the untreated (vehicle) control group and this increase was significantly reduced by the addition of OH14, TRAIL or the combination of the two (Fig 4.14A). The effect of treatment with OH14 and TRAIL after paclitaxel was significantly more than single agent TRAIL after paclitaxel but not OH14 after paclitaxel

When evaluating the effect of OH14 alone after paclitaxel, for both the MDA-MB-231 and SUM149 cell lines, there was a significant reduction of the highly significant increase in ALDH+ seen with paclitaxel, with the addition of OH14 (Figs 4.14 B and C). As shown previously, in the MDA-MB-231 cell line, there was a significant reduction in the ALDH+ population with single agent OH14 without chemotherapy. Interestingly, there was a much larger increase in the ALDH+ population in the SUM149 cell line compared to the MDA-MB-231 cell line.

A

ALDH+ve

130
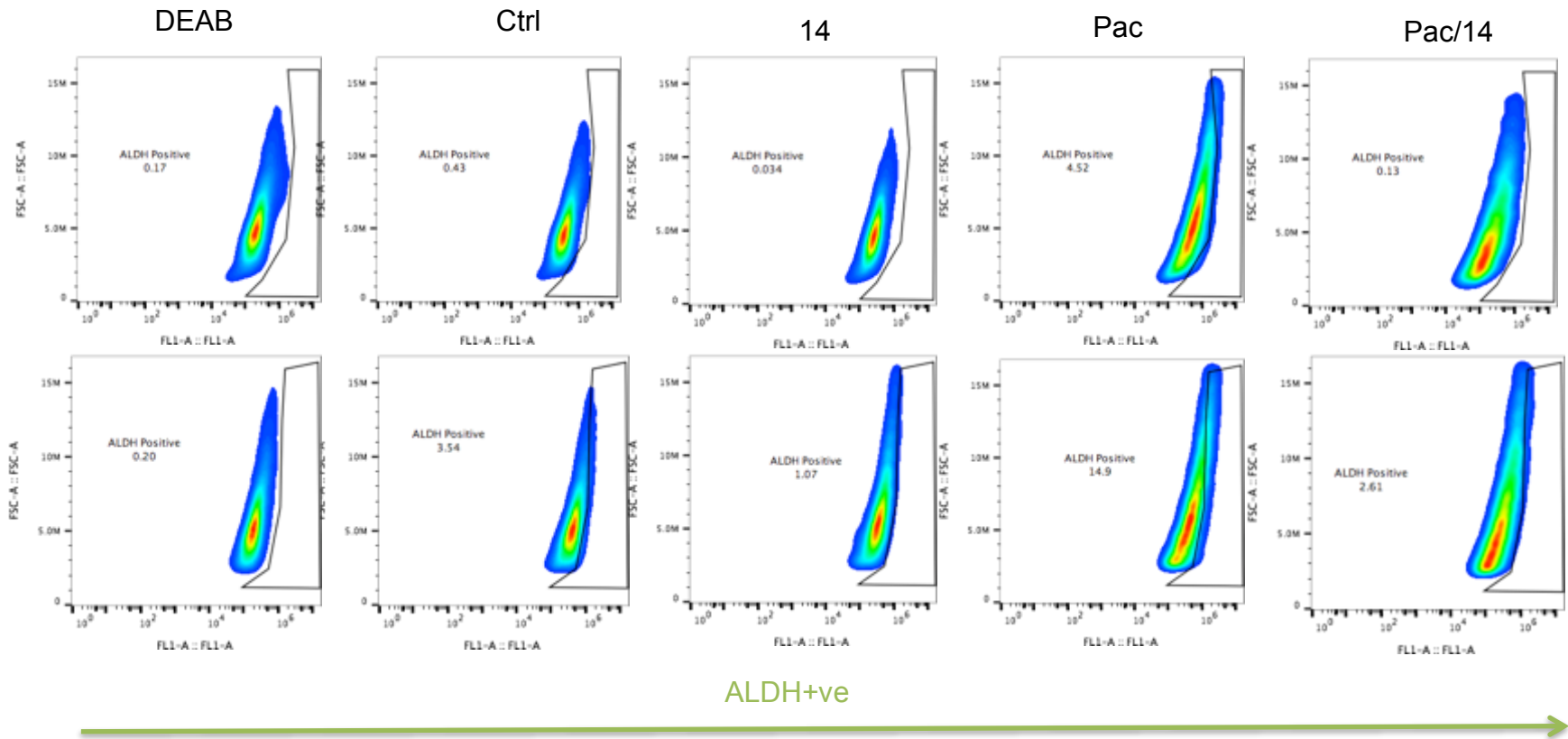
B
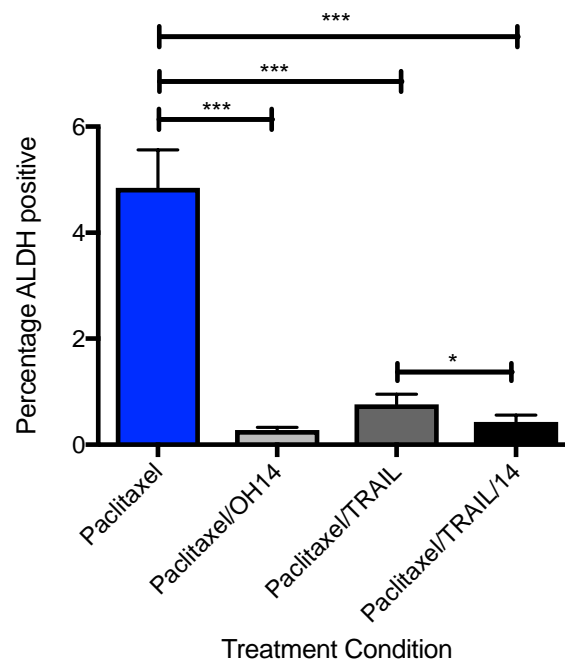
C
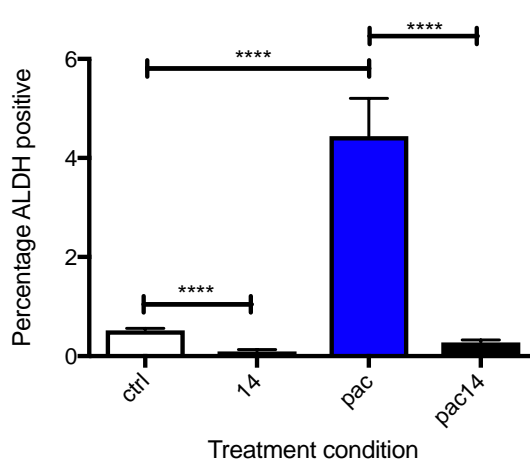
D
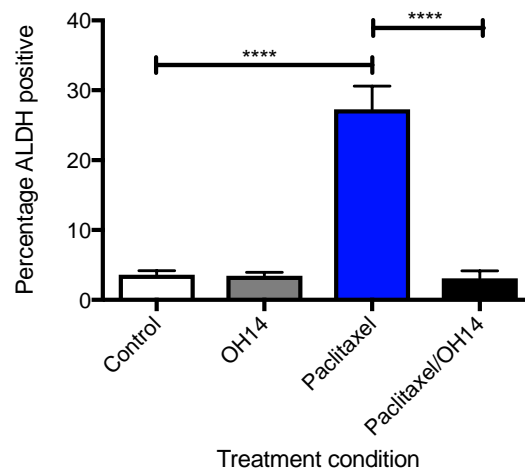
Figure 4.14 Effect of OH14, TRAIL and Paclitaxel on TNBC ALDH+ cells

The MDA-MB-231 (B and C) and SUM149 (D) cell lines were plated into adherent conditions for 96 hours and 72 hrs later treated with Ctrl, OH14, TRAIL or TRAIL+OH14 for 24 hours. Cells were dissociated and underwent flow cytometry using the Aldefluor assay following the manufacturers protocol. Representative plots are shown in A. Error bars represent SEM of the mean and results are an average of three experiments performed in triplicate (SUM149 Flow cytometry was 2 repeats). (T-test, *=p<0.1, **=p<0.01, ***=p<0.001 ****=p<0.0001).

4.2.9   Confirming an 'on-target' effect of OH14

4.2.9.1 SiRNA-mediated knockdown of cFLIP sensitises TNBC cell lines
to paclitaxel

It has previously been shown that overexpression of cFLIP led to a reduction
in the cytotoxicity of paclitaxel in both leukaemic and the MCF7 breast cancer
cell lines (Day et al. 2006).   In addition, paclitaxel mediates its apoptotic
effects through the extrinsic apoptosis pathway in a ligand-independent
manner (Day, Huang, and Safa 2008a) meaning that a sound rationale exists
to combine an agent targeting cFLIP with paclitaxel. Previously in this chapter
we demonstrated that OH14, a novel compound targeted against a binding
pocket of cFLIP on FADD, sensitised TNBC cell lines to paclitaxel (Section
4.2.4.1). Next an assessment as to whether using siRNA-mediated
knockdown of cFLIP levels led to a similar reduction in viability to OH14
(compared to a scrambled RNA control) in two TNBC cell lines. The MDA-MB-
231 and SUM149 cell lines were transfected as described in Chapter 2, left for
48 hrs and then treated overnight with 10nM of paclitaxel to replicate the
conditions used in the previous OH14 experiment.

In both the MDA-MB-231 and SUM149 cell lines, use of siRNA against cFLIP
led to a significant increase in the toxicity of paclitaxel over the level seen with
scrambled RNA (Fig. 4.15). This mirrored the effect of OH14 seen previously
(Fig. 4.9).

A
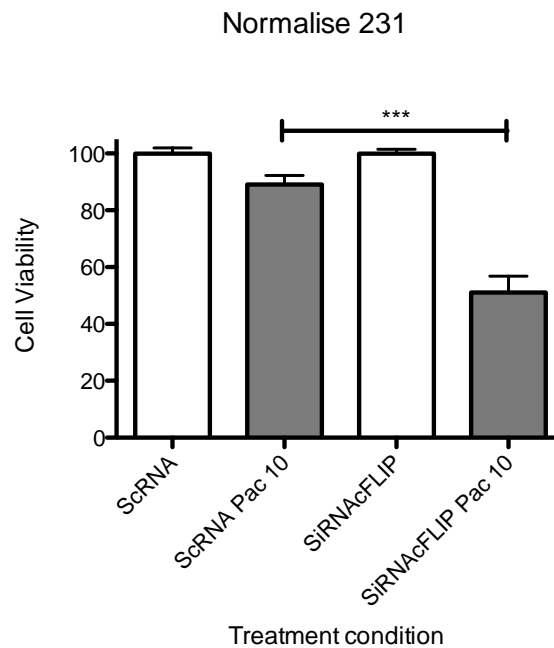
B
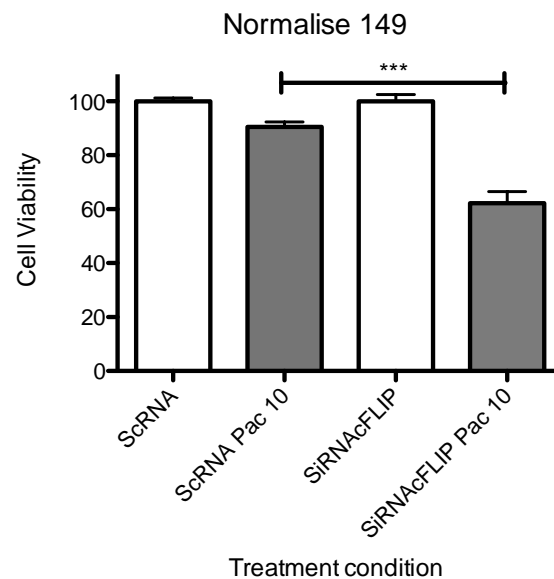
Figure 4.15- Effect of siRNA knockdown on TNBC cell lines in combination with paclitaxel

The MDA-MB-231 and SUM149 cell line was plated into adherent conditions and 24 hours later treated with either scRNA or siRNA against cFLIP. 48 hours later paclitaxel was added at 10nM and left on for 24 hours. Cell viability was then evaluated using CellTiter Blue. Error bars represent SEM of the mean and results are an average of three experiments performed in triplicate (SUM149 Flow cytometry was 2 repeats). (T-test, *=$p<0.1$, **=$p<0.01$, ***=$p<0.001$ ****=$p<0.0001$).

4.2.9.2 Paclitaxel-induced mammosphere formation is reduced by the SiRNA-mediated knockdown of cFLIP

We then sought to assess whether reducing cFLIP levels led to a reduction in PAC-induced mammosphere formation. MDA-MB-231 and SUM149 cells were treated with scRNA or SiRNA against cFLIP for 24hours and then treated with paclitaxel and left for 96 hours. Then the cells were dissociated and plated into non-adherent mammopshere conditions at a fixed concentration and counted seven days later (Passage 1) or following a subsequent passage (Passage 2).

SiRNA treated cells exhibited smaller spheres and reduced the paclitaxel-mediated increase in sphere numbers seen when scRNA cells were treated with Paclitaxel (Fig 4.16)

A

ScRNA　　　　　　　SiRNA cFLIP
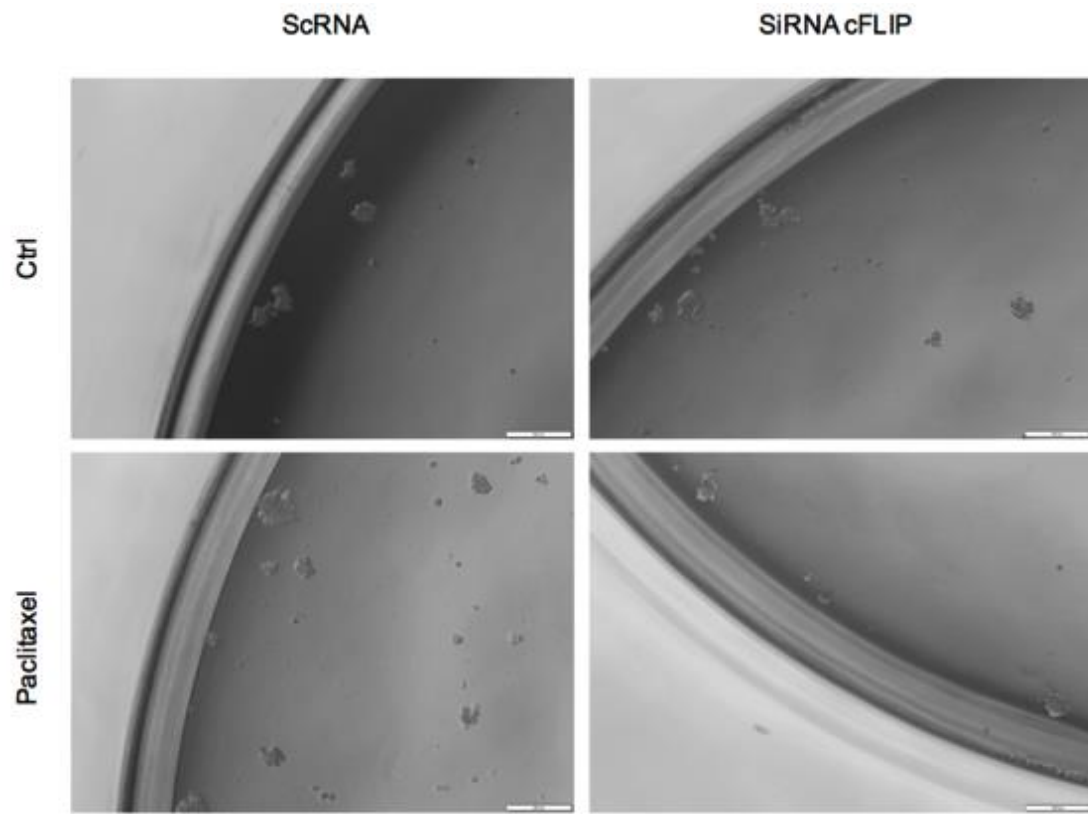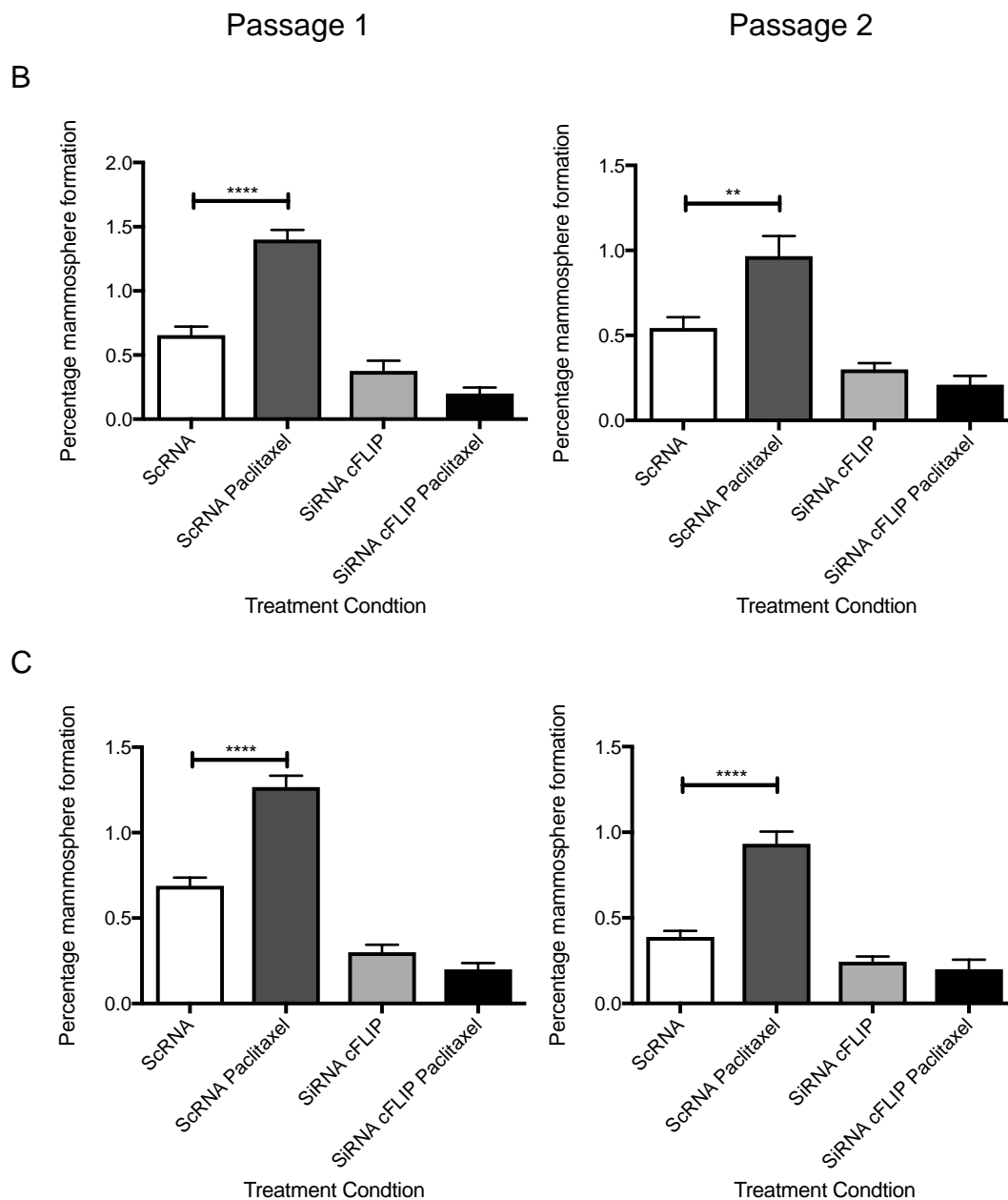
Figure 4.16 Effect of SiRNA-mediated cFLIP knockdown on mammosphere formation after paclitaxel

The MDA-MB-231 (A and B) and SUM149 cell lines (C) were plated into adherent conditions and 24 hours later treated with either scRNA or siRNA against cFLIP. 24 hours later paclitaxel was added and left on for 96 hours. Cells were then dissociated and plated into non-adherent conditions at a fixed cell concentration. After 7 days they were counted (Passage 1, B), dissociated and plated as single cells again at a fixed cell concentration and a further 7 days they were counted again (Passage 2, C). A shows representative pictures in the MDA-MB-231 cell line at the end of Passage 2. Error bars represent SEM of the mean and results are an average of three experiments performed in triplicate. (T-test, *=p<0.1, **=p<0.01, ***=p<0.001 ****=p<0.0001).

4.2.10 *In vivo* experiments using OH14, TRAIL and paclitaxel suggest OH14 targets CSC-like cells in vivo

The gold standard assay for CSC-like activity within a tumour cell population is the ability of cells to initiate tumour growth in vivo. Thus in order to determine how the in vitro responses of CSC-like activity influenced tumour establishment in vivo, two different xenograft models of TNBC were employed.

4.2.10.1 Determination of tumour establishment by TNBC cell lines

Before using the TNBC cell lines MDA-MB-231 or SUM 149 in mouse experiments we wanted to establish the efficiency of tumour growth when cells were implanted into the mammary fat pads of mice with matrigel.

We injected a range of cells bilaterally into NOD/SCID mice (MDA-MB-231 100000, 10000, 1000 cells and SUM149 5000, 500, 100 cells) to assess how successfully tumours formed. Tumours were measured twice a week. Using 4 mice per cell line, all the dilutions of MDA-MB-231 cells grew tumours around a month after injection whereas in the SUM149 cell line, both tumours at 5000 cells formed tumours and one tumour formed in a mouse with 500 cells (Table 4.1).

MDA-MD-231 Cells injected	Tumour take	SUM149 Cells Injected	Tumour take
100000	2/2	5000	2/2
10000	3/3	500	1/3
1000	3/3	100	0/3

Table 4.1 – Rates of tumour take in NOD-SCID mice when injected with varying concentrations of TNBC cells

MDA-MB-231 and SUM149 cells were harvested from adherent culture and diluted in matrigel (50%) before injection into mammary fat pads of NOD/SCID mice. Mice were then checked twice a week until tumour formation was noted. The cell numbers were lower in SUM149 due to previous reports of superior tumour efficacy of the SUM149 cells compared to MDA-MB-231 cells

4.2.10.1.1 Pre-treatment with OH14 and TRAIL reduced tumour initiation in mice

Having established that an injection of either 10000 or 1000 cells of the MDA-MB-231 cell line established tumours, we then set out to assess the effect of TRAIL and OH14 on tumour initiation. 10000, 1000 or 100 cells were injected bilaterally into recipient mice and the latency of tumour establishment determined. This provides a relative assessment of the proportion of viable tumour-initiating cells in a given tumour cell population.

Cells were seeded *in vitro* and allowed to grow for 72hrs prior to the addition of TRAIL/OH14/vehicle for 24 hours. Attached (ie predominantly viable) cells were then harvested with trypsin, washed three times in additive-free RPMI and then suspended in a solution of 50% matrigel and 50% additive-free RPMI. 100µL of solution was injected into each mammary fat pad and tumours were observed for growth twice weekly. Three mice with two tumours each were used to give a total potential of six tumours per condition. A determination of stem cell frequency and statistical comparison was undertaken using the ELDA calculator available online (http://bioinf.wehi.edu.au/software/elda/). This is a widely cited formula for determining CSC number in limiting dilution experiments (Hu and Smyth 2009)

At 10000 cells per mammary fat pad, single OH14 led to a small reduction in tumour formation from 6/6 to 4/6 (Fig 4.17). Whilst single agent TRAIL had no effect on tumour formation at this cell density, which is perhaps surprising seeing as in our *in vitro* experiments it led to a significant reduction in mammosphere formation as a single agent, the combination of both agents had a large effect with only 1/6 tumours forming. At 1000 cells per mammary fat pad, fewer tumours formed in the control arm (2/6) and this was halved by treatment with single agent OH14 or TRAIL and completely abolished by combined treatment. At 100 cells, no tumours formed in any treatment arm. Our stem cell calculator demonstrated a large reduction in CSC frequency for OH14, slightly less for TRAIL and the largest reduction for combined treatment with OH14 and TRAIL.

A

B

No. of cells	Control	14	TRAIL	TRAIL/14
10000	6/6	4/6	6/6	1/6
1000	2/6	1/6	1/6	0/6
100	0/6	0/6	0/6	0/6
CSC freq **(95% CI)**	1/2340 (1/862-1/6351)	1/8447 (1/3335-1/21391)	1/3220 (1/1281-1/8144)	1/61464 (1/8705-1/434007)

Significant differences in CSCs (p value, Chi Squared test)				Ctrl- 0.000173 14- 0.0341 TRAIL- 0.000868

Figure 4.17- Tumour take of MDA-MB-231 cells when treated with OH14, TRAIL or a combination and calculation of stem cell frequency

MDA-231-wells were plated into adherent conditions, left for 96 hours and then treated with either control (DMSO vehicle), OH14, TRAIL or OH14/TRAIL for 24 hours. They were then injected bilaterally into mammary fat pads of NOD/SCID mice in a 50:50 mix of serum-free media and matrigel and observed twice weekly for tumour growth. 3 mice were used per condition with bilateral tumours in each. A, graphical representation of tumour formation. B, The number of stem cells was estimated using ELDA software (http://bioinf.wehi.edu.au/software/elda/) and comparison made via Chi squared test as described in (Hu and Smyth 2009)

4.2.10.1.2 Treatment with paclitaxel increases tumour formation that is likely abrogated by a combination of OH14 and TRAIL

Cells were seeded *in vitro* and allowed to grow for 24hrs prior to the addition of paclitaxel. 72 hours later TRAIL/OH14/vehicle was added for 24 hours. Attached (ie predominantly viable) cells were then harvested with trypsin, washed three times in additive-free RPMI and then suspended in a solution of 50% matrigel and 50% additive-free RPMI. 100µL of solution was injected into each mammary fat pad and tumours were observed for growth twice weekly. Three mice with two tumours each were used to give a total potential of six tumours per condition. We again used the ELDA calculator available online (http://bioinf.wehi.edu.au/software/elda/) to calculate CSC frequency and statistical significance.

Paclitaxel alone led to a 6/6 tumour formation rate at 10000 and 1000 cells (compared to 2/6 in the 1000 cell arm in the control group). There was also tumour formation in half of the mice that were injected with 100 cells compared to none in both the control arm (Fig 4.18) and with any other treatment in this group. This is clearly indicative of an increased CSC-like population remaining at the end of *in vitro* paclitaxel treatment. The combination of paclitaxel with OH14 resulted in a lack of tumour formation in the 100 cell arm suggesting that OH14 did potentially reverse the paclitaxel-mediated increase in CSCs. Single agent TRAIL after paclitaxel had a better effect with tumour formation being halved at highest cell concentration (10000 cells, 3/6 tumours) with an even stronger effect at the 1000 cells per injection concentration (1/6 tumours) and 100 cells (0/6). The relationship between tumour formation for the combined treatment of OH14 and TRAIL after paclitaxel is more complicated, whilst at 10000 cells there as a 50% reduction in tumour forming ability (6/6 to 3/6) and at 100 cells there was no tumour formation (from 3/6) at 1000 cells per injection there was a surprising increase. It is likely this reflects a degree of technical variability in this biological assay, and it will be necessary to repeat this experiment in the future to determine whether this unexpected result is reproduced.

Our CSC frequency calculator again confirmed these findings, with a significantly higher proportion of CSCs in paclitaxel compared to untreated control that was reduced by combination of paclitaxel with OH14 and paclitaxel OH14 and TRAIL. However, the combination of paclitaxel and OH14 had the lowest frequency- again confirming that the technical variability of this assay

A
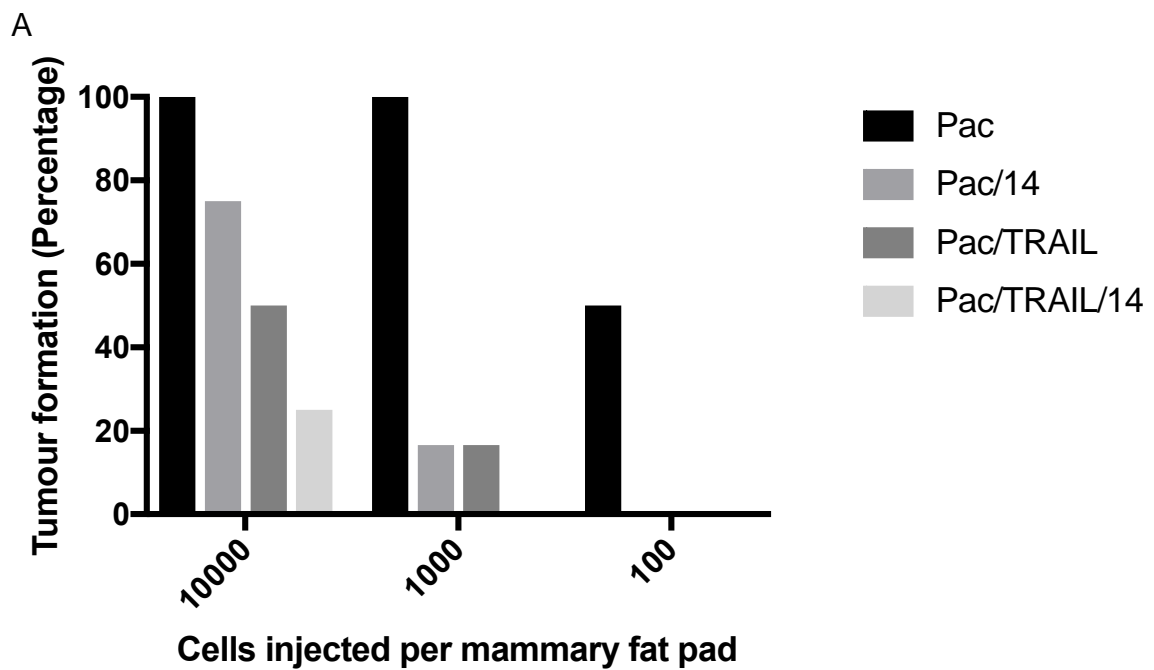
B

No. of cells	Pac	Pac/14	Pac/TRAIL	Pac/TRAIL/14
10000	6/6	3/4	2/4	1/4
1000	6/6	1/6	1/6	0/6
100	3/6	0/6	0/6	0/6
CSC freq (95% CI)	1/142 (1/47.4-1/428)	1/6896 (1/2408-1/19742)	1/11556 (1/3525-1/37877)	1/41399 (1/5899-1/290524)
Significant differences in CSCs (p value, Chi Squared test)		Ctrl- 8.45×10^{-8}	Ctrl- 2.01×10^{-9}	Ctrl- 8.02×10^{-12}

Figure 4.18 Effect of OH14 and TRAIL after paclitaxel on tumour formation *in vivo* and calculation of stem cell frequency

MDA-231-wells were plated into adherent conditions, left for 24 hours and then treated with paclitaxel followed by either control (DMSO vehicle), OH14, TRAIL or OH14/TRAIL7 2 hours later for 24 hours. They were then injected bilaterally into mammary fat pads of NOD/SCID mice in a 50:50 mix of serum-free media and matrigel and observed twice weekly for tumour growth. 3 mice were used per condition with bilateral tumours in each. . A, graphical representation of tumour formation. B, The number of stem cells was estimated using ELDA software (http://bioinf.wehi.edu.au/software/elda/) and comparison made by chi-squared test as described in (Hu and Smyth 2009)

4.2.10.1.3 Treatment with OH14 with paclitaxel stops the recurrence of tumours in an *in vivo* TNBC model

Having shown that the combination of OH14 and Paclitaxel was potentially effective in targeting bCSCs in pretreatment of TNBC cell line xenografts, we wanted to assess the potential for *in vivo* administration of OH14/paclitaxel on established tumours. The expected outcome of targeting CSCs in this context relies on the ability of the chemotherapy to regress, or partially regress tumour growth by diminishing bulk-cell viability, followed by an increased latency of relapse occurring through the suppression of tumour-initiating (CSC) activity within the remaining tumour cell population. TRAIL was not tested in this experiment due to the financial cost of the experiment. 500000 MDA-MB-231 cells were implanted into each mammary fat pad of an athymic mouse and allowed to grow until tumours measured over 5mm in their longest dimension. The mice were then divided into four arms: control (DMSO), OH14, Paclitaxel (with DMSO) and Paclitaxel and OH14. They were then treated twice a week with paclitaxel at 20mg/kg or control for a total of seven doses (represented by arrows on in Fig 4.19A). During this 20-day period some mice were also treated with OH14 at 20mg/kg or DMSO control five days a week. Tumour volume was measured at least twice weekly.

The mice in the control and OH14 alone arms had a rapid tumour growth that led to the mice in those groups being culled (due to maximum permitted tumour size being reached) at around 18 days on average in the control group and around 22 days in the OH14 arm (Fig 4.19A).

There was a marked response to paclitaxel treatment with both paclitaxel alone or paclitaxel/OH14. Tumour regression was sustained for a minimum 47 days whereupon one of the paclitaxel treated tumours began to rapidly grow, followed at Day 69, by the remaining paclitaxel treated mouse. In contrast, the two OH14/paclitaxel treated mice remained tumour free for up to Day 141 (Fig 4.19B), whereupon the animals were culled as a humane endpoint to the experiment.

A
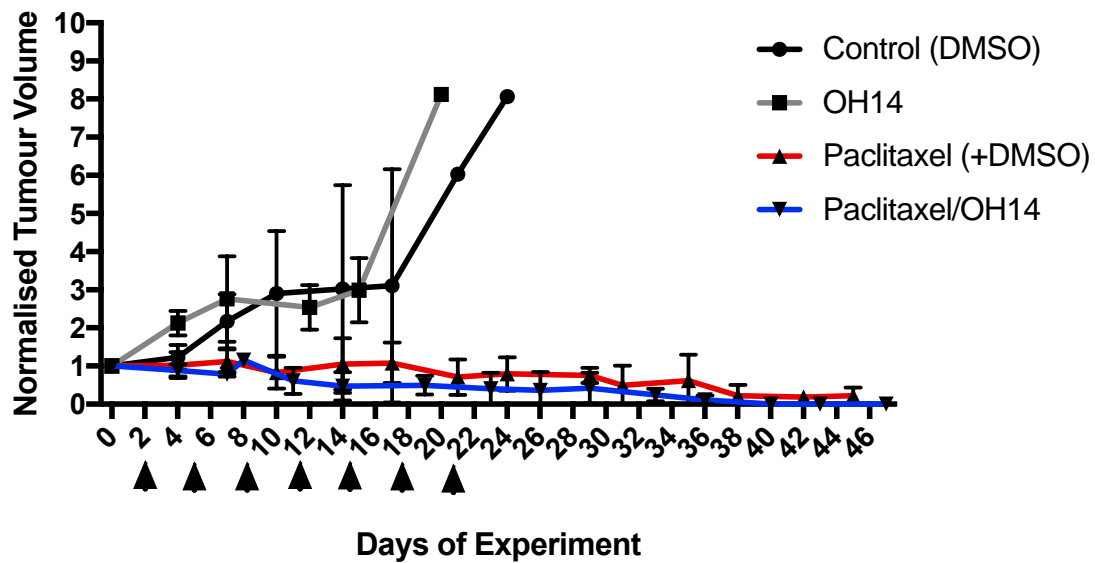
B
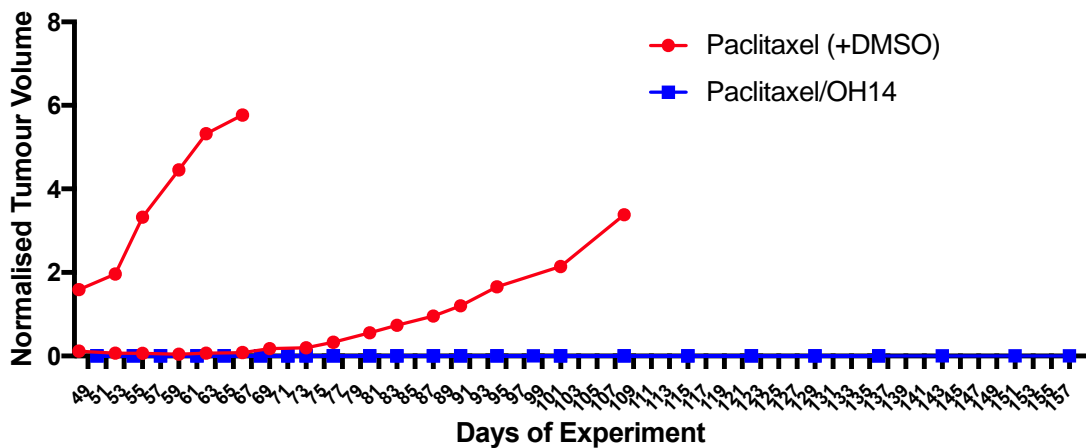
Figure 4.19 Treatment of MDA-MB-231 xenografts with paclitaxel and OH14.

500000 MDA-MB-231cells were injected bilaterally into mammary fat pads of athymic mice in a 50:50 solution of serum-free media and matrigel. Once tumours reached a minimum of 5mm in one dimension, they were either treated with control, OH14, paclitaxel or paclitaxel and OH14 for a total of seven doses (Represented by arrows on graph). Tumour size was then measured until culling criteria was met. In the case of the Paclitaxel and OH14 treated mice, no tumour growth was detected at 141 days and the experiment was ended.

4.3 Discussion

Having established a model in Chapter 3 to demonstrate that chemotherapy increased CSC-like activity in a panel of cell lines, we sought to assess whether TRAIL, with and without the novel cFLIP inhibitor OH14, could successfully target this induced CSC-like population. Furthermore, previous work without chemotherapy had demonstrated that the combination of cFLIP inhibition alongside TRAIL led to a reduction in CSC-like activity (Piggott et al. 2011; French et al. 2015) and we wanted to assess whether this was still the case after chemotherapy.

Using the MCF7 and SUM149 cell lines, representing two key subtypes of breast cancer – and two contrasting cell types with respect to their known sensitivity to TRAIL, we initially assessed the cytotoxicity of OH14, TRAIL and their combination on bulk-cell viability and mammosphere formation (Figs 4.3-4.5). We employed the same mathematical model as in Chapter 3 to demonstrate that both OH14 and TRAIL reduced absolute CSC numbers (Fig. 4.6). The effect on CSC-like behaviour was more marked than in bulk cells suggesting that OH14/TRAIL preferentially target CSC-like cells over bulk tumour cells.

We then demonstrated that the increase in mammosphere formation seen with FEC, paclitaxel and docetaxel chemotherapy was abrogated with the addition of OH14 and TRAIL (Fig. 4.7). Interestingly, in the SUM149 cell line, there was a highly significant reduction in mammosphere formation using OH14 alone after chemotherapy in all passages with FEC, paclitaxel and docetaxel and that this reduction was greater than seen with TRAIL (Figs 4.7 D-F and 4.8). Although not completely wanting to rule out the combination of chemotherapy, OH14 and TRAIL, this led to the possibility that OH14 alone after chemotherapy could be a viable therapeutic option. As stated at the beginning of the chapter, it was clear from previous studies that paclitaxel seemed to exert its effects predominantly through the extrinsic apoptosis pathway and as such there was a sound scientific rationale for combining paclitaxel with OH14 (Day, Huang, and Safa 2008b; Day et al. 2006; Park et al. 2004). As we had seen the greatest effect in the SUM149 cell line, and

TNBC is an area of breast cancer in urgent need of novel treatment strategies, the focus of this work switched mainly towards assessing whether OH14 alone after paclitaxel in TNBC would be a viable treatment strategy.

An initial experiment on a panel of TNBC cell lines, MDA-MB-231, MDA-MB-436 and SUM149, showed that an overnight treatment of paclitaxel at 10nM decreased viability when OH14 was added 1 hour before and this effect was not seen in the MCF-7 and HCC 1954 (both non-TNBC) cell lines (Fig 4.9). This confirmed that TNBC seemed like a reasonable choice in which to assess this combination. Given more time, an exploration of whether this effect on the bulk cell population was synergistic could be explored by using log-fold dose increases of both paclitaxel and OH14.

However, our main focus was on the effect of OH14 in combination with paclitaxel on the CSC-like formation within TNBC. As previously discussed in Chapter 3, our mathematical model of mammosphere formation had concluded that paclitaxel caused an increase in the absolute number of mammosphere forming cells (CSC-like cells) in the treated cell pool, which suggested that CSCs were not only more resistant to paclitaxel than bulk-cells, as suggested previously (Samanta et al. 2014; Alamgeer et al. 2014), but that they were actively promoted by paclitaxel.

In this chapter we found that OH14 reduced this paclitaxel-induced CSC population, and diminished CSC numbers to below untreated levels (Figs 4.11, 4,12, 4.13 and 4.16A and C-D). For example, in our model (Fig 4.13) of MDA-MB-231 cells, the total number of CSCs fell from 34 to 11, a 67.3% reduction- this correlated with a reduction in overall cell viability of 60.7%. Therefore, we postulate that OH14, by reducing the total number of CSCs to below control levels, is potentially enabling paclitaxel to target CSC-like cells, but also blocking the signaling pathways that lead to CSC-like cell formation. This raises the possibility that treatment with paclitaxel, whilst increasing absolute CSC number and mammosphere formation, leaves an 'Achilles Heel' that can be targeted by the addition of OH14 alone.

We used siRNA-mediated knockdown of cFLIP to confirm these observations - demonstrating that OH14 was likely having an 'on-target' effect.

As described in Chapter 3, the relationship between ALDH+ and mammosphere formation was not exact. When examining the effect of paclitaxel on ALDH+ we saw a similar 10-fold increase between the MDA-MB-231 and SUM149 cell lines (0.52 in control to 4.84 with paclitaxel in the former and 3.5 to 27.3 in the later) though the SUM149 cells consistently had more ALDH+ at baseline (Fig 4.14). This was far more than the 2-3 fold increase in mammosphere formation at Passage 2 for both of these cell lines (Fig 4.11). The SUM149 cell line represents an inflammatory breast cancer, a type of breast cancer where ALDH has been shown to represent a CSC-like population and correlate with both metastases and survival (Charafe-Jauffret et al. 2010). It is possible that the higher ALDH+ in the SUM149 cell line is due to its inflammatory origin.

Not wanting to exclude TRAIL from our experiments completely at this point, the effect of the combination of OH14 and TRAIL alone on mammosphere formation and with paclitaxel on cell viability of the SUM149 and MDA-MB-231 cell lines was investigated, We demonstrated that the combination of OH14 and TRAIL leads to a significant reduction in viability compared to control, OH14 and TRAIL alone (though the later only in the MDA-MB-231 cell line) and that the combination of OH14 and TRAIL after chemotherapy lead to the most significant reduction in viability (Fig 4.10). In the MCF7 and SUM149 cell line, OH14 did not have an effect on mammosphere formation but TRAIL and TRAIL/OH14 did (Figs 4.3-4.4). In the MDA-MB-231 cell line, single agent OH14 significantly reduced mammosphere formation, though the effect was greater with TRAIL and TRAIL/OH14. In the MDA-MB-231 and SUM149 cell lines, the effect of TRAIL +/- OH14 on the ALDH+ was investigated and had a significant effect on ALDH positivity (Fig 4.15). In the SUM149 cells there was a significant effect of OH14, TRAIL and TRAIL/OH14 on the ALDH+ positive population that was not replicated in mammosphere conditions where OH14 had no effect (Fig 4.4). In the MDA-MB-231 cell line, the greatest reduction in ALDH+ cells came with the use of single agent OH14, with

smaller reductions seen in the TRAIL and TRAIL/OH14 arms. Although a significant reduction in mammosphere formation was seen with single agent OH14, the effect of TRAIL and TRAIL/OH14 on mammosphere formation was greater than OH14 alone.

Lastly, we used two *in vivo* experiments to assess whether these results could be replicated in the MDA-MB-231 cell line. Firstly, we performed a serial dilution experiment that tests the ability of cells to form tumours in mice. We performed these experiments again with TRAIL as we did not want to disregard it at this point. Without chemotherapy, OH14 alone led to a slight reduction in tumour formation at the highest concentration of cells injected (10000 per mammary fat pad) but that combination treatment of OH14 and TRAIL was the most effective reducing tumour formation. When repeating the experiments with paclitaxel we saw a marked increase in tumour formation. This correlates with the increase in both mammosphere formation and ALDH+ cells that we saw *in vitro*. These results were confirmed by a model calculating CSC in each of the arms (Figs 4.19 and 4.20)

We next wanted to assess the effect of combination treatment *in vivo* on both a MDA–MB–231model as well as a patient derived TNBC cell line called PDX 151 as patient derived samples are taking on increasing importance in assessing tumour behaviour (Bruna et al. 2016). Unfortunately, the strain of mouse used for the PDX experiment (NOD/SCID/Balbc, Charles River Laboratories, Wilmington, US) did not tolerate the combined treatment with all three mice being treated with a combination of OH14 and paclitaxel dying within 48 hours of administration. This is an experiment that we would like to repeat. In the athymic mice used to evaluate the MDA-MB-231 cell line the mice tolerated treatment well, maintaining weight and appearing healthy. Here we saw a marked regression in tumour size after 7 doses of paclitaxel (given twice a week) with OH14 being given 5 times a week whilst the paclitaxel was being given. Of the initial three mice, one of the paclitaxel mice did not respond to paclitaxel and was culled early in the experiment due to tumour size. One of the paclitaxel/OH14 mice was also culled due to the presence of an intra-abdominal tumour meaning that there were only two mice

per arm for comparison. The profound increased latency in tumour relapse observed in the OH14/paclitaxel combined treatment arm helps support our *in vitro* data that OH14 seems effective at targeting a CSC-like population that could be responsible for tumour initiation associated with tumour relapse (Fig 4.19). A larger cohort of animals would help to confirm these promising findings.

Therefore, having established that OH14 seems to target the CSC-like population in TNBC cell lines our attention turns to possible mechanisms through which this may be occurring. There is a possibility that this is due to apoptosis in that paclitaxel has been shown to induce its apoptotic effect in a non-ligand dependent manner through the extrinsic apoptotic pathway (Day, Huang, and Safa 2008a). As an antagonist of this pathway, cFLIP is a natural target to increase the cytotoxicity of paclitaxel with previous evidence that over-expressing cFLIP protects cells from paclitaxel-mediated apoptosis (Day et al. 2006). We would hypothesise that this effect may be more significant in CSC-like cells as more of an effect was observed on mammosphere formation than than with bulk cell viability. Another possibility is that OH14 is targeting a component of CSC signalling that is induced by paclitaxel and two signalling pathways are worthy of consideration. The first is the WNT/ β-catenin pathway that has been shown in other work to be down-regulated with suppression of cFLIP (French et al. 2015) and the second is HIF1α. HIF1α has been shown to be prognostic in TNBC and blocking HIF1α using digoxin after paclitaxel has been shown to reduce CSC-like activity in TNBC cell lines (Samanta et al. 2014). Aggregates of cFLIP have been shown to interfere with the ubiquitynation and degradation of both molecules, leading to increased cellular levels (Ishioka et al. 2007; Safa 2012). These mechanisms will be explored in Chapter 5.

5 Investigating the mechanisms of cFLIP-mediated decreased viability and CSC-like activtity

5.1 Introduction

Results in previous chapters have demonstrated that firstly, chemotherapy leads to an increase in CSC-like behaviour (Chapter 3) and that secondly, this effect can be reversed with a combination of OH14 and TRAIL (Chapter 4). Interestingly, the use of single agent OH14 in combination with paclitaxel led to a significant reduction both in viability and in CSC-like behaviour in TNBC cell lines and in a mouse model using the combined treatment *in* vivo.

This chapter seeks to explore the mechanism behind this observed effect. As stated in the conclusion to Chapter 4, our mathematical model demonstrated that paclitaxel led to an increase in the number of CSCs compared to control (Fig. 4.13). Previous work has shown that chemotherapy can lead to the induction of a CSC-like phenotype (H. Liu, Lv, and Yang 2015) and as such this led to the generation of two hypotheses for the role of OH14 in suppressing the expansion of the CSC pool: Firstly, that OH14 may be having an additional pro-apoptotic effect on cells treated with chemotherapy-lowering the apoptotic threshold in the CSC population. Other compounds, such as salinomycin, have been shown to target CSCs in this manner (P. B. Gupta et al. 2009). Secondly, that cFLIP suppression may inhibit the upregulation of CSC signalling induced by chemotherapy such as β-catenin and HIF1α, resulting in the prevention of the generation of CSCs.

It has previously been shown that over-expression of cFLIP protects cancer cell lines from paclitaxel-induced apoptosis and as such reducing levels of cFLIP could lead to an increased sensitivity to paclitaxel (Day et al. 2006; S.-J. Park et al. 2004). Paclitaxel has been shown to lead to apoptosis through the extrinsic apoptosis pathway. As shown in Fig. 5.1A in this pathway FADD usually binds to Caspases 8 and 10, forming the Death Inducing Signalling Complex (DISC) and lead to the induction of the apoptotic pathway. cFLIP can inhibit this pathway by binding to Caspases 8 and 10 and FADD thereby preventing formation of the DISC (Safa 2012) (Fig 5.1B and Section 1.10.5). With the addition of OH14, that binds to the DED1 domain of cFLIP (Hayward et al, unpublished work), we could prevent the inhibition of DISC formation by cFLIP, allowing apoptosis to occur (Fig. 5.1C).

In TNBC, as outlined in Chapter 1, HIF1α has been shown to both be induced by chemotherapy and be prognostic (Samanta et al. 2014; Lu et al. 2015). It has been demonstrated that overexpression of cFLIP increases levels of HIF1α and β-catenin. These proteins would usually be degraded by the Ubiquitin Proteosome System (UPS) leading to their reduced intracellular levels (Fig 5.2A). cFLIP can lead to elevation of HIF1α and β-catenin through forming cellular aggregates that interfere with the functioning of the UPS (Fig 5.2B) (Naito et al. 2004; Ishioka et al. 2007). Interfering with the UPS through using the proteasome inhibitor MG132 reversed the increase protein levels of HIF1α and β-catenin when cFLIP was overexpressed. In addition, mutating the DEDs of cFLIP led to a similar effect, as binding through DEDs are thought to be responsible for the aggregation of cFLIP and UPS inhibition (Ishioka et al. 2007). OH14, our novel cFLIP inhibitor, has been designed to target the DED1 domain of cFLIP and therefore we hypothesise that we should see a reduction in HIF1α and β-catenin levels due to OH14 blocking cFLIP aggregate formation (Fig. 5.2C). Previous work undertaken in our laboratory, though not in combination with chemotherapy, has demonstrated that siRNA-mediated knockdown of cFLIP in combination with TRAIL selectively targets CSC-like behaviour across a broad panel of breast cancer cell lines and increases levels of cell death in the bulk population (Piggott et al. 2011). Further work has demonstrated that SiRNA-mediated cFLIP suppression leads to a reduction in β-catenin (French et al. 2015)

This main aim of this chapter is to assess whether the mechanism of a cFLIP-mediated reduction in CSC function in the context of chemotherapy is mediated through an increased apoptotic effect or through reduced CSC-signalling.
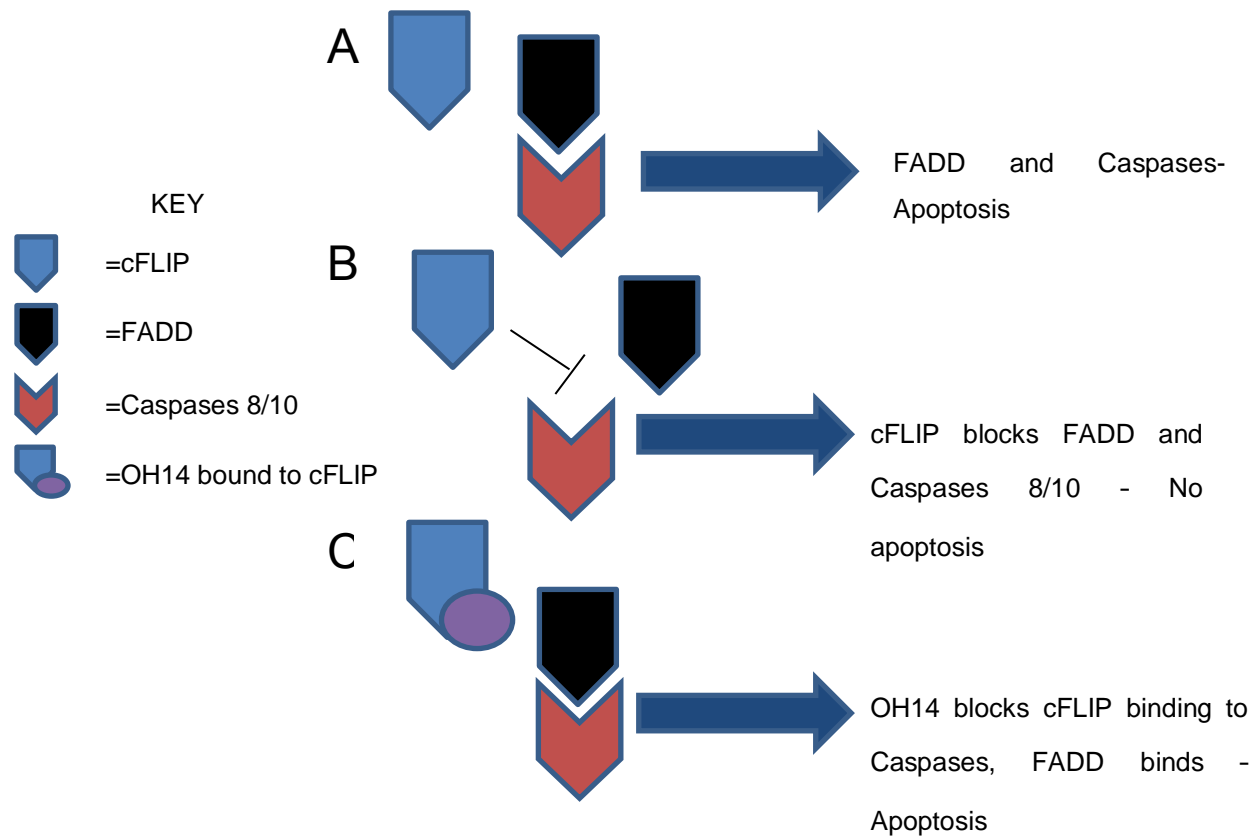
Figure 5.1 Potential effect of OH14 on apoptosis

Diagram representing the potential anti-apoptotic effects of OH14. A, FADD (black) binds to Caspases 8/10 (red) and triggers apoptosis via the extrinsic apoptotic pathway. B, cFLIP (blue) prevents apoptosis. C, OH14 blocks cFLIP (blue with yellow circle) allowing Caspases 8/10 to initiate apoptosis.
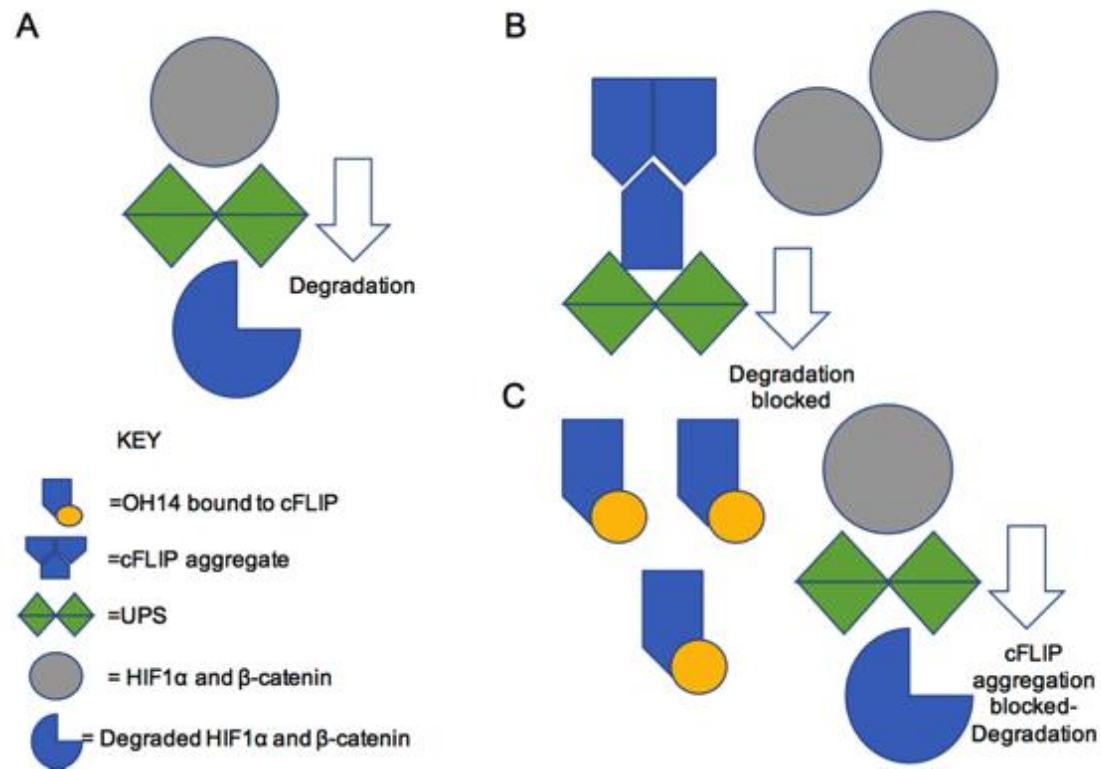
Figure 5.5.2 Potential effect of OH14 on cFLIP aggregation and UPS function

A diagram demonstrating the effect of OH14 on HIF1α and β-catenin degradation. A, HIF1α and β-catenin (grey circle) are degraded (leading to blue three-quarter circle) by the UPS (Green triangles). B, if cFLIP aggregates (blue trapezoids) the UPS is inhibited and HIF1α and β-catenin are not detgraded. C, when OH14 binds cFLIP (blue chevrons with yellow circle), OH14 allows HIF1α and β-catenin to be degraded by the UPS.

5.2 Results

5.2.1 Investigating the role of apoptosis

5.2.1.1 cFLIP inhibition and TRAIL lead to increased apoptosis and cell death in the bulk MDA-MB-231 cell population with and without paclitaxel

An assessment as to whether OH14 was having its intended effect through increasing apoptosis on the general cell population was carried out by Annexin V assay. MDA-MB-231 cells were plated into adherent conditions and left overnight before the addition of paclitaxel at its IC50 value. Then 72 hours later, control (vehicle), 10μM OH14, TRAIL or a combination of the two were added and left for 24hours before the cells were dissociated and stained with antibodies as per manufacturers protocols.

Without chemotherapy OH14 did not lead to an increase in either apoptosis or cell death whereas TRAIL led to a drop in viable cells to 47% as a single agent. The addition of OH14 to TRAIL led to a significant further drop of 16% compared to TRAIL alone (Figure 5.3 A and C)

The addition of paclitaxel saw a reduction in the mean percentage of viable cells to 65% from 88% in the DMSO treated control (Fib 5.3B and C). The addition of single agent OH14 or TRAIL significantly reduced this remaining viable population to 54%. The combination of OH14 and TRAIL resulted in 29% of the population remaining viable at the end of treatment, this was a significant reduction compared to paclitaxel, paclitaxel and OH14 or paclitaxel and TRAIL.

A

Control   14

TRAIL   14/TRAIL

DAPI

Annexin V (FITC)
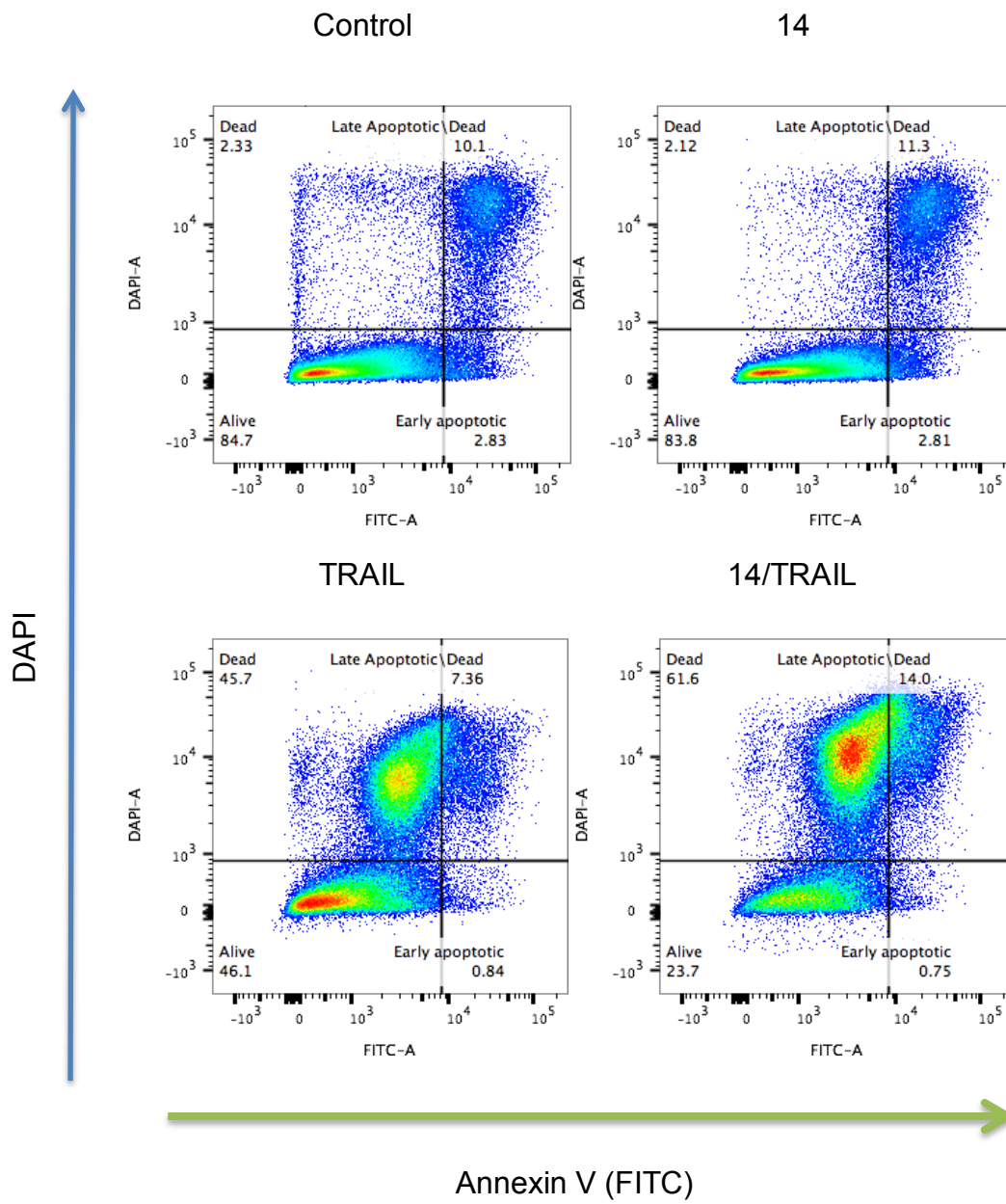
B
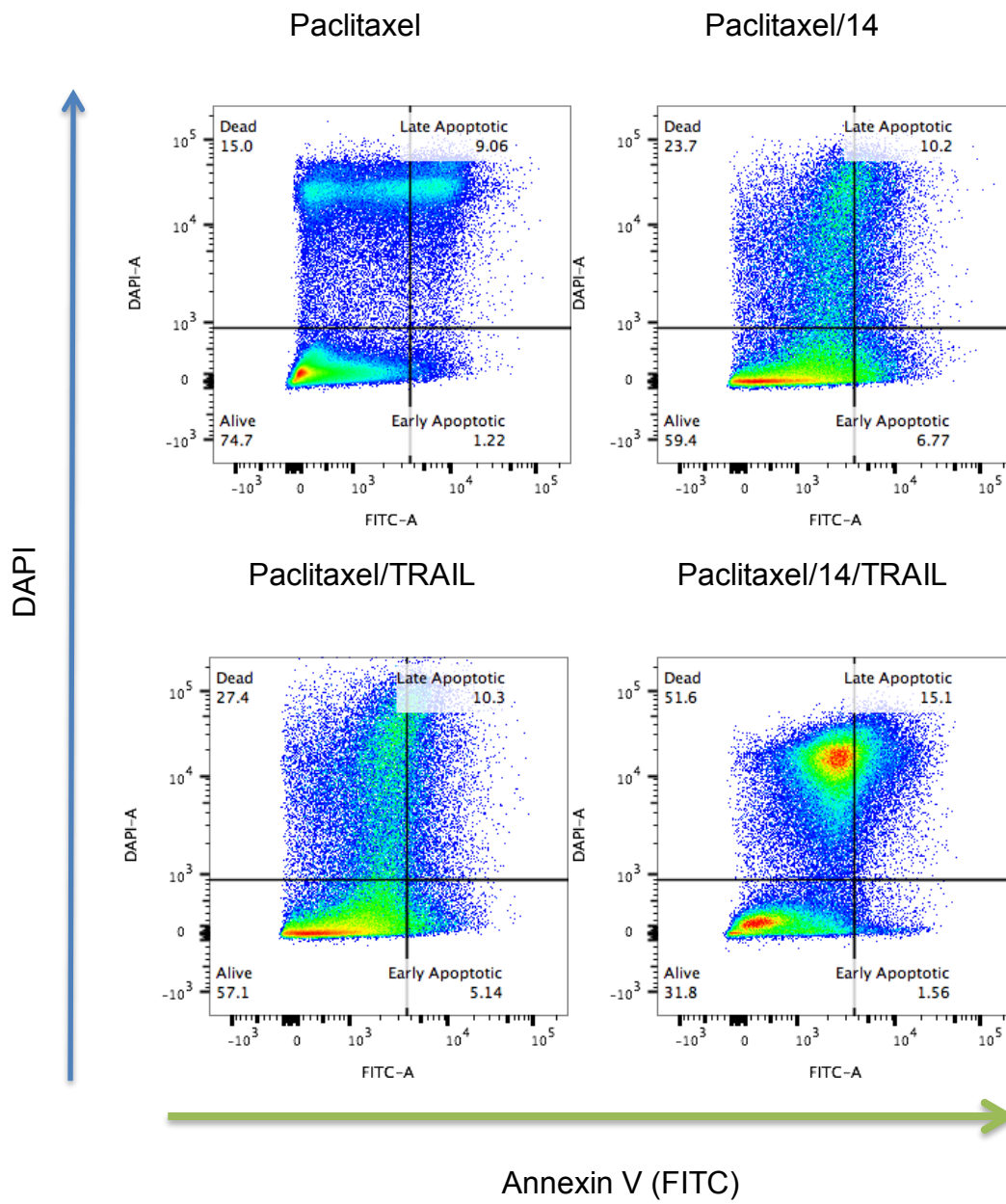
C
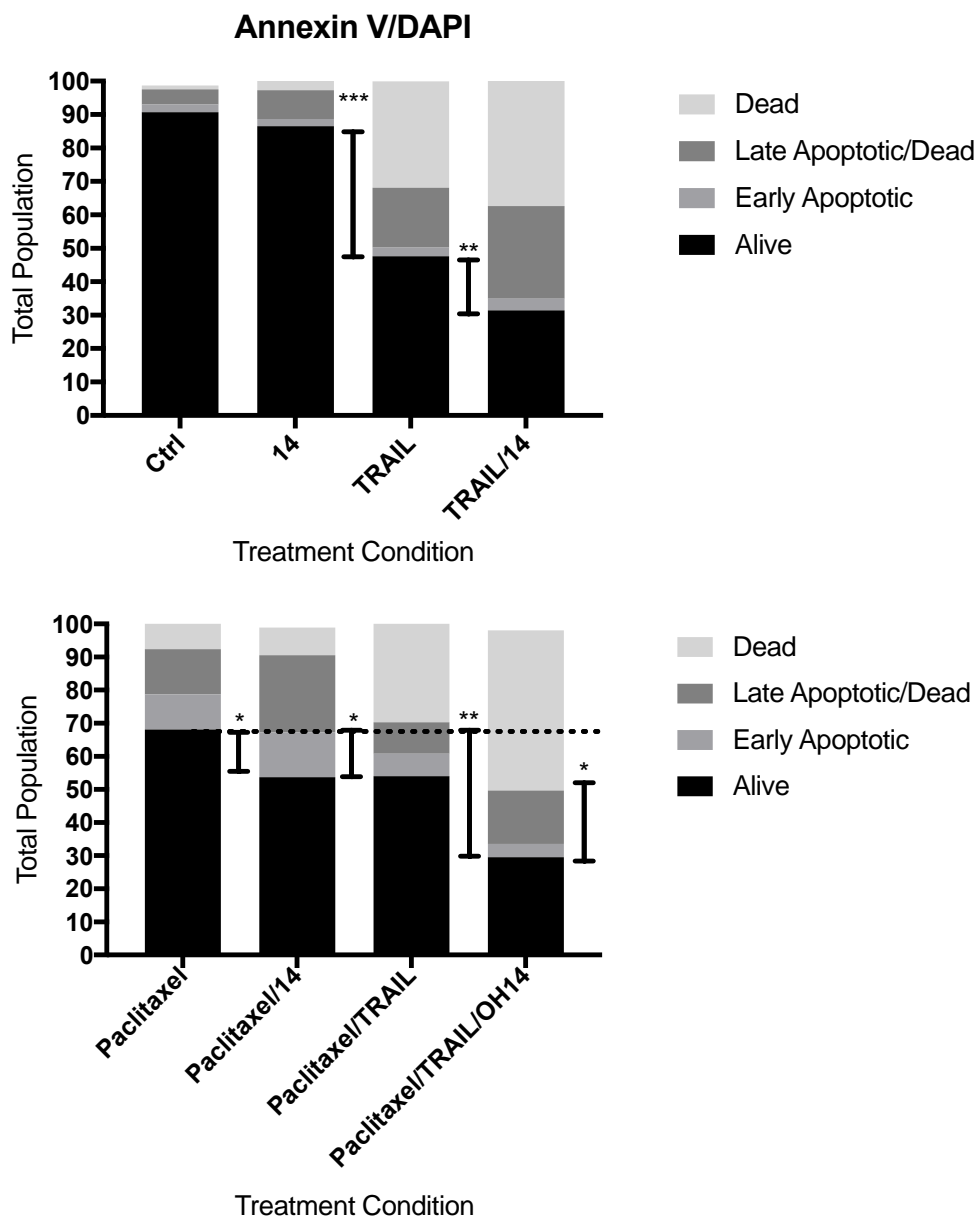
Figure 5.3 – TRAIL and OH14 lead to increased cell death and apoptosis with and without chemotherapy

MDA-MB-231 cells were treated with OH14 and TRAIL with/without paclitaxel before being trypsinised and undergoing flow cytometry with the Annexin V and DAPI stain. This gives an alive, early apoptotic, late apoptotic and dead population. Figs 5.3 A-B show representative pictures whereas Fig 5.3C shows a graphical representation of the results without error bars to ease interpretation. Dotted line is the alive population after paclitaxel treatment to allow comparison. Results are an average of three experiments performed in triplicate. (T-test, *=p<0.1, **=p<0.01, ***=p<0.001 ****=p<0.0001).

5.2.1.2 The effect of blocking apoptosis on the viability of TNBC cell lines in response to OH14

As OH14 was designed as a pro-apoptotic molecule that, by binding to the DED1 domain of cFLIP (Hayward et al, unpublished work), leads to increased apoptosis mediated through the extrinsic apoptosis pathway, we wanted to investigate whether blocking apoptosis using a pan-caspase inhibitor lead to a reversal of the effect seen with OH14 on both bulk and CSC-like cells.

Using two representative TNBC cell lines, SUM149 and MDA-MB-231, we assessed the effect of adding Z-VAD-FMK on both the overall cell viability of treated cells. Cells were plated into adherent conditions, left overnight and then treated with their respective IC50 values of paclitaxel. 72 hours after chemotherapy, OH14 or vehicle was added, with Z-VAD-FMK added one hour before, and left for a further 24 hours. Cell viability was then assessed by Cell Titer Blue assay.

Addition of Z-VAD-FMK led to a significant increase in the viability of the remaining cells in all conditions in both the MDA-MB-231 as well as the SUM149 cell lines apart from the SUM149 control group (Fig. 5.4). Interestingly, this effect was also observed for the control and the paclitaxel conditions – even though in the case of the latter it was added 72 hours after the addition of the chemotherapy or vehicle. With single agent OH14, paclitaxel and paclitaxel/OH14 the increase in viability after addition of Z-VAD-FMK was 15-20% across all conditions in both cell lines.

A
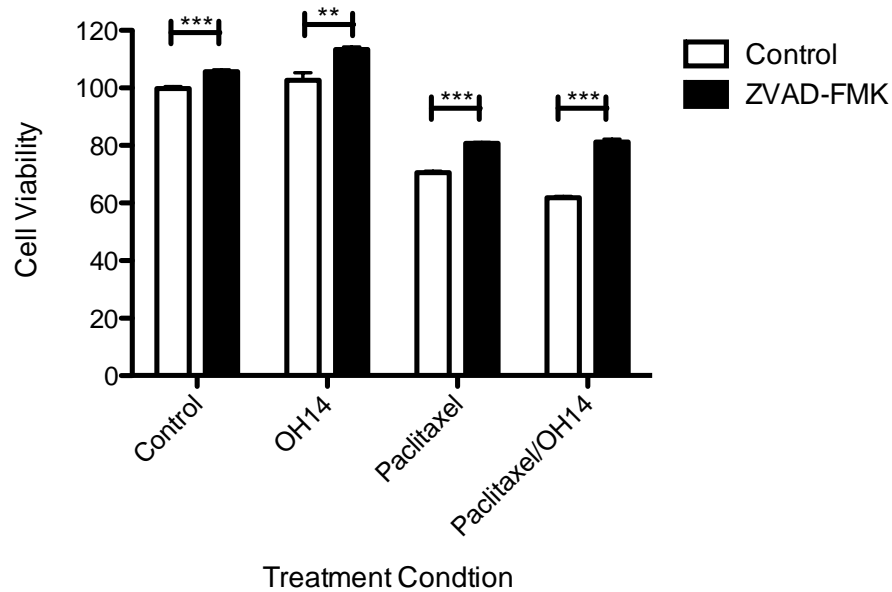
B
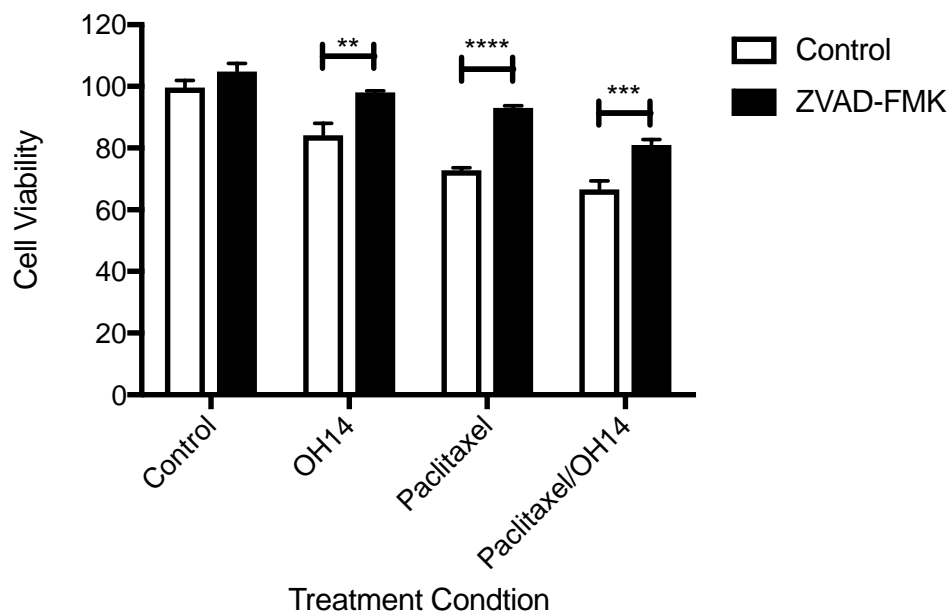
Figure 5.4- Caspase inhibition leads to an increase in viability in both the MDA-MB-231 and SUM 149 cells when treated with either paclitaxel, OH14 or a combination of the two

A) MDA-MB-231 and B) SUM149 cell lines were treated with their IC50 value of paclitaxel before OH14 was added 72hrs later +/-Z-VAD-FMK Caspase inhibition (CI) 1hr before. Viability was assessed via Cell Titer Blue. Error bars represent SEM of the mean and results are an average of three experiments performed in triplicate. (T-test, *=p<0.1, **=p<0.01, ***=p<0.001 ****=p<0.0001).

5.2.1.3 Caspase inhibition decreases the effect of OH14 on mammosphere formation in the MDA-MB-231 cell line

As we particularly wanted to examine the potential role of apoptosis in mediating the effect of OH14 on CSC-like behaviour, we repeated the mammosphere forming experiments with paclitaxel and OH14 with and without caspase inhibition (CI). We again combined our viability and mammosphere data to construct our mathematical model combining viability and mammosphere data as used in previous chapters (See Sections 3.17 and 4.26). MDA-MB-231 cells were treated as per Section 5.1.1.2 and then plated into mammosphere conditions with mammospheres being counted at 7 days (Passage 1), dissociated into single cells and plated again into non-adherent conditions at a fixed cell density for a further seven days and counted again (Passage 2).

As previously described in Chapter 4, paclitaxel led to a significant increase in mammosphere formation that was reduced by the addition of OH14. (Figs 5.5 A and B and 5.6). If the effect of OH14 on CSC-like cells was dependent upon apoptosis, we would expect there to be a significant difference between the magnitude of difference in mammosphere formation between CI and control arms in the OH14 treated cells compared to the control treated cells. For example, if in the control treated cells, there was a difference 0.2% in the mammosphere formation between control and CI arms, we would expect the difference in the OH14 group to be much larger, for example 0.4%.

CI with ZVAD-FMK significantly increased mammosphere formation in control conditions, an effect that could be due to increased resistance to anoikis due to inhibition of apoptosis. This effect was seen again and in the presence of OH14 and paclitaxel/OH14 though the magnitude of difference between the control and CI arms in each treatment condition was similar. (Figs 5.5A and B). This suggests that OH14 is not having a significant effect on mammosphere formation that is mediated through apoptosis. The addition of Z-VAD-FMK to paclitaxel alone however led to a non-significant reduction in sphere formation.

This is confirmed by our mathematical model. In our control arm there was an increase in absolute CSC numbers from 89 in the control arm to 129 with CI. With OH14 the magnitude of increase was similar- increasing from 100 to 145 without paclitaxel and from 63 to 110 with paclitaxel without and with CI respectively (Fig. 5.6). There was no significant difference between the actual numbers of CSCs between the control and CI treated cells, possibly because the CI was added 72 hours after the paclitaxel and apoptosis had already occurred.

A
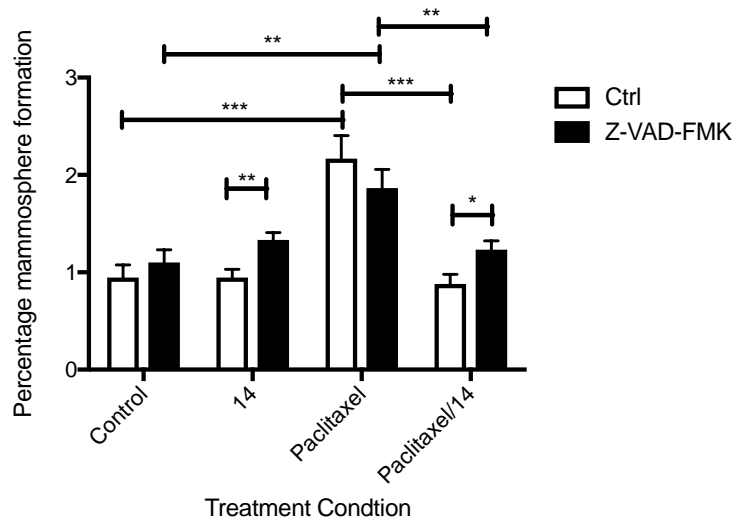
B
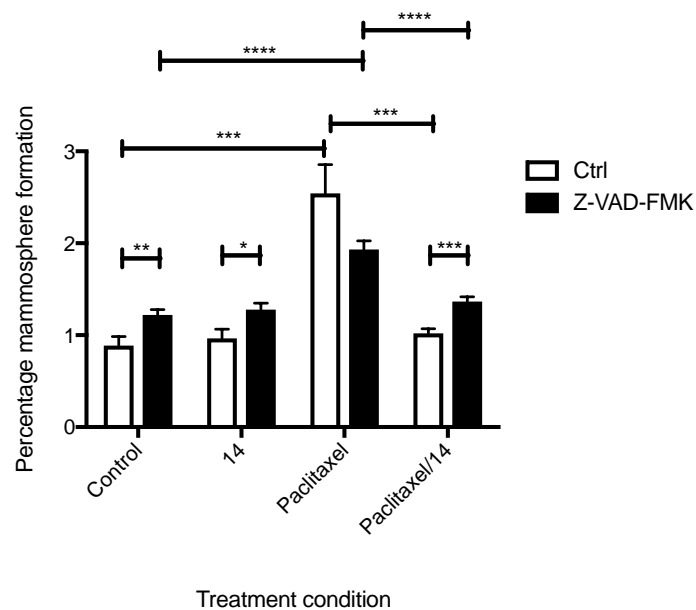
Figure 5.5 – Effect of caspase inhibition on mammosphere formation in TNBC is complex

MDA-MB-231 cells were treated with their IC50 value of paclitaxel before OH14 was added 72hrs later +/-Z-VAD-FMK Caspase inhibition (CI) 1hr before. After 24hrs they were plated into mammosphere conditions and counted at Passage 1 (A) and Passage 2 (B). Error bars represent SEM of the mean and results are an average of three experiments performed in triplicate. (T-test, *=p<0.1, **=p<0.01, ***=p<0.001 ****=p<0.0001).

| Treatment Condition	Viability (%)	Cell number (100%-10000)	P2 sphere formation (%)	Total number of CSCs
Control	99.8	9980	0.89	89
OH14	102.8	10280	0.97	100
Paclitaxel	70.7	7070	2.54	180
Paclitaxel/OH14	61.9	6190	1.02	63

Treatment Condition	Viability (%)	Cell number (100%-10000)	P2 sphere formation (%)	Total number of CSCs
Control with CI	105.8	10580	1.22	129
OH14 with CI	113.5	11350	1.28	145
Paclitaxel with CI	80.8	8080	1.93	156
Paclitaxel/OH14 with CI	81.2	8120	1.36	110
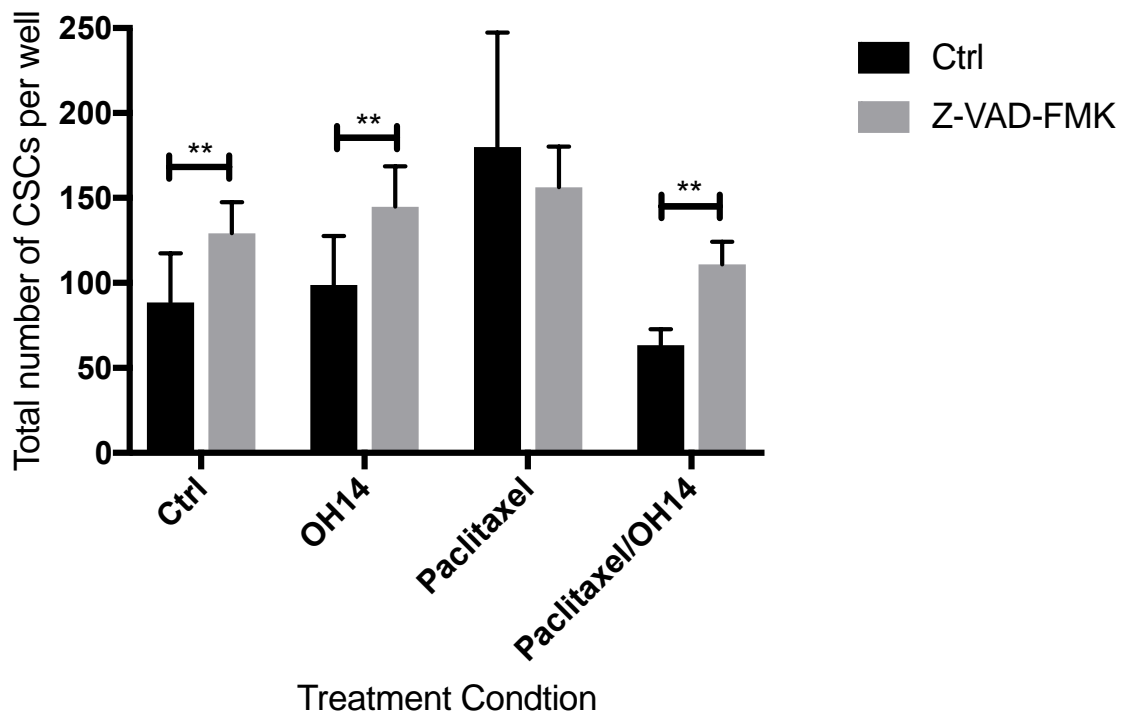
Figure 5.6 – Table and Graphical Representation of mathematical CSC model in MDA-MB-231 cells with or without Caspase Inhibition

The overall cell viability of the MDA-MB-231 cell line was multiplied by the percentage mammosphere formation at the end of Passage 2 for the respective treatment condition to give an absolute CSC number remaining at the end of adherent treatment Error bars represent SEM of the mean and results are an average of three experiments performed in triplicate. (T-test, *=p<0.1, **=p<0.01, ***=p<0.001 ****=p<0.0001).

5.2.1.4 Caspase inhibition also decreases the effect of OH14 on mammosphere formation in the SUM149 cell line

SUM149 cells were treated as above (5.2.1.2) and again the effect on mammosphere formation was observed.

As in the previous section, if the effect of OH14 on CSC-like behaviour was mediated by apoptosis we would expect there to a proportional difference in the effect of CI on OH14 treated cells as compared to control.

In this cell line, addition of Z-VAD-FMK had a significant effect on mammosphere formation or actual CSC number (Figs 5.7 and 5.8). There was however a small increase in mammosphere formation seen in both OH14 and OH14 combined with paclitaxel treated cells of around 40 (148 to 189 in OH14 treated cells and 86 and 127 in combined treated cells without and with CI repectively (Fig 5.8). Again, there was no effect on the paclitaxel treated cells. Although this is different to the MDA-MB-231 cell line, the overall trend of data is the same.

Taken together, the results in our two cell lines suggest that the effect of OH14 after paclitaxel is minimally dependent upon apoptosis and that another mechanism must be involved. As discussed in the introduction to this chapter (Section 5.1), the other major hyppthesised mechanism of action of OH14 on CSC-like function is CSC signalling.

A
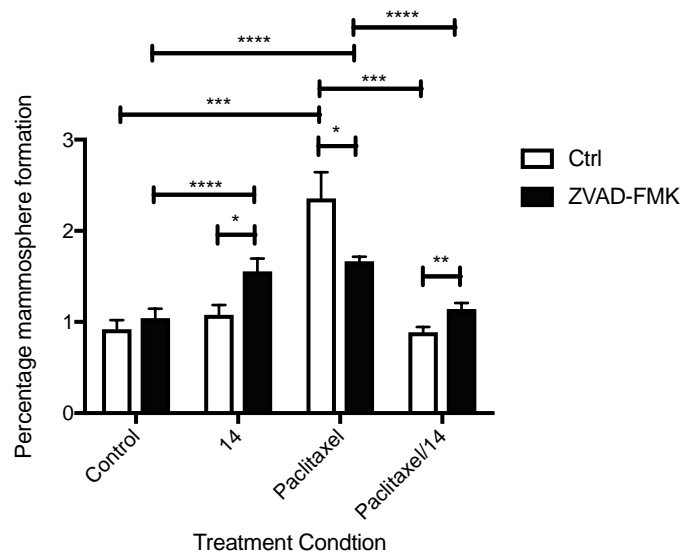
B
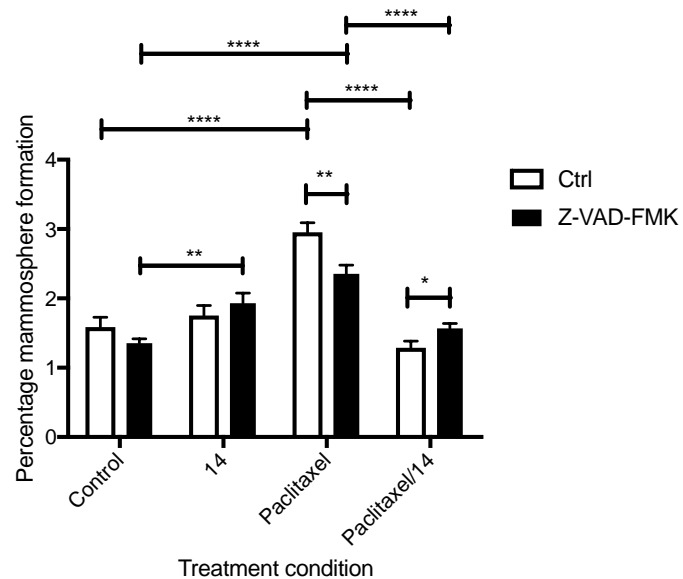
Figure 5.7 Mammosphere formation in the SUM 149 cell line is altered by Caspase inhibition

SUM149 cells were treated with their IC50 value of paclitaxel before OH14 was added 72hrs later +/-Z-VAD-FMK Caspase inhibition (CI) 1hr before. After 24hrs they were plated into mammosphere conditions and counted at Passage 1 (A) and Passage 2 (B). Error bars represent SEM of the mean and results are an average of three experiments performed in triplicate. (T-test, *=p<0.1, **=p<0.01, ***=p<0.001   ****=p<0.0001).

Treatment Condition	Viability (%)	Cell number (100%-10000)	P2 sphere formation (%)	Total number of CSCs
Control	99.7	9970	1.59	159
OH14	84.2	8420	1.76	148
Paclitaxel	72.8	7280	2.96	215
Paclitaxel/OH14	66.7	6670	1.29	86

Treatment Condition	Viability (%)	Cell number (100%-10000)	P2 sphere formation (%)	Total number of CSCs
Control with CI	104.9	10490	1.36	143
OH14 with CI	98	9800	1.93	189
Paclitaxel with CI	93	9300	2.36	219
Paclitaxel/OH14 with CI	81.1	8110	1.57	127
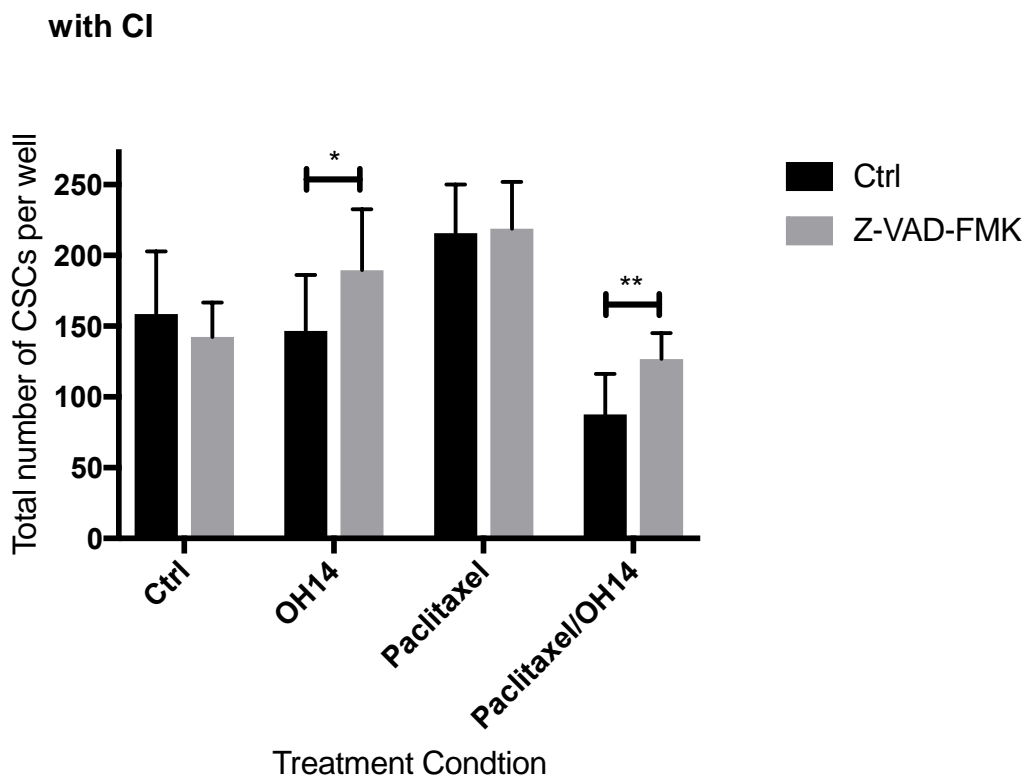
Figure 5.8 – Table and Graphical Representation of mathematical CSC model in SUM149 cells with or without Caspase Inhibition

The overall cell viability of the SUM149 cell line was multiplied by the percentage mammosphere formation at the end of Passage 2 for the respective treatment condition to give an absolute CSC number remaining at the end of adherent treatment. Error bars represent SEM of the mean and results are an average of three experiments performed in triplicate. (T-test, *=p<0.1, **=p<0.01, ***=p<0.001   ****=p<0.0001)

5.2.2 Investigating the role of OH14 in paclitaxel-induced CSC signaling

Having established in the previous sections that pan-caspase inhibition did not significantly restore the effect of OH14 on paclitaxel-induced CSC-like behaviour, we wanted to assess the role of OH14 on CSC signalling. This section will address our alternative hypothesis that OH14 prevented the acquisition of CSC-like characteristics, either through trans-differentiation or proliferation of CSCs following paclitaxel treatment. Two representative cell lines, SUM 149 and MDA-MB-231 were chosen to study the mechanisms underlying a cFLIP-mediated anti-CSC signalling effect.

5.2.2.1 Paclitaxel leads to an increase in HIF1α but not β-catenin protein expression at 96 hours

The elevation of CSC markers such as HIF1α and β-catenin in response to chemotherapy has been previously reported. In a panel of breast cancer cell lines treated with the chemotherapeutics paclitaxel and gemcitabine, it took 96 hours for the elevation of HIF1α to occur (Samanta et al. 2014). HIF1α has been shown to be elevated in response to chemotherapy, particularly in TNBC and to be prognostic (Lu et al. 2015; Buffa et al. 2010; Rohwer and Cramer 2011). It has also been shown to promote EMT (W. Zhang et al. 2015). β-catenin is also known to be associated with EMT and CSC-like behaviour and its inhibition has been shown to increase the cytotoxicity of a number of different chemotherapeutics across a broad-range of cancer types (Saifo et al. 2010). However, it has been demonstrated in breast cancer that neoadjuvant chemotherapy did not lead to altered β-catenin levels (as measured by immunohistochemistry) and that β-catenin could not be used to predict treatment resistance (Rosa et al. 2015). These proteins are both of interest as, as has been previously discussed, both potentially have an association with cFLIP and β-catenin has already been demonstrated in our laboratory to be affected by cFLIP- though this was not in association with chemotherapy (Safa 2012; French et al. 2015; Ishioka et al. 2007).

As our results to date (Chapter 3 and Chapter 4) have shown that paclitaxel increases CSC-like mammosphere over an extended perioded of time (4

days). We wanted to assess the levels of these proteins in response to chemotherapy over a similar extended period of time to assess whether they correlated with mammosphere formation.

Two representative TNBC cell lines (MDA-MB-231 and SUM 149) were treated with the 96-hour IC50 value of paclitaxel that had been established. Cells were harvested at 24, 48, 72 and 96 hours after the addition of chemotherapy. Western blotting was used to examine the effect of chemotherapy on HIF1α, β-catenin and cFLIP protein levels in total cell lysates. qPCR was then used to confirm the levels of both HIF1α and β-catenin at the transcriptional level.

In both cell lines all three proteins exhibited increases in expression over the 96 hour time course, yet only HIF1α was significantly elevated in both cell lines by the 96-hours time point (Fig 5.9).

A
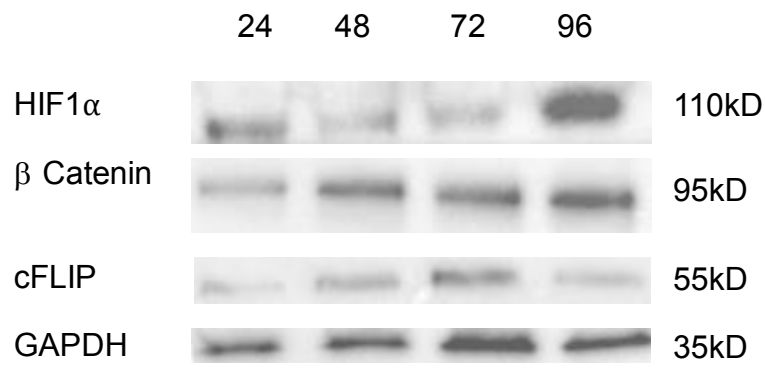
B
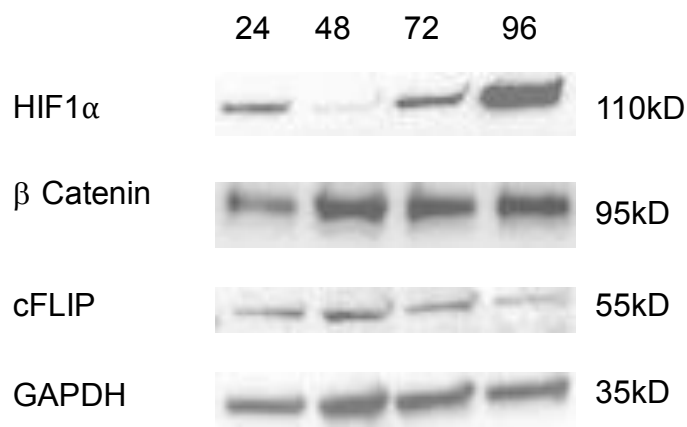
C
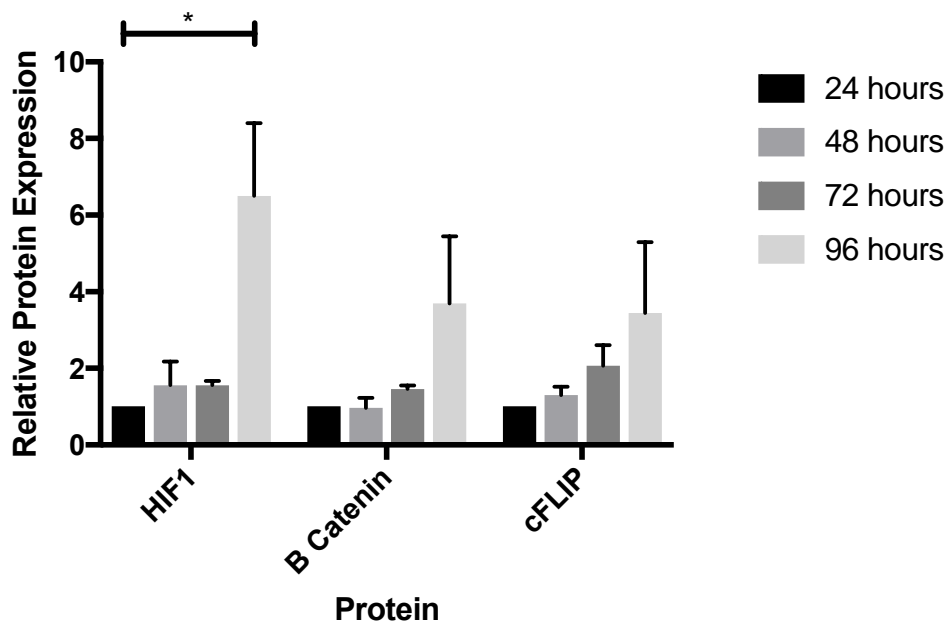
D
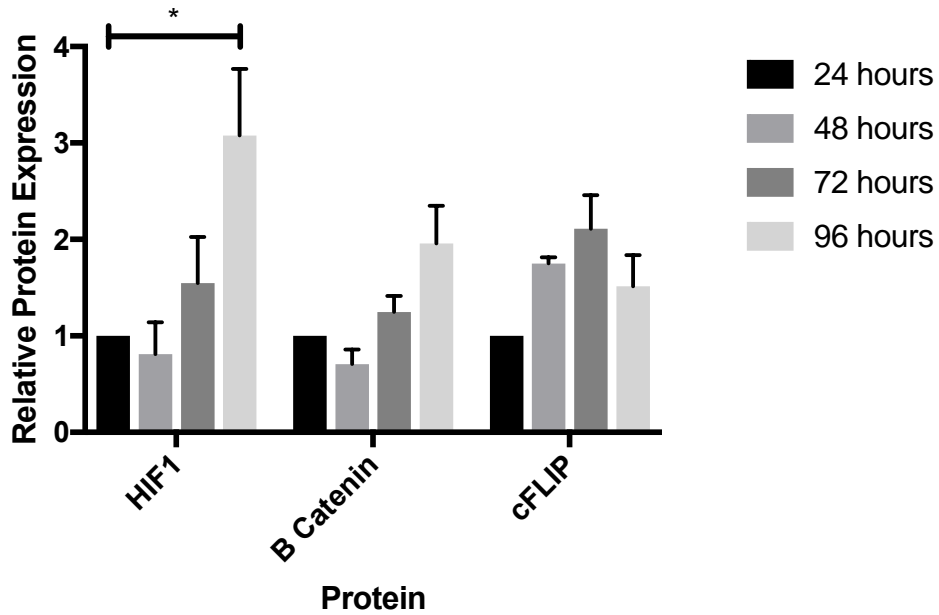
Figure 5.9- Time course of protein expression in response to paclitaxel in TNBC cell lines

The MDA-MB-231 (A and C) and SUM149 (B and D) cell lines were treated with paclitaxel and cells were harvested at 24,48,72 and 96 hours for protein analysis. A and B are representative pictures and C and D are a graphical representation of results. Error bars represent SEM of the mean and results are an average of three experiments. (T-test, *=p<0.1, **=p<0.01, ***=p<0.001   ****=p<0.0001).

5.2.3 HIF1α mediated gene expression is increased in a time-dependent manner

Having demonstrated that HIF1α, but not β-catenin, is significantly elevated by chemotherapy at 96 hours we examined HIF1α- gene expression and downstream HIF-α -dependent gene expression over the same time course. Again, we treated both MDA-MB-231 and SUM149 cell lines with their respective IC50 values of paclitaxel and harvested cells for RNA at 24,48, 72 and 96 hours. Targets of HIF1α that we wanted to examine were IL6, IL8, MDR1 and Snail, all of which have been shown to be under control of HIF1α (Shujing Liu et al. 2011; L. Zhang et al. 2013; Samanta et al. 2014).

In the MDA-MB-231 cell line there was significant upregulation of IL6, IL8, MDR1 and Snail prior to the 96 hours time point but the increase was largest at 96 hours for all targets and, for HIF1α itself, only significant at this time point (Fig 5.10A). In the SUM149 cell line (Fig 5.10B), there is a similar picture, with all targets upregulated before 96 hours but most markedly so at this point, with the exception of Snail that was most elevated at 24 hours.

A

B
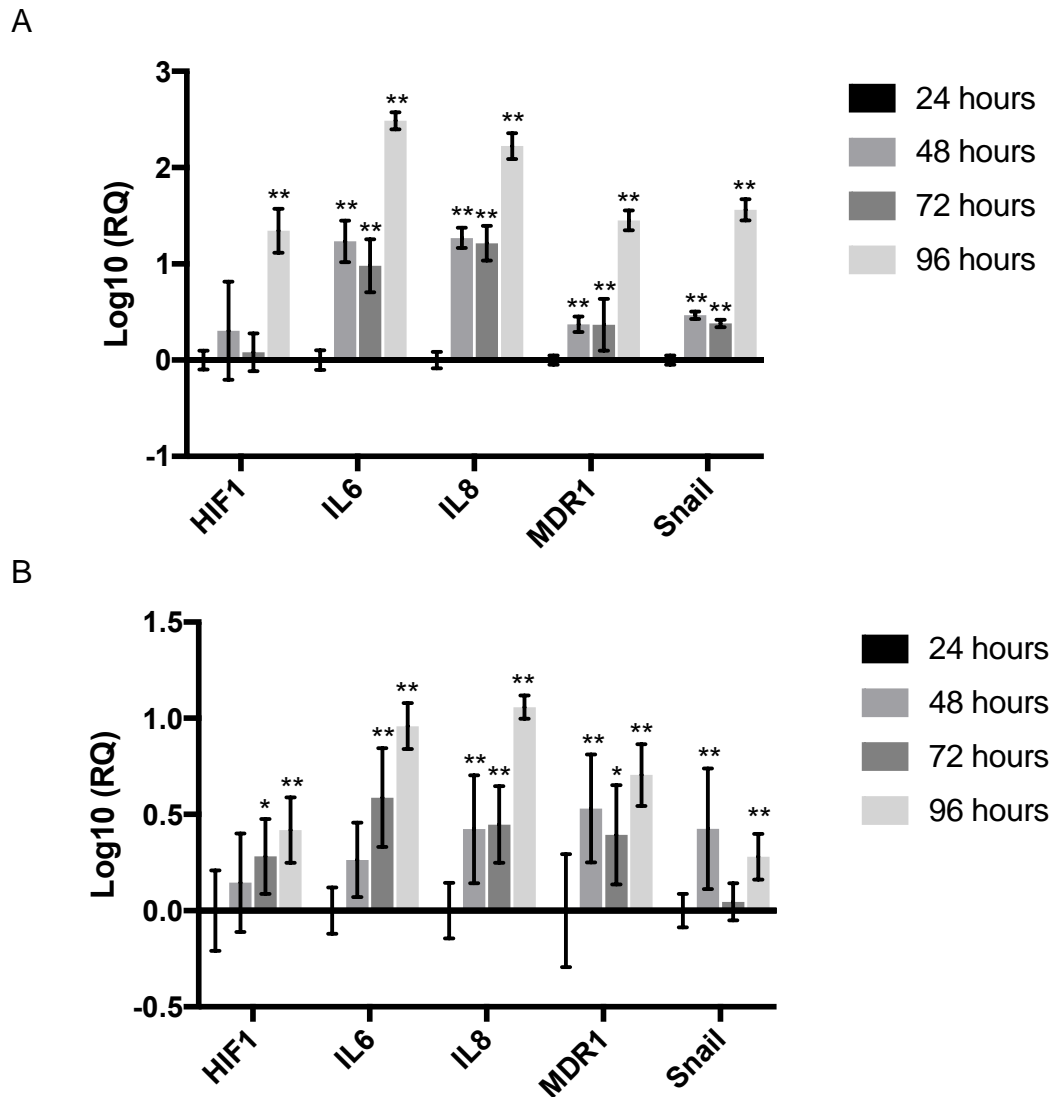
Figure 5.10 HIF1α-mediated gene expression increases over time in TNBC cell lines in response to paclitaxel

The MDA-MB-231 (A) and SUM149 (B) cell lines were treated with paclitaxel and cells were harvested at 24,48,72 and 96 hours for RNA analysis. Error bars represent CI of the mean and results are an average of three experiments each performed in triplicate. Statistical analysis was then performed by assessing the overlap between 95% confidence intervals (Cumming, Fidler, and Vaux 2007) (*=p<0.1, **=p<0.01).

5.2.4 The paclitaxel-mediated increase in HIF1α protein levels and gene-expression is reversed by OH14

Next we wanted to assess whether the increase in HIF1α that was seen with paclitaxel could be reversed by the addition of OH14, our novel cFLIP inhibitor. As previously described, cFLIP has been shown to interfere with the breakdown of HIF1α and therefore we hypothesised that OH14 would lead to increased breakdown of HIF1α mediated by the ubiquitin proteosome system (UPS) (Ishioka et al. 2007; Safa 2012). Thus we predicted that protein levels, but not mRNA levels of HIF1α would be affected by OH14, while downstream HIF1a-dependent gene targets would also be reduced. We also wanted to evaluate any potential effect on β-catenin and cFLIP.

The MDA-MB-231 or SUM149 cell lines were plated into adherent conditions, the relevant IC50 value of paclitaxel was added after cells were allowed to adhere overnight and left for 96 hours with OH14 +/- TRAIL being added 72hours later for the final 24 hours of the experiment. Cells were harvested and stored for either analysis of protein levels via Western Blotting or RNA analysis by RT-PCR.

Confirming our previous time course data, in both the MDA-MB-231 (Fig 5.11 A and B) and SUM149 (Fig 5.11 A and C) there was a significant rise in HIF1α protein expression when treated with paclitaxel. This increase was reversed by the addition of OH14, though in the MDA-MB-231 cell line the level of HIF1α was still significantly more than the control group. In the SUM149 cells, the levels of HIF1α were higher in the combined paclitaxel/OH14 group than control but this was not significant. In both cell lines, there were no significant differences between treatment arms seen with either β-catenin or cFLIP.

The effect of paclitaxel on HIF1α gene expression differed between the two cell lines. As expected MDA-MB-231 cells exhibited no transcriptional increase in HIF1α, suggesting that increased protein levels were due to stabilisation and/or post-translational modification. HIF1α gene expression in the SUM149 cell line however exhibited a significant increase, suggesting an

alternative, or additional, mechanism of regulation. However, the effect of OH14 on HIF1α gene expression was consistent, with both cell lines exhibiting a significant decrease in HIF1α mRNA levels with combined treatment.

The effect of OH14 on paclitaxel-mediated HIF1a-induced gene expression was also consistent between the cell lines, with OH14 inhibiting downstream paclitaxel-mediated gene transcription. In the SUM149 cell line, OH14 alone had the unexpected effect of reducing baseline transcription in 3 of the 4 downstream HIF1α gene targets.

A

	MDA-MB-231	SUM149	
	Ctrl 14 Pac Pac/14	Ctrl 14 Pac Pac/14	
HIF1α			110kD
β Catenin			95kD
cFLIP			55kD
GAPDH			35kD

B

C

Figure 5.11 Effect of paclitaxel and OH14 on HIF1α, β-catenin and cFLIP protein expression and HIF1α-mediated gene expression

The MDA-MB-231 (Figs A, B and D) and SUM149 cell lines (A, C and E) were treated with paclitaxel before the addition of OH14 72 hours later. After 24 hours they were harvested for either protein or RNA analysis. For Western blots, Error bars represent SEM of the mean and results are an average of three experiments. (T-test, *=p<0.1, **=p<0.01, ***=p<0.001 ****=p<0.0001). For RT-PCR error bars represent CI of the mean and results are an average of three experiments performed in triplicate. Statistical analysis was performed by assessing the overlap between 95% confidence intervals (Cumming, Fidler, and Vaux 2007) (*=p<0.1, **=p<0.01).

5.2.5 Confirming the role of HIF1α in TNBC CSC-like activity

5.2.5.1 HIF1α plays an important role in viability and mammosphere formation both with and without chemotherapy

Having established in the previous section that HIF1α, but not β-catenin, was affected by OH14 we sought to investigate the role of HIF1α further. HIF1α is known to play an important role in tumourigenesis, slow down tumour initiation *in vivo* and abrogate mammosphere formation in mammary tumour epithelial cells derived from mice in a MMTV-Cre model (Schwab et al. 2012; H. Zhang et al. 2015). For these experiments, MDA-MB-231 cells were plated overnight and then either scRNA or SiRNA HIF1α was added the next day before chemotherapy was added the day afterwards and allowed to remain in culture for another 96 hours. Cells were then examined for either viability using Cell Titer Blue or transferred into mammosphere conditions as described in Section 2.6. In addition cells were harvested between 24-96 hours to check the efficacy and duration of knockdown of HIF1α.

The siRNA-mediated knockdown of HIF1α was both persistent (lasting up to 96 hours) and highly significant at all time points (Fig 5.12A). There was no effect of siHIF1α alone, but a small yet significant difference in cell viability when paclitaxel treated cells were treated with SiRNA compared to scRNA (mean 69% with scRNA and 60% with SiRNA HIF1α). When examining the effect of mammosphere formation, the effect of knocking down HIF1α is highly significant. In both Passage 1 and Passage 2, there was a highly significant increase with paclitaxel in the scRNA group as has been seen in our previous experiments. Knockdown of HIF1α led to not only a significant reduction in mammosphere formation compared to scRNA in both Passage 1 and Passage 2 (Fig 5.13 A-C) but also abrogated the increase in mammosphere formation seen in both passages with paclitaxel. When combining our data into our mathematical model, it can be seen that knockdown of HIF1α leads to a significant reduction in absolute CSC number from 133 in the scRNA group to 61. It also leads to a 50% reduction in absolute CSC number with chemotherapy (61 to 31) compared to the 25% increase seen with paclitaxel with scRNA (Fig 5.14).

A
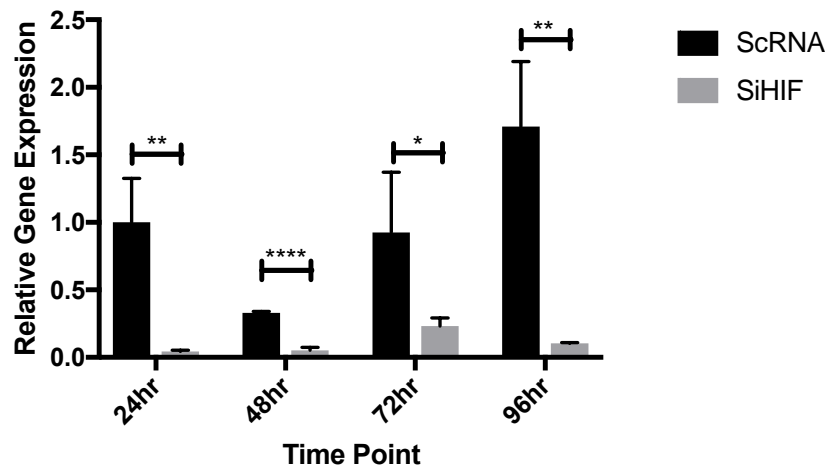
B
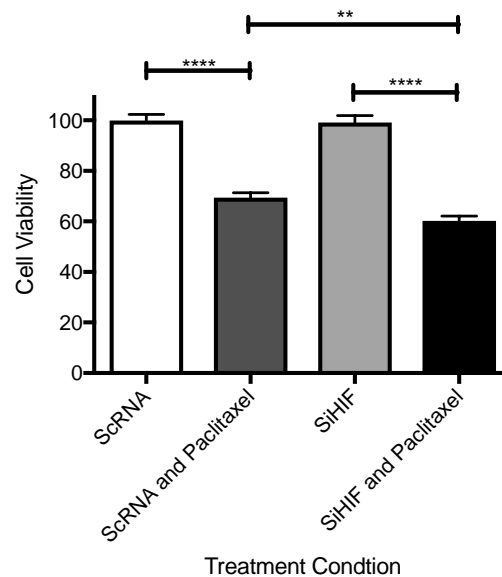
Figure 5.12 Effect of siRNA against HIF1α on cell viability in combination with paclitaxel

MDA-MB-231 cells were plated overnight and then either scRNA or SiRNA HIF1α was added the next day. A, to confirm knockdown of HIF1α cells were harvested for RNA between 24 and 96hrs. B, after knockdown chemotherapy was added the day afterwards and allowed to remain in culture for another 96 hours. Cells were then examined for either viability using Cell Titer Blue. For RT-PCR error bars represent CI of the mean and results are an average of three experiments performed in triplicate. Statistical analysis was performed by assessing the overlap between 95% confidence intervals (Cumming, Fidler, and Vaux 2007) (*=p<0.1, **=p<0.01). For viability, error bars represent standard error of the mean and results are an average of three experiments performed in triplicate. (T-test, *=p<0.1, **=p<0.01, ***=p<0.001 ****=p<0.0001).

A

Treatment Condtion

B

Treatment condition

C

| Control | Paclitaxel |

scRNA

siHIF1
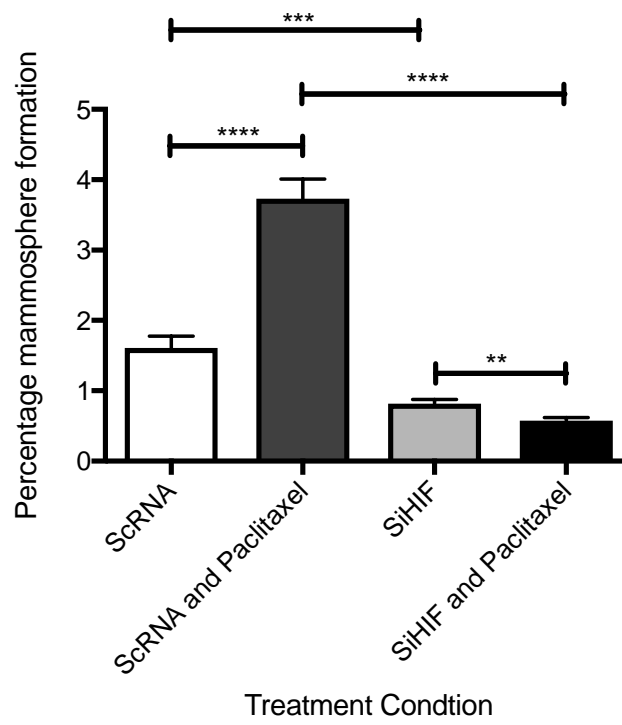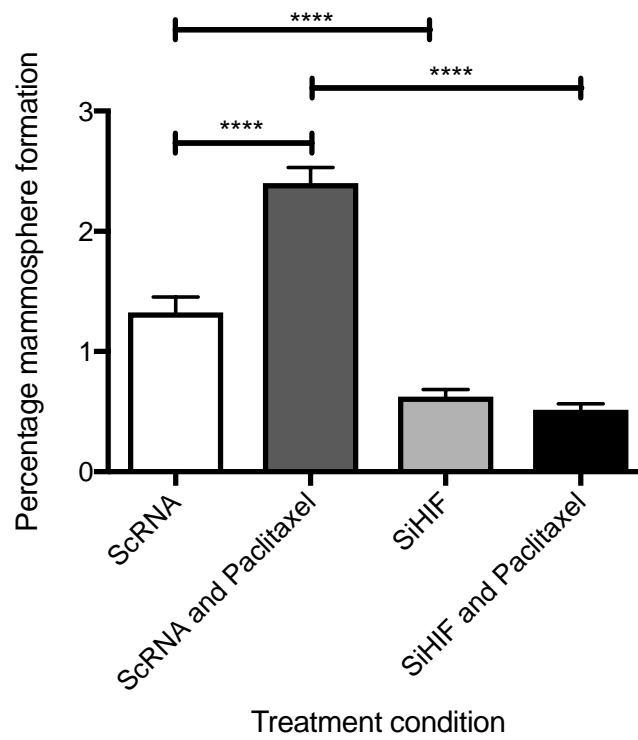
Figure 5.13- Knockdown of HIF1α stops the increase in mammosphere formation seen in the MDA-MB-231 cell line with paclitaxel

MDA-MB-231 cells were plated overnight and then either scRNA or SiRNA HIF1α was added the next day before chemotherapy was added the day afterwards and allowed to remain in culture for another 96 hours. Cells were then dissociated and plated at a fixed density in mammosphere conditions. After 7 days they were counted (Passage 1, A), dissociated and plated again at a fixed concentration. 7 days later they were counted again (Passage 2, B). C, Pictures at the end of Passage 2.   Error bars represent standard error of the mean and results are an average of three experiments performed in triplicate. (T-test, *=p<0.1, **=p<0.01, ***=p<0.001 ****=p<0.0001).

Treatment Condition	Viability (%)	Cell number (100%-10000)	P2 sphere formation (%)	Total number of CSCs
scRNA	100	10000	1.325	133
scRNA with Paclitaxel	69.4	6940	2.4	167
siRNA HIF1	99.1	9910	0.62	61
siRNA HIF1 with paclitaxel	60.3	6030	0.52	31
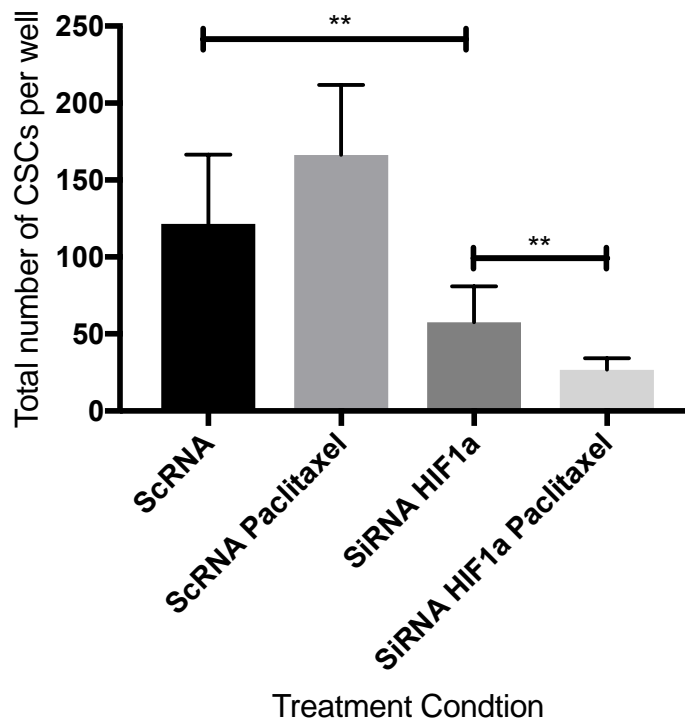
Figure 5.14 – Table and Graphical Representation of mathematical CSC model in MDA-MB-231 cells with or without Caspase Inhibition

The overall cell viability of the MDA-MB-231 cell line was multiplied by the percentage mammosphere formation at the end of Passage 2 for the respective treatment condition to give an absolute CSC number remaining at the end of adherent treatment. Error bars represent standard error of the mean and results are an average of three experiments performed in triplicate. (T-test, *=p<0.1, **=p<0.01, ***=p<0.001 ****=p<0.0001).

5.2.5.2 Establishing the role of apoptosis in HIF1α-mediated CSC suppression

Hypoxia has been shown to play an anti-apoptotic role with mechanisms mediated both with and without HIF1α (Flamant et al. 2010). Flamant and co-workers eloquently showed in the MDA-MB-231 cell line that HIF1α is involved in hypoxia-induced protection against paclitaxel-induced apoptosis. In addition, hypoxia led to lower expression of extrinsic apoptosis pathway genes such as Caspases 8 and 10 as well as TRAIL receptor family that was reversed by knockdown of HIF1α by siRNA. This has important implications and suggests that OH14, as an antagonist of cFLIP activity, could be having a duality of effect on CSC-like activity. Firstly, it may increase apoptosis by directly blocking the antagonostic activity of cFLIP on the extrinsic apoptosis pathway. By reducing HIF1α levels, through allowing its degradation through the UPS, it also potentially increases the gene expression of components of this pathway. This would also result in the reduction of paclitaxel induced HIF1α-mediated gene expression of genes associated with CSC-like behaviour such as IL6, IL8 and MDR1 (Section 5.1.4).

In this section we therefore sought to assess the effect of Caspase Inhibition (CI) on both viability and mammosphere formation in HIF1a-siRNA treated MDA-MB-231 cells. Cells were plated, allowed to seed overnight, treated with siRNA HIF1α and then treated with paclitaxel 24 hours later for 96 hours. CI was added one hour before paclitaxel. Cells were then analysed for viability by Cell Titer Blue or trypsinised, dissociated and plated into mammosphere condition as described in detail in Section 2.6. To conclude that apoptosis was an important mechanism in altering CSC-like behaviour in the context of HIFα suppression and paclitaxel, we would expect CI to cause a significant change in the magnitude of the effect of paclitaxel in the context of HIFα suppression compared to the control group with no paclitaxel.

CI led to a significant increase in cell viability when combined with paclitaxel with viability increasing from 66 to 76% (Fig 5.15). The effects of CI on mammosphere formation in both Passage 1 and Passage 2, with and without paclitaxel, (Fig 5.16A and 5.16B respectively) were similar. As seen in

Sections 5.1.1.3 and 5.1.1.4, CI led to a significant increase in mammosphere formation in all conditions. However, as there was no differences between the control and paclitaxel treated groups we conclude that apoptosis is unlikely to play a major role.

The mathematical model that combines cell viability with mammosphere formation yields similar results. Without CI, when HIF1α is suppressed paclitaxel leads to a significant fall in CSC numbers and this effect persists with CI. (Fig 5.16). This does not suggest that apoptosis is playing a signicant role in the HIF1α-mediated effect on CSC number induced by paclitaxel
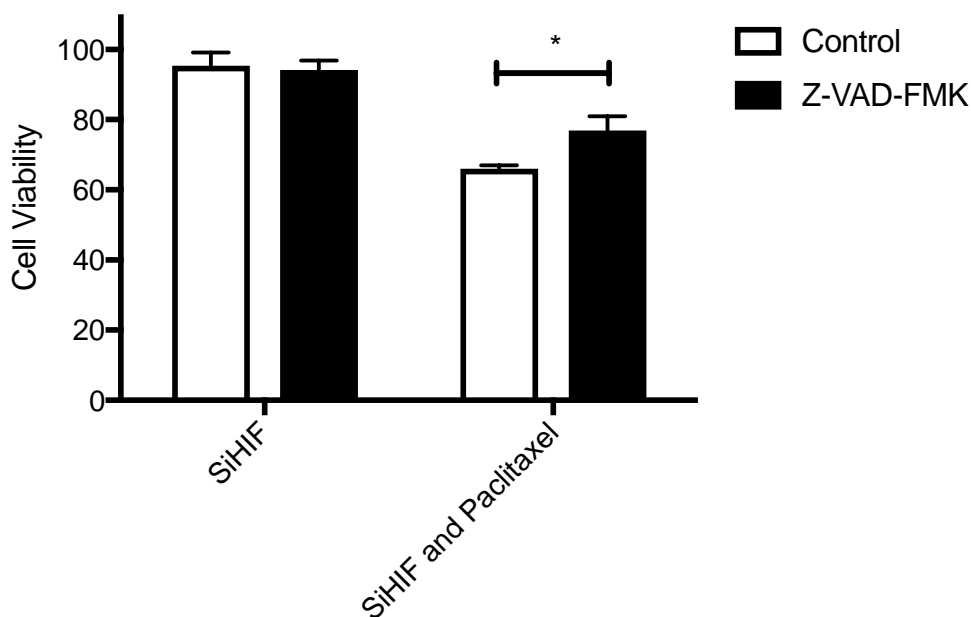
Figure 5.15- Effect of Caspase Inhibition on cell viability in combination with paclitaxel and siRNA-mediated knockdown of HIF1α

MDA-MB-231 cells were plated overnight and then either scRNA or SiRNA HIF1α was added the next day before chemotherapy was added the day afterwards and allowed to remain in culture for another 96 hours. Z-VAD-FMK was added one hours before chemotherapy. Cells were then examined for either viability using Cell Titer Blue. Error bars represent standard error of the mean and results are an average of three experiments performed in triplicate. (T-test, *=p<0.1, **=p<0.01, ***=p<0.001 ****=p<0.0001).

A
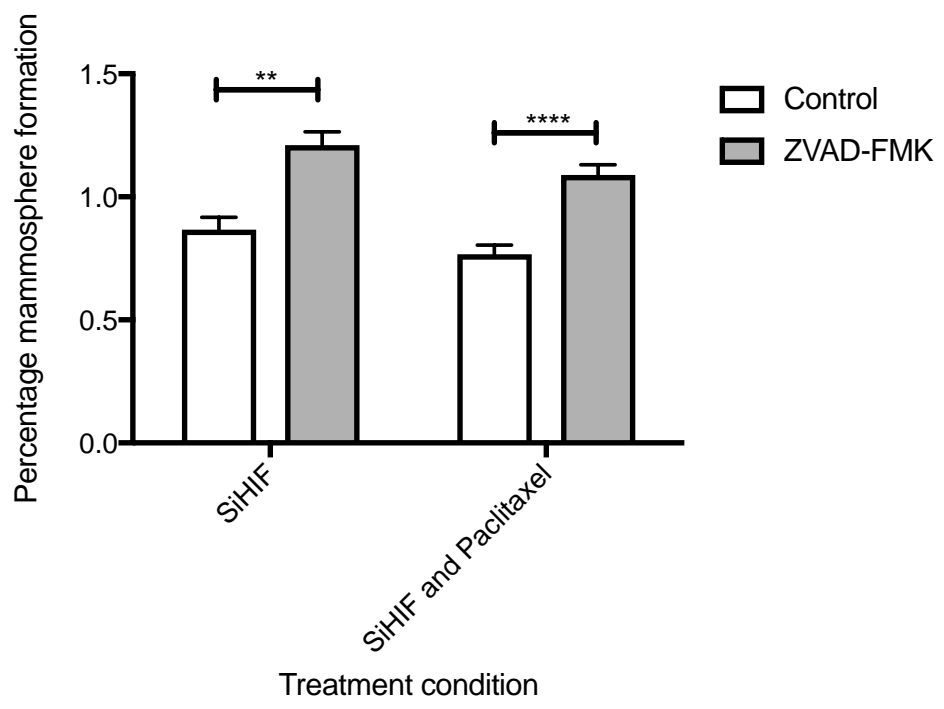
B

C
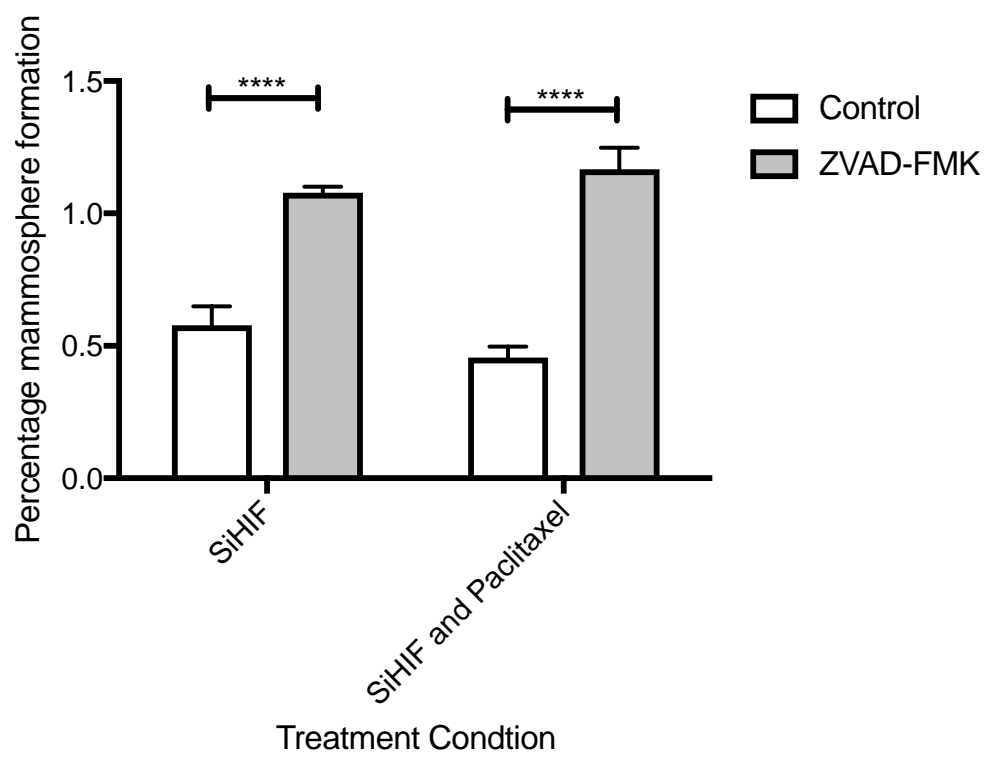
Treatment Condition	Viability (%)	Cell number (100%-10000)	P2 sphere formation (%)	Total number of CSCs
siRNA HIF1	95.4	9540	0.58	55
siRNA HIF1 with paclitaxel	66	6600	0.46	30
siRNA HIF1 with CI	94.2	9420	1.08	101
siRNA HIF1 with paclitaxel and CI	76.9	7690	1	76.9
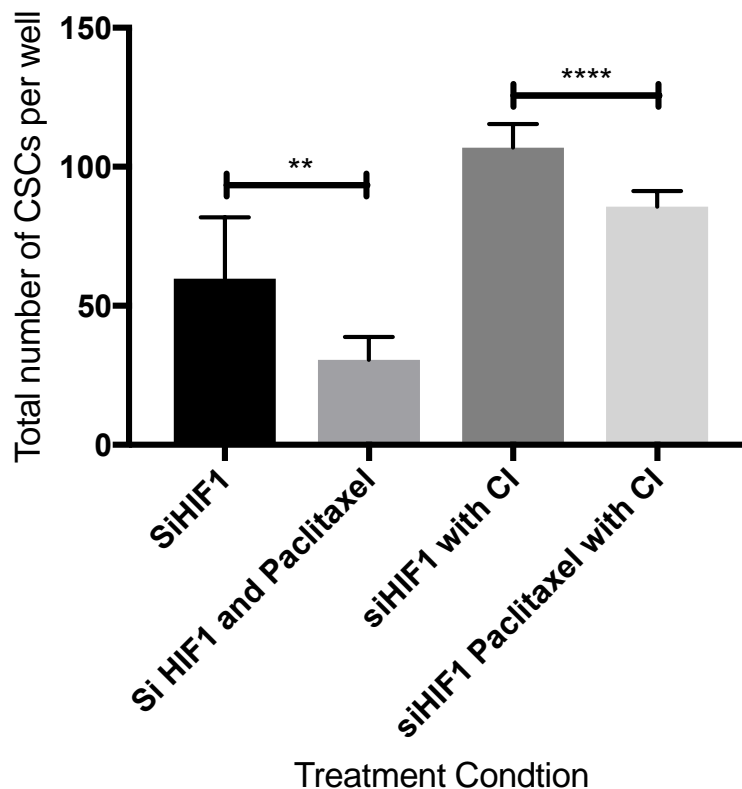
Figure 5.16 Effect of CI on CSC-like activity with paclitaxel and siRNA-mediated knockdown of HIF1α

MDA-MB-231 cells were plated overnight, SiRNA HIF1α was added 24hr later, before chemotherapy was added 24hr later again (+/- CI 1hr before) for 96 hours. Cells were dissociated and plated into mammosphere conditions. After 7 days they were counted (Passage 1, A), dissociated and plated again at a fixed concentration. 7 days later they were counted again (Passage 2, B). C, the overall cell viability of the MDA-MB-231 cell line was multiplied by

the percentage mammosphere formation at the end of Passage 2 for the respective treatment condition to give an absolute CSC number remaining at the end of adherent treatment. Error bars represent standard error of the mean and results are an average of three experiments performed in triplicate. (T-test, *=p<0.1, **=p<0.01, ***=p<0.001   ****=p<0.0001).
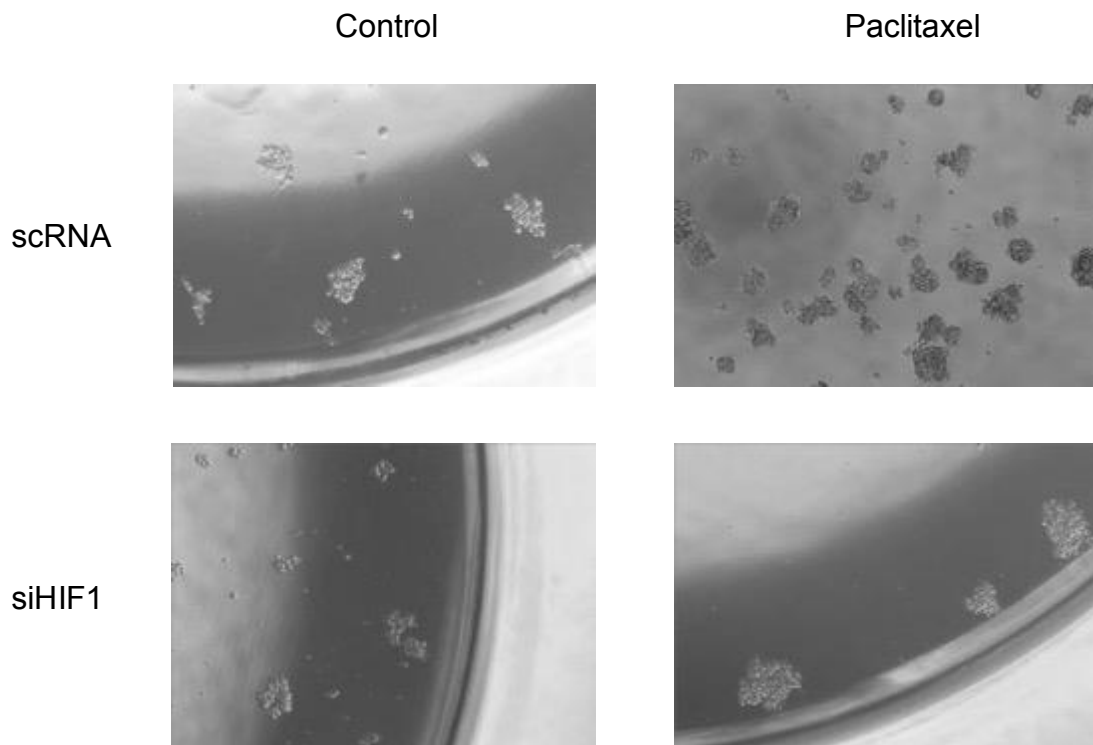
5.2.5.3 Inhibiting the proteasome pathway, reverses the reduction in HIF1α seen in response to cFLIP inhibtion

Having established that OH14 leads to a reduction in HIF1α and that supressing HIF1α leads to a suppression of mammosphere activity, with and without paclitaxel, we wanted to establish a mechanism of action. Previous studies have shown that over expression of cFLIP led to upregulation of both HIF1α and β-catenin that was reversed through using MG132, a proteasome inhibitor that disrupts the ubiquitin proteasome system (UPS) (Ishioka et al. 2007; Naito et al. 2004). This effect was replicated by mutating the DEDs of cFLIP, one of which (DED1) is known to be bound by our novel compound OH14 (Hayward et al, unpublished work).

We therefore assessed the effect of MG132 on reversing the reduction of both HIF1α and β-catenin by siRNA-mediated knockdown of cFLIP and HIF1α in the MDA-MB-231 cell line. In these experiments we stimulated HIF1α through hypoxic conditions, rather than using chemotherapy. This is because MG132 is toxic to cells and therefore combining it with chemotherapy would lead to too much cell death. Cells were treated with either a scrambled siRNA control or siRNA targeted against cFLIP or HIF1α for 48hrs and then treated with 10µM of MG132 for 5 hours whilst in a 1% O_2/ 5% CO_2 incubator at 37°C. Western blotting (Fig 5.15A) showed that in scrambled control the level of HIF1α and β-catenin went up with MG132 (shown graphically with white bars in Fig 5.15B for HIF1α and Fig 5.15C for β-Catenin). cFLIP, although known to be degraded by the UPS (Safa 2012) did not change (Fig 5.15D, white bars).

Knocking down cFLIP led to a 60% reduction in HIF1α (Fig 5.15B) that was significantly reversed with MG132. Although suppression of cFLIP had not previously been shown to cause a reduction in β-Catenin in the MDA-MB-231 cell line, there was a trend but no significant increase in β-Catenin with MG132 following knockdown of cFLIP (Fig 5.15C). cFLIP levels were suppressed by an average of 85% at 48hrs with siRNA and therefore were not affected by MG132 (Fig 5.15D).

Finally, suppression of HIF1α led to an 80% reduction in HIF1α levels that was not changed by MG132 (Fig 5.15B), though there was a small but non-significant increase in β-Catenin and decrease in cFLIP seen with MG132 after knockdown (Figs 5.15C and 5.15D respectively).

A
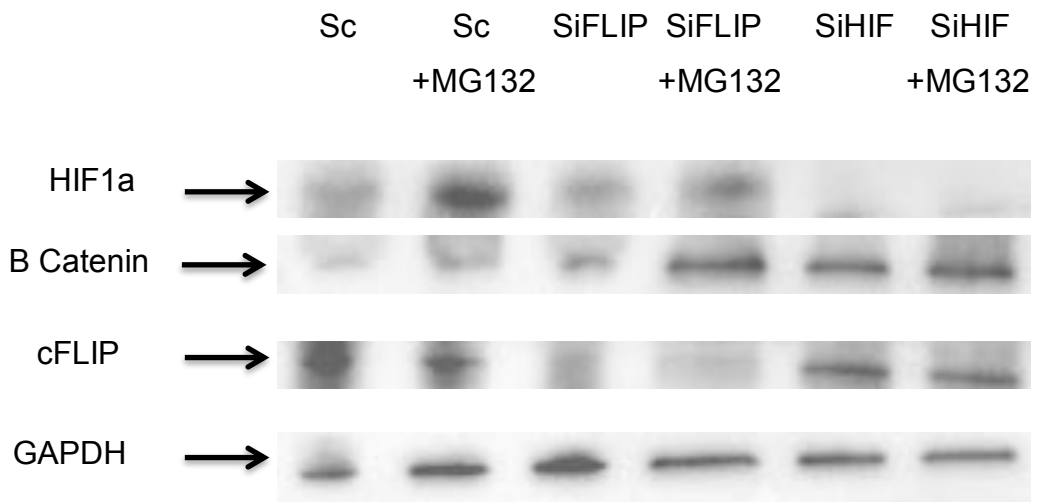
B
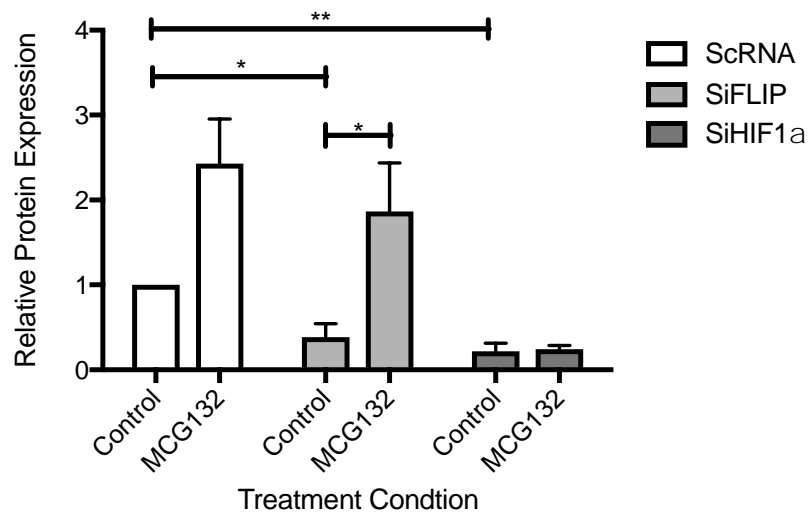
C
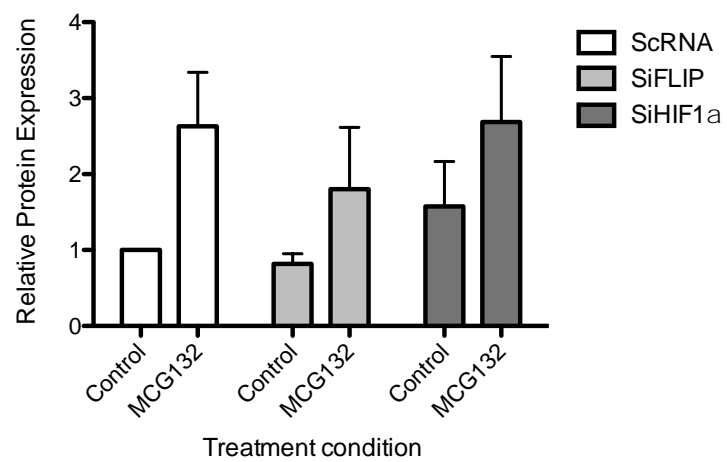
D
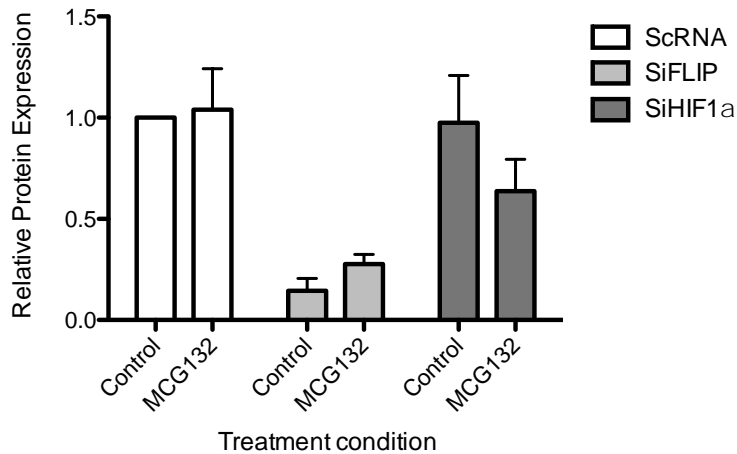
Figure 5.17- Inhibition of the UPS reverses the reduction in HIF1α levels in response to siRNA mediated knockdown of cFLIP

The MDA-MB-231 cell line was treated with either scRNA, siRNA against cFLIP or siRNA against HIF1α for 48hrs before being placed in hypoxic condition for 5 hrs with or without the proteasome inhibitor MG132. Cells were then harvested for protein analysis. A, representative Western Blot. B, graphical representation of effect of siRNA on HIF1α. C, graphical representation of effect of siRNA on β-Catenin. D, graphical representation of effect of siRNA on cFLIP. Error bars represent SEM of the mean and results are an average of three experiments. (T-test, *=p<0.1, **=p<0.01, ***=p<0.001 ****=p<0.0001).

5.2.5.4 OH14 reverses the increase in colony forming ability seen with hypoxia in MDA-MB-231 cells

Next we wanted to assess whether OH14 could block any increase in colony formation ability (CFA) of MDA-MB-231 cells when they were plated at low confluency and left for a period of time in either hypoxic (1% O_2/5%CO_2) or normoxic (20% O_2/5%CO_2) conditions. The CFA is an *in vitro* assay which tests one of the functional characteristics of stem cells: the ability to propagate colonies from single cells through enhanced proliferative potential (Locke et al. 2005). Hypoxia has previously been shown to increase the stem cell markers and colony forming ability of the MDA-MB-231 cell line (Xie et al. 2016). In this experiment, MDA-MB-231 cells were plated at a confluency of 185 cells/ml into a 12 well dish, allowed to adhere overnight, then treated with either DMSO control or 10µM OH14, placed in differing oxygen concentrations and then left for 6 days. This experimental design was chosen as the passaging step of the mammosphere experiment would have involved passaging cells in non-hypoxic conditions- potentially altering the outcome.

Hypoxia led to a highly significant increase in the colony forming ability of the cells (20% average 115.5 colonies, 1% 194.5 colonies, a 68% increase) (Fig 5.16 below). In normoxia, OH14 significantly reduced colony formation (115.5 to 101.5 colonies on average, a 12% decrease) but under hypoxic condition, the addition of OH14 greatly reduced the ability of the cells to form colonies (194.5 to 118.8, a 39% decrease).
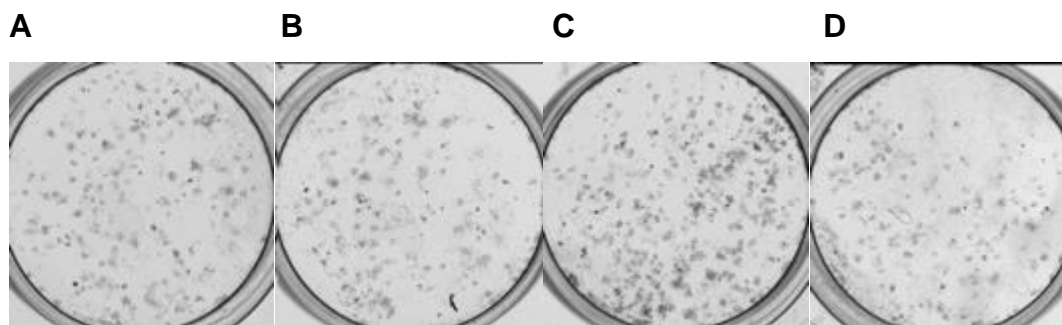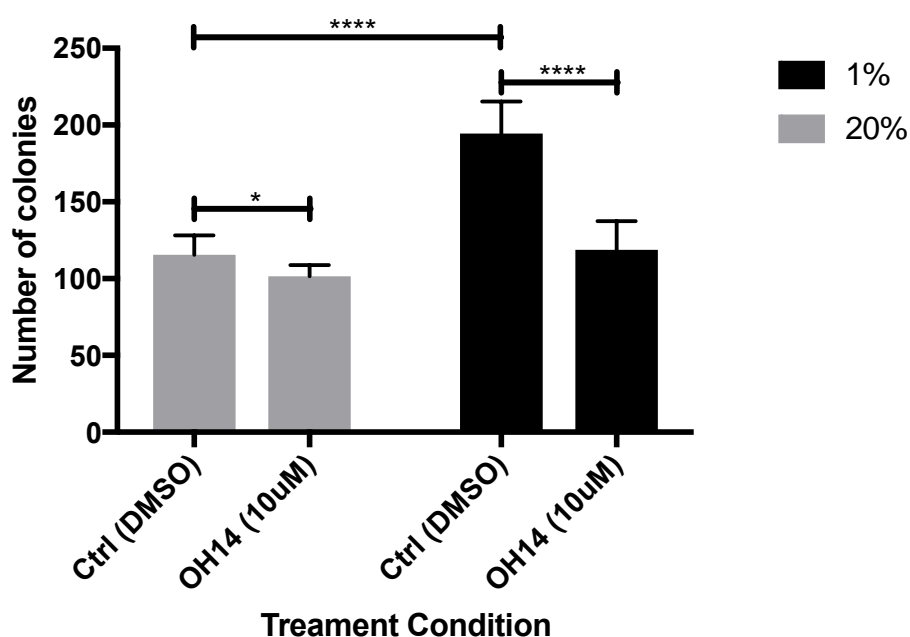
Figure 5.18- Effect of OH14 on CFA of the MDA-MB-231 cell line

A-D, representative pictures of different treatment condition (A, 20% control, B, 20% OH14, C, 1% Control, D, 1% OH14) after being left for 6 days in respective treatment conditions. E, Graphical representation of results. Error bars represent SEM of the mean and results are an average of three experiments. (T-test, *=p<0.1, **=p<0.01, ***=p<0.001 ****=p<0.0001).

5.3   Discussion

Previous work in our laboratory had shown that the combination of cFLIP suppression and TRAIL was effective against CSCs in a broad panel of breast cancer cell lines without chemotherapy (Piggott et al. 2011). The original aim of this thesis was to assess whether the combination of cFLIP suppression, using the subsequently developed cFLIP inhibitor OH14, and TRAIL abrogated CSC-like activity as effectively in breast cancer cell lines that had been treated with chemotherapy. It was demonstrated in Chapter 3 that chemotherapy led to an increased CSC-like phenotype across a panel of breast cancer cell lines and then in Chapter 4 that the combination of paclitaxel and OH14 alone led to a significant effect on CSC-like activity in TNBC cell lines alone without TRAIL. Although, not wanting to discount TRAIL entirely, the aim of this chapter was to assess the mechanism through which OH14, or cFLIP suppression using siRNA, may be leading to a reduction in a CSC-phenotype in the context of chemotherapy.

There were two main mechanisms that we wished to explore- apoptosis and CSC-like signalling. As described in Section 5.1, cFLIP has an important antagonistic role in the extrinsic apoptosis pathway and its overexpression has been shown to protect against the apoptosis induced by paclitaxel in particular (Safa 2012; Day, Huang, and Safa 2008a; Day et al. 2006). CSC-signalling has been shown to be induced by chemotherapy and two targets were of interest- HIF1α and β-catenin. Whilst both have been implicated in CSC-like behaviour, the former has been shown to be both induced by chemotherapy and to be prognostic in TNBC (Samanta et al. 2014; Lu et al. 2015). Although such a strong link does not exist for β-catenin, it has been shown to be involved in EMT, a key mechanism through which cancerous cells acquire CSC-like attributes (Mani et al. 2008; Rosa et al. 2015). The degradation of both these proteins has been shown to be under the control of the ubiquitin proteasome system (UPS), of which cFLIP is an inhibitor (Ishioka et al. 2007). Indeed, previous work in our laboratory has shown that siRNA-mediated suppression of cFLIP leads to a reduction in β-catenin and here we wanted to assess whether this remained the case both in using OH14 rather than siRNA and in the context of chemotherapy (French et al. 2015).

Wanting to firstly assess the role of apoptosis, the Annexin V and DAPI assay was used to examine apoptosis and cell death via flow cytometry in the MDA-MB-231 cell line. We demonstrated that without chemotherapy OH14 did little to effect overall cell viability as a single agent (Fig 5.3), TRAIL alone led a highly significant drop to 47% of control that was further increased by 16% to 31% overall alive population with the combination of both TRAIL and OH14 together. With the addition of paclitaxel, both OH14 and TRAIL led to a reduction in viability compared to paclitaxel alone, though interestingly for TRAIL the overall viable population was higher with the combination of paclitaxel and TRAIL than TRAIL alone (54% v 47%) though this was not statistically significant. This is somewhat surprising as a previous synergistic relationship has been shown between paclitaxel and TRAIL and paclitaxel has been shown to up regulate the death receptors to which TRAIL binds (Buchsbaum et al. 2003; de Miguel et al. 2016) and therefore we would expect the viability to decrease above single agent TRAIL as we previously saw with our Cell Titre Blue assay in Section 4.2.4. The combination of OH14 and TRAIL led to an increase in cell death with only 30% of the population remaining viable.

We then wanted to assess whether blocking apoptosis using a pan-caspase inhibitor (CI) Z-VAD-FMK led to OH14 having different effects on both overall viability and CSC-like activity (Figs 5.4-5.8). When examining the effect of CI on overall cell viability, in both the MDA-MB-231 and SUM149 cell lines, CI led to an increased viability in control, OH14 paclitaxel and paclitaxel/OH14 arms. This effect was broadly similar across all treatment arms suggesting that OH14 was not having a marked effect on the overall bulk cell population through apoptotic pathways. We subsequently went on to examine the effect of CI on mammosphere formation, hypothesising that in previous Chapters OH14 had affected CSC-like activity more than its effects on a bulk cell population. In these experiments, CI led to an increase in mammosphere formation and actual CSC number across all treatment groups- likely because anoikis uses apoptosis pathways to induce cell death and this is a key biological process in resisting death in non-adherent cell culture conditions.

(Gilmore 2005). We again explored as to whether there as a difference in magnitude different conditions had CI added. In none of our treatment conditions did CI lead to a change in magnitude of either mammospheres or numbers of CSCs in our mathematical models. This suggests that the primary anti-CSC activity of OH14 is not dependent upon apoptosis. Further experiments examining the effect of OH14 on apoptosis in CSCs could be undertaken on a purified CSC population (fox example that had been FACS sorted by ALDH[+]) and could include either recalculation of an IC50 value on these cells compared to an overall cell population or an Annexin V/DAPI assay.

Having shown that OH14 was not having a major effect through apoptosis, we examined the role of the CSC-signalling proteins HIF1α and β-catenin. As shown in Fig 5.9, there was no significant increase in β-catenin with paclitaxel at any time point after chemotherapy but HIF1α levels increased significantly at 96hrs. This could explain why, in Chapter 3, no increase in mammosphere formation was seen at 72hrs but was at 96 hrs. Indeed, others have shown that it takes 96hrs for HIF1α levels to be elevated in response to chemotherapy in breast cancer cell lines (Samanta et al. 2014)- although the same laboratory subsequently published a paper showing an increase in mammosphere formation after 72hrs of treatment (Zhang et al. 2015). Further experiments will be undertaken to assess whether β-catenin gene expression was increased despite no increase in protein levels. This could be through a mechanism such as nuclear localisation and therefore nuclear and cytoplasmic levels of β-catenin could be examined. In addition, further experiments using reporter assays for both HIF1α and β-catenin (for example luciferase reporters) could be undertaken to examine both the time course of any increase in response to chemotherapy and also the effect of OH14 on this process.

Having demonstrated an increased in HIF1α protein levels, we wanted to assess whether HIF1α-mediated gene expression also increased at this time point using qRT-PCR (Fig 5.10). The results showed that at the 48, 72 and 96 hours, there was an increase in IL6, IL8, MDR1 and Snail expression but

that this effect was most profound at 96 hours. Whilst IL6, IL8 and MDR1 are known to be under the influence of HIF1α, expression of IL6 and IL8 has been shown to be increased by paclitaxel in ovarian cancer cell lines after 24 hours (Wang et al. 2006; Lee et al. 1997) and therefore it is likely that increased expression was non-HIF1α dependent. A potential mechanism could include activation of the c-Jun N-terminal kinase (JNK) and Nuclear Factor-κB (NFκB) pathways that have been shown to be upregulated by paclitaxel and lead to increases in anti-apoptotic proteins such as MDR1 and IL6 and IL8. (Wang et al. 2006).

The next experiments set out to evaluate the effect of OH14 on HIF1α protein levels and gene expression. When examining protein levels, paclitaxel led to a significant increase in HIF1α that was abrogated by the addition of OH14 (Fig. 5.11). The effect of paclitaxel on HIF1α gene expression differed between the two cell lines. As expected MDA-MB-231 cells exhibited no transcriptional increase in HIF1α, suggesting that increased protein levels were due to stabilisation and/or post-translational modification. HIF1α gene expression in the SUM149 cell line however exhibited a significant increase, suggesting an alternative, or additional, mechanism of regulation. However, the effect of OH14 on HIF1α gene expression was consistent, with both cell lines exhibiting a significant decrease in HIF1α mRNA levels with combined treatment.

The effect of OH14 on paclitaxel-mediated HIF1 α -induced gene expression was also consistent between the cell lines, with OH14 inhibiting downstream paclitaxel-mediated gene transcription. In the SUM149 cell line, OH14 alone had the unexpected effect of reducing baseline transcription in 3 of the 4 downstream HIF1α gene targets whereas in the MDA-MB-231 cell line, OH14 increase all 4 targets. These experiments firstly need repeating to ensure that this is a true effect but this is a potentially interesting observation, suggesting that there may be differences in biology between the two cell lines. One potential mechanism is through the JNK mediated proteasomal degradation of cFLIP, leading to enhanced apoptosis (L. Chang et al. 2006). An isoform of cFLIP, cFLIP-L, has been shown to inhibit the JNK pathway (Nakajima et al.

2006). OH14, by binding to cFLIP, may be inhibiting this inhibition, therefore leading to elevation of JNK and an elevation of IL6 levels. When examining potential mechanisms of IL8 elevation with OH14, there is a potential complex mechanism involving both pro- and anti-inflammatory signalling involving both cFLIP and NF-κB signaling. cFLIP has also been shown to inhibit the death receptor induced activation and induction of the NFκB target gene IL8. Therefore inhibiting cFLIP with OH14 may stop this process causing elevation of IL8 (Kavuri et al. 2011). Further experiments looking at both protein levels of the JNK and NFκB pathways could be undertaken should this effect persist in repeat experiments.

Together, these data demonstrated that paclitaxel induced HIF1α and that OH14 seemed to have an effect on both protein levels and HIF1α-mediated gene expression when combined with paclitaxel. We therefore sought to confirm the role of HIF1α in CSC-like behaviour. As can be seen in Fig 5.12, siRNA-mediated knockdown of HIF1α led to both an increased in the cytotoxicity of paclitaxel on the bulk cell population of MDA-MB-231 cells as well as significantly reducing mammosphere formation compared to scrambled control. It also reversed the increase in mammosphere formation seen with paclitaxel. Using our mathematical model confirmed that blocking HIF1α led to an almost proportional reduction in CSCs as compared to the reduction in overall cell viability. Cell viability decreased from 99.1% with siRNA HIF1α to 60.3% with siRNA HIF1α and paclitaxel (a 60.8% reduction), with a drop in absolute CSC numbers from 61 to 31 (a 50.8% drop). This suggests that HIF1α may also have a role in potentiating the apoptotic effect of paclitaxel. We sought to evaluate this further by using a CI to examine this effect on both cell viability and mammosphere formation. As seen with OH14 and paclitaxel there were no differences in the proportion of increase with the addition of CI in siRNA treated cells both with and without paclitaxel suggesting that HIF1α was not having its predominant effect through apoptosis (Fig 5.16 A and B). In our CSC model (Fig 5.16C), paclitaxel after siRNA-mediated knockdown of HIF1α led to reduction in CSC number that was maintained with the addition of CI. These results suggest a minor role for

apoptosis in the HIF1α-mediated reduction in CSC-like behaviour but further work could look at examining the levels of Caspase activation in response to HIF1α knockdown.

Having established the role of HIF1α, we wanted to confirm the mechanism of reduction in HIF1α by cFLIP suppression. Using MG132, a proteasome inhibitor, we sought to show that cFLIP prevented the ubiquitin proteasome system (UPS) from degrading HIF1α as has been shown by others previously (Ishioka et al. 2007). Our results showed that in hypoxic conditions (to elevate HIF1α), siRNA-mediated knockdown of cFLIP led to a significant reduction in HIF1α levels that was reversed by MG132 (Fig 5.15). This confirms that the mechanism of action of OH14 is via the UPS.

Lastly, we demonstrated that hypoxia increased colony formation in the MDA-MB-231 cell line and that this effect was reversed by the addition of OH14 (Fig 5.16). This experiment was chosen rather than a mammsophere experiment as we wanted to avoid the handling of cells (for example during the passage step of the mammosphere experiment).

This chapter has therefore demonstrated that OH14 is having its effect on CSC-like behaviour in two ways: Firstly, and primarily, through increasing the degradation of HIF1α that is induced by chemotherapy and secondly, through increasing apoptosis in CSCs. HIF1α leads to the expression of a number of genes that are associated with CSC-like behaviour and drug resistance, such as IL6, IL8 and MDR1.

6 Discussion and Future Work

6.1 Discussion

There has been a significant improvement in breast cancer survival over the last few decades with much of this improvement attributable to a combination of earlier detection of breast cancer, improvement in systemic therapy and improved surgical techniques (J.-H. Park, Anderson, and Gail 2015). Despite this, breast cancer remains that largest cause of cancer death in females in the Western world and novel treatment strategies are needed to improve survival (Turner et al. 2016).

The importance of inter tumour heterogeneity in breast cancer has long been recognised, for example through the oestrogen, progesterone and Her2 receptors. We know and appreciate that these markers have a large impact on disease progression, response to treatment and overall prognosis (Prat and Perou 2011). Nevertheless, it is only in the last 10 to 15 years that the concept of intra tumour heterogeneity has been both appreciated and studied. The emergence of the cancer stem cell hypothesis over the last 15 years has led to possible explanations to previously poorly understood clinical concepts such as tumour dormancy, metastases and recurrence (Al-Hajj et al. 2003; Azizi and Wicha 2013).

Naturally, there has been a focus on how chemotherapeutic agents in use affect this population. A large body of previous work has demonstrated that chemotherapy poorly targets the CSCs within many tumours, including breast cancer (Suling Liu and Wicha 2010). When treating patients in clinic, both the physician and the patient are reassured that chemotherapy seems to shrink tumours and 'cure' patients- only for the disease to return, often at a distant site. This phenomenon can increasingly be understood through the CSC model and the characteristics that these cells possess such as resistance to apoptosis and drug efflux (hence resistance to chemotherapy) as well as tumour dormancy and the ability to migrate through EMT (Pattabiraman and Weinberg 2014). In most tumour types, the establishment of metastatic disease heralds incurable disease and increasingly it is recognised that this could be due to CSCs residing at metastatic niches throughout the body

where they can resist treatment, lie dormant and eventually thrive (Plaks, Kong, and Werb 2015). In a few tumour types, such as germ cell cancer, metastatic disease is not incurable as the tumours are exquisitely sensitive to chemotherapy with cure rates of over 90%. Germ cell tumours have been shown to have very low levels of MDR proteins, as well as having an increased susceptibility to apoptosis, perhaps offering a window in which to study the differential responses of the CSCs of these types to chemotherapy (Savage 2016).

Work demonstrating that CSCs are increased in chemotherapy has led to intensive efforts to target this population using both novel and other compounds, whose use has been repurposed after recognition that they seem to possess some anti-CSC activity. Such examples include digoxin, a cardiac glycoside used for atrial fibrilliation, and salinomycin, an antibiotic that is widely-used in chicken feed, that was identified through high-throughput screening to target breast cancer CSCs 100 times more effectively than paclitaxel (P. B. Gupta et al. 2009; Lu et al. 2015).

Previous work in our laboratory has identified that the apoptotic-inducing ligand TRAIL seems to target CSCs in a broad range of molecular subtypes and that this effect is potentiated by inhibiting the anti-apoptotic protein cFLIP (Piggott et al. 2011). Whilst demonstrating that the method of synergy was through increased apoptosis previous work been demonstrated that aggregates of cFLIP can interfere with the degradation of HIF1α and β-catenin, two known CSC signalling pathways (Naito et al. 2004; Ishioka et al. 2007; Safa 2012). A relationship between cFLIP and β-catenin was subsequently confirmed by other members of our laboratory (French et al. 2015). HIF1α has been shown to be prognostic in breast cancer, upregulated by chemotherapy, lead to a CSC phenotype in breast cancer and induce EMT (Lu et al. 2015; H. Zhang et al. 2015; Samanta et al. 2014; W. Zhang et al. 2015).

This led to the development of a novel cFLIP inhibitor, OH14, that was designed to work concurrently with TRAIL to target CSC-like behaviour in

breast cancer and hopefully lead to an improvement in the, so far, disappointing activity of TRAIL in the breast clinic- despite promising pre-clinical activity (Oliver et al. 2012; Holland 2014; Forero-Torres et al. 2015).

The aims of this project were therefore to: 1) to establish an *in vitro* to model to demonstrate that different chemotherapeutic agents in use in the clinic led to an increase in CSC-like behaviour; 2) show whether the combination of OH14 and TRAIL could effectively target this population; and 3) characterise the mechanism through which OH14 and TRAIL was having this effect.

In Chapter 3, we began by establishing IC50 values of chemotherapeutics in use in the breast clinic such as FEC and docetaxel in a panel of three cell lines representing a broad range of molecular subtypes of breast cancer (MCF-7- ER positive, HCC1954- Her2 positive and SUM149- Triple negative). We then assessed the effect of chemotherapy on mammosphere formation, a recognised and established surrogate of CSC-like behaviour (Dontu et al. 2003). However, our initial results did not show an increase in mammosphere formation something that we felt went against the weight of previously published evidence. After trying multiple variables, an increase in the treatment time from 72 to 96 hours led to an increase in mammosphere formation and we speculated that this may have been due to an increase in HIF1α that had previously been shown in an *in vitro* model to take 96 hours to be upregulated by chemotherapy (Samanta et al. 2014). A mathematical model that we had constructed by combining viability and mammosphere data demonstrated that chemotherapy not only poorly targeted CSCs but, across most cell lines and chemotherapeutics, led to an increase in overall CSC number suggesting that CSC signalling was being induced by chemotherapy. This was most marked in our TNBC SUM149 cell line.

Having established this 96 hour time point to use as our model of CSC-like behaviour, in Chapter 4 we tested the effect of OH14 and TRAIL after chemotherapy in the MCF7 and SUM149 cell line. Whilst demonstrating the combination was effective across all cell lines, in the SUM149, triple negative line, the use of single agent OH14 led to a greater effect that the use of the

combination of OH14 and TRAIL. A literature search identified that a particular chemotherapy drug, paclitaxel, worked predominantly through the apoptosis pathway under negative regulation of cFLIP and therefore was chosen to investigate the effect of single agent OH14 after chemotherapy in TNBC (Day, Huang, and Safa 2008b; Day et al. 2006). TNBC cell lines were used to demonstrate that single agent OH14 seemed to target mammosphere formation and the ALDH+ cell population, both surrogate markers of CSCs, after paclitaxel. The same mathematical model confirmed that the addition of OH14 was leading to an overall reduction in CSCs, suggesting that it was both increasing the cytotoxic of paclitaxel against CSCs as well as potentially influencing CSC signalling. *In vivo* serial dilution experiments confirmed that paclitaxel increased tumour formation compared to untreated controls and that OH14 and TRAIL without paclitaxel decreased tumour formation. However, our results combining OH14 and TRAIL with paclitaxel were confusing in that no effect was seen and these experiments are being repeated. *In vivo* treatment of established TNBC cell line tumours showed that single agent OH14 had no effect on tumour growth but that both paclitaxel and the combination of paclitaxel and OH14 led to a dramatic reduction in tumour size. Interestingly, many weeks later the paclitaxel only treated mice begun to rapidly regrow tumours whilst those treated with OH14 and paclitaxel continued disease free. This could potentially be explained by our CSC hypothesis- undetectable TNBC cells continued to exist within the mice that begun to regrow after time. In those mice treated with OH14, this process was interrupted. This experiment is again being repeated with larger numbers of mice to confirm this effect.

Lastly, we wanted to show a potential mechanism of the relationship between OH14 and paclitaxel. In the MDA-MB-231 TNBC cell line, we demonstrated that both TRAIL and OH14 with TRAIL increased cell death and apoptosis in a bulk cell population without paclitaxel. With paclitaxel, single agent OH14 and TRAIL led to a significant reduction in viability suggesting a synergy between paclitaxel and these two compounds. Nevertheless, the most significant decrease in viability was seen by using both agents together with paclitaxel- suggesting that the combination of OH14 and TRAIL in combination with

paclitaxel is a therapeutic option worth exploring. Blocking apoptosis with a pan-caspase inhibitor in two TNBC cell lines demonstrated little effect on both cell viability and mammosphere formation. This suggests that apoptosis is only having a minor role in the activity of OH14 on CSC-like activity after chemotherapy. This effect could be examined further by testing the effect of caspase inhibition on a pure CSC population and also investigating whether any effect is related to Caspases 8 and 10, the initiator caspases in the extrinsic apoptosis pathway.

We subsequently demonstrated in two TNBC cell lines, that the increase in HIF1α protein levels did occur at 96 hours post-paclitaxel, a finding that was in concordance with others (Samanta et al. 2014) and went someway towards showing why our mammospheres only increased after 96 hours in Chapter 3. However, our rRT-PCR data showed a more complex picture with elevation of HIF1α-mediated gene expression before 96 hours, though at lower levels. Others have shown that IL6 and IL8, two genes under control of HIF1α, were elevated by chemotherapy at earlier time points and therefore there is likely to be a non- HIF1α dependent mechanism occurring, such as through the JNK pathway (Wang et al. 2006) and this could be investigated further.

Next we showed that the paclitaxel-induced increase in HIF1α protein expression was abrogated by OH14. Paclitaxel increased the HIF1α mediated gene-expression of IL6, IL6, MDR1 and Snail that was reversed by the addition of OH14. However, in the MDA-MB-231 cell line, single agent OH14 led to an increase in IL6, IL8, Snail and MDR1 gene expression that was reversed when OH14 was combined with paclitaxel. This was not seen in the SUM149 inflammatory breast cancer cell line. If time had allowed, I would have liked to explore the relationship between OH14, the MAPK and NFκB pathways and IL6 and IL8 signalling. Of particular interest would be the different effects seen between the MDA-MB-231 cell line and the SUM149, inflammatory breast cancer cell line, as NFκB has been shown to be upregulated in inflammatory breast cancer (Lerebours et al. 2008).

The importance of HIF1α in mammosphere formation was shown by siRNA-mediated knockdown that closely mirrored the effect of both OH14 and siRNA against cFLIP. Blocking apoptosis with z-VAD-FMK, did not alter the relationship between control and paclitaxel treated cells suggesting that the effect was not mediated through apoptosis.

Blocking the degradation of HIF1α using the proteasome inhibitor MG132 reversed the reduction in HIF1α protein levels seen with siRNA-mediated knockdown of cFLIP. This supports previously published evidence suggesting that aggregates of cFLIP inhibit the proteasome system and lead to increased levels of proteins such as HIF1α (Ishioka et al. 2007). Finally, we used hypoxic conditions to show that hypoxia increased colony formation and that this increase was reversed by the addition of OH14.

In conclusion, and as shown in Figure 6.1 below, our data show that paclitaxel targets differentiated cells leading to cell death but leads to an induction of a CSC-like phenotype. This is either through resistance of existing CSCs to its effects or, and more likely, through induction of CSC-signalling and conversion of differentiated cells into CSCs (through the process of plasticity, See Section 1.5.7). HIF1α is an important mediator of increased CSC signalling and may also lead to plasticity between differentiated cancer cells and cancer stem cells. cFLIP is both an inhibitor of apoptotic pathway and inhibits the degradation of HIF1α. OH14, our novel cFLIP inhibitor, reverses the increase in CSC-like behaviour seen with paclitaxel and has a small effect on increasing apoptosis. OH14 may have an important role in the treatment of cancer, both in combination with chemotherapy and TRAIL, potentially increasing the effect of the latter as an antagonist of the extrinsic apoptosis pathway and the former by inhibiting induced CSC-signalling. There may be more cancer types that benefit from a combination of paclitaxel and OH14 treatment with notable examples being castrate-resistant prostate cancer (McCourt et al. 2012) and also pancreatic cancer (Haag et al. 2011), where cFLIP has been shown to be over-expressed, and also inflammatory breast cancer, where complex interactions may lie with immune signalling pathways.
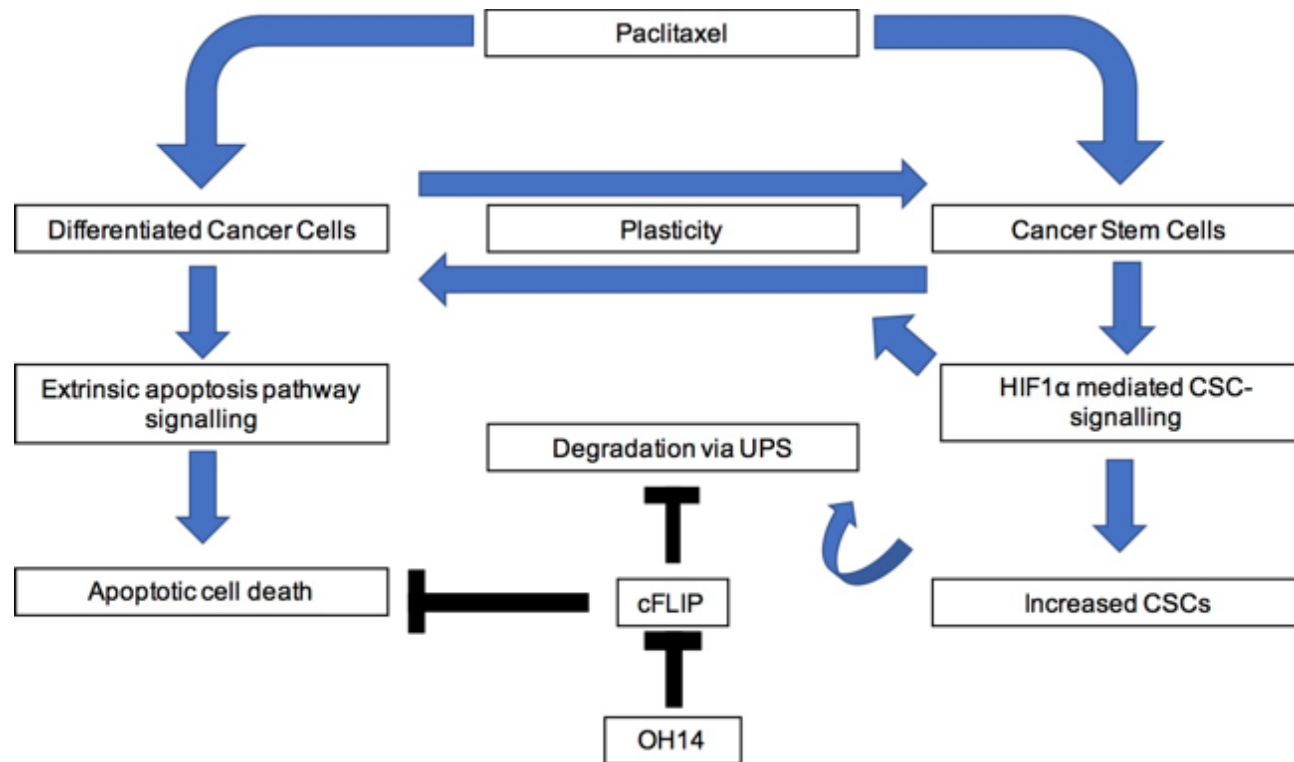
Figure 6.1 The effect of cFLIP and OH14 on paclitaxel-induced effects on cancer cells

Paclitaxel leads to both apoptosis (primarily in Differentiated cells) and an induction of CSC-signalling mediated by HIF1α. This may induce non-CSCs into a CSC state. cFLIP leads to resistance to paclitaxel through both inhibiting apoptosis and inhibiting the breakdown of HIF1α through the Ubiquitin Proteosome System (UPS). OH14 blocks this inhibition, leading to a reduction in CSC-signalling and an increase in apoptosis.

7 Bibliography

Abdulghani, Junaid, Joshua E. Allen, David T. Dicker, Yingqiu Yvette Liu, David Goldenberg, Charles D. Smith, Robin Humphreys, and Wafik S. El-Deiry. 2013. "Sorafenib Sensitizes Solid Tumors to Apo2L/TRAIL and Apo2L/TRAIL Receptor Agonist Antibodies by the Jak2-Stat3-Mcl1 Axis." *PLoS ONE* 8 (9):e75414. https://doi.org/10.1371/journal.pone.0075414.

Abdullah, Lissa Nurrul, and Edward Kai-Hua Chow. 2013. "Mechanisms of Chemoresistance in Cancer Stem Cells." *Clinical and Translational Medicine* 2 (January):3. https://doi.org/10.1186/2001-1326-2-3.

Abedini, Mohammad R., Emilie J. Muller, Jan Brun, Richard Bergeron, Douglas A. Gray, and Benjamin K. Tsang. 2008. "Cisplatin Induces p53-Dependent FLICE-like Inhibitory Protein Ubiquitination in Ovarian Cancer Cells." *Cancer Research* 68 (12):4511–17. https://doi.org/10.1158/0008-5472.CAN-08-0673.

Acloque, Herve, Meghan S. Adams, Katherine Fishwick, Marianne Bronner-Fraser, and M. Angela Nieto. 2009. "Epithelial-Mesenchymal Transitions: The Importance of Changing Cell State in Development and Disease." *The Journal of Clinical Investigation* 119 (6):1438–49. https://doi.org/10.1172/JCI38019.

Alamgeer, Muhammad, Vinod Ganju, Beena Kumar, Jane Fox, Stewart Hart, Michelle White, Marion Harris, et al. 2014. "Changes in Aldehyde Dehydrogenase-1 Expression during Neoadjuvant Chemotherapy Predict Outcome in Locally Advanced Breast Cancer." *Breast Cancer Research* 16 (2):R44. https://doi.org/10.1186/bcr3648.

Al-Hajj, Muhammad, Max S. Wicha, Adalberto Benito-Hernandez, Sean J. Morrison, and Michael F. Clarke. 2003. "Prospective Identification of Tumorigenic Breast Cancer Cells." *Proceedings of the National Academy of Sciences* 100 (7):3983–88. https://doi.org/10.1073/pnas.0530291100.

Amirikia, Kathryn C., Paul Mills, Jason Bush, and Lisa A. Newman. 2011. "Higher Population-Based Incidence Rates of Triple-Negative Breast Cancer among Young African-American Women : Implications for Breast Cancer Screening Recommendations." *Cancer* 117 (12):2747–53. https://doi.org/10.1002/cncr.25862.

Angeloni, Valentina, Paola Tiberio, Valentina Appierto, and Maria Grazia Daidone. 2015. "Implications of Stemness-Related Signaling Pathways in Breast Cancer Response to Therapy." *Seminars in Cancer Biology*, Intracellular Signaling and Response to Anti-Cancer Therapy, 31 (April):43–51. https://doi.org/10.1016/j.semcancer.2014.08.004.

———. n.d. "Implications of Stemness-Related Signaling Pathways in Breast Cancer Response to Therapy." *Seminars in Cancer Biology*. Accessed October 1, 2014. https://doi.org/10.1016/j.semcancer.2014.08.004.

Ari, Ferda, Rudolf Napieralski, Engin Ulukaya, Egemen Dere, Christoph Colling, Katja Honert, Achim Krüger, Marion Kiechle, and Manfred Schmitt. 2011. "Modulation of Protein Expression Levels and DNA Methylation Status of Breast Cancer Metastasis Genes by Anthracycline-Based Chemotherapy and the Demethylating Agent Decitabine." *Cell Biochemistry and Function* 29 (8):651–59. https://doi.org/10.1002/cbf.1801.

Ashkenazi, A, and V M Dixit. 1998. "Death Receptors: Signaling and Modulation." *Science (New York, N.Y.)* 281 (5381):1305–8.

Ashkenazi, Avi, Pamela Holland, and S. Gail Eckhardt. 2008. "Ligand-Based Targeting of Apoptosis in Cancer: The Potential of Recombinant Human Apoptosis Ligand 2/Tumor Necrosis Factor–Related Apoptosis-Inducing Ligand (rhApo2L/TRAIL)." *Journal of Clinical Oncology* 26 (21):3621–30. https://doi.org/10.1200/JCO.2007.15.7198.

Aulmann, Sebastian, Nina Waldburger, Roland Penzel, Mindaugas Andrulis, Peter Schirmacher, and Hans Peter Sinn. 2010. "Reduction of CD44+/CD24− Breast Cancer Cells by Conventional Cytotoxic Chemotherapy." *Human Pathology* 41 (4):574–81. https://doi.org/10.1016/j.humpath.2009.08.023.

Azizi, Ebrahim, and Max S. Wicha. 2013. "Point: Cancer Stem Cells—The Evidence Accumulates." *Clinical Chemistry* 59 (1):205–7. https://doi.org/10.1373/clinchem.2012.195990.

Beerling, Evelyne, Daniëlle Seinstra, Elzo de Wit, Lennart Kester, Daphne van der Velden, Carrie Maynard, Ronny Schäfer, et al. 2016. "Plasticity between Epithelial and Mesenchymal States Unlinks EMT from

Metastasis-Enhancing Stem Cell Capacity." *Cell Reports* 14 (10):2281–88. https://doi.org/10.1016/j.celrep.2016.02.034.

Bhola, Neil E., Justin M. Balko, Teresa C. Dugger, María Gabriela Kuba, Violeta Sánchez, Melinda Sanders, Jamie Stanford, Rebecca S. Cook, and Carlos L. Arteaga. 2013. "TGF-β Inhibition Enhances Chemotherapy Action against Triple-Negative Breast Cancer." *Journal of Clinical Investigation* 123 (3):1348–58. https://doi.org/10.1172/JCI65416.

Blum, Barak, Ori Bar-Nur, Tamar Golan-Lev, and Nissim Benvenisty. 2009. "The Anti-Apoptotic Gene Survivin Contributes to Teratoma Formation by Human Embryonic Stem Cells." *Nature Biotechnology* 27 (3):281–87. https://doi.org/10.1038/nbt.1527.

Bonadonna, G, E Brusamolino, P Valagussa, A Rossi, L Brugnatelli, C Brambilla, M De Lena, et al. 1976. "Combination Chemotherapy as an Adjuvant Treatment in Operable Breast Cancer." *The New England Journal of Medicine* 294 (8):405–10. https://doi.org/10.1056/NEJM197602192940801.

Brabletz, Thomas, Andreas Jung, Simone Spaderna, Falk Hlubek, and Thomas Kirchner. 2005. "Migrating Cancer Stem Cells — an Integrated Concept of Malignant Tumour Progression." *Nature Reviews Cancer* 5 (9):744–49. https://doi.org/10.1038/nrc1694.

Britton, Kelly M., John A. Kirby, Thomas W.J. Lennard, and Annette P. Meeson. 2011. "Cancer Stem Cells and Side Population Cells in Breast Cancer and Metastasis." *Cancers* 3 (2):2106–30. https://doi.org/10.3390/cancers3022106.

Brufman, G., E. Colajori, N. Ghilezan, M. Lassus, M. Martoni, N. Perevodchikova, C. Tosello, D. Viaro, and C. Zielinski. 1997. "Doubling Epirubicin Dose Intensity (100 Mg/m2 versus 50 Mg/m2) in the FEC Regimen Significantly Increases Response Rates. An International Randomised Phase III Study in Metastatic Breast Cancer." *Annals of Oncology* 8 (2):155–62.

Bruna, Alejandra, Oscar M. Rueda, Wendy Greenwood, Ankita Sati Batra, Maurizio Callari, Rajbir Nath Batra, Katherine Pogrebniak, et al. 2016. "A Biobank of Breast Cancer Explants with Preserved Intra-Tumor

Heterogeneity to Screen Anticancer Compounds." *Cell* 0 (0).
https://doi.org/10.1016/j.cell.2016.08.041.

Buchsbaum, Donald J., Tong Zhou, William E. Grizzle, Patsy G. Oliver,
Charlotte J. Hammond, Sijian Zhang, Mark Carpenter, and Albert F.
LoBuglio. 2003. "Antitumor Efficacy of TRA-8 Anti-DR5 Monoclonal
Antibody Alone or in Combination with Chemotherapy And/Or
Radiation Therapy in a Human Breast Cancer Model." *Clinical Cancer
Research* 9 (10):3731–41.

Buffa, F. M., A. L. Harris, C. M. West, and C. J. Miller. 2010. "Large Meta-
Analysis of Multiple Cancers Reveals a Common, Compact and Highly
Prognostic Hypoxia Metagene." *British Journal of Cancer* 102 (2):428–
35. https://doi.org/10.1038/sj.bjc.6605450.

Cancer Genome Atlas Network. 2012. "Comprehensive Molecular Portraits of
Human Breast Tumours." *Nature* 490 (7418):61–70.
https://doi.org/10.1038/nature11412.

Canellos, George P., Vincent T. Devita, G. Lennard Gold, Bruce A. Chabner,
Philip S. Schein, and Robert C. Young. 1974. "Cyclical Combination
Chemotherapy for Advanced Breast Carcinoma." *BMJ* 1 (5901):218–
20. https://doi.org/10.1136/bmj.1.5901.218.

Cao, Yiting, Joseph M. Eble, Ejung Moon, Hong Yuan, Douglas H. Weitzel,
Chelsea D. Landon, Charleen Yu-Chih Nien, et al. 2013a. "Tumor Cells
Upregulate Normoxic HIF-1α in Response to Doxorubicin." *Cancer
Research* 73 (20):6230–42. https://doi.org/10.1158/0008-5472.CAN-
12-1345.

Cardoso, F., N. Harbeck, L. Fallowfield, S. Kyriakides, and E. Senkus. 2012.
"Locally Recurrent or Metastatic Breast Cancer: ESMO Clinical
Practice Guidelines for Diagnosis, Treatment and Follow-Up." *Annals
of Oncology* 23 (suppl 7):vii11-vii19.
https://doi.org/10.1093/annonc/mds232.

Carey LA, Perou CM, Livasy CA, and et al. 2006. "RAce, Breast Cancer
Subtypes, and Survival in the Carolina Breast Cancer Study." *JAMA*
295 (21):2492–2502. https://doi.org/10.1001/jama.295.21.2492.

Carey, Lisa A., E. Claire Dees, Lynda Sawyer, Lisa Gatti, Dominic T. Moore,
Frances Collichio, David W. Ollila, Carolyn I. Sartor, Mark L. Graham,

and Charles M. Perou. 2007. "The Triple Negative Paradox: Primary Tumor Chemosensitivity of Breast Cancer Subtypes." *Clinical Cancer Research* 13 (8):2329–34. https://doi.org/10.1158/1078-0432.CCR-06-1109.

Chang, Jenny C., Eric C. Wooten, Anna Tsimelzon, Susan G. Hilsenbeck, M. Carolina Gutierrez, Yee-Lu Tham, Mamta Kalidas, et al. 2005. "Patterns of Resistance and Incomplete Response to Docetaxel by Gene Expression Profiling in Breast Cancer Patients." *Journal of Clinical Oncology* 23 (6):1169–77. https://doi.org/10.1200/JCO.2005.03.156.

Chang, Lufen, Hideaki Kamata, Giovanni Solinas, Jun-Li Luo, Shin Maeda, K. Venuprasad, Yun-Cai Liu, and Michael Karin. 2006. "The E3 Ubiquitin Ligase Itch Couples JNK Activation to TNFα-Induced Cell Death by Inducing c-FLIPL Turnover." *Cell* 124 (3):601–13. https://doi.org/10.1016/j.cell.2006.01.021.

Charafe-Jauffret, Emmanuelle, Christophe Ginestier, Flora Iovino F, Carole Tarpin, Mark Diebel, Benjamin Esterni, Gilles Houvenaeghel, et al. 2010. "ALDH1-Positive Cancer Stem Cells Mediate Metastasis and Poor Clinical Outcome in Inflammatory Breast Cancer." *Clinical Cancer Research : An Official Journal of the American Association for Cancer Research* 16 (1):45–55. https://doi.org/10.1158/1078-0432.CCR-09-1630.

Charafe-Jauffret, Emmanuelle, Christophe Ginestier, Flora Iovino, Carole Tarpin, Mark Diebel, Benjamin Esterni, Gilles Houvenaeghel, et al. 2010. "Aldehyde Dehydrogenase 1–Positive Cancer Stem Cells Mediate Metastasis and Poor Clinical Outcome in Inflammatory Breast Cancer." *American Association for Cancer Research* 16 (1):45–55. https://doi.org/10.1158/1078-0432.CCR-09-1630.

Charafe-Jauffret, Emmanuelle, Christophe Ginestier, Flora Iovino, Julien Wicinski, Nathalie Cervera, Pascal Finetti, Min-Hee Hur, et al. 2009. "Breast Cancer Cell Lines Contain Functional Cancer Stem Cells with Metastatic Capacity and a Distinct Molecular Signature." *Cancer Research* 69 (4):1302–13. https://doi.org/10.1158/0008-5472.CAN-08-2741.

Chatterjee, D., I. Schmitz, A. Krueger, K. Yeung, S. Kirchhoff, P. H. Krammer, M. E. Peter, J. H. Wyche, and P. Pantazis. 2001. "Induction of Apoptosis in 9-Nitrocamptothecin-Treated DU145 Human Prostate Carcinoma Cells Correlates with de Novo Synthesis of CD95 and CD95 Ligand and down-Regulation of c-FLIP(short)." *Cancer Research* 61 (19):7148–54.

Chen, Feng, Hai-Hong Zhu, Lin-Fu Zhou, Shan-Shan Wu, Jing Wang, and Zhi Chen. 2010. "Inhibition of c-FLIP Expression by miR-512-3p Contributes to Taxol-Induced Apoptosis in Hepatocellular Carcinoma Cells." *Oncology Reports* 23 (5):1457–62.

Cho, K R, and B Vogelstein. 1992. "Genetic Alterations in the Adenoma-- Carcinoma Sequence." *Cancer* 70 (6 Suppl):1727–31.

Chou, T C, and P Talalay. 1984. "Quantitative Analysis of Dose-Effect Relationships: The Combined Effects of Multiple Drugs or Enzyme Inhibitors." *Advances in Enzyme Regulation* 22:27–55.

Chou, Ting-Chao. 2006. "Theoretical Basis, Experimental Design, and Computerized Simulation of Synergism and Antagonism in Drug Combination Studies." *Pharmacological Reviews* 58 (3):621–81. https://doi.org/10.1124/pr.58.3.10.

Chun, Yun Shin, Prasad S. Adusumilli, and Yuman Fong. 2005. "Employing Tumor Hypoxia for Oncolytic Therapy in Breast Cancer." *Journal of Mammary Gland Biology and Neoplasia* 10 (4):311–18. https://doi.org/10.1007/s10911-006-9004-6.

Conley, Sarah J., Elizabeth Gheordunescu, Pramod Kakarala, Bryan Newman, Hasan Korkaya, Amber N. Heath, Shawn G. Clouthier, and Max S. Wicha. 2012. "Antiangiogenic Agents Increase Breast Cancer Stem Cells via the Generation of Tumor Hypoxia." *Proceedings of the National Academy of Sciences of the United States of America* 109 (8):2784–89. https://doi.org/10.1073/pnas.1018866109.

Creighton, Chad J., Xiaoxian Li, Melissa Landis, J. Michael Dixon, Veronique M. Neumeister, Ashley Sjolund, David L. Rimm, et al. 2009. "Residual Breast Cancers after Conventional Therapy Display Mesenchymal as Well as Tumor-Initiating Features." *Proceedings of the National*

Academy of Sciences 106 (33):13820–25.
https://doi.org/10.1073/pnas.0905718106.

CRUK, Cancer Research. 2014. "Breast Cancer Incidence Statistics."
Document. May 29, 2014. http://www.cancerresearchuk.org/cancer-
info/cancerstats/types/breast/incidence/uk-breast-cancer-incidence-
statistics.

Cryns, Vincent, and Junying Yuan. 1998. "Proteases to Die for." *Genes &
Development* 12 (11):1551–70. https://doi.org/10.1101/gad.12.11.1551.

Cumming, Geoff, Fiona Fidler, and David L. Vaux. 2007. "Error Bars in
Experimental Biology." *The Journal of Cell Biology* 177 (1):7–11.
https://doi.org/10.1083/jcb.200611141.

Day, Travis W., Su Huang, and Ahmad R. Safa. 2008a. "C-FLIP Knockdown
Induces Ligand-Independent DR5-, FADD-, Caspase-8-, and Caspase-
9-Dependent Apoptosis in Breast Cancer Cells." *Biochemical
Pharmacology* 76 (12):1694–1704.
https://doi.org/10.1016/j.bcp.2008.09.007.

Day, Travis W, Su Huang, and Ahmad R Safa. 2008b. "C-FLIP Knockdown
Induces Ligand-Independent DR5-, FADD-, Caspase-8-, and Caspase-
9-Dependent Apoptosis in Breast Cancer Cells." *Biochemical
Pharmacology* 76 (12):1694–1704.
https://doi.org/10.1016/j.bcp.2008.09.007.

Day, Travis W., Farhad Najafi, Ching-Huang Wu, and Ahmad R. Safa. 2006.
"Cellular FLICE-like Inhibitory Protein (c-FLIP): A Novel Target for
Taxol-Induced Apoptosis." *Biochemical Pharmacology* 71 (11):1551–
61. https://doi.org/10.1016/j.bcp.2006.02.015.

De Luca, Antonella, Amelia D'Alessio, Marianna Gallo, Monica R Maiello, Ann
M Bode, and Nicola Normanno. 2014. "Src and CXCR4 Are Involved in
the Invasiveness of Breast Cancer Cells with Acquired Resistance to
Lapatinib." *Cell Cycle* 13 (1):148–56. https://doi.org/10.4161/cc.26899.

DeLeo, Albert B. 2012. "Targeting Cancer Stem Cells with ALDH1A1-Based
Immunotherapy." *Oncoimmunology* 1 (3):385–87.
https://doi.org/10.4161/onci.18826.

Denduluri, Neelima, Mark R. Somerfield, Andrea Eisen, Jamie N. Holloway,
Arti Hurria, Tari A. King, Gary H. Lyman, et al. 2016. "Selection of

Optimal Adjuvant Chemotherapy Regimens for Human Epidermal Growth Factor Receptor 2 (HER2) -Negative and Adjuvant Targeted Therapy for HER2-Positive Breast Cancers: An American Society of Clinical Oncology Guideline Adaptation of the Cancer Care Ontario Clinical Practice Guideline." *Journal of Clinical Oncology: Official Journal of the American Society of Clinical Oncology*, April. https://doi.org/10.1200/JCO.2016.67.0182.

Dent, Rebecca, Maureen Trudeau, Kathleen I. Pritchard, Wedad M. Hanna, Harriet K. Kahn, Carol A. Sawka, Lavina A. Lickley, Ellen Rawlinson, Ping Sun, and Steven A. Narod. 2007. "Triple-Negative Breast Cancer: Clinical Features and Patterns of Recurrence." *Clinical Cancer Research* 13 (15):4429–34. https://doi.org/10.1158/1078-0432.CCR-06-3045.

DeVita, Vincent T., and Edward Chu. 2008. "A History of Cancer Chemotherapy." *Cancer Research* 68 (21):8643–53. https://doi.org/10.1158/0008-5472.CAN-07-6611.

Dey, Devaveena, Meera Saxena, Anurag N. Paranjape, Visalakshi Krishnan, Rajashekhar Giraddi, M. Vijaya Kumar, Geetashree Mukherjee, and Annapoorni Rangarajan. 2009. "Phenotypic and Functional Characterization of Human Mammary Stem/Progenitor Cells in Long Term Culture." *PLoS ONE* 4 (4). https://doi.org/10.1371/journal.pone.0005329.

DiMeo, Theresa A., Kristen Anderson, Pushkar Phadke, Chang Feng, Charles M. Perou, Steven Naber, and Charlotte Kuperwasser. 2009. "A Novel Lung Metastasis Signature Links Wnt Signaling with Cancer Cell Self-Renewal and Epithelial-Mesenchymal Transition in Basal-like Breast Cancer." *Cancer Research* 69 (13):5364–73. https://doi.org/10.1158/0008-5472.CAN-08-4135.

Dontu, Gabriela, Wissam M. Abdallah, Jessica M. Foley, Kyle W. Jackson, Michael F. Clarke, Mari J. Kawamura, and Max S. Wicha. 2003. "In Vitro Propagation and Transcriptional Profiling of Human Mammary Stem/Progenitor Cells." *Genes & Development* 17 (10):1253–70. https://doi.org/10.1101/gad.1061803.

Dragu, Denisa L, Laura G Necula, Coralia Bleotu, Carmen C Diaconu, and Mihaela Chivu-Economescu. 2015. "Therapies Targeting Cancer Stem Cells: Current Trends and Future Challenges." *World Journal of Stem Cells* 7 (9):1185–1201. https://doi.org/10.4252/wjsc.v7.i9.1185.

Drake, John W., Brian Charlesworth, Deborah Charlesworth, and James F. Crow. 1998. "Rates of Spontaneous Mutation." *Genetics* 148 (4):1667–86.

Early Breast Cancer Trialists' Collaborative Group (EBCTCG). 2012. "Comparisons between Different Polychemotherapy Regimens for Early Breast Cancer: Meta-Analyses of Long-Term Outcome among 100 000 Women in 123 Randomised Trials." *Lancet* 379 (9814):432–44. https://doi.org/10.1016/S0140-6736(11)61625-5.

Eccles, Suzanne A, Eric O Aboagye, Simak Ali, Annie S Anderson, Jo Armes, Fedor Berditchevski, Jeremy P Blaydes, et al. 2013. "Critical Research Gaps and Translational Priorities for the Successful Prevention and Treatment of Breast Cancer." *Breast Cancer Research : BCR* 15 (5):R92. https://doi.org/10.1186/bcr3493.

El-Zawahry, Ahmed, John McKillop, and Christina Voelkel-Johnson. 2005. "Doxorubicin Increases the Effectiveness of Apo2L/TRAIL for Tumor Growth Inhibition of Prostate Cancer Xenografts." *BMC Cancer* 5 (January):2. https://doi.org/10.1186/1471-2407-5-2.

Farmer, Pierre, Hervé Bonnefoi, Pascale Anderle, David Cameron, Pratyakasha Wirapati, Véronique Becette, Sylvie André, et al. 2009. "A Stroma-Related Gene Signature Predicts Resistance to Neoadjuvant Chemotherapy in Breast Cancer." *Nature Medicine* 15 (1):68–74. https://doi.org/10.1038/nm.1908.

Ferlay, Jacques, Hai-Rim Shin, Freddie Bray, David Forman, Colin Mathers, and Donald Maxwell Parkin. 2010. "Estimates of Worldwide Burden of Cancer in 2008: GLOBOCAN 2008." *International Journal of Cancer. Journal International Du Cancer* 127 (12):2893–2917. https://doi.org/10.1002/ijc.25516.

Ferrand, Nathalie, Anne Gnanapragasam, Guillaume Dorothee, Gérard Redeuilh, Annette K. Larsen, and Michèle Sabbah. 2014. "Loss of WISP2/CCN5 in Estrogen-Dependent MCF7 Human Breast Cancer

Cells Promotes a Stem-Like Cell Phenotype." *PLoS ONE* 9 (2). https://doi.org/10.1371/journal.pone.0087878.

Fischer, Kari R., Anna Durrans, Sharrell Lee, Jianting Sheng, Fuhai Li, Stephen Wong, Hyejin Choi, et al. 2015. "EMT Is Not Required for Lung Metastasis but Contributes to Chemoresistance." *Nature* 527 (7579):472–76. https://doi.org/10.1038/nature15748.

Flamant, Lionel, Annick Notte, Noelle Ninane, Martine Raes, and Carine Michiels. 2010. "Anti-Apoptotic Role of HIF-1 and AP-1 in Paclitaxel Exposed Breast Cancer Cells under Hypoxia." *Molecular Cancer* 9 (July):191. https://doi.org/10.1186/1476-4598-9-191.

Forero-Torres, Andres, Katherine E. Varley, Vandana Abramson, Yufeng Li, Christos Vaklavas, Nancy U. Lin, Minetta C. Liu, et al. 2015. "TBCRC 019: Phase II Trial of Nab-PAC With/Without the Anti-Death Receptor 5 Monoclonal Antibody Tigatuzumab in Patients with Triple Negative Breast Cancer." *Clinical Cancer Research: An Official Journal of the American Association for Cancer Research*, March. https://doi.org/10.1158/1078-0432.CCR-14-2780.

Forsythe, J. A., B. H. Jiang, N. V. Iyer, F. Agani, S. W. Leung, R. D. Koos, and G. L. Semenza. 1996. "Activation of Vascular Endothelial Growth Factor Gene Transcription by Hypoxia-Inducible Factor 1." *Molecular and Cellular Biology* 16 (9):4604–13.

French, Rhiannon, Olivia Hayward, Samuel Jones, William Yang, and Richard Clarkson. 2015. "Cytoplasmic Levels of cFLIP Determine a Broad Susceptibility of Breast Cancer Stem/Progenitor-like Cells to TRAIL." *Molecular Cancer* 14 (1):209. https://doi.org/10.1186/s12943-015-0478-y.

Frew, Ailsa J., Ralph K. Lindemann, Ben P. Martin, Christopher J. P. Clarke, Janelle Sharkey, Desiree A. Anthony, Kellie-Marie Banks, et al. 2008. "Combination Therapy of Established Cancer Using a Histone Deacetylase Inhibitor and a TRAIL Receptor Agonist." *Proceedings of the National Academy of Sciences of the United States of America* 105 (32):11317–22. https://doi.org/10.1073/pnas.0801868105.

Fulda, Simone. 2013. "Regulation of Apoptosis Pathways in Cancer Stem Cells." *Cancer Letters* 338 (1):168–73. https://doi.org/10.1016/j.canlet.2012.03.014.

Gage, Michele M., Martin Rosman, W. Charles Mylander, Erica Giblin, Hyun-Seok Kim, Leslie Cope, Christopher Umbricht, Antonio C. Wolff, and Lorraine Tafra. 2015. "A Validated Model for Identifying Patients Unlikely to Benefit From the 21-Gene Recurrence Score Assay." *Clinical Breast Cancer*, April. https://doi.org/10.1016/j.clbc.2015.04.006.

Galluzzi, Lorenzo, Oliver Kepp, and Guido Kroemer. 2012. "Mitochondria: Master Regulators of Danger Signalling." *Nature Reviews Molecular Cell Biology* 13 (12):780–88. https://doi.org/10.1038/nrm3479.

Garimella, Sireesha V, Kristie Gehlhaus, Jennifer L Dine, Jason J Pitt, Magdalena Grandin, Sirisha Chakka, Marion M Nau, Natasha J Caplen, and Stanley Lipkowitz. 2014. "Identification of Novel Molecular Regulators of Tumor Necrosis Factor-Related Apoptosis-Inducing Ligand (TRAIL)-Induced Apoptosis in Breast Cancer Cells by RNAi Screening." *Breast Cancer Research : BCR* 16 (2):R41. https://doi.org/10.1186/bcr3645.

Garimella, Sireesha V, Andrea Rocca, and Stanley Lipkowitz. 2012. "WEE1 Inhibition Sensitizes Basal Breast Cancer Cells to TRAIL-Induced Apoptosis." *Molecular Cancer Research* 10 (1):75–85. https://doi.org/10.1158/1541-7786.MCR-11-0500.

Gilkes, Daniele M., and Gregg L. Semenza. 2013. "Role of Hypoxia-Inducible Factors in Breast Cancer Metastasis." *Future Oncology (London, England)* 9 (11):1623–36. https://doi.org/10.2217/fon.13.92.

Gilmore, A. P. 2005. "Anoikis." *Cell Death & Differentiation* 12 (S2):1473–77. https://doi.org/10.1038/sj.cdd.4401723.

Ginestier, Christophe, Min Hee Hur, Emmanuelle Charafe-Jauffret, Florence Monville, Julie Dutcher, Marty Brown, Jocelyne Jacquemier, et al. 2007. "ALDH1 Is a Marker of Normal and Malignant Human Mammary Stem Cells and a Predictor of Poor Clinical Outcome." *Cell Stem Cell* 1 (5):555–67. https://doi.org/10.1016/j.stem.2007.08.014.

Gong, Chang, Herui Yao, Qiang Liu, Jingqi Chen, Junwei Shi, Fengxi Su, and Erwei Song. 2010. "Markers of Tumor-Initiating Cells Predict Chemoresistance in Breast Cancer." *PLoS ONE* 5 (12):e15630. https://doi.org/10.1371/journal.pone.0015630.

Gong, Yun, Jeff Wang, Lei Huo, Wei Wei, Naoto T. Ueno, and Wendy A. Woodward. 2014. "Aldehyde Dehydrogenase 1 Expression in Inflammatory Breast Cancer as Measured by Immunohistochemical Staining." *Clinical Breast Cancer* 14 (3):e81–88. https://doi.org/10.1016/j.clbc.2013.12.006.

Gottesman, Michael M., Tito Fojo, and Susan E. Bates. 2002. "Multidrug Resistance in Cancer: Role of ATP–dependent Transporters." *Nature Reviews Cancer* 2 (1):48–58. https://doi.org/10.1038/nrc706.

Gray, L. H., A. D. Conger, M. Ebert, S. Hornsey, and O. C. A. Scott. 1953. "The Concentration of Oxygen Dissolved in Tissues at the Time of Irradiation as a Factor in Radiotherapy." *The British Journal of Radiology* 26 (312):638–48. https://doi.org/10.1259/0007-1285-26-312-638.

Gupta, Gaorav P., and Joan Massagué. 2006. "Cancer Metastasis: Building a Framework." *Cell* 127 (4):679–95. https://doi.org/10.1016/j.cell.2006.11.001.

Gupta, Piyush B., Tamer T. Onder, Guozhi Jiang, Kai Tao, Charlotte Kuperwasser, Robert A. Weinberg, and Eric S. Lander. 2009. "Identification of Selective Inhibitors of Cancer Stem Cells by High-Throughput Screening." *Cell* 138 (4):645–59. https://doi.org/10.1016/j.cell.2009.06.034.

Gupta, Piyush B., Christine M. Fillmore, Guozhi Jiang, Sagi D. Shapira, Kai Tao, Charlotte Kuperwasser, and Eric S. Lander. 2011. "Stochastic State Transitions Give Rise to Phenotypic Equilibrium in Populations of Cancer Cells." *Cell* 146 (4):633–44. https://doi.org/10.1016/j.cell.2011.07.026.

Haag, Christian, Dominic Stadel, Shaoxia Zhou, Max G. Bachem, Peter Möller, Klaus-Michael Debatin, and Simone Fulda. 2011. "Identification of c-FLIP(L) and c-FLIP(S) as Critical Regulators of Death Receptor-

Induced Apoptosis in Pancreatic Cancer Cells." *Gut* 60 (2):225–37.
https://doi.org/10.1136/gut.2009.202325.

Habib, Joyce G., and Joyce A. O'Shaughnessy. 2016. "The Hedgehog
Pathway in Triple-Negative Breast Cancer." *Cancer Medicine*, August,
n/a-n/a. https://doi.org/10.1002/cam4.833.

Hamburger, A W, and S E Salmon. 1977. "Primary Bioassay of Human Tumor
Stem Cells." *Science (New York, N.Y.)* 197 (4302):461–63.

Hanahan, Douglas, and Robert A. Weinberg. 2011. "Hallmarks of Cancer: The
Next Generation." *Cell* 144 (5):646–74.
https://doi.org/10.1016/j.cell.2011.02.013.

Harris, Adrian L. 2002. "Hypoxia--a Key Regulatory Factor in Tumour Growth."
Nature Reviews. Cancer 2 (1):38–47. https://doi.org/10.1038/nrc704.

Hartman, Zachary C., Graham M. Poage, Petra den Hollander, Anna
Tsimelzon, Jamal Hill, Nattapon Panupinthu, Yun Zhang, et al. 2013.
"Growth of Triple-Negative Breast Cancer Cells Relies upon
Coordinate Autocrine Expression of the Proinflammatory Cytokines IL-
6 and IL-8." *Cancer Research* 73 (11):3470–80.
https://doi.org/10.1158/0008-5472.CAN-12-4524-T.

Hassan, Mohamed, Hidemichi Watari, Ali AbuAlmaaty, Yusuke Ohba, and
Noriaki Sakuragi. 2014. "Apoptosis and Molecular Targeting Therapy in
Cancer." *BioMed Research International* 2014.
https://doi.org/10.1155/2014/150845.

Hennessy, Bryan T., Ana-Maria Gonzalez-Angulo, Katherine Stemke-Hale,
Michael Z. Gilcrease, Savitri Krishnamurthy, Ju-Seog Lee, Jane
Fridlyand, et al. 2009. "Characterization of a Naturally Occurring Breast
Cancer Subset Enriched in Epithelial-to-Mesenchymal Transition and
Stem Cell Characteristics." *Cancer Research* 69 (10):4116–24.
https://doi.org/10.1158/0008-5472.CAN-08-3441.

Hermann, Patrick C., Stephan L. Huber, Tanja Herrler, Alexandra Aicher,
Joachim W. Ellwart, Markus Guba, Christiane J. Bruns, and
Christopher Heeschen. 2007. "Distinct Populations of Cancer Stem
Cells Determine Tumor Growth and Metastatic Activity in Human
Pancreatic Cancer." *Cell Stem Cell* 1 (3):313–23.
https://doi.org/10.1016/j.stem.2007.06.002.

Hirsch, Heather A., Dimitrios Iliopoulos, Philip N. Tsichlis, and Kevin Struhl. 2009. "Metformin Selectively Targets Cancer Stem Cells, and Acts Together with Chemotherapy to Block Tumor Growth and Prolong Remission." *Cancer Research* 69 (19):7507–11. https://doi.org/10.1158/0008-5472.CAN-09-2994.

Hoffmeyer, Katrin, Angelo Raggioli, Stefan Rudloff, Roman Anton, Andreas Hierholzer, Ignacio Del Valle, Kerstin Hein, Riana Vogt, and Rolf Kemler. 2012. "Wnt/β-Catenin Signaling Regulates Telomerase in Stem Cells and Cancer Cells." *Science* 336 (6088):1549–54. https://doi.org/10.1126/science.1218370.

Holland, Pamela M. 2014. "Death Receptor Agonist Therapies for Cancer, Which Is the Right TRAIL?" *Cytokine & Growth Factor Reviews*. https://doi.org/10.1016/j.cytogfr.2013.12.009.

Hu, Yifang, and Gordon K. Smyth. 2009. "ELDA: Extreme Limiting Dilution Analysis for Comparing Depleted and Enriched Populations in Stem Cell and Other Assays." *Journal of Immunological Methods* 347 (1–2):70–78. https://doi.org/10.1016/j.jim.2009.06.008.

Huang, L. E., J. Gu, M. Schau, and H. F. Bunn. 1998. "Regulation of Hypoxia-Inducible Factor 1alpha Is Mediated by an O2-Dependent Degradation Domain via the Ubiquitin-Proteasome Pathway." *Proceedings of the National Academy of Sciences of the United States of America* 95 (14):7987–92.

Hughes, Michelle A., Ian R. Powley, Rebekah Jukes-Jones, Sebastian Horn, Maria Feoktistova, Louise Fairall, John W. R. Schwabe, Martin Leverkus, Kelvin Cain, and Marion MacFarlane. 2016. "Co-Operative and Hierarchical Binding of c-FLIP and Caspase-8: A Unified Model Defines How c-FLIP Isoforms Differentially Control Cell Fate." *Molecular Cell* 61 (6):834–49. https://doi.org/10.1016/j.molcel.2016.02.023.

Iliopoulos, Dimitrios, Heather A. Hirsch, Guannan Wang, and Kevin Struhl. 2011. "Inducible Formation of Breast Cancer Stem Cells and Their Dynamic Equilibrium with Non-Stem Cancer Cells via IL6 Secretion." *Proceedings of the National Academy of Sciences of the United States*

of America 108 (4):1397–1402.
https://doi.org/10.1073/pnas.1018898108.

Ishioka, Toshiyasu, Ryohei Katayama, Ryo Kikuchi, Michie Nishimoto, Shinji Takada, Ritsuko Takada, Shu-ichi Matsuzawa, John C. Reed, Takashi Tsuruo, and Mikihiko Naito. 2007. "Impairment of the Ubiquitin-Proteasome System by Cellular FLIP." *Genes to Cells* 12 (6):735–44. https://doi.org/10.1111/j.1365-2443.2007.01087.x.

Izbicka, Elzbieta, David Campos, Gilbert Carrizales, and Anthony Tolcher. 2005. "Biomarkers for Sensitivity to Docetaxel and Paclitaxel in Human Tumor Cell Lines In Vitro." *Cancer Genomics - Proteomics* 2 (4):219–26.

Januchowski, Radosław, Karolina Wojtowicz, and Maciej Zabel. 2013. "The Role of Aldehyde Dehydrogenase (ALDH) in Cancer Drug Resistance." *Biomedicine & Pharmacotherapy = Biomedecine & Pharmacotherapie* 67 (7):669–80. https://doi.org/10.1016/j.biopha.2013.04.005.

Jemal, Ahmedin, Rebecca Siegel, Elizabeth Ward, Yongping Hao, Jiaquan Xu, and Michael J. Thun. 2009. "Cancer Statistics, 2009." *CA: A Cancer Journal for Clinicians* 59 (4):225–49. https://doi.org/10.3322/caac.20006.

Jensen, Mette Munk, Jesper Tranekjaer Jørgensen, Tina Binderup, and Andreas Kjaer. 2008. "Tumor Volume in Subcutaneous Mouse Xenografts Measured by microCT Is More Accurate and Reproducible than Determined by 18F-FDG-microPET or External Caliper." *BMC Medical Imaging* 8 (October):16. https://doi.org/10.1186/1471-2342-8-16.

Jones, Stephen E., Michael A. Savin, Frankie Ann Holmes, Joyce A. O'Shaughnessy, Joanne L. Blum, Svetislava Vukelja, Kristi J. McIntyre, et al. 2006. "Phase III Trial Comparing Doxorubicin plus Cyclophosphamide with Docetaxel plus Cyclophosphamide as Adjuvant Therapy for Operable Breast Cancer." *Journal of Clinical Oncology: Official Journal of the American Society of Clinical Oncology* 24 (34):5381–87. https://doi.org/10.1200/JCO.2006.06.5391.

Jordan, M. A., R. J. Toso, D. Thrower, and L. Wilson. 1993. "Mechanism of Mitotic Block and Inhibition of Cell Proliferation by Taxol at Low

Concentrations." *Proceedings of the National Academy of Sciences* 90 (20):9552–56.

Jung, Hae-Yun, and Jing Yang. 2015. "Unraveling the TWIST between EMT and Cancer Stemness." *Cell Stem Cell* 16 (1):1–2. https://doi.org/10.1016/j.stem.2014.12.005.

Kao, Jessica, Keyan Salari, Melanie Bocanegra, Yoon-La Choi, Luc Girard, Jeet Gandhi, Kevin A. Kwei, et al. 2009. "Molecular Profiling of Breast Cancer Cell Lines Defines Relevant Tumor Models and Provides a Resource for Cancer Gene Discovery." *PloS One* 4 (7):e6146. https://doi.org/10.1371/journal.pone.0006146.

Kavuri, Shyam M., Peter Geserick, Daniela Berg, Diana Panayotova Dimitrova, Maria Feoktistova, Daniela Siegmund, Harald Gollnick, Manfred Neumann, Harald Wajant, and Martin Leverkus. 2011. "Cellular FLICE-Inhibitory Protein (cFLIP) Isoforms Block CD95- and TRAIL Death Receptor-Induced Gene Induction Irrespective of Processing of Caspase-8 or cFLIP in the Death-Inducing Signaling Complex." *The Journal of Biological Chemistry* 286 (19):16631–46. https://doi.org/10.1074/jbc.M110.148585.

Khan, Khurum H., Montserrat Blanco-Codesido, and L. Rhoda Molife. n.d. "Cancer Therapeutics: Targeting the Apoptotic Pathway." *Critical Reviews in Oncology/Hematology*. Accessed March 20, 2014. https://doi.org/10.1016/j.critrevonc.2013.12.012.

Khramtsov, Andrey I., Galina F. Khramtsova, Maria Tretiakova, Dezheng Huo, Olufunmilayo I. Olopade, and Kathleen H. Goss. 2010. "Wnt/Beta-Catenin Pathway Activation Is Enriched in Basal-like Breast Cancers and Predicts Poor Outcome." *The American Journal of Pathology* 176 (6):2911–20. https://doi.org/10.2353/ajpath.2010.091125.

Kida, Kumiko, Takashi Ishikawa, Akimitsu Yamada, Kazutaka Narui, Sadataka Sugae, Mikiko Tanabe, Yasushi Ichikawa, and Itaru Endo. 2015. "Abstract P2-06-16: The Impact of ALDH1 on Chemo-Resistance and Prognosis according to Intrinsic Subtype in Breast Cancers." *Cancer Research* 75 (9 Supplement):P2-6-16-P2-06–16. https://doi.org/10.1158/1538-7445.SABCS14-P2-06-16.

Kiely, Belinda E., Yu Yang Soon, Martin H. N. Tattersall, and Martin R. Stockler. 2011. "How Long Have I Got? Estimating Typical, Best-Case, and Worst-Case Scenarios for Patients Starting First-Line Chemotherapy for Metastatic Breast Cancer: A Systematic Review of Recent Randomized Trials." *Journal of Clinical Oncology* 29 (4):456–63. https://doi.org/10.1200/JCO.2010.30.2174.

Kisim, Asli, Harika Atmaca, Burcu Cakar, Bulent Karabulut, Canfeza Sezgin, Selim Uzunoglu, Ruchan Uslu, and Burcak Karaca. 2012. "Pretreatment with AT-101 Enhances Tumor Necrosis Factor-Related Apoptosis-Inducing Ligand (TRAIL)-Induced Apoptosis of Breast Cancer Cells by Inducing Death Receptors 4 and 5 Protein Levels." *Journal of Cancer Research and Clinical Oncology* 138 (7):1155–63. https://doi.org/10.1007/s00432-012-1187-1.

Kitagawa, M., S. Hatakeyama, M. Shirane, M. Matsumoto, N. Ishida, K. Hattori, I. Nakamichi, A. Kikuchi, K. Nakayama, and K. Nakayama. 1999. "An F-Box Protein, FWD1, Mediates Ubiquitin-Dependent Proteolysis of Beta-Catenin." *The EMBO Journal* 18 (9):2401–10. https://doi.org/10.1093/emboj/18.9.2401.

Klaus, Alexandra, and Walter Birchmeier. 2008. "Wnt Signalling and Its Impact on Development and Cancer." *Nature Reviews. Cancer* 8 (5):387–98. https://doi.org/10.1038/nrc2389.

Konecny, Gottfried, Manuel Fritz, Michael Untch, Annette Lebeau, Margrit Felber, Sandra Lude, Malgorzata Beryt, Hermann Hepp, Dennis Slamon, and Mark Pegram. 2001. "HER-2/Neu Overexpression and in Vitro Chemosensitivity to CMF and FEC in Primary Breast Cancer." *Breast Cancer Research and Treatment* 69 (1):53–63. https://doi.org/10.1023/A:1012226006395.

Kreso, Antonija, and John E. Dick. 2014. "Evolution of the Cancer Stem Cell Model." *Cell Stem Cell* 14 (3):275–91. https://doi.org/10.1016/j.stem.2014.02.006.

Kruyt, Frank A. E. 2008. "TRAIL and Cancer Therapy." *Cancer Letters* 263 (1):14–25. https://doi.org/10.1016/j.canlet.2008.02.003.

Lapidot, Tsvee, Christian Sirard, Josef Vormoor, Barbara Murdoch, Trang Hoang, Julio Caceres-Cortes, Mark Minden, Bruce Paterson, Michael

A. Caligiuri, and John E. Dick. 1994. "A Cell Initiating Human Acute Myeloid Leukaemia after Transplantation into SCID Mice." *Nature* 367 (6464):645–48. https://doi.org/10.1038/367645a0.

LeBlanc, H. N., and A. Ashkenazi. 2003. "Apo2L/TRAIL and Its Death and Decoy Receptors." *Cell Death & Differentiation* 10 (1):66–75. https://doi.org/10.1038/sj.cdd.4401187.

Lee, H E, J H Kim, Y J Kim, S Y Choi, S-W Kim, E Kang, I Y Chung, et al. 2011. "An Increase in Cancer Stem Cell Population after Primary Systemic Therapy Is a Poor Prognostic Factor in Breast Cancer." *British Journal of Cancer* 104 (11):1730–38. https://doi.org/10.1038/bjc.2011.159.

Lee, Justine C., and Marcus E. Peter. 2003. "Regulation of Apoptosis by Ubiquitination." *Immunological Reviews* 193 (June):39–47.

Lee, L F, J S Haskill, N Mukaida, K Matsushima, and J P Ting. 1997. "Identification of Tumor-Specific Paclitaxel (Taxol)-Responsive Regulatory Elements in the Interleukin-8 Promoter." *Molecular and Cellular Biology* 17 (9):5097–5105.

Lehmann, Brian D., Joshua A. Bauer, Xi Chen, Melinda E. Sanders, A. Bapsi Chakravarthy, Yu Shyr, and Jennifer A. Pietenpol. 2011. "Identification of Human Triple-Negative Breast Cancer Subtypes and Preclinical Models for Selection of Targeted Therapies." *The Journal of Clinical Investigation* 121 (7):2750–67. https://doi.org/10.1172/JCI45014.

Lemke, J, S von Karstedt, J Zinngrebe, and H Walczak. 2014. "Getting TRAIL Back on Track for Cancer Therapy." *Cell Death and Differentiation* 21 (9):1350–64. https://doi.org/10.1038/cdd.2014.81.

Lerebours, Florence, Sophie Vacher, Catherine Andrieu, Marc Espie, Michel Marty, Rosette Lidereau, and Ivan Bieche. 2008. "NF-Kappa B Genes Have a Major Role in Inflammatory Breast Cancer." *BMC Cancer* 8 (February):41. https://doi.org/10.1186/1471-2407-8-41.

Li, Xiaoxian, Michael T. Lewis, Jian Huang, Carolina Gutierrez, C. Kent Osborne, Meng-Fen Wu, Susan G. Hilsenbeck, et al. 2008. "Intrinsic Resistance of Tumorigenic Breast Cancer Cells to Chemotherapy."

Journal of the National Cancer Institute 100 (9):672–79.
https://doi.org/10.1093/jnci/djn123.

Li, Yanyan, Katharine Atkinson, and Tao Zhang. 2017. "Combination of
Chemotherapy and Cancer Stem Cell Targeting Agents: Preclinical and
Clinical Studies." *Cancer Letters*.
https://doi.org/10.1016/j.canlet.2017.03.008.

Liu, Gentao, Xiangpeng Yuan, Zhaohui Zeng, Patrizia Tunici, Hiushan Ng,
Iman R Abdulkadir, Lizhi Lu, Dwain Irvin, Keith L Black, and John S Yu.
2006. "Analysis of Gene Expression and Chemoresistance of CD133+
Cancer Stem Cells in Glioblastoma." *Molecular Cancer* 5
(December):67. https://doi.org/10.1186/1476-4598-5-67.

Liu, Haiguang, Lin Lv, and Kai Yang. 2015. "Chemotherapy Targeting Cancer
Stem Cells." *American Journal of Cancer Research* 5 (3):880–93.

Liu, Shujing, Suresh M. Kumar, James S. Martin, Ruifeng Yang, and Xiaowei
Xu. 2011. "Snail1 Mediates Hypoxia-Induced Melanoma Progression."
The American Journal of Pathology 179 (6):3020–31.
https://doi.org/10.1016/j.ajpath.2011.08.038.

Liu, Suling, Yang Cong, Dong Wang, Yu Sun, Lu Deng, Yajing Liu, Rachel
Martin-Trevino, et al. 2013. "Breast Cancer Stem Cells Transition
between Epithelial and Mesenchymal States Reflective of Their Normal
Counterparts." *Stem Cell Reports* 2 (1):78–91.
https://doi.org/10.1016/j.stemcr.2013.11.009.

Liu, Suling, and Max S. Wicha. 2010. "Targeting Breast Cancer Stem Cells."
Journal of Clinical Oncology 28 (25):4006–12.
https://doi.org/10.1200/JCO.2009.27.5388.

Liu, Xiangping, Jing Wang, Haibo Wang, Shihai Liu, Ye Liang, Zhidong Lv,
Quan Zhou, and Weili Ding. 2013. "Combination of Ad-sTRAIL with the
Chemotherapeutic Drug Cisplatin Synergistically Enhances Their pro-
Apoptotic Ability in Human Breast Cancer Cells." *Oncology Reports* 30
(4):1913–19. https://doi.org/10.3892/or.2013.2653.

Locke, Matthew, Matthew Heywood, Stuart Fawell, and Ian C. Mackenzie.
2005. "Retention of Intrinsic Stem Cell Hierarchies in Carcinoma-
Derived Cell Lines." *Cancer Research* 65 (19):8944–50.
https://doi.org/10.1158/0008-5472.CAN-05-0931.

Longley, D. B., T. R. Wilson, M. McEwan, W. L. Allen, U. McDermott, L. Galligan, and P. G. Johnston. 2005. "C-FLIP Inhibits Chemotherapy-Induced Colorectal Cancer Cell Death." *Oncogene* 25 (6):838–48. https://doi.org/10.1038/sj.onc.1209122.

López-Knowles, Elena, Sarah J. Zardawi, Catriona M. McNeil, Ewan K. A. Millar, Paul Crea, Elizabeth A. Musgrove, Robert L. Sutherland, and Sandra A. O'Toole. 2010. "Cytoplasmic Localization of Beta-Catenin Is a Marker of Poor Outcome in Breast Cancer Patients." *Cancer Epidemiology, Biomarkers & Prevention: A Publication of the American Association for Cancer Research, Cosponsored by the American Society of Preventive Oncology* 19 (1):301–9. https://doi.org/10.1158/1055-9965.EPI-09-0741.

Louie, Elizabeth, Sara Nik, Juei-Suei Chen, Marlies Schmidt, Bo Song, Christine Pacson, Xiu Fang Chen, Seonhye Park, Jingfang Ju, and Emily I. Chen. 2010. "Identification of a Stem-like Cell Population by Exposing Metastatic Breast Cancer Cell Lines to Repetitive Cycles of Hypoxia and Reoxygenation." *Breast Cancer Research: BCR* 12 (6):R94. https://doi.org/10.1186/bcr2773.

Lowe, S. W., S. Bodis, A. McClatchey, L. Remington, H. E. Ruley, D. E. Fisher, D. E. Housman, and T. Jacks. 1994. "p53 Status and the Efficacy of Cancer Therapy in Vivo." *Science (New York, N.Y.)* 266 (5186):807–10.

Lu, Haiquan, Debangshu Samanta, Lisha Xiang, Huimin Zhang, Hongxia Hu, Ivan Chen, John W. Bullen, and Gregg L. Semenza. 2015. "Chemotherapy Triggers HIF-1–dependent Glutathione Synthesis and Copper Chelation That Induces the Breast Cancer Stem Cell Phenotype." *Proceedings of the National Academy of Sciences* 112 (33):E4600–4609. https://doi.org/10.1073/pnas.1513433112.

Luengo-Fernandez, Ramon, Jose Leal, Alastair Gray, and Richard Sullivan. 2013. "Economic Burden of Cancer across the European Union: A Population-Based Cost Analysis." *The Lancet Oncology* 14 (12):1165–74. https://doi.org/10.1016/S1470-2045(13)70442-X.

Maddams, J., D. Brewster, A. Gavin, J. Steward, J. Elliott, M. Utley, and H. Møller. 2009. "Cancer Prevalence in the United Kingdom: Estimates for

2008." *British Journal of Cancer* 101 (3):541–47. https://doi.org/10.1038/sj.bjc.6605148.

Maddams, J., M. Utley, and H. Møller. 2012. "Projections of Cancer Prevalence in the United Kingdom, 2010-2040." *British Journal of Cancer* 107 (7):1195–1202. https://doi.org/10.1038/bjc.2012.366.

Madjd, Zahra, Ali Zare Mehrjerdi, Ali Mohammad Sharifi, Saadat Molanaei, Shahriar Zohourian Shahzadi, and Mohsen Asadi-Lari. 2009. "CD44+ Cancer Cells Express Higher Levels of the Anti-Apoptotic Protein Bcl-2 in Breast Tumours." *Cancer Immunity : A Journal of the Academy of Cancer Immunology* 9 (April). http://www.ncbi.nlm.nih.gov/pmc/articles/PMC2935767/.

Magni, M., S. Shammah, R. Schiró, W. Mellado, R. Dalla-Favera, and A. M. Gianni. 1996. "Induction of Cyclophosphamide-Resistance by Aldehyde-Dehydrogenase Gene Transfer." *Blood* 87 (3):1097–1103.

Mani, Sendurai A., Wenjun Guo, Mai-Jing Liao, Elinor Ng. Eaton, Ayyakkannu Ayyanan, Alicia Y. Zhou, Mary Brooks, et al. 2008. "The Epithelial-Mesenchymal Transition Generates Cells with Properties of Stem Cells." *Cell* 133 (4):704–15. https://doi.org/10.1016/j.cell.2008.03.027.

Martin, Lainie P., Thomas C. Hamilton, and Russell J. Schilder. 2008. "Platinum Resistance: The Role of DNA Repair Pathways." *Clinical Cancer Research* 14 (5):1291–95. https://doi.org/10.1158/1078-0432.CCR-07-2238.

Martín, Miguel, Alvaro Rodríguez-Lescure, Amparo Ruiz, Emilio Alba, Lourdes Calvo, Manuel Ruiz-Borrego, Blanca Munárriz, et al. 2008. "Randomized Phase 3 Trial of Fluorouracil, Epirubicin, and Cyclophosphamide Alone or Followed by Paclitaxel for Early Breast Cancer." *Journal of the National Cancer Institute* 100 (11):805–14. https://doi.org/10.1093/jnci/djn151.

Mathieu, Julie, Zhan Zhang, Wenyu Zhou, Amy J. Wang, John M. Heddleston, Claudia M. A. Pinna, Alexis Hubaud, et al. 2011. "HIF Induces Human Embryonic Stem Cell Markers in Cancer Cells." *Cancer Research* 71 (13):4640–52. https://doi.org/10.1158/0008-5472.CAN-10-3320.

McCourt, Clare, Pamela Maxwell, Roberta Mazzucchelli, Rodolfo Montironi, Marina Scarpelli, Manuel Salto-Tellez, Joe M. O'Sullivan, Daniel B.

Longley, and David J.J. Waugh. 2012. "ELEVATION OF C-FLIP IN CASTRATE-RESISTANT PROSTATE CANCER ANTAGONIZES THERAPEUTIC RESPONSE TO ANDROGEN-RECEPTOR TARGETED THERAPY." *Clinical Cancer Research : An Official Journal of the American Association for Cancer Research* 18 (14):3822–33. https://doi.org/10.1158/1078-0432.CCR-11-3277.

Miguel, D. de, J. Lemke, A. Anel, H. Walczak, and L. Martinez-Lostao. 2016. "Onto Better TRAILs for Cancer Treatment." *Cell Death & Differentiation* 23 (5):733–47. https://doi.org/10.1038/cdd.2015.174.

Miyoshi, Yuichiro, Tadahiko Shien, Akiko Ogiya, Naoko Ishida, Kieko Yamazaki, Rie Horii, Yoshiya Horimoto, et al. 2016. "Differences in Expression of the Cancer Stem Cell Marker Aldehyde Dehydrogenase 1 among Estrogen Receptor-Positive/Human Epidermal Growth Factor Receptor Type 2-Negative Breast Cancer Cases with Early, Late, and No Recurrence." *Breast Cancer Research: BCR* 18 (1):73. https://doi.org/10.1186/s13058-016-0731-3.

Moja, Lorenzo, Cinzia Brambilla, Anna Compagnoni, and Vanna Pistotti. 2012. "Trastuzumab Containing Regimens for Early Breast Cancer." In *Cochrane Database of Systematic Reviews*, edited by The Cochrane Collaboration. Chichester, UK: John Wiley & Sons, Ltd. http://doi.wiley.com/10.1002/14651858.CD006243.

Morel, Anne-Pierre, Marjory Lièvre, Clémence Thomas, George Hinkal, Stéphane Ansieau, and Alain Puisieux. 2008. "Generation of Breast Cancer Stem Cells through Epithelial-Mesenchymal Transition." *PLoS ONE* 3 (8). https://doi.org/10.1371/journal.pone.0002888.

Moulder-Thompson, Stacey. n.d. "Women's Triple-Negative, First-Line Treatment: Improving Outcomes in Triple-Negative Breast Cancer (TNBC) Using Molecular Triaging and Diagnostic Imaging to Guide Neoadjuvant Therapy (NACT)." *Journal of Clinical Oncology*. Accessed June 10, 2016. http://meetinglibrary.asco.org/content/153158-156.

Naito, Mikihiko, Ryohei Katayama, Toshiyasu Ishioka, Akiko Suga, Kohei Takubo, Masahiro Nanjo, Chizuko Hashimoto, et al. 2004. "Cellular FLIP Inhibits Beta-Catenin Ubiquitylation and Enhances Wnt

Signaling." *Molecular and Cellular Biology* 24 (19):8418–27.
https://doi.org/10.1128/MCB.24.19.8418-8427.2004.

Nakajima, Akihito, Sachiko Komazawa-Sakon, Mutsuhiro Takekawa,
Tomonari Sasazuki, Wen-Chen Yeh, Hideo Yagita, Ko Okumura, and
Hiroyasu Nakano. 2006. "An Antiapoptotic Protein, c-FLIPL, Directly
Binds to MKK7 and Inhibits the JNK Pathway." *The EMBO Journal* 25
(23):5549–59. https://doi.org/10.1038/sj.emboj.7601423.

Neve, Richard M., Koei Chin, Jane Fridlyand, Jennifer Yeh, Frederick L.
Baehner, Tea Fevr, Laura Clark, et al. 2006. "A Collection of Breast
Cancer Cell Lines for the Study of Functionally Distinct Cancer
Subtypes." *Cancer Cell* 10 (6):515–27.
https://doi.org/10.1016/j.ccr.2006.10.008.

Newsom-Davis, Thomas, Silvia Prieske, and Henning Walczak. 2009. "Is
TRAIL the Holy Grail of Cancer Therapy?" *Apoptosis* 14 (4):607–23.
https://doi.org/10.1007/s10495-009-0321-2.

Nowell, P C. 1976. "The Clonal Evolution of Tumor Cell Populations." *Science
(New York, N.Y.)* 194 (4260):23–28.

O'Brien, Catherine A, Aaron Pollett, Steven Gallinger, and John E Dick. 2007.
"A Human Colon Cancer Cell Capable of Initiating Tumour Growth in
Immunodeficient Mice." *Nature* 445 (7123):106–10.
https://doi.org/10.1038/nature05372.

Oh, Bora, SoJung Park, Jhang Ho Pak, and InKi Kim. 2012. "Downregulation
of Mcl-1 by Daunorubicin Pretreatment Reverses Resistance of Breast
Cancer Cells to TNF-Related Apoptosis-Inducing Ligand." *Biochemical
and Biophysical Research Communications* 422 (1):42–47.
https://doi.org/10.1016/j.bbrc.2012.04.093.

Ohi, Yasuyo, Yoshihisa Umekita, Takako Yoshioka, Masakazu Souda,
Yoshiaki Rai, Yoshiaki Sagara, Yasuaki Sagara, Yoshiatsu Sagara,
and Akihide Tanimoto. 2011. "Aldehyde Dehydrogenase 1 Expression
Predicts Poor Prognosis in Triple-Negative Breast Cancer."
Histopathology 59 (4):776–80. https://doi.org/10.1111/j.1365-
2559.2011.03884.x.

Oliver, Patsy G., Albert F. LoBuglio, Tong Zhou, Andres Forero, Hyunki Kim,
Kurt R. Zinn, Guihua Zhai, Yufeng Li, Choo H. Lee, and Donald J.

Buchsbaum. 2012. "Effect of Anti-DR5 and Chemotherapy on Basal-like Breast Cancer." *Breast Cancer Research and Treatment* 133 (2):417–26. https://doi.org/10.1007/s10549-011-1755-0.

Park, Ju-Hyun, William F. Anderson, and Mitchell H. Gail. 2015. "Improvements in US Breast Cancer Survival and Proportion Explained by Tumor Size and Estrogen-Receptor Status." *Journal of Clinical Oncology: Official Journal of the American Society of Clinical Oncology* 33 (26):2870–76. https://doi.org/10.1200/JCO.2014.59.9191.

Park, Sojung, Sang-Mi Shim, Sang-Hee Nam, Ladislav Andera, Nayoung Suh, and Inki Kim. 2014. "CGP74514A Enhances TRAIL-Induced Apoptosis in Breast Cancer Cells by Reducing X-Linked Inhibitor of Apoptosis Protein." *Anticancer Research* 34 (7):3557–62.

Park, Soo-Jung, Ching-Haung Wu, John D. Gordon, Xiaoling Zhong, Armaghan Emami, and Ahmad R. Safa. 2004. "Taxol Induces Caspase-10-Dependent Apoptosis." *Journal of Biological Chemistry* 279 (49):51057–67. https://doi.org/10.1074/jbc.M406543200.

Parker, Joel S., Michael Mullins, Maggie C.U. Cheang, Samuel Leung, David Voduc, Tammi Vickery, Sherri Davies, et al. 2009. "Supervised Risk Predictor of Breast Cancer Based on Intrinsic Subtypes." *Journal of Clinical Oncology* 27 (8):1160–67. https://doi.org/10.1200/JCO.2008.18.1370.

Pastan, I., and M. M. Gottesman. 1991. "Multidrug Resistance." *Annual Review of Medicine* 42:277–86. https://doi.org/10.1146/annurev.me.42.020191.001425.

Pattabiraman, Diwakar R., and Robert A. Weinberg. 2014. "Tackling the Cancer Stem Cells — What Challenges Do They Pose?" *Nature Reviews Drug Discovery* 13 (7):497–512. https://doi.org/10.1038/nrd4253.

Piggott, Luke, Nader Omidvar, Salvador Marti Perez, Matthias Eberl, and Richard WE Clarkson. 2011. "Suppression of Apoptosis Inhibitor c-FLIP Selectively Eliminates Breast Cancer Stem Cell Activity in Response to the Anti-Cancer Agent, TRAIL." *Breast Cancer Research : BCR* 13 (5):R88. https://doi.org/10.1186/bcr2945.

Plaks, Vicki, Niwen Kong, and Zena Werb. 2015. "The Cancer Stem Cell Niche: How Essential Is the Niche in Regulating Stemness of Tumor Cells?" *Cell Stem Cell* 16 (3):225–38. https://doi.org/10.1016/j.stem.2015.02.015.

Plati, Jessica, Octavian Bucur, and Roya Khosravi-Far. 2011. "Apoptotic Cell Signaling in Cancer Progression and Therapy." *Integrative Biology : Quantitative Biosciences from Nano to Macro* 3 (4):279–96. https://doi.org/10.1039/c0ib00144a.

Polakis, P. 2000. "Wnt Signaling and Cancer." *Genes & Development* 14 (15):1837–51.

Prat, Aleix, Joel S Parker, Olga Karginova, Cheng Fan, Chad Livasy, Jason I Herschkowitz, Xiaping He, and Charles M Perou. 2010. "Phenotypic and Molecular Characterization of the Claudin-Low Intrinsic Subtype of Breast Cancer." *Breast Cancer Research : BCR* 12 (5):R68. https://doi.org/10.1186/bcr2635.

Prat, Aleix, and Charles M. Perou. 2011. "Deconstructing the Molecular Portraits of Breast Cancer." *Molecular Oncology* 5 (1):5–23. https://doi.org/10.1016/j.molonc.2010.11.003.

Prosperi, Jenifer R., and Kathleen H. Goss. 2010. "A Wnt-Ow of Opportunity: Targeting the Wnt/Beta-Catenin Pathway in Breast Cancer." *Current Drug Targets* 11 (9):1074–88.

Rahman, Monzur, Sean R. Davis, Janet G. Pumphrey, Jing Bao, Marion M. Nau, Paul S. Meltzer, and Stanley Lipkowitz. 2009. "TRAIL Induces Apoptosis in Triple-Negative Breast Cancer Cells with a Mesenchymal Phenotype." *Breast Cancer Research and Treatment* 113 (2):217–30. https://doi.org/10.1007/s10549-008-9924-5.

Rahman, Monzur, Janet G. Pumphrey, and Stanley Lipkowitz. 2009a. "Chapter 3 The TRAIL to Targeted Therapy of Breast Cancer." In *Advances in Cancer Research*, edited by George F. Vande Woude and George Klein, Volume 103:43–73. Advances in Cancer Research. Academic Press. http://www.sciencedirect.com/science/article/pii/S0065230X09030036.

———. 2009b. "The TRAIL to Targeted Therapy of Breast Cancer." *Advances in Cancer Research* 103:43–73. https://doi.org/10.1016/S0065-230X(09)03003-6.

Ramalingam, Suresh. n.d. "Galaxy-2 Trial (NCT01798485): A Randomized Phase 3 Study of Ganetespib in Combination with Docetaxel versus Docetaxel Alone in Patients with Advanced Lung Adenocarcinoma." *Journal of Clinical Oncology*. Accessed June 21, 2016. http://meetinglibrary.asco.org/content/132601-144.

Rampurwala, Murtuza M., Gabrielle B. Rocque, and Mark E. Burkard. 2014. "Update on Adjuvant Chemotherapy for Early Breast Cancer." *Breast Cancer: Basic and Clinical Research* 8:125–33. https://doi.org/10.4137/BCBCR.S9454.

Ranji, Peyman, Tayyebali Salmani Kesejini, Sara Saeedikhoo, and Ali Mohammad Alizadeh. 2016. "Targeting Cancer Stem Cell-Specific Markers And/Or Associated Signaling Pathways for Overcoming Cancer Drug Resistance." *Tumor Biology*, August, 1–17. https://doi.org/10.1007/s13277-016-5294-5.

Ratcliffe, Peter J., Christopher W. Pugh, and Patrick H. Maxwell. 2000. "Targeting Tumors through the HIF System." *Nature Medicine* 6 (12):1315–16. https://doi.org/10.1038/82113.

Ray, Subrata, and Alex Almasan. 2003. "Apoptosis Induction in Prostate Cancer Cells and Xenografts by Combined Treatment with Apo2 Ligand/Tumor Necrosis Factor-Related Apoptosis-Inducing Ligand and CPT-11." *Cancer Research* 63 (15):4713–23.

Ricci-Vitiani, Lucia, Dario G. Lombardi, Emanuela Pilozzi, Mauro Biffoni, Matilde Todaro, Cesare Peschle, and Ruggero De Maria. 2007. "Identification and Expansion of Human Colon-Cancer-Initiating Cells." *Nature* 445 (7123):111–15. https://doi.org/10.1038/nature05384.

Roché, Henri, Pierre Fumoleau, Marc Spielmann, Jean-Luc Canon, Thierry Delozier, Daniel Serin, Michel Symann, et al. 2006. "Sequential Adjuvant Epirubicin-Based and Docetaxel Chemotherapy for Node-Positive Breast Cancer Patients: The FNCLCC PACS 01 Trial." *Journal of Clinical Oncology: Official Journal of the American Society of Clinical Oncology* 24 (36):5664–71. https://doi.org/10.1200/JCO.2006.07.3916.

Rohwer, Nadine, and Thorsten Cramer. 2011. "Hypoxia-Mediated Drug Resistance: Novel Insights on the Functional Interaction of HIFs and Cell Death Pathways." *Drug Resistance Updates* 14 (3):191–201. https://doi.org/10.1016/j.drup.2011.03.001.

Roizin-Towle, L., and E. J. Hall. 1978. "Studies with Bleomycin and Misonidazole on Aerated and Hypoxic Cells." *British Journal of Cancer* 37 (2):254–60. https://doi.org/10.1038/bjc.1978.34.

Rosa, Marilin, Hyo Sook Han, Roohi Ismail-Khan, Pushpa Allam-Nandyala, and Marilyn M. Bui. 2015. "Beta-Catenin Expression Patterns in Matched Pre- and Post-Neoadjuvant Chemotherapy-Resistant Breast Cancer." *Annals of Clinical and Laboratory Science* 45 (1):10–16.

Roy, R., P. M. Willan, R. Clarke, and G. Farnie. 2010. "Differentiation Therapy: Targeting Breast Cancer Stem Cells to Reduce Resistance to Radiotherapy and Chemotherapy." *Breast Cancer Research* 12 (Suppl 1):O5. https://doi.org/10.1186/bcr2496.

Safa, A R. 2012. "C-FLIP, a Master Anti-Apoptotic Regulator." *Experimental Oncology* 34 (3):176–84.

Saifo, Maher S., Donald R. Rempinski, Youcef M. Rustum, and Rami G. Azrak. 2010. "Targeting the Oncogenic Protein Beta-Catenin to Enhance Chemotherapy Outcome against Solid Human Cancers." *Molecular Cancer* 9 (December):310. https://doi.org/10.1186/1476-4598-9-310.

Samanta, Debangshu, Daniele M. Gilkes, Pallavi Chaturvedi, Lisha Xiang, and Gregg L. Semenza. 2014. "Hypoxia-Inducible Factors Are Required for Chemotherapy Resistance of Breast Cancer Stem Cells." *Proceedings of the National Academy of Sciences*, December, 201421438. https://doi.org/10.1073/pnas.1421438111.

Sansone, Pasquale, Gianluca Storci, Simona Tavolari, Tiziana Guarnieri, Catia Giovannini, Mario Taffurelli, Claudio Ceccarelli, et al. 2007. "IL-6 Triggers Malignant Features in Mammospheres from Human Ductal Breast Carcinoma and Normal Mammary Gland." *The Journal of Clinical Investigation* 117 (12):3988–4002. https://doi.org/10.1172/JCI32533.

Savage, Philip. 2016. "Chemotherapy Curable Malignancies and Cancer Stem Cells: A Biological Review and Hypothesis." *BMC Cancer* 16:906. https://doi.org/10.1186/s12885-016-2956-z.

Scheel, Christina, and Robert A. Weinberg. 2011. "Phenotypic Plasticity and Epithelial-Mesenchymal Transitions in Cancer and Normal Stem Cells?" *International Journal of Cancer* 129 (10):2310–2314. https://doi.org/10.1002/ijc.26311.

Schott, Anne F., Melissa D. Landis, Gabriela Dontu, Kent A. Griffith, Rachel M. Layman, Ian Krop, Lacey A Paskett, et al. 2013. "Preclinical and Clinical Studies of Gamma Secretase Inhibitors with Docetaxel on Human Breast Tumors." *Clinical Cancer Research : An Official Journal of the American Association for Cancer Research* 19 (6):1512–24. https://doi.org/10.1158/1078-0432.CCR-11-3326.

Schwab, Luciana P., Danielle L. Peacock, Debeshi Majumdar, Jesse F. Ingels, Laura C. Jensen, Keisha D. Smith, Richard C. Cushing, and Tiffany N. Seagroves. 2012. "Hypoxia-Inducible Factor 1α Promotes Primary Tumor Growth and Tumor-Initiating Cell Activity in Breast Cancer." *Breast Cancer Research: BCR* 14 (1):R6. https://doi.org/10.1186/bcr3087.

Semenza, G. L. 2013. "Cancer-Stromal Cell Interactions Mediated by Hypoxia-Inducible Factors Promote Angiogenesis, Lymphangiogenesis, and Metastasis." *Oncogene* 32 (35):4057–63. https://doi.org/10.1038/onc.2012.578.

Semenza, Gregg L. 2013. "HIF-1 Mediates Metabolic Responses to Intratumoral Hypoxia and Oncogenic Mutations." *The Journal of Clinical Investigation* 123 (9):3664–71. https://doi.org/10.1172/JCI67230.

———. 2014. "Oxygen Sensing, Hypoxia-Inducible Factors, and Disease Pathophysiology." *Annual Review of Pathology* 9:47–71. https://doi.org/10.1146/annurev-pathol-012513-104720.

———. 2015. "Regulation of the Breast Cancer Stem Cell Phenotype by Hypoxia-Inducible Factors." *Clinical Science* 129 (12):1037–45. https://doi.org/10.1042/CS20150451.

———. 2016. "Hypoxia-inducible Factors: Coupling Glucose Metabolism and Redox Regulation with Induction of the Breast Cancer Stem Cell Phenotype." *The EMBO Journal*, December, e201695204. https://doi.org/10.15252/embj.201695204.

Senkus, E., S. Kyriakides, F. Penault-Llorca, P. Poortmans, A. Thompson, S. Zackrisson, and F. Cardoso. 2013. "Primary Breast Cancer: ESMO Clinical Practice Guidelines for Diagnosis, Treatment and Follow-Up." *Annals of Oncology* 24 (suppl 6):vi7-vi23. https://doi.org/10.1093/annonc/mdt284.

Senkus, Elżbieta, Fatima Cardoso, and Olivia Pagani. 2014. "Time for More Optimism in Metastatic Breast Cancer?" *Cancer Treatment Reviews* 40 (2):220–28. https://doi.org/10.1016/j.ctrv.2013.09.015.

Seufferlein, T., J. B. Bachet, E. Van Cutsem, and P. Rougier. 2012. "Pancreatic Adenocarcinoma: ESMO–ESDO Clinical Practice Guidelines for Diagnosis, Treatment and Follow-Up." *Annals of Oncology* 23 (suppl 7):vii33-vii40. https://doi.org/10.1093/annonc/mds224.

Shamimi-Noori, S., W.-S. Yeow, M. F. Ziauddin, H. Xin, T. L. N. Tran, J. Xie, A. Loehfelm, et al. 2008. "Cisplatin Enhances the Antitumor Effect of Tumor Necrosis Factor-Related Apoptosis-Inducing Ligand Gene Therapy via Recruitment of the Mitochondria-Dependent Death Signaling Pathway." *Cancer Gene Therapy* 15 (6):356–70. https://doi.org/10.1038/sj.cgt.7701120.

Shankar, Sharmila, Xufen Chen, and Rakesh K. Srivastava. 2005. "Effects of Sequential Treatments with Chemotherapeutic Drugs Followed by TRAIL on Prostate Cancer in Vitro and in Vivo." *The Prostate* 62 (2):165–186. https://doi.org/10.1002/pros.20126.

Shankar, Sharmila, Thiyam Ramsing Singh, and Rakesh K. Srivastava. 2004. "Ionizing Radiation Enhances the Therapeutic Potential of TRAIL in Prostate Cancer in Vitro and in Vivo: Intracellular Mechanisms." *The Prostate* 61 (1):35–49. https://doi.org/10.1002/pros.20069.

Shaw, Frances L., Hannah Harrison, Katherine Spence, Matthew P. Ablett, Bruno M. Simões, Gillian Farnie, and Robert B. Clarke. 2012. "A

Detailed Mammosphere Assay Protocol for the Quantification of Breast Stem Cell Activity." *Journal of Mammary Gland Biology and Neoplasia* 17 (2):111–17. https://doi.org/10.1007/s10911-012-9255-3.

Shin, Sung-Young, Oliver Rath, Armin Zebisch, Sang-Mok Choo, Walter Kolch, and Kwang-Hyun Cho. 2010. "Functional Roles of Multiple Feedback Loops in Extracellular Signal-Regulated Kinase and Wnt Signaling Pathways That Regulate Epithelial-Mesenchymal Transition." *Cancer Research* 70 (17):6715–24. https://doi.org/10.1158/0008-5472.CAN-10-1377.

Sims-Mourtada, Jennifer, Lynn M. Opdenaker, Joshua Davis, Kimberly M. Arnold, and Daniel Flynn. 2014. "Taxane-Induced Hedgehog Signaling Is Linked to Expansion of Breast Cancer Stem-like Populations after Chemotherapy." *Molecular Carcinogenesis*, September, n/a-n/a. https://doi.org/10.1002/mc.22225.

Singh, A., and J. Settleman. 2010. "EMT, Cancer Stem Cells and Drug Resistance: An Emerging Axis of Evil in the War on Cancer." *Oncogene* 29 (34):4741–51. https://doi.org/10.1038/onc.2010.215.

Singh, Sheila K., Cynthia Hawkins, Ian D. Clarke, Jeremy A. Squire, Jane Bayani, Takuichiro Hide, R. Mark Henkelman, Michael D. Cusimano, and Peter B. Dirks. 2004. "Identification of Human Brain Tumour Initiating Cells." *Nature* 432 (7015):396–401. https://doi.org/10.1038/nature03128.

Song, Jin H., Doyoun K. Song, Meenhard Herlyn, Kenneth C. Petruk, and Chunhai Hao. 2003. "Cisplatin down-Regulation of Cellular Fas-Associated Death Domain-like Interleukin-1beta-Converting Enzyme-like Inhibitory Proteins to Restore Tumor Necrosis Factor-Related Apoptosis-Inducing Ligand-Induced Apoptosis in Human Melanoma Cells." *Clinical Cancer Research: An Official Journal of the American Association for Cancer Research* 9 (11):4255–66.

Sorlie, Therese, Charles M. Perou, Robert Tibshirani, Turid Aas, Stephanie Geisler, Hilde Johnsen, Trevor Hastie, et al. 2001. "Gene Expression Patterns of Breast Carcinomas Distinguish Tumor Subclasses with Clinical Implications." *Proceedings of the National Academy of*

Sciences of the United States of America 98 (19):10869–74. https://doi.org/10.1073/pnas.191367098.

Sparano, Joseph A., Molin Wang, Silvana Martino, Vicky Jones, Edith A. Perez, Tom Saphner, Antonio C. Wolff, George W. Sledge, William C. Wood, and Nancy E. Davidson. 2008. "Weekly Paclitaxel in the Adjuvant Treatment of Breast Cancer." *The New England Journal of Medicine* 358 (16):1663–71. https://doi.org/10.1056/NEJMoa0707056.

Stone, Albert A., and Timothy C. Chambers. 2000. "Microtubule Inhibitors Elicit Differential Effects on MAP Kinase (JNK, ERK, and p38) Signaling Pathways in Human KB-3 Carcinoma Cells." *Experimental Cell Research* 254 (1):110–19. https://doi.org/10.1006/excr.1999.4731.

Takebe, Naoko, Ronald Q Warren, and S Percy Ivy. 2011. "Breast Cancer Growth and Metastasis: Interplay between Cancer Stem Cells, Embryonic Signaling Pathways and Epithelial-to-Mesenchymal Transition." *Breast Cancer Research : BCR* 13 (3):211. https://doi.org/10.1186/bcr2876.

Tanei, Tomonori, Koji Morimoto, Kenzo Shimazu, Seung Jin Kim, Yoshio Tanji, Tetsuya Taguchi, Yasuhiro Tamaki, and Shinzaburo Noguchi. 2009. "Association of Breast Cancer Stem Cells Identified by Aldehyde Dehydrogenase 1 Expression with Resistance to Sequential Paclitaxel and Epirubicin-Based Chemotherapy for Breast Cancers." *Clinical Cancer Research* 15 (12):4234–41. https://doi.org/10.1158/1078-0432.CCR-08-1479.

Tanimoto, K., Y. Makino, T. Pereira, and L. Poellinger. 2000. "Mechanism of Regulation of the Hypoxia-Inducible Factor-1 Alpha by the von Hippel-Lindau Tumor Suppressor Protein." *The EMBO Journal* 19 (16):4298–4309. https://doi.org/10.1093/emboj/19.16.4298.

Thiery, Jean Paul, Hervé Acloque, Ruby Y. J. Huang, and M. Angela Nieto. 2009. "Epithelial-Mesenchymal Transitions in Development and Disease." *Cell* 139 (5):871–90. https://doi.org/10.1016/j.cell.2009.11.007.

Tibbetts, Michael D., Lixin Zheng, and Michael J. Lenardo. 2003. "The Death Effector Domain Protein Family: Regulators of Cellular Homeostasis." *Nature Immunology* 4 (5):404–9. https://doi.org/10.1038/ni0503-404.

Tiezzi, Daniel Guimarães, Willian Simões Clagnan, Larissa Raquel Mouro
Mandarano, Christiani Bisinoto de Sousa, Heitor Ricardo Cosiski
Marana, Marcelo Guimarães Tiezzi, and Jurandyr Moreira de Andrade.
2013. "Expression of Aldehyde Dehydrogenase after Neoadjuvant
Chemotherapy Is Associated with Expression of Hypoxia-Inducible
Factors 1 and 2 Alpha and Predicts Prognosis in Locally Advanced
Breast Cancer." *Clinics* 68 (5):592–98.
https://doi.org/10.6061/clinics/2013(05)03.

Tsuji, Takanori, Soichiro Ibaragi, Kaori Shima, Miaofen G. Hu, Miki Katsurano,
Akira Sasaki, and Guo-fu Hu. 2008. "Epithelial-Mesenchymal Transition
Induced by Growth Suppressor p12CDK2-AP1 Promotes Tumor Cell
Local Invasion but Suppresses Distant Colony Growth." *Cancer
Research* 68 (24):10377–86. https://doi.org/10.1158/0008-5472.CAN-
08-1444.

Turner, Nicholas C., Patrick Neven, Sibylle Loibl, and Fabrice Andre. 2016.
"Advances in the Treatment of Advanced Oestrogen-Receptor-Positive
Breast Cancer." *Lancet (London, England)*, December.
https://doi.org/10.1016/S0140-6736(16)32419-9.

UK, Cancer Research. 2014. "Worldwide Cancer Statistics." Document.
February 14, 2014. http://www.cancerresearchuk.org/cancer-
info/cancerstats/world/cancer-worldwide-the-global-picture.

Unruh, Annika, Anke Ressel, Hamid G. Mohamed, Randall S. Johnson, Roger
Nadrowitz, Eckart Richter, Dörthe M. Katschinski, and Roland H.
Wenger. 2003. "The Hypoxia-Inducible Factor-1 Alpha Is a Negative
Factor for Tumor Therapy." *Oncogene* 22 (21):3213–20.
https://doi.org/10.1038/sj.onc.1206385.

Vargo-Gogola, Tracy, and Jeffrey M. Rosen. 2007. "Modelling Breast Cancer:
One Size Does Not Fit All." *Nature Reviews Cancer* 7 (9):659–72.
https://doi.org/10.1038/nrc2193.

Vaupel, Peter, Michael Höckel, and Arnulf Mayer. 2007. "Detection and
Characterization of Tumor Hypoxia Using pO2 Histography."
Antioxidants & Redox Signaling 9 (8):1221–35.
https://doi.org/10.1089/ars.2007.1628.

Velasco-Velázquez, Marco A., Nora Homsi, Marisol De La Fuente, and Richard G. Pestell. 2012. "Breast Cancer Stem Cells." *The International Journal of Biochemistry & Cell Biology* 44 (4):573–77. https://doi.org/10.1016/j.biocel.2011.12.020.

Vermeulen, Louis, Felipe de Sousa e Melo, Dick J Richel, and Jan Paul Medema. 2012. "The Developing Cancer Stem-Cell Model: Clinical Challenges and Opportunities." *The Lancet Oncology* 13 (2):e83–89. https://doi.org/10.1016/S1470-2045(11)70257-1.

Vidot, Susanne, James Witham, Roshan Agarwal, Sebastian Greenhough, Harnoor S. Bamrah, Gabor J. Tigyi, Stanley B. Kaye, and Alan Richardson. 2010. "Autotaxin Delays Apoptosis Induced by Carboplatin in Ovarian Cancer Cells." *Cellular Signalling* 22 (6):926–35. https://doi.org/10.1016/j.cellsig.2010.01.017.

Visvader, Jane E., and Geoffrey J. Lindeman. 2008. "Cancer Stem Cells in Solid Tumours: Accumulating Evidence and Unresolved Questions." *Nature Reviews Cancer* 8 (10):755–68. https://doi.org/10.1038/nrc2499.

Walczak, Henning, Robert E. Miller, Kiley Ariail, Brian Gliniak, Thomas S. Griffith, Marek Kubin, Wilson Chin, et al. 1999. "Tumoricidal Activity of Tumor Necrosis Factor–related Apoptosis–inducing Ligand in Vivo." *Nature Medicine* 5 (2):157–63. https://doi.org/10.1038/5517.

Wang, T.-H., Y.-H. Chan, C.-W. Chen, W.-H. Kung, Y.-S. Lee, S.-T. Wang, T.-C. Chang, and H.-S. Wang. 2006. "Paclitaxel (Taxol) Upregulates Expression of Functional Interleukin-6 in Human Ovarian Cancer Cells through Multiple Signaling Pathways." *Oncogene* 25 (35):4857–66. https://doi.org/10.1038/sj.onc.1209498.

Wang, Tzu-Hao, Hsin-Shih Wang, and Yung-Kwei Soong. 2000. "Paclitaxel-Induced Cell Death." *Cancer* 88 (11):2619–28. https://doi.org/10.1002/1097-0142(20000601)88:11<2619::AID-CNCR26>3.0.CO;2-J.

Wang, Zhuo, Robert Goulet, Katie J. Stanton, Miral Sadaria, and Harikrishna Nakshatri. 2005. "Differential Effect of Anti-Apoptotic Genes Bcl-xL and c-FLIP on Sensitivity of MCF-7 Breast Cancer Cells to Paclitaxel and Docetaxel." *Anticancer Research* 25 (3C):2367–79.

Wilson, Catherine, Timothy Wilson, Patrick G. Johnston, Daniel B. Longley, and David J. J. Waugh. 2008. "Interleukin-8 Signaling Attenuates TRAIL- and Chemotherapy-Induced Apoptosis through Transcriptional Regulation of c-FLIP in Prostate Cancer Cells." *Molecular Cancer Therapeutics* 7 (9):2649–61. https://doi.org/10.1158/1535-7163.MCT-08-0148.

Wu, Yanyuan, Marianna Sarkissyan, and Jaydutt V. Vadgama. 2016. "Epithelial-Mesenchymal Transition and Breast Cancer." *Journal of Clinical Medicine* 5 (2). https://doi.org/10.3390/jcm5020013.

Xiang, Lisha, Daniele M. Gilkes, Pallavi Chaturvedi, Weibo Luo, Hongxia Hu, Naoharu Takano, Houjie Liang, and Gregg L. Semenza. 2014. "Ganetespib Blocks HIF-1 Activity and Inhibits Tumor Growth, Vascularization, Stem Cell Maintenance, Invasion, and Metastasis in Orthotopic Mouse Models of Triple-Negative Breast Cancer." *Journal of Molecular Medicine (Berlin, Germany)* 92 (2):151–64. https://doi.org/10.1007/s00109-013-1102-5.

Xiang, Lisha, Daniele M. Gilkes, Hongxia Hu, Naoharu Takano, Weibo Luo, Haiquan Lu, John W. Bullen, Debangshu Samanta, Houjie Liang, and Gregg L. Semenza. 2014. "Hypoxia-Inducible Factor 1 Mediates TAZ Expression and Nuclear Localization to Induce the Breast Cancer Stem Cell Phenotype." *Oncotarget* 5 (24):12509–27. https://doi.org/10.18632/oncotarget.2997.

Xie, Jing, Yong Xiao, Xiao-yan Zhu, Zhou-yu Ning, Hai-fan Xu, and Hui-min Wu. 2016. "Hypoxia Regulates Stemness of Breast Cancer MDA-MB-231 Cells." *Medical Oncology (Northwood, London, England)* 33. https://doi.org/10.1007/s12032-016-0755-7.

Xing, F., H. Okuda, M. Watabe, A. Kobayashi, S. K. Pai, W. Liu, P. R. Pandey, et al. 2011. "Hypoxia-Induced Jagged2 Promotes Breast Cancer Metastasis and Self-Renewal of Cancer Stem-like Cells." *Oncogene* 30 (39):4075–86. https://doi.org/10.1038/onc.2011.122.

Xu, Jing, Zhengfan Xu, Jun-Ying Zhou, Zhengping Zhuang, Enhua Wang, Julie Boerner, and Gen Sheng Wu. 2013. "Regulation of the Src-PP2A Interaction in Tumor Necrosis Factor (TNF)-Related Apoptosis-Inducing Ligand (TRAIL)-Induced Apoptosis." *The Journal of Biological*

Chemistry 288 (46):33263–71.
https://doi.org/10.1074/jbc.M113.508093.

Xu, Jinhua, Jenifer R. Prosperi, Noura Choudhury, Olufunmilayo I. Olopade, and Kathleen H. Goss. 2015. "β-Catenin Is Required for the Tumorigenic Behavior of Triple-Negative Breast Cancer Cells." *PLoS ONE* 10 (2). https://doi.org/10.1371/journal.pone.0117097.

Yang, Annie, Nicholas S Wilson, and Avi Ashkenazi. 2010. "Proapoptotic DR4 and DR5 Signaling in Cancer Cells: Toward Clinical Translation." *Current Opinion in Cell Biology*, Cell differentiation / Cell division, growth and death, 22 (6):837–44. https://doi.org/10.1016/j.ceb.2010.08.001.

Yang, Jing, and Robert A. Weinberg. 2008. "Epithelial-Mesenchymal Transition: At the Crossroads of Development and Tumor Metastasis." *Developmental Cell* 14 (6):818–29. https://doi.org/10.1016/j.devcel.2008.05.009.

Yang, Wanjuan, Jorge Soares, Patricia Greninger, Elena J. Edelman, Howard Lightfoot, Simon Forbes, Nidhi Bindal, et al. 2013. "Genomics of Drug Sensitivity in Cancer (GDSC): A Resource for Therapeutic Biomarker Discovery in Cancer Cells." *Nucleic Acids Research* 41 (D1):D955–61. https://doi.org/10.1093/nar/gks1111.

Yin, Shuping, Arun K. Rishi, and Kaladhar B. Reddy. 2015. "Anti-Estrogen‑resistant Breast Cancer Cells Are Sensitive to Cisplatin plus TRAIL Treatment." *Oncology Reports* 33 (3):1475–80. https://doi.org/10.3892/or.2015.3721.

Yin, Shuping, Liping Xu, Sudeshna Bandyopadhyay, Seema Sethi, and Kaladhar B. Reddy. 2011. "Cisplatin and TRAIL Enhance Breast Cancer Stem Cell Death." *International Journal of Oncology* 39 (4):891–98. https://doi.org/10.3892/ijo.2011.1085.

Yoo, Young A., Myoung Hee Kang, Hyun Joo Lee, Baek-hui Kim, Jong Kuk Park, Hyun Koo Kim, Jun Suk Kim, and Sang Cheul Oh. 2011. "Sonic Hedgehog Pathway Promotes Metastasis and Lymphangiogenesis via Activation of Akt, EMT, and MMP-9 Pathway in Gastric Cancer."

Cancer Research 71 (22):7061–70. https://doi.org/10.1158/0008-5472.CAN-11-1338.

Zhang, Cathy C., Zhengming Yan, Qing Zong, Douglas D. Fang, Cory Painter, Qin Zhang, Enhong Chen, Maruja E. Lira, Annette John-Baptiste, and James G. Christensen. 2013. "Synergistic Effect of the γ-Secretase Inhibitor PF-03084014 and Docetaxel in Breast Cancer Models." *Stem Cells Translational Medicine* 2 (3):233–42. https://doi.org/10.5966/sctm.2012-0096.

Zhang, Huimin, Haiquan Lu, Lisha Xiang, John W. Bullen, Chuanzhao Zhang, Debangshu Samanta, Daniele M. Gilkes, Jianjun He, and Gregg L. Semenza. 2015. "HIF-1 Regulates CD47 Expression in Breast Cancer Cells to Promote Evasion of Phagocytosis and Maintenance of Cancer Stem Cells." *Proceedings of the National Academy of Sciences* 112 (45):E6215–23. https://doi.org/10.1073/pnas.1520032112.

Zhang, Lin, Gang Huang, Xiaowu Li, Yujun Zhang, Yan Jiang, Junjie Shen, Jia Liu, et al. 2013. "Hypoxia Induces Epithelial-Mesenchymal Transition via Activation of SNAI1 by Hypoxia-Inducible Factor -1α in Hepatocellular Carcinoma." *BMC Cancer* 13:108. https://doi.org/10.1186/1471-2407-13-108.

Zhang, Mei, Rachel L. Atkinson, and Jeffrey M. Rosen. 2010. "Selective Targeting of Radiation-Resistant Tumor-Initiating Cells." *Proceedings of the National Academy of Sciences of the United States of America* 107 (8):3522–27. https://doi.org/10.1073/pnas.0910179107.

Zhang, Wenjing, Xinpeng Shi, Ying Peng, Meiyan Wu, Pei Zhang, Ruyi Xie, Yao Wu, Qingqing Yan, Side Liu, and Jide Wang. 2015. "HIF-1α Promotes Epithelial-Mesenchymal Transition and Metastasis through Direct Regulation of ZEB1 in Colorectal Cancer." *PloS One* 10 (6):e0129603. https://doi.org/10.1371/journal.pone.0129603.

Zinonos, Irene, Agatha Labrinidis, Vasilios Liapis, Shelley Hay, Vasilios Panagopoulos, Mark Denichilo, Vladimir Ponomarev, et al. 2014. "Doxorubicin Overcomes Resistance to Drozitumab by Antagonizing Inhibitor of Apoptosis Proteins (IAPs)." *Anticancer Research* 34 (12):7007–20.

Zobalova, Renata, Laura McDermott, Marina Stantic, Katerina Prokopova, Lan-Feng Dong, and Jiri Neuzil. 2008. "CD133-Positive Cells Are Resistant to TRAIL due to up-Regulation of FLIP." *Biochemical and Biophysical Research Communications* 373 (4):567–71. https://doi.org/10.1016/j.bbrc.2008.06.073.